Synthesis, Fluorescent and Metal Sensor Properties of Hydrazone Derivatives

Patcharaporn Jansrisewangwong

A Thesis Submitted in Partial Fulfillment of the Requirements for the Degree of

Master of Science in Inorganic Chemistry

Prince of Songkla University

2012

Thesis Title	Synthesis, Fluorescent and Metal Sensor Properties of Hydrazone Derivatives
Author	Miss Patcharaporn Jansrisewangwong
Major Program	Inorganic Chemistry

Major Advisor:

……..
(Assoc. Prof. Dr. Suchada Chantrapromma)

Co-Advisor:

…….....
(Assoc. Prof. Dr. Chatchanok Karalai)

Examining Committee:

……..…….Chairperson
(Dr. Anob Kantacha)

……..…….....…
(Assoc. Prof. Dr. Suchada Chantrapromma)

……..……
(Assoc. Prof. Dr. Chatchanok Karalai)

……..……
(Asst. Prof. Darunee Bhongsuwan)

The Graduate School, Prince of Songkla University, has approved this thesis as partial fulfillment of the requirements for the Master of Science Degree in Inorganic Chemistry

…..……
(Prof. Dr. Amornrat Phongdara)
Dean of Graduate School

ชื่อวิทยานิพนธ์	การสังเคราะห์ สมบัติฟลูออเรสเซนซ์และการตรวจจับโลหะของสารประกอบอนุพันธ์ Hydrazones
ผู้เขียน	นางสาวพัชราภรณ์ จันทร์ศรีสว่างวงค์
สาขาวิชา	เคมีอินทรีย์
ปีการศึกษา	2554

บทคัดย่อ

สังเคราะห์สารประกอบอนุพันธ์ hydrazones (**PJ1**-**PJ17**) จำนวน 17 ชนิด และทำการวิเคราะห์โครงสร้างด้วยเทคนิค ^{1}H NMR FT-IR และ UV-Vis spectroscopy ศึกษาสมบัติฟลูออเรสเซนซ์ของสารในตัวทำละลายคลอโรฟอร์มที่อุณหภูมิห้อง พบว่า สารประกอบ hydrazones (**PJ1**-**PJ17**) แสดงสมบัติฟลูออเรสเซนซ์ และมีลักษณะของ fluorescence emission คล้ายคลึงกัน และเมื่อทำการกระตุ้นพลังงานที่ความยาวคลื่น 300 nm พบว่าสารแสดงค่า λ_{em} เท่ากับ 413, 412, 411, 406, 404, 410, 412, 407, 408, 409, 409, 404, 412, 405, 404, 410 และ 404 nm ตามลำดับ และมีสเปกตรัม fluorescence excitation แสดงค่า λ_{ex} เท่ากับ 296, 300, 293, 298, 294, 302, 304, 298, 302, 299, 298, 298, 300, 299, 302, 300 และ 302 nm ตามลำดับ เมื่อกำหนดค่า emission ที่ความยาวคลื่น 420 nm และสารประกอบ **PJ7** สามารถแสดงสมบัติเซนเซอร์ต่อโลหะ Cu(I) และ Cu(II) และศึกษาผลการเซนเซอร์ด้วยเกลือของโลหะ Cu ได้แก่ CuBr, CuCl, CuI, $CuCl_2$, $Cu(NO_3)_2$, $Cu(OAc)_2$ และ $CuSO_4$ พบว่า แถบดูดกลืนแสงเปลี่ยนแปลงอย่างเห็นได้ชัดต่อ $CuCl_2$ และ $Cu(NO_3)_2$ จาก 370 nm เป็น 452 nm ตามลำดับ นอกจากนั้นได้ทำการหาโครงสร้างด้วยเทคนิคการเลี้ยวเบนของรังสีเอกซ์บนผลึกเดี่ยวของสารประกอบ **PJ1**, **PJ10**, **PJ11**, **PJ14** และ **PJ15** พบว่าระบบผลึกเป็นมอโนคลีนิก (monoclinic) มีหมู่ปริภูมิเป็น $P2_1/c$ ส่วน **PJ2** และ **PJ6** พบว่าระบบผลึกเป็นไตรคลีนิค (triclinic) มีหมู่ปริภูมิเป็น $P\bar{1}$

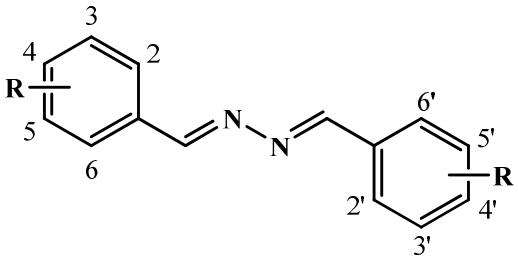

(**A**)

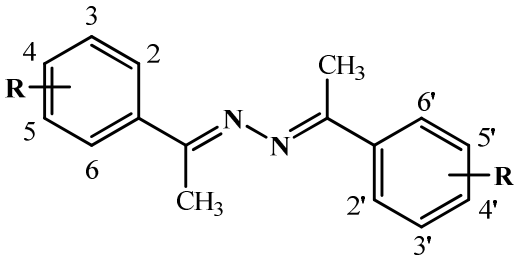

(**B**)

Code	R
PJ1	2,4,5-trimethoxy
PJ2	2,4,6-trimethoxy
PJ3	3,4,5-trimethoxy
PJ4	3-OH,4-NO_2
PJ5	4-OH,3-NO_2

Code	R	Code	R
PJ6	2-OCH_3	PJ12	3-OCH_3
PJ7	2-NH_2	PJ13	3-NH_2
PJ8	2-NO_2	PJ14	3-NO_2
PJ9	2-Cl	PJ15	3-Cl
PJ10	2-Br	PJ16	3-Br
PJ11	4-OH	PJ17	3-F

Thesis Title	Synthesis, Fluorescent and Metal Sensor Properties of Hydrazone Derivatives
Author	Miss. Patcharaporn Jansrisewangwong
Major Program	Inorganic Chemistry
Academic Year	2554

Abstract

Seventeen hydrazones (**PJ1**-**PJ17**) were synthesized and characterized by ^{1}H NMR, FT-IR and UV-Vis spectroscopies. Their fluorescent properties were studied in chloroform solution at room temperature. It was found that compounds (**PJ1**-**PJ17**) show fluorescent properties and their emission spectra have similar pattern. **PJ1**-**PJ17** present the maxima emission wavelength (λ_{em}) at 413, 412, 411, 406, 404, 410, 412, 407, 408, 409, 409, 404, 412, 405, 404, 410 and 404 nm, respectively, when was excited at 300 nm. The spectra of **PJ1**-**PJ17** compounds show maxima excitation wavelength (λ_{ex}) at 296, 300, 293, 298, 294, 302, 304, 298, 302, 299, 298, 298, 300, 299, 302, 300 and 302 nm, respectively, when the emission wavelength was fixed at 420 nm. **PJ7** shows metal sensor property for Cu(I) and Cu(II) ions. The metal sensor property was also studied with various Cu salts which are CuBr, CuCl, CuI, $CuCl_2$, $Cu(NO_3)_2$, $Cu(OAc)_2$ and $CuSO_4$ and it was found that the maxima absorption wavelength was considerable changed for $CuCl_2$ and $Cu(NO_3)_2$ from 370 to 430 and 452 nm, respectively. In addition, single crystal X-ray structure determination was also studies and found that **PJ1**, **PJ10**, **PJ11**, **PJ14** and **PJ15** were recrystallized crystallize in monoclinic $P2_1/c$ space group whereas **PJ2** and **PJ6** crystallize in triclinic $P\bar{1}$ space group.

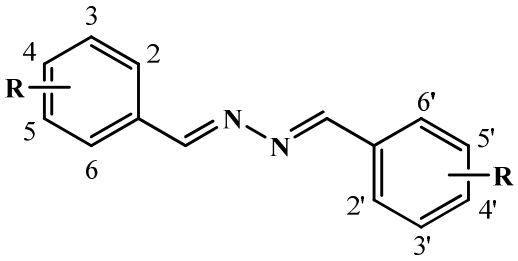

(**A**)

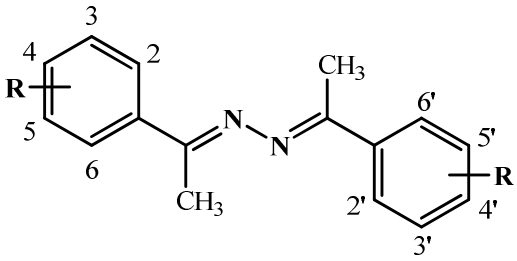

(**B**)

Code	R
PJ1	2,4,5-trimethoxy
PJ2	2,4,6-trimethoxy
PJ3	3,4,5-trimethoxy
PJ4	3-OH,4-NO_2
PJ5	4-OH,3-NO_2

Code	R	Code	R
PJ6	2-OCH_3	PJ12	3-OCH_3
PJ7	2-NH_2	PJ13	3-NH_2
PJ8	2-NO_2	PJ14	3-NO_2
PJ9	2-Cl	PJ15	3-Cl
PJ10	2-Br	PJ16	3-Br
PJ11	4-OH	PJ17	3-F

CONTENTS

CONTENTS (Continued)

CONTENTS (Continued)

CONTENTS (Continued)

CONTENTS (Continued)

LIST OF TABLES

LIST OF TABLES (Continued)

LIST OF ILLUSTRATIONS

LIST OF ILLUSTRATIONS (Continued)

LIST OF ILLUSTRATIONS (Continued)

LIST OF ILLUSTRATIONS (Continued)

LIST OF ILLUSTRATIONS (Continued)

ABBREVIATIONS AND SYMBOLS

s	=	singlet
d	=	doublet
t	=	triplet
dd	=	doublet of doublet
dt	=	doublet of triplet
g	=	gram
nm	=	nanometer
ml	=	milliliter
mp.	=	melting point
cm^{-1}	=	reciprocal centimeter (wave number)
δ	=	chemical shift relative to TMS
J	=	coupling constant
λ_{max}	=	maximum wavelength
ν	=	absorption frequencies
ε	=	molar extinction frequencies
°C	=	degree celcius
MHz	=	Megahertz
Hz	=	Hertz
ppm	=	part per million
Φ_F	=	fluorescence quantum yield
λ_{ex}	=	excitation wavelength
λ_{em}	=	emission wavelength
Å	=	Angstrom
hr	=	hour
aq	=	aqueous solution
μM	=	micromolar

ABBREVIATIONS AND SYMBOLS (Continued)

Trp	=	tryptophan
DTC	=	3,3’-diethylthiacarbocyanine
LEDs	=	light-emitting diodes
NLO	=	non-linear optic
DMADHC	=	4’-dimethylamino-2,5-dihydroxychalcone
DMC	=	4’-*N*,*N*-dimethylamino-4-methylacryloylamino chalcone
DMATP	=	3-(4’-dimethylaminophenyl)-1-(2-thienyl)prop-2-en-1-one
DMAFP	=	3-(4’-dimethylaminophenyl)-1-(2-furanyl)prop-2-en-1-one
XRD	=	X-ray diffraction
FT-IR	=	Fourier transform-infrared
UV-Vis	=	Ultraviolet-Visible
NMR	=	Nuclear magnetic resonance
TMS	=	tetramethylsilane
$CDCl_3$	=	deuterochloroform
DMSO-d_6	=	hexadeutero-dimethyl sulphoxide
KBr	=	potassium bromide

CHAPTER 1
INTRODUCTION

1.1 Motivation of Research

At the beginning of the twentieth century, there has been the first observation of fluorescence from a quinine solution in sunlight. It is interesting to notice that the first known fluorophore, quinine, was responsible for stimulating the development of the first spectrofluorometers that appeared in the 1950s. To this day the fluorescence of quinine remains one of the most used and most beautiful examples of blue fluorescence.

Fluorescence occurs when an orbital electron of a molecule, atom or nanostructure relaxes to its ground state by emitting a photon of light after being excited to a higher quantum state. There are many natural and synthetic compounds that exhibit fluorescence, and they have a number of applications which can be used in many fields such as fluorescent dyes (Arun *et al*., 2009), light-emitting diodes; LEDs (Li *et al*., 2005), fluorescent probes (Houdier *et al*., 1999) and fluorescent sensors (Jiménez-Pulido *et al*., 2009). Some of hydrazone derivatives exhibit fluorescence (Qin *et al*., 2009).

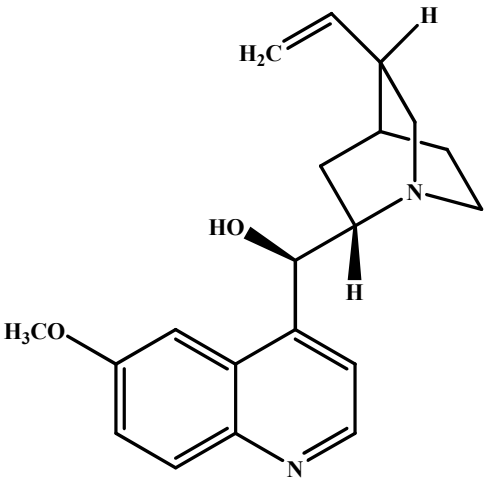

Quinine

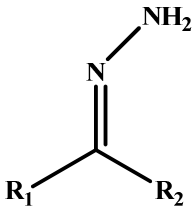

Hydrazone

Scheme 1. Structures of quinine and hydrazone.

In this work, the researcher was interested in studying fluorescent properties of organic synthesized compounds. The seventeen novel hydrazone derivatives were synthesized and characterized, their fluorescent properties and metal sensor were also investigated.

1.2 Luminescence

Luminescence is the emission of light from any substance, and occurs from electronically excited states. The term luminescence is used to describe a process by which light is produced other than by heating. The Sun gives off both heat and light as a result of nuclear reactions in its core. An incandescent light bulb gives off light when a wire filament inside the bulb is heated to white heat. One can read by the light of a candle flame because burning wax gives off both heat and light. But light can also be produced by other processes in which heat is not involved. For example, fireflies produce light by means of chemical reactions that take place within their bodies. They convert a compound known as luciferin from one form into another. As that process occurs, light is given off.

Luminescence occurs, the system loses energy and if the emission is to be continuous, some form of energy must be supplied from elsewhere. The various types of luminescence are classified according to the mode of excitation. Thus the radioluminescence emitted from a luminous clock face is supplied by high energy particles from the radioactive material in the phosphor and the electroluminescence of a gas discharge lamp is derived from the passage of an electric current through an ionized gas. Other such phenomena include chemiluminescence, when occurs a chemical reaction from eletronic excited molecule return to the ground state. When the chemiluminescence reactions take place within living organisms is called bioluminescence such as firefly, some types of jelly fish, bacteria and crustacean. The external energy supply is by means of the absorption of ultraviolet, visible or infrared light, the emitted light is called photoluminescence.

The ultraviolet and visible regions of the spectrum are of most interest in fluorometry and absorption in these regions causes the excitation of the outermost electrons of the molecule. The energy associated with radiation of this frequency is quite high, around 100 kilogram calories per einstein, and is sometimes sufficient to break down the absorbing molecules, as for instance with the fading of dyes by the action of sunlight.

The absorption of light results in the formation of excited molecules which can in turn dissipate their energy by decomposition, reaction, or re-emission.

Luminescence is the emission of light from any substance and occurs from electronically excited states. Luminescence is formally divided into two types which are fluorescence and phosphorescence

Phosphorescence is emission of light from triplet-excited states (T_1), in which the electron in the excited orbital has the same spin orientation as the ground-state electron. Transitions to the ground state are forbidden and the emission rates are slow (10^3-10^0 s^{-1}). So that phosphorescence lifetimes are typically milliseconds to seconds (10^{-3}-10^2 s). Even longer lifetimes are possible, as is seen from “glow-in-the-dark”

Fluorescence is emission light from singlet-excited states, in which the electron in the excited orbital is paired (of opposite sign) to the second electron in the ground-state orbital. Return to the ground state is spin-allowed and occurs rapidly by emission of a photon. The emission rates of fluorescence are typically 10^8 s^{-1}, so that a typical fluorescence lifetime is near 10 ns ($10^{-9} \times 10^{-7}$ s). The lifetime of a fluorophore is the average time between its excitation and its return to the ground state. It is valuable to consider a 1-ns lifetime within the context of the speed of light.

From above mentioned, the fluorescence properties of Hydrazones was selected to study in this thesis.

1.3 Origin of Fluorescence

Fluorescence is found as a special optical phenomenon in some substances, fluorescence was first observed by Nicolas Monardes in 1565, he reported that the extract from the 'Lignum nephriticum' showed blue emission fluorescence (Valeur, 2002). Based on his reports, others-including Newton-investigated the phenomenon, but it was not understood. In 1833, Sir David Brewster noted that chlorophylls can also emit red fluorescence light. Following important observations by Brewster and Herschel in the nineteenth century, Sir George Gabriel Stokes demonstrated in 1852 that fluorescence was an emission of light following the absorption of light (Stokes, 1852). Stokes was also responsible for coining the term "fluorescence" which are the name was given as a description of the essence of the mineral fluorite, composed of calcium fluoride, which gave a visible emission when illuminated with 'invisible radiation' (UV radiation). After that, fluorescence spectroscopy has been widely used as chemistry analysis techniques in many fields. The theory of fluorescence has been described thoroughly by Lakowicz (Lakowicz, 1999) and will be shortly summarized.

1.4 Theory of Fluorescence

The processes which occur between the absorption and emission of light are usually illustrated by a Jablonski diagram. A typical Jablonski diagram is shown in **Figure 1.** The Jablonski diagram is a concise summary of the radiative and non-radiative transitions occurring between electronic states in a molecule. The figure 1 shows the transition that are common to all systems. The ground, first and second electronic states are depicted by S_0, S_1 and S_2, respectively.

At each of these electronic energy levels the fluorophores can exist in a number of vibrational energy levels (denoted by 0, 1, 2, etc.). Transitions between states are depicted as vertical lines to illustrate the instantaneous nature of light absorption. Transitions occur in about 10^{-15} seconds, a time too short for significant displacement of nuclei. A fluorophore is usually excited to some higher vibrational

level of either S_1 or S_2. With a few rare exceptions, molecules in condensed phases rapidly relax to the lowest vibrational level of S_1. This process, called internal conversion, is nonradiative and takes place in 10^{-12} seconds or less. Since fluorescence lifetimes are typically near 10^{-8} s, internal conversion is generally complete prior to emission. Hence, fluorescence emission generally results from a thermally equilibrated excited state, that is, the lowest energy vibrational state of S_1. Return to the ground state occurs to a higher excited vibrational ground-state level, which then quickly (10^{-12} s) reaches thermal equilibrium. An interesting consequence of emission to a higher vibrational ground state is that the emission spectrum is typically a mirror image of the absorption spectrum of the $S_0 \rightarrow S_1$ transition. This similarity occurs because electronic excitation does not greatly alter the nuclear geometry. Hence the spacing of the vibrational energy levels of the excited states is similar to that of the ground state. As a result, the vibrational structures seen in the absorption and the emission spectra are similar. Molecules in the S_1 state can also undergo a spin conversion to the first triplet state T_1. Emission from T_1 is termed phosphorescence, and is generally shifted to longer wavelengths (lower energy) relative to the fluorescence. Conversion of S_1 to T_1 is called intersystem crossing. Transition from T_1 to the singlet ground state is forbidden, and as a result the rate constants for triplet emission are several orders of magnitude smaller than those for fluorescence. Molecules containing heavy atoms such as bromine and iodine are frequently phosphorescent. The heavy atoms facilitate intersystem crossing and thus enhance phosphorescence quantum yields.

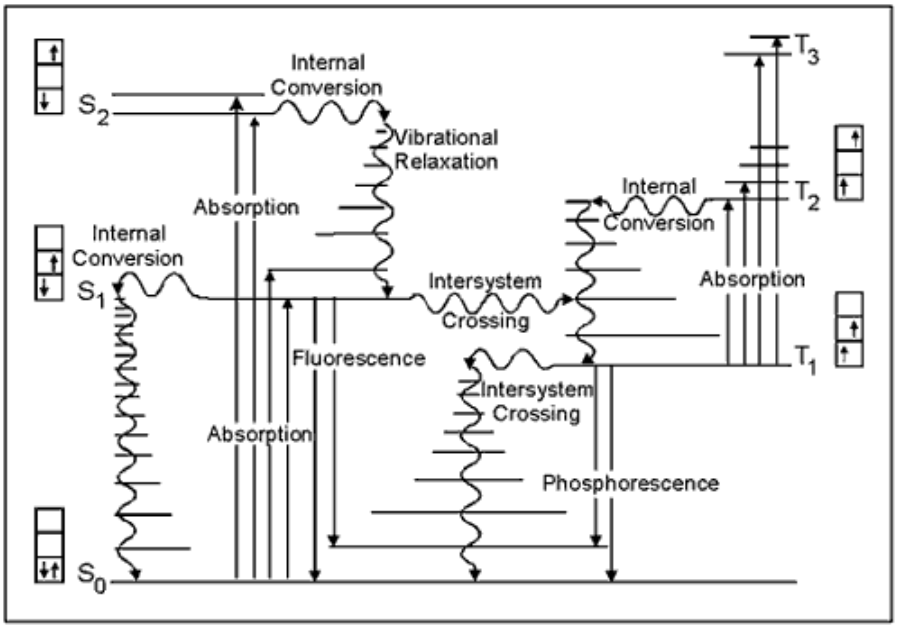

Figure 1 A simplified Jablonski diagram with absorption, internal conversion, fluorescence, intersystem crossing and phosphorescence.

1.4.1 Absorption, Excitation, and Emission

Absorption of energy by fluorochromes occurs between the closely spaced vibrational and rotational energy levels of the excited states in different molecular orbitals. The various energy levels involved in the absorption and emission of light by a fluorophore are classically presented by a Jablonski energy diagram (**Figure 1**), named in honor of the Polish physicist Professor Alexander Jablonski. A typical Jablonski diagram illustrates the singlet ground (S_0) state, as well as the first (S_1) and second (S_2) excited singlet states as a stack of horizontal lines. In **Figure 1**, transitions between the states are illustrated as straight or wavy arrows, depending upon whether the transition is associated with absorption or emission of a photon (straight arrow) or results from a molecular internal conversion or non-radiative relaxation process (wavy arrows). Vertical upward arrows are utilized to indicate the instantaneous nature of excitation processes, while the wavy arrows are reserved for those events that occur on a much longer timescale.

Absorption of light occurs very quickly (approximately a femtosecond, the time necessary for the photon to travel a single wavelength) in discrete amounts termed quanta and corresponds to excitation of the fluorophore from the ground state to an excited state. Likewise, emission of a photon through fluorescence or phosphorescence is also measured in terms of quanta. The energy in a quantum (Planck's Law) is expressed by the equation:

$$E = h\nu = hc/\lambda \qquad (2)$$

where E is the energy, h is Planck's constant, ν and λ are the frequency and wavelength of the incoming photon, and c is the speed of light. Planck's Law dictates that the radiation energy of an absorbed photon is directly proportional to the frequency and inversely proportional to the wavelength, meaning that shorter incident wavelengths possess a greater quantum of energy. The absorption of a photon of energy by a fluorophore, which occurs due to an interaction of the oscillating electric field vector of the light wave with charges (electrons) in the molecule, is an all or none phenomenon and can only occur with incident light of specific wavelengths known as absorption bands. If the absorbed photon contains more energy than is necessary for a simple electronic transition, the excess energy is usually converted into vibrational and rotational energy. However, if a collision occurs between a molecule and a photon having insufficient energy to promote a transition, no absorption occurs. The spectrally broad absorption band arises from the closely spaced vibrational energy levels plus thermal motion that enables a range of photon energies to match a particular transition. Because excitation of a molecule by absorption normally occurs without a change in electron spin-pairing, the excited state is also a singlet. In general, fluorescence investigations are conducted with radiation having wavelengths ranging from the ultraviolet to the visible regions of the electromagnetic spectrum (250 to 700 nanometers).

With ultraviolet or visible light, common fluorophores are usually excited to higher vibrational levels of the first (S_1) or second (S_2) singlet energy state. One of the absorption (or excitation) transitions presented in **Figure 1** occurs from

the lowest vibrational energy level of the ground state to a higher vibrational level in the second excited state (a transition denoted as S_0 to S_2). A second excitation transition is depicted from the second vibrational level of the ground state to the highest vibrational level in the first excited state (denoted as S_0 to S_1). In a typical fluorophore, irradiation with a wide spectrum of wavelengths will generate an entire range of allowed transitions that populate the various vibrational energy levels of the excited states. Some of these transitions will have a much higher degree of probability than others, and when combined, will constitute the absorption spectrum of the molecule. Note that for most fluorophores, the absorption and excitation spectra are distinct, but often overlap and can sometimes become indistinguishable. In other cases (fluorescein, for example) the absorption and excitation spectra are clearly separated.

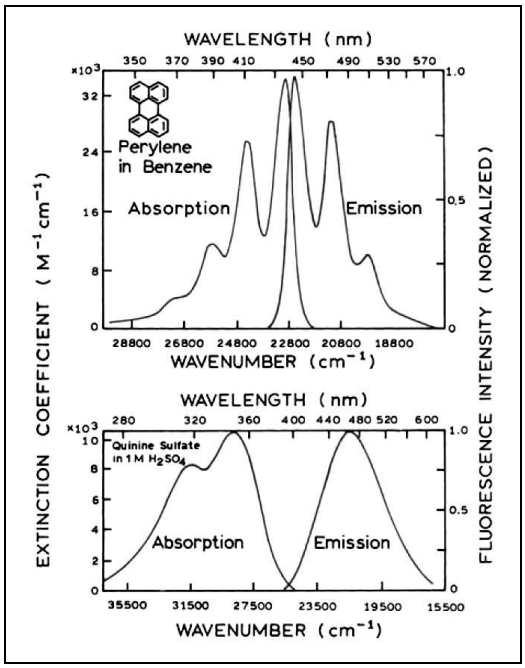

Figure 2 Absorption and fluorescence emission spectra of perylene and quinine. Emission spectra cannot be correctly presented on both the wavelength and wavenumber scales. The wavenumber presentation is correct in this instance. Wavelengths are shown for convenience.

Fluorescence spectral data are generally presented as emission spectra. A fluorescence emission spectrum is a plot of the fluorescence intensity versus

wavelength (nanometers) or wavenumber (cm^{-1}). Two typical fluorescence emission spectra are shown in **Figure 2**. Emission spectra vary widely and are dependent upon the chemical structure of the fluorophore and the solvent in which it is dissolved. The spectra of some compounds, such as perylene, show significant structure due to the individual vibrational energy levels of the ground state and excited states. Other compounds, such as quinine, show spectra which are devoid of vibrational structure.

1.4.2 Stokes Shift

Stokes shift is the difference (in wavelength or frequency units) between positions of the band maxima of the absorption and emission spectra (fluorescence and Raman being two examples) of the same electronic transition. It is named after Irish physicist George G. Stokes.

When a system (be it a molecule or atom) absorbs a photon, it gains energy and enters an excited state. One way for the system to relax is to emit a photon, thus losing its energy (another method would be the loss of heat energy). When the emitted photon has less energy than the absorbed photon, this energy difference is the Stokes shift. If the emitted photon has more energy, the energy difference is called an anti-Stokes shift; this extra energy comes from dissipation of thermal phonons in a crystal lattice, cooling the crystal in the process. Yttrium oxysulfide doped with gadolinium oxysulfide is a common industrial anti-Stokes pigment, absorbing in the near-infrared and emitting in the visible portion of the spectrum.

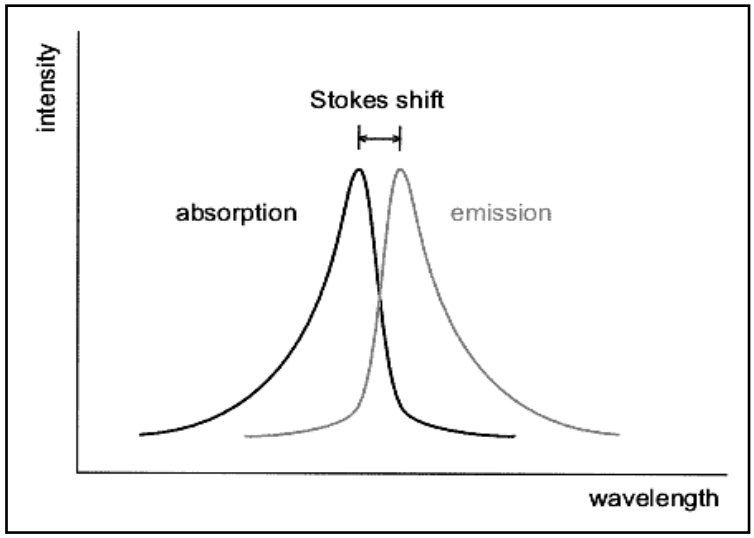

Figure 3 Stokes shift between λ_{max} of absorption and emission spectra

1.5 Structural requirements for fluorophores

Fluorophores, small molecules that can be part of a molecule (intrinsic fluorophores) or added to it (extrinsic fluorophores), can be found in different cells, and so they can be used as natural indicators to study the structure, dynamics, and metabolism of living cells. Their fluorescence properties are dependent on their structure and on the surrounding environment. Each fluorophore has its own specific fluorescence properties.

Fluorescence typically occurs from aromatic molecules. Some typical fluorescent substances (fluorophores) are shown in **Figure 4**

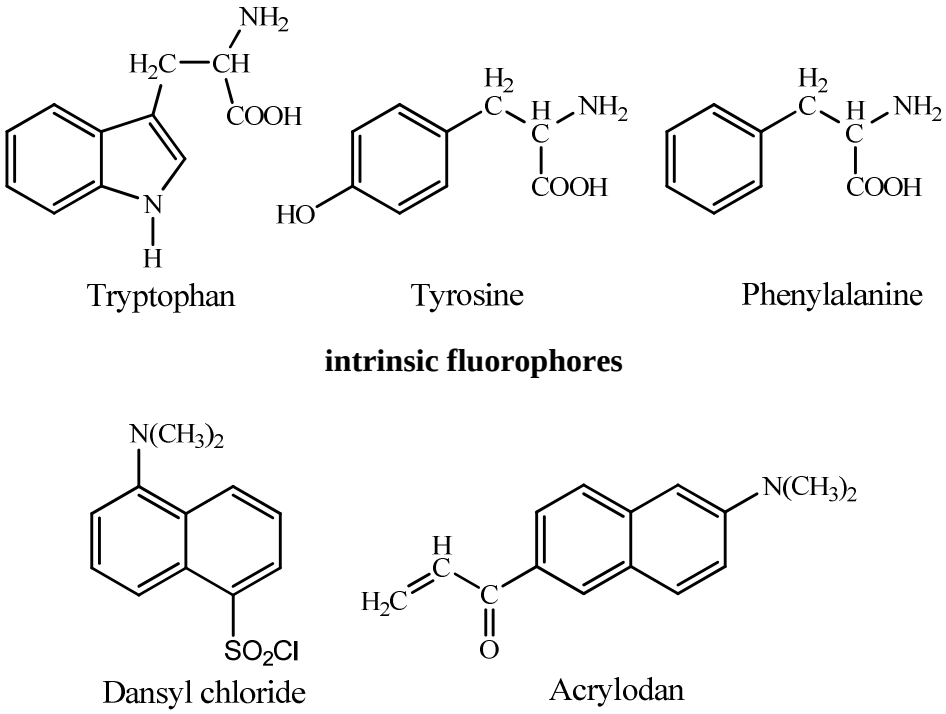

Figure 4 Structures of typical fluorescent substances.

Types of fluorophores, there are many possible ways in which to group similar fluorophores into distinct classes.

- Intrinsic or natural fluorophores: Fluorescent compounds are found in many living systems. These include the fluorescence amino acids tryptophan, tyrosine, and phenylalanine found in proteins, as well as enzyme cofactor such as NADH, FAD, and riboflavin found in cells and tissues. While intrinsic fluorophores can be used to study cellular dynamics and protein structure, more offen they serve as an unwanted background “autofluorescence” that must be separated from the desired signal.

- Covalent protein-labeling fluorophores: These fluorophores are designed with reactive groups for labeling proteins with a fluorescent tag, allowing us monitor their behavior. A wide variety of reactive derivatives are available. For example, sulfhydryl groups can be labeled through reaction with iodocaetamides or malemides and amine groups through reaction with isothiocyanates, sulfonyl chlorides.

Molecular structures which can interact as fluorophore were shown here:

- The compounds contained the electron which can cause the transition by using low energy because causing π to π* which are aromatic functional group.

- The compounds contained conjugated multiple double bonds which can see that aliphatic and alicyclic carbonyl structures have conjugated multiple bonds less than aromatic system.

- Aromatic hydrocarbons which have not substituted groups will increase the fluorescence if the number of ring is increase. Resulting in the increase in Quantum Efficiency in the **Table 1**

Table 1 Fluorescence and Quantum Efficiency of linear aromatics

Compounds	Quantum Efficiency (Φ_f)	Excitation wavelength λ_{ex} (nm)	Emission wavelength λ_{em} (nm)
Benzene	0.11	205	278
Naphthalene	0.29	286	321
Anthracene	0.46	365	400
Tetracene	0.60	390	480
Pentacene	0.52	580	640

It can be seen that increasing of conjugation is the cause of increasing fluorescence quantum yield. In addition, when transition energy was decreased, the fluorescence spectrum will shift to the longer wavelength.

- Heterocyclic compounds, for example, pyridine, furan, thiophene and pyrrole show low fluorescent properties because of it transition from n to π* and change to Triplet state quickly. But, compounds which are fused rings and have long conjugate which have heterocyclic nucleus shows fluorescence property such as quinolin, isoquinolin and indole etc.

- Substituted groups in benzene ring have influence for fluorescence which was shown in **Table 2**

Table 2 Substitution effect on the fluorescence of benzene in ethanol solution

Compound	**Formula**	**Fluorescence wavelength (nm.)**	**Fluorescence relative intensity**
Benzene	C_6H_6	270-310	10
Toluene	$C_6H_5CH_3$	270-320	17
Propylbenzene	$C_6H_5C_3H_7$	270-320	17
Phenol	C_6H_5OH	285-365	18
Phenolate ion	$C_6H_5O^-$	310-400	10
Anisole	$C_6H_5OCH_3$	285-345	20
Aniline	$C_6H_5NH_2$	310-405	20
Benzonitrile	C_6H_5CN	280-360	20
Fluorobenzene	C_6H_5F	270-320	10
Chlorobenzene	C_6H_5Cl	275-345	7
Bromobenzene	C_6H_5Br	290-380	5
Iodobenzene	C_6H_5I	-	0
Anilinium ion	$C_6H_5NH_3^+$	-	0
Benzoic acid	C_6H_5COOH	310-390	3
Nitrobenzene	$C_6H_5NO_2$	-	0

1.6 Metal ion sensor

Metal ion sensor is employed in application ranging from clinical toxicology, environmental bioinorganic chemistry, bioremediation and waste management and much attention has focused to the development of sensing devices for copper. Copper compounds are also employed for plant diseases treatment, water treatment and as preservatives for wood and leather. Nonetheless, while a low-level background intake of copper is indispensable, high doses of copper can be harmful and even toxic to biological system.

Many sensing methods for detecting Cu^{2+} have been described, such as colorimetric and fluorescent chemosensors, and electrochemical methods. Colorimetric sensors are promising due to the simplicity of assay. Furthermore, colorimetric assays have a significantly lower capital cost than closely related methods, such as fluorescent sensors, for which both spectrophotometric equipment and UV light source are required.

An attractive feature of photoreceptors with donor-acceptor character is the possibility of synthetically tuning the transition energy of their internal charge transfer (ICT) states to allow colorimetric 'naked eye' response.

1.7 Hydrazone derivatives

Hydrazones are a special group of the Schiff base compounds and they are characterized by the presence >C=N-N=C< and reaction of hydrazone, shown in **Figure 5**. The presence of two inter-linked nitrogen atoms was separated from imines, oximes, etc. They have applications including biologically active compounds such as antibacterial, antifungal (El-Tabl *et al*., 2008), antimalarial (Melnyk *et al*., 2006), anti-inflammatory (El-Sherif *et al*., 2009), antioxidant (Qin *et al*., 2009), hydrazones find applications in the treatment of diseases such as tuberculosis (Patole *et al*., 2003), non-linear optic (NLO) (Baughman *et al*., 2004) and electroactive fluorescent materials which are used as fluorescent dyes (Arun *et al*., 2009), light-emitting diodes (LEDs) (Li *et al*., 2005), fluorescent probes (Houdier *et al*., 1999) and

fluorescent sensors (Jiménez-Pulido *et al*., 2009), etc. They also find applications as indicators and spot test reagents (Dubey *et al*., 1985)

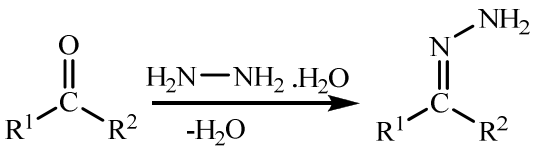

Figure 5 The structure and reaction of hydrazone

In general, the compounds which can emit fluorescence light (fluorophore) in visible region under ultraviolet or visible excitation frequently contain mixing structures of aromatic with long π-conjugate system or aliphatic/alicyclic carbonyl corresponding to the structure of hydrazone derivatives.

1.8 Review of Literatures

Chen *et al*., 2009 synthesized new rhodamine derivatives bearing binaphthyl group and studied for fluorescent properties and colorimetric sensors for Cu^{2+} and found that they are highly selective “off–on” type fluorescent.

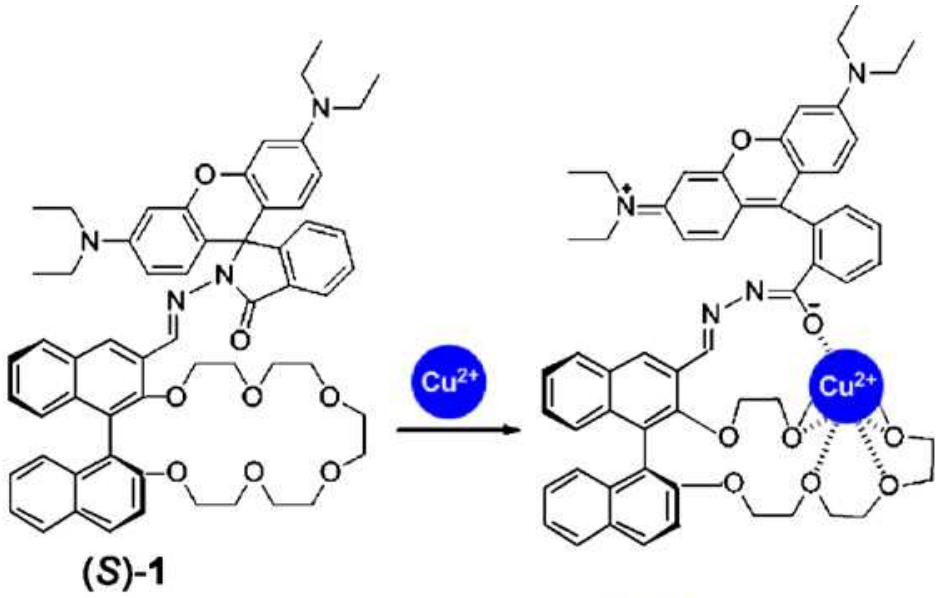

Scheme 2. Proposed binding mechanism for (S)-1 with Cu^{2+} and colorimetric/ fluorescent changes of 50 μM (S)-1 treated with 10 eq. Cu^{2+}

Dang *et al.*, 2010 synthesized hydrazone derivatives and their complexes and luminescent properties and studied for strength of bond of *N*,*N*'-bis(furan-2-ylmethylene)hydrazine ligand which have O and N donor atoms in the reaction with Ag(I) ion.

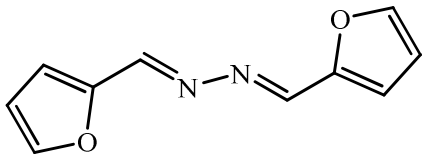

Scheme 3. *N*,*N*'-bis(furan-2-ylmethylene)hydrazine

Dilek *et al.*, 2008 synthesized hydrazone derivatives of boron dipyrromethene (BODIPY or BDP) possessing a 3-hydrazinyl substituent which prepared by nucleophilic substitution reactions for use as bioorthogonal fluorescent labels of aldehydes and ketones.

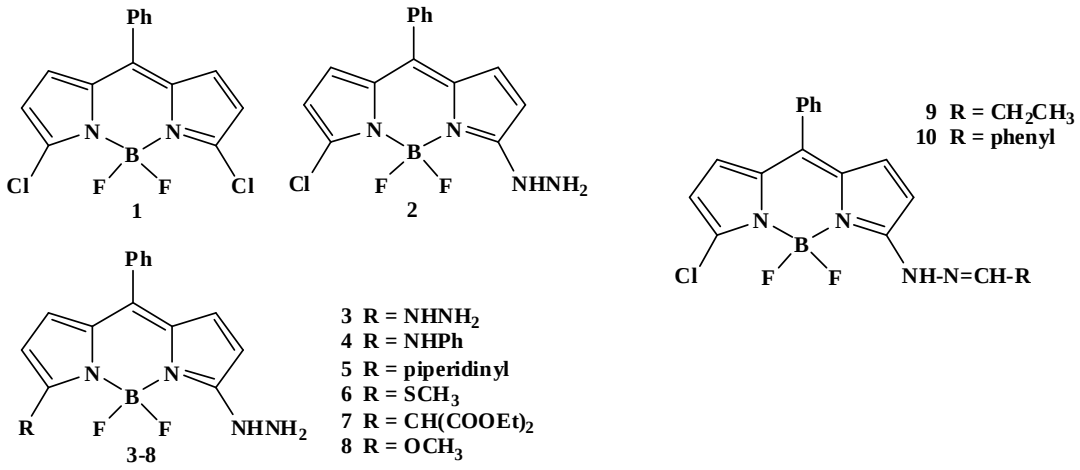

Scheme 4. Structure of BDPs (1-8) and hydrazones (9-10)

Han *et al.*, 2007 synthesized derivatives of bisthiocarbonohydrazones and found to be a class of sensitive, selective, ratiometric and colorimetric chemosensors of anions such as fluoride (F^-) or acetate (Ac^-) and study for switch-on fluorescent chemosensor for F^- and Ac^-.

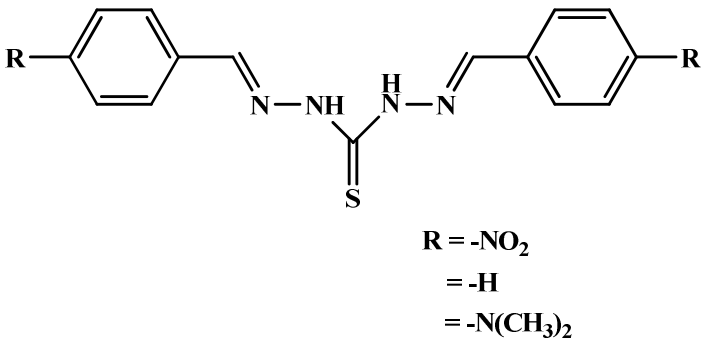

Scheme 5. Structure of hydrazones ligand

Huh *et al*., 2008 synthesized and studied for fluorescent properties of hydrazone derivatives and their complexes of 5 compounds by layer diffusion (dichloromethane–methanol solution) and found that $[Ag_2L_2(NO_3)_2]$ complex with L_2 = 1,2-bis(furan-2-ylmethylene)hydrazine exhibited blue-green photo- luminescence at room temperature in the solid state.

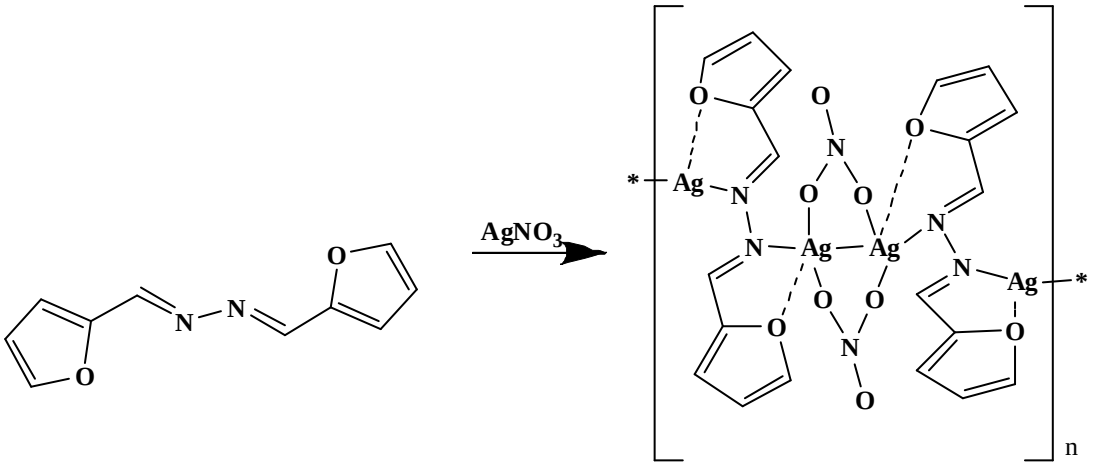

Scheme 6. $[Ag_2$(1,2-bis(furan-2-ylmethylene)hydrazine$)(NO_3)_2]$

Jiménez-Pulido *et al*., 2009 synthesized pteridine-benzoylhydrazone ligand (BZLMH = benzoyl- hydrazone of 6-acetyl-1,3,7-trimethyllumazine, lumazine = (1*H*,3*H*)-pteridin-2,4-dione) and studied for fluorescent properties and the fluorescence band shift and changes in intensity which is modulated by complexation with different metal ions (Ni^{2+}, Zn^{2+} and Hg^{2+}). The BZLMH system show good affinity for Hg^{2+} due to the pronounced changes in photophysical properties such as emission wavelength and intensity of Hg(II) complexes.

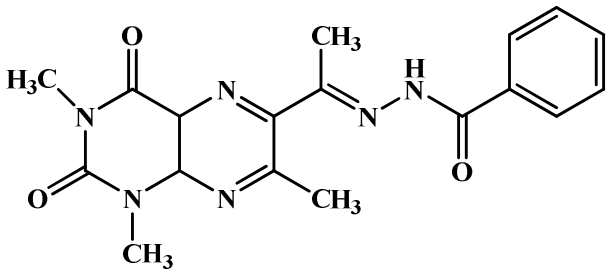

Scheme 7. Benzoylhydrazone of 6-acetyl-1,3,7-trimethyllumazine (BZLMH)

Liu *et al*., 2010 synthesized hydrazone derivatives and their complexes and studied for fluorescent properties such as *N*-(2-acetic acid)salicyloyl hydrazone ($C_9H_8N_2O_4$, H_3L) and imidazole. The cadmium(II) complex exhibits good fluorescence properties.

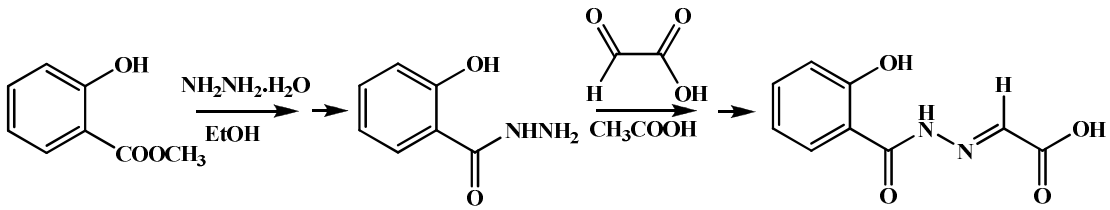

Scheme 8. Synthesis of H_3L ligand

Lu *et al*., 2008 synthesized hydrazone derivatives and their complexes such as *N*-(1,3-diphenyl-4-propylene-5-pyrazolone)salicylidene hydrazone (1) *N*-(1,3-diphenyl-4-ethylene-5-pyrazolone) salicylidene hydrazone (2) *N*-(1,3-diphenyl-4-benzylidene-5-pyrazolone)salicylidene hydrazone (3) *N*-(1,3-diphenyl-4-phenyl ethylene-5-pyrazolone)salicylidene hydrazone (4) and studied for fluorescent properties both in the solid state and in solution of ligand, they are in the following order 1 > 2 > 3, which is consistent with the red-shift of the emission spectra. However, it was found that the energy gap of ligand 4 does not correspond to the redshift.

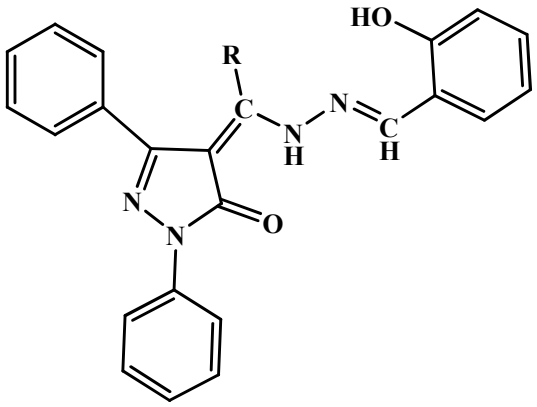

R = CH_2CH_3 1

= CH_3 2

= 3

= H_3C 4

Scheme 9. hydrazone derivatives (1-4)

Mashraqui *et al*., 2010 synthesized hydrazone derivative and complex such as Michler's ketone benzhydrazide (MIZON) by condensing Michler's ketone with 4-(*N*,*N*'-dimethylamino)benzhydrazide and studies for fluorescent properties which MIZON was found to interact selectively with Cu^{2+}, inducing remarkably high absorbance red shift by 240 nm. Therefore it is clearly available that MIZON can be used to detect Cu^{2+} in micromolar range via dual visible color change from yellow to green and fluorescence switch-on response.

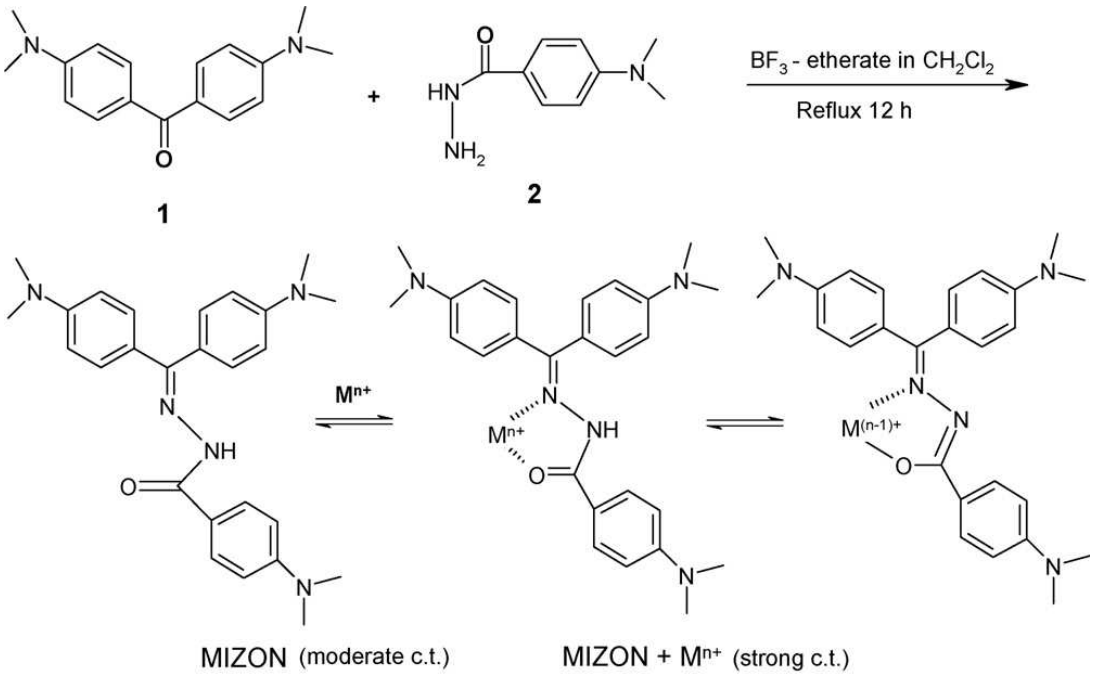

Scheme 10. Synthesis and the proposed interaction of MIZON with metal ions (M^{n+}).

Wang *et al*., 2009 synthesized and characterized hydrazone derivatives and their complexes such as 7-methoxychromone-3-carbaldehyde-(4'-hydroxy) benzoylhydrazone (ligand) and Ln(III) complexes (Ln = La, Eu). It was found that the Eu(III) complex exhibits characteristic fluorescence of europium ion in different organic solvents.

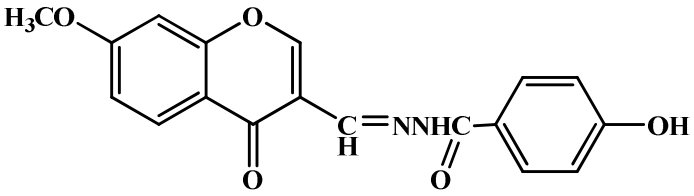

Scheme 11. 7-methoxychromone-3-carbaldehyde-(4'-hydroxy)benzoylhydrazone

1.9 Objectives and outline of this study

The objectives of this study are:

1. To synthesize and characterize hydrazone derivatives by spectroscopic techniques.
2. To determine the structures of hydrazone derivatives which can be crystallized out in single crystals form by X-ray diffraction method.
3. To study fluorescent property and metal sensor of hydrazone derivatives.

Much attentions have been given to fluorescent materials because of their promising applications such as fluorescent dyes, fluorescent tubes, fluorescent probes and fluorescent sensors. In this thesis, the seventeen compounds of hydrazone derivatives which are expected to exhibit fluorescent property will be synthesized. Their structures will be elucidated by spectroscopy techniques. Single crystal X-ray structure determination will also be studied for those compounds which can be crystallized out in order to study for their structures and crystal packings.

The seventeen synthesized hydrazones were designed base on π conjugated structure and different in substituted groups (shown in **Figure 6**) and studied for their fluorescent properties.

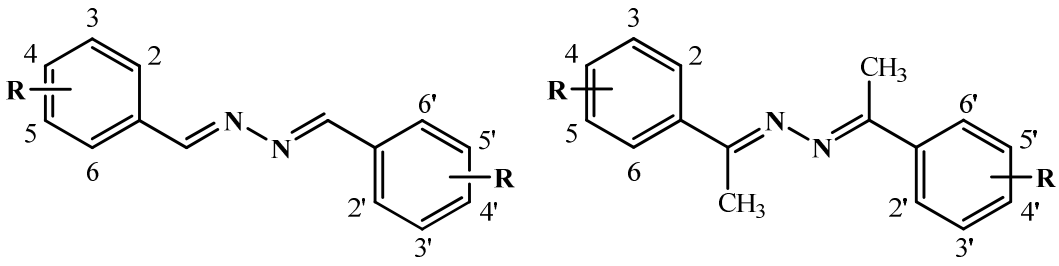

(**A**) (**B**)

Code	R
PJ1	2,4,5-trimethoxy
PJ2	2,4,6-trimethoxy
PJ3	3,4,5-trimethoxy
PJ4	3-OH,4-NO_2
PJ5	4-OH,3-NO_2

Code	R	Code	R
PJ6	2-OCH_3	PJ12	3-OCH_3
PJ7	2-NH_2	PJ13	3-NH_2
PJ8	2-NO_2	PJ14	3-NO_2
PJ9	2-Cl	PJ15	3-Cl
PJ10	2-Br	PJ16	3-Br
PJ11	4-OH	PJ17	3-F

Figure 6 The seventeen synthesized hydrazone derivatives.

In this study, focus will be on effect of different in substituted groups of hydrazones (**Figure 6**) which are expected to exhibit the fluorescent property along with comparison of their emission fluorescence. Crystals of a size and quality suitable for single crystal X-ray diffraction studies were grown with the objective to study their structures in solid state.

This thesis is divided into four parts, which are introduction, experimental, results and discussion, and conclusion.

2. EXPERIMENT

2.1 Instruments and chemicals

2.1.1 Instruments

Ultraviolet and visible (UV-Vis) absorption spectra were recorded using a SPECORD S 100 (Analytikjena) and principle bands (λ_{max}) were recorded as wavelengths (nm) and logε. Proton nuclear magnetic resonance spectra were recorded on FT-NMR Bruker Ultra Shield^{TM} 300 MHz. Spectra were recorded in deuterochloroform or hexadeutero-dimethyl sulphoxide solution and were recorded as δ value in ppm downfield from TMS (internal standard δ 0.00). Melting point was recorded in °C and was measured using an Electrothermal melting point apparatus. Infrared spectra were recorded by using FTS 165 FT-IR spectrophotometer. Major bands (ν) were recorded in wave numbers (cm^{-1}). Single crystal X-ray diffraction measurements were collected using a Bruker Apex2 CCD diffractometer with a graphite monochromated $MoK_{\propto}$ radiation. (λ = 0.71073 Å) at a detector distance of 5 cm and with APEX2 software. The collected data were reduced using *SAINT* (Bruker, 2005) program, and the empirical absorption corrections were performed using *SADABS* program. The structures were solved by direct methods and refined by least-squares using the *SHELXTL* (Sheldrick, 2008) software package. Fluorescence excitation and emission spectra were recorded on a Perkin-Elmer LS 55 Luminescence Spectrometer at the ambient temperature. The yields were reported as percentage of products.

2.1.2 Chemicals

All chemicals used in this study are AR grade and were used without further purification.

1) Hydrazine hydrate from Sigma-Aldrich, Inc, USA
2) 2,4,5-Trimethoxybenzaldehyde from Fluka Chemica, Switzerland
3) 2,4,6-Trimethoxybenzaldehyde from Fluka Chemica, Switzerland
4) 3,4,5-Trimethoxybenzaldehyde from Fluka Chemica, Switzerland
5) 3-Hydroxy-4-nitrobenzaldehyde from Fluka Chemica, Switzerland
6) 4-Hydroxy-3-nitrobenzaldehyde from Fluka Chemica, Switzerland
7) 2-Methoxyacetophenone from Sigma-Aldrich, Inc, USA
8) 2-Aminoacetophenone from Sigma-Aldrich, Inc, USA
9) 2-Nitroacetophenone from Sigma-Aldrich, Inc, USA
10) 2-Chloroacetophenone from Sigma-Aldrich, Inc, USA
11) 2-Bromoacetophenone from Sigma-Aldrich, Inc, USA
12) 4-Hydroxyacetophenone from Fluka Chemica, Switzerland
13) 3-Methoxyacetophenone from Fluka Chemica, Switzerland
14) 3-Aminoacetophenone from Fluka Chemica, Switzerland
15) 3-Nitroacetophenone from Fluka Chemica, Switzerland
16) 3-Fluoroacetophenone from Fluka Chemica, Switzerland
17) 3-Chloroacetophenone from Fluka Chemica, Switzerland
18) 3-Bromoacetophenone from Fluka Chemica, Switzerland
19) Ethanol (AR grade) from Merck, Germany
20) Chloroform (AR grade) from Merck, Germany
21) Acetonitrile (AR grade) from Merck, Germany
22) Acetone (AR grade) from Merck, Germany
23) Magnesium (II) chloride hexahydrate from Carlo, France
24) Calcium (II) chloride dehydrate from Merck, Germany
25) Manganese (II) chloride tetrahydrate from Fluka Chemica, Switzerland
26) Ferric (II) chloride tetrahydrate from Fluka Chemica, Switzerland

27) Cobalt (II) chloride from Fluka Chemica, Switzerland
28) Nickel (II) chloride from Scharlau, Spain
29) Zinc (II) chloride from Fisher, Malaysia
30) Mercury (II) chloride from Carlo, France
31) Cadmium (II) chloride from Scharlau, Spain
32) Cupper (I) bromide from Fluka Chemica, Switzerland
33) Cupper (I) chloride from M&B, England
34) Cupper (I) iodide from M&B, England
35) Cupper (II) chloride from Scharlau, Spain
36) Copper (II) sulfate pentahydrate from Scharlau, Spain
37) Cupper (II) acetate monohydrate from Fluka Chemica, Switzerland
38) Cupper (II) nitrate from Carlo, France

2.2 Synthesis of hydrazone derivatives

All compounds were synthesized by mixing hydrazine hydrate and various acetophenones or aldehydes in 1:2 molar ratio. A straightforward approach to synthesize the series of hydrazone derivatives.

2.3 Synthesis and characterization of hydrazones

2.3.1 (1*E*,2*E*)-1,2-bis(2,4,5-trimethoxybenzylidene)hydrazine (PJ1)

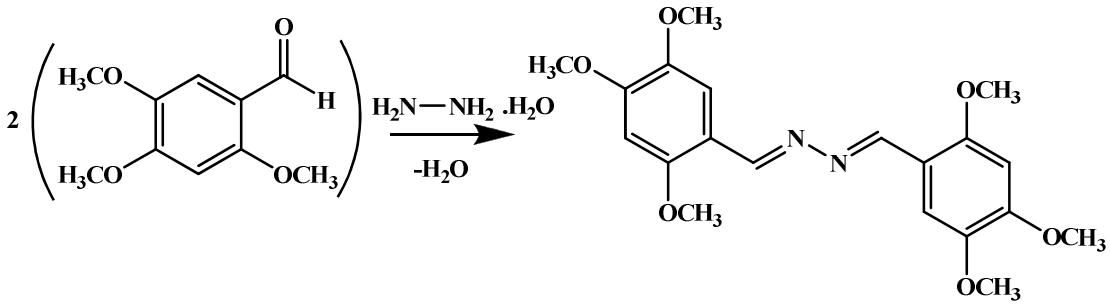

2,4,5-trimethoxy-benzaldehyde hydrazine hydrate (**PJ1**)

Compound **PJ1** was synthesized by condensation reaction, the solution of hydrazine hydrate (0.01 ml, 2 mmol) and 2,4,5-trimethoxybenzaldehyde (0.785 g, 4 mmol) in EtOH (20 ml). The resulting solution was refluxed for 5 hrs. The purity of the compounds was confirmed by thin-layer chromatography, yielding the yellow solid. The resultant solid was filtered off and washed with MeOH, dried in vacuum and purified by repeated recrystallization from CH_3COCH_3 to give a yellow crystal of compound **PJ1** (76% yield), mp. 250 °C (decompose), UV-Vis ($CHCl_3$) λ_{max} (nm) (ε x10^4): 270 (2.20), 379 (0.40). FT-IR (KBr) ν(cm^{-1}): 2937 (sp^2 C-H aromatic stretching), 1608 (C=N stretching), 1514 (C=C aromatic stretching), 1184 (C-O stretching). ^{1}H NMR (see **Table 3**).

2.3.2 (1*E*,2*E*)-1,2-bis(2,4,6-trimethoxybenzylidene)hydrazine (PJ2)

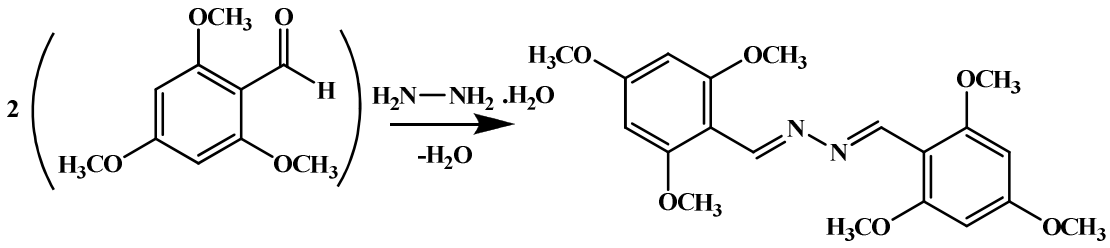

2,4,6-trimethoxy-benzaldehyde hydrazine hydrate (**PJ2**)

Compound **PJ2** was synthesized by condensation reaction, the solution of hydrazine hydrate (0.01 ml, 2 mmol) and 2,4,6-trimethoxybenzaldehyde (0.785 g, 4 mmol) in EtOH (20 ml). The resulting solution was refluxed for 5 hrs. The purity of the compounds was confirmed by thin-layer chromatography, yielding the yellow solid. The resultant solid was filtered off and washed with MeOH, dried in vacuum and purified by repeated recrystallization from CH_3COCH_3/EtOH to give a yellow crystal of compound **PJ2** (72% yield), mp. 211-213 °C, UV-Vis ($CHCl_3$) λ_{max} (nm) (ε x10^4): 205 (3.18), 342 (0.90). FT-IR (KBr) ν(cm^{-1}): 2937 (sp^2 C-H aromatic stretching), 1574 (C=N stretching), 1457 (C=C aromatic stretching), 1187 (C-O stretching). ^{1}H NMR (see **Table 7**).

2.3.3 *(1E,2E)*-1,2-bis(3,4,5-trimethoxybenzylidene)hydrazine (PJ3)

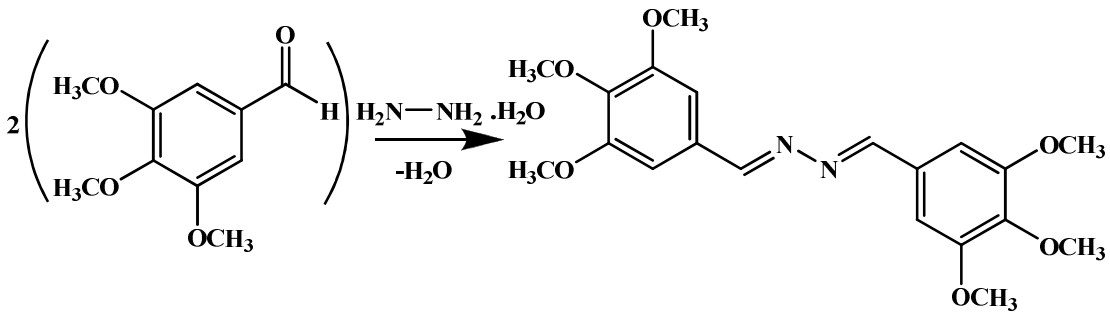

3,4,5-trimethoxy-benzaldehyde | hydrazine hydrate | (**PJ3**)

Compound **PJ3** was synthesized by condensation reaction, the solution of hydrazine hydrate (0.01 ml, 2 mmol) and 3,4,5-trimethoxybenzaldehyde (0.785 g, 4 mmol) in EtOH (20 ml). The resulting solution was refluxed for 4 hrs. The purity of the compounds was confirmed by thin-layer chromatography, yielding the pale yellow solid. The resultant solid was filtered off and washed with MeOH, dried in vacuum and purified by repeated recrystallization from CH_3COCH_3 of compound **PJ3** (73% yield), mp. 190-192 °C, UV-Vis ($CHCl_3$) λ_{max} (nm) (ε x10^4): 211 (5.40), 335 (3.80). FT-IR (KBr) ν(cm^{-1}): 2936 (sp^2 C-H aromatic stretching), 1616 (C=N stretching), 1581 (C=C aromatic stretching), 1182 (C-O stretching). ^{1}H NMR (see **Table 11**).

2.3.4 (1*E*,2*E*)-1,2-bis(3-hydroxy-4-nitrobenzylidene)hydrazine (PJ4)

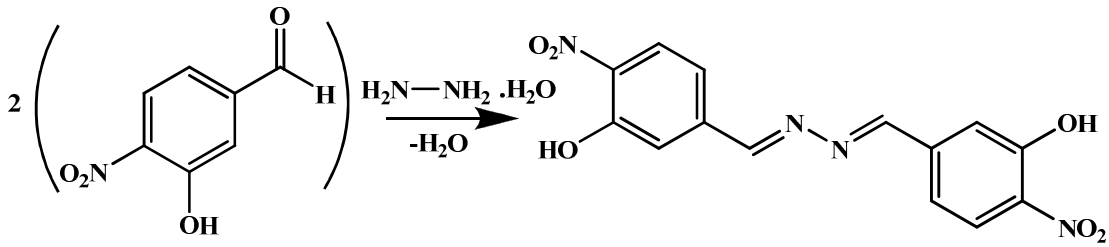

3-hydroxy-4-nitro-benzaldehyde hydrazine hydrate (**PJ4**)

Compound **PJ4** was synthesized by condensation reaction, the solution of hydrazine hydrate (0.01 ml, 2 mmol) and 3-hydroxy-4-nitrobenzaldehyde (0.67 g, 4 mmol) in EtOH (20 ml). The resulting solution was refluxed for 4 hrs. The purity of the compounds was confirmed by thin-layer chromatography, yielding the orange solid. The resultant solid was filtered off and washed with MeOH, dried in vacuum and purified by repeated recrystallization from CH_3COCH_3 to give a yellow crystal of compound **PJ4** (82% yield), mp. 156-158 °C, UV-Vis ($CHCl_3$) λ_{max} (nm) (ε x10^4): 227 (1.70), 371 (2.40). FT-IR (KBr) ν(cm^{-1}): 3406 (O-H stretching), 2994 (sp^2 C-H aromatic stretching), 1614 (C=N stretching), 1557 (N=O asymmetric stretching), 1327 (N=O symmetric stretching), 1259 (C-O stretching), 1152(C-N stretching). ^{1}H NMR (see **Table 12**).

2.3.5 *(1E,2E)*-1,2-bis(4-hydroxy-3-nitrobenzylidene)hydrazine (PJ5)

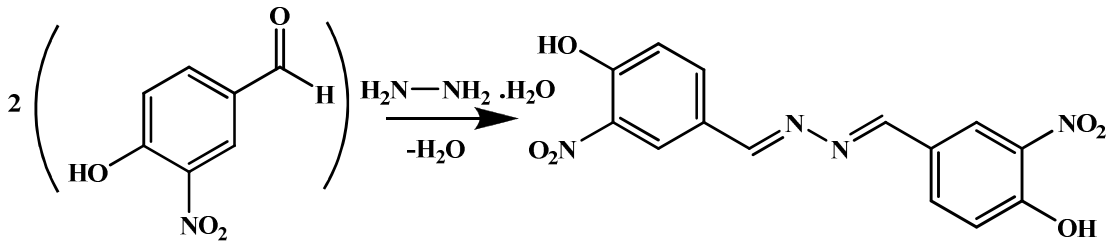

4-hydroxy-3-nitro-benzaldehyde hydrazine hydrate (**PJ5**)

Compound **PJ5** was synthesized by condensation reaction, the solution of hydrazine hydrate (0.01 ml, 2 mmol) and 4-hydroxy-3-nitrobenzaldehyde (0.67 g, 4 mmol) in EtOH (20 ml). The resulting solution was refluxed for 4 hrs. The purity of the compounds was confirmed by thin-layer chromatography, yielding the orange solid. The resultant solid was filtered off and washed with MeOH, dried in vacuum and purified by repeated recrystallization from CH_3COCH_3 of compound **PJ5** (81% yield), mp. 250 °C (decompose), UV-Vis ($CHCl_3$) λ_{max} (nm) (ε x10^4): 206 (2.40), 264 (0.60), 369 (0.92). FT-IR (KBr) ν(cm^{-1}): 3266 (O-H stretching), 3057 (sp^2 C-H aromatic stretching), 1610 (C=N stretching), 1507 (N=O asymmetric stretching), 1327 (N=O symmetric stretching), 1210 (C-O stretching), 1165 (C-N stretching). ^{1}H NMR (see **Table 13**).

2.3.6 (1*E*,2*E*)-1,2-bis(1-(2-methoxyphenyl)ethylidene)hydrazine (PJ6)

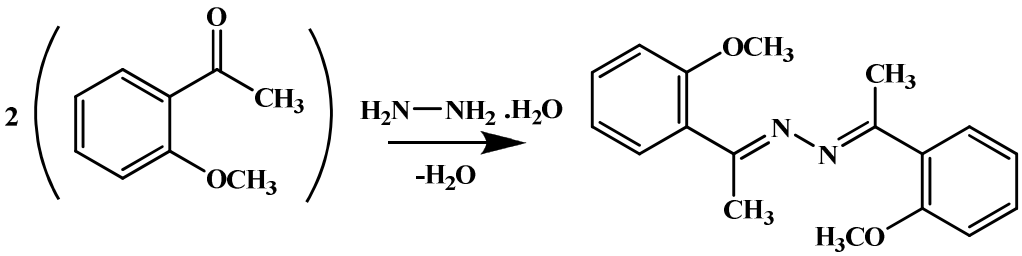

2-methoxy-acetophenone | hydrazine hydrate | (**PJ6**)

Compound **PJ6** was synthesized by condensation reaction, the solution of hydrazine hydrate (0.01 ml, 2 mmol) and 2-methoxyacetophenone (0.55 g, 4 mmol) in EtOH (20 ml). The resulting solution was refluxed for 5 hrs. The purity of the compounds was confirmed by thin-layer chromatography, yielding the pale brown solid. The resultant solid was filtered off and washed with MeOH, dried in vacuum and purified by repeated recrystallization from CH_3COCH_3/EtOH to give a pale yellow crystal of compound **PJ6** (79% yield), mp. >300 °C, UV-Vis ($CHCl_3$) λ_{max} (nm) (ε x10^4): 248 (1.28), 287 (0.76). FT-IR (KBr) ν(cm^{-1}): 3069 (sp^2 C-H aromatic stretching), 2967 (C-H stretching), 1602 (C=N stretching), 1492 (C=C aromatic stretching), 1240 (C-O stretching). ^{1}H NMR (see **Table 14**).

2.3.7 (1*E*,2*E*)-1,2-bis(1-(2-aminophenyl)ethylidene)hydrazine (PJ7)

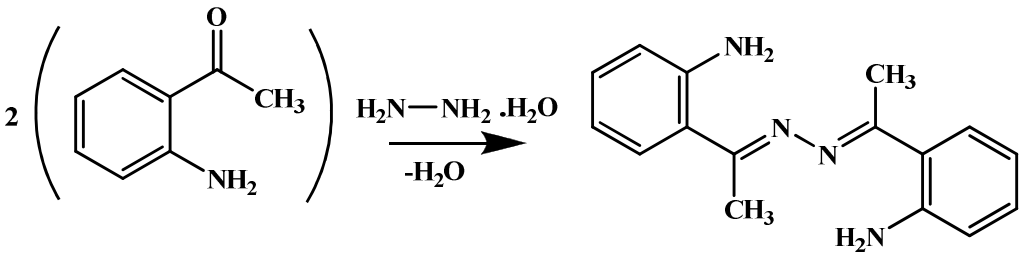

2-amino-acetophenone | hydrazine hydrate | (**PJ7**)

Compound **PJ7** was synthesized by condensation reaction, the solution of hydrazine hydrate (0.01 ml, 2 mmol) and 2-aminoacetophenone (0.49 g, 4 mmol) in EtOH (20 ml). The resulting solution was refluxed for 3 hrs. The purity of the compounds was confirmed by thin-layer chromatography, yielding the yellow solution and purified by repeated recrystallization from CH_3COCH_3 to give a yellow crystal of compound **PJ7** (84% yield), mp. 179-180 °C, UV-Vis ($CHCl_3$) λ_{max} (nm) (ε x10^4): 238 (1.28), 379 (0.30). FT-IR (KBr) ν(cm^{-1}): 3348 (N-H stretching), 3187 (sp^2 C-H aromatic stretching), 2961 (C-H stretching), 1609 (C=N stretching), 1546 (C=C aromatic stretching), 1293 (C-N stretching). ^{1}H NMR (see **Table 18**).

2.3.8 (1*E*,2*E*)-1,2-bis(1-(2-nitrophenyl)ethylidene)hydrazine (PJ8)

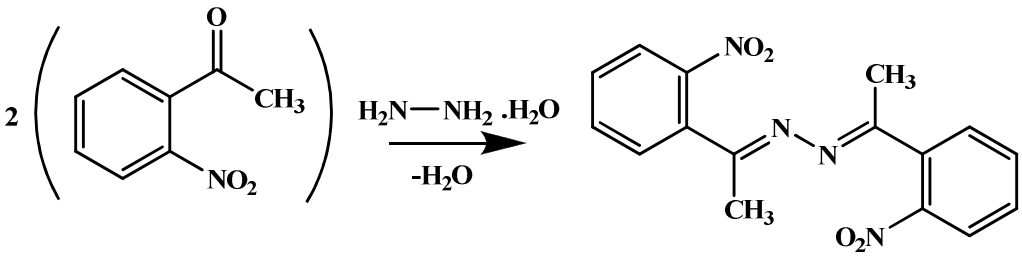

2-nitro-acetophenone | hydrazine hydrate | (**PJ8**)

Compound **PJ8** was synthesized by condensation reaction, the solution of hydrazine hydrate (0.01 ml, 2 mmol) and 2-nitroacetophenone (0.53 ml, 4 mmol) in EtOH (20 ml). The resulting solution was refluxed for 3 hrs. The purity of the compounds was confirmed by thin-layer chromatography, yielding the yellow solid. The resultant solid was filtered off and washed with MeOH, dried in vacuum and purified by repeated recrystallization from CH_3COCH_3 to give a yellow crystal of compound **PJ8** (78% yield), mp. 171-173 °C, UV-Vis ($CHCl_3$) λ_{max} (nm) (ε x10^4): 235 (0.50). FT-IR (KBr) ν(cm^{-1}): 3063 (sp^2 C-H aromatic stretching), 2861 (C-H stretching), 1623 (C=N stretching), 1545 (N=O asymmetric stretching), 1358 (N=O symmetric stretching). ^{1}H NMR (see **Table 19**).

2.3.9 (1*E*,2*E*)-1,2-bis(1-(2-chlorophenyl)ethylidene)hydrazine (PJ9)

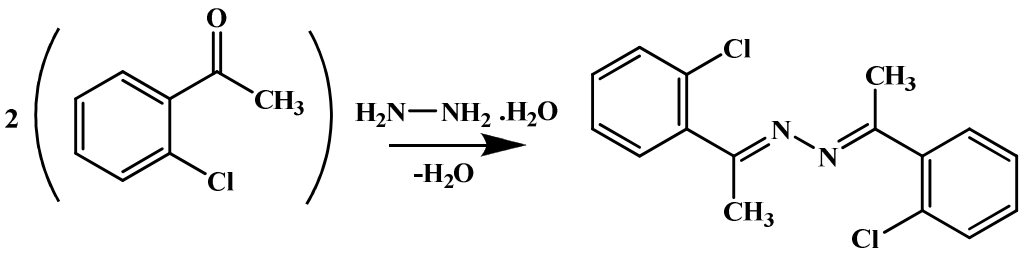

2-chloro-acetophenone | hydrazine hydrate | (**PJ9**)

Compound **PJ9** was synthesized by condensation reaction, the solution of hydrazine hydrate (0.01 ml, 2 mmol) and 2-chloroacetophenone (0.52 ml, 4 mmol) in EtOH (20 ml). The resulting solution was refluxed for 5 hrs. The purity of the compounds was confirmed by thin-layer chromatography, yielding the yellow solution and purified by repeated recrystallization from CH_3COCH_3 to give a yellow crystal of compound **PJ9** (67% yield), mp. 92-93 °C, UV-Vis ($CHCl_3$) λ_{max} (nm) (ε x10^4): 242 (3.20). FT-IR (KBr) ν(cm^{-1}): 3045 (sp^2 C-H aromatic stretching), 2995 (C-H stretching), 1612 (C=N stretching), 1431 (C=C aromatic stretching), 737 (C-Cl stretching). ^{1}H NMR (see **Table 20**).

2.3.10 (1*E*,2*E*)-1,2-bis(1-(2-bromophenyl)ethylidene)hydrazine (PJ10)

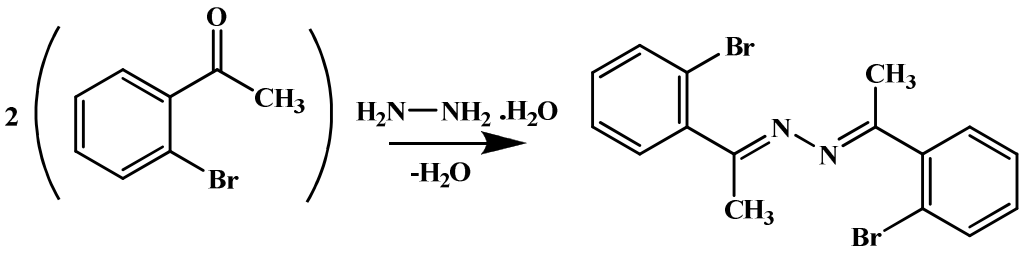

2-bromo-acetophenone | hydrazine hydrate | (**PJ10**)

Compound **PJ10** was synthesized by condensation reaction, the solution of hydrazine hydrate (0.01 ml, 2 mmol) and 2-bromoacetophenone (0.54 ml, 4 mmol) in EtOH (20 ml). The resulting solution was refluxed for 5 hrs. The purity of the compounds was confirmed by thin-layer chromatography, yielding the white solid. The resultant solid was filtered off and washed with MeOH, dried in vacuum and purified by repeated recrystallization from CH_3COCH_3 to give a colorless crystal of compound **PJ10** (89% yield), mp. 114-116 °C, UV-Vis ($CHCl_3$) λ_{max} (nm) (ε x10^4): 207 (6.00). FT-IR (KBr) ν(cm^{-1}): 3058 (sp^2 C-H aromatic stretching), 2994 (C-H stretching), 1615 (C=N stretching), 1559 (C=C aromatic stretching), 575 (C-Br stretching). ^{1}H NMR (see **Table 21**).

2.3.11 (1*E*,2*E*)-1,2-bis(1-(4-hydroxyphenyl)ethylidene)hydrazine (PJ11)

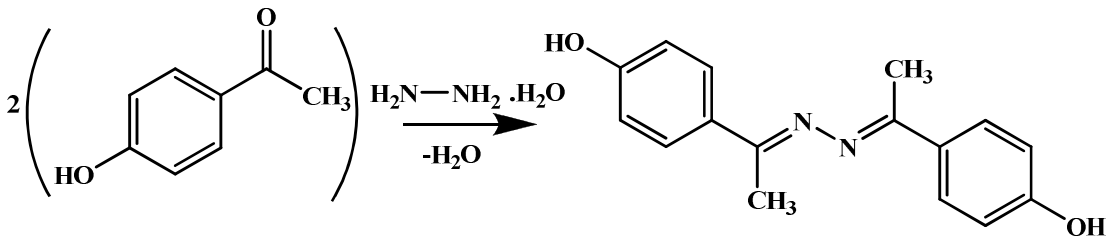

4-hydroxy-acetophenone | hydrazine hydrate | (**PJ11**)

Compound **PJ11** was synthesized by condensation reaction, the solution of hydrazine hydrate (0.01 ml, 2 mmol) and 4-hydroxyacetophenone (0.54 ml, 4 mmol) in EtOH (20 ml). The resulting solution was refluxed for 5 hrs. The purity of the compounds was confirmed by thin-layer chromatography, yielding the brown solid. The resultant solid was filtered off and washed with MeOH, dried in vacuum and purified by repeated recrystallization from CH_3COCH_3 to give a brown crystal of compound **PJ11** (82% yield), mp. 210-212 °C, UV-Vis ($CHCl_3$) λ_{max} (nm) (ε x10^4): 223 (2.60), 306 (4.00). FT-IR (KBr) ν(cm^{-1}): 2900-3400 (O-H stretching), (*sp*^{2} C-H aromatic stretching), (C-H stretching), 1666 (C=N stretching), 1595 (C=C aromatic stretching), 1225 (C-O stretching). ^{1}H NMR (see **Table 25**).

2.3.12 (1*E*,2*E*)-1,2-bis(1-(3-methoxyphenyl)ethylidene)hydrazine (PJ12)

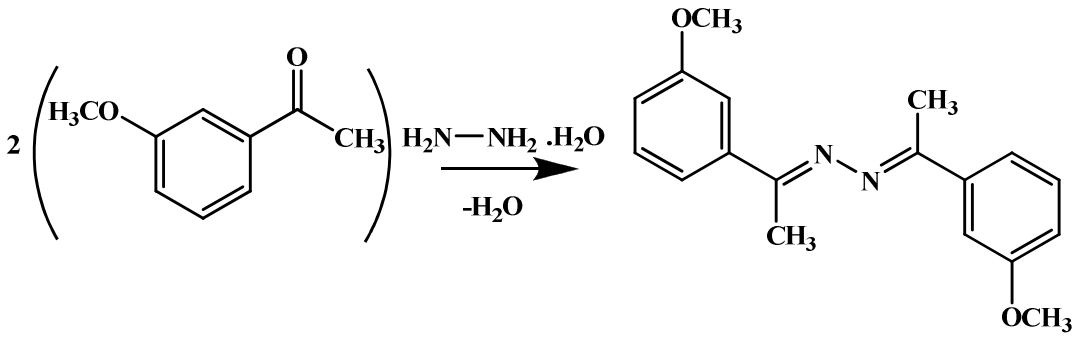

3-methoxy-acetophenone | hydrazine hydrate | (**PJ12**)

Compound **PJ12** was synthesized by condensation reaction, the solution of hydrazine hydrate (0.01 ml, 2 mmol) and 3-methoxyacetophenone (0.55 ml, 4 mmol) in EtOH (20 ml). The resulting solution was refluxed for 5 hrs. The purity of the compounds was confirmed by thin-layer chromatography, yielding the yellow solid. The resultant solid was filtered off and washed with MeOH, dried in vacuum and purified by repeated recrystallization from CH_3COCH_3 to give a yellow crystal of compound **PJ12** (81% yield), mp. 95-97 °C, UV-Vis ($CHCl_3$) λ_{max} (nm) (ε x10^4): 222 (2.40), 267 (2.50). FT-IR (KBr) ν(cm^{-1}): 3104 (sp^2 C-H aromatic stretching), 2954 (C-H stretching), 1605 (C=N stretching), 1575 (C=C aromatic stretching), 1218 (C-O stretching). ^{1}H NMR (see **Table 29**).

2.3.13 (1*E*,2*E*)-1,2-bis(1-(3-aminophenyl)ethylidene)hydrazine (PJ13)

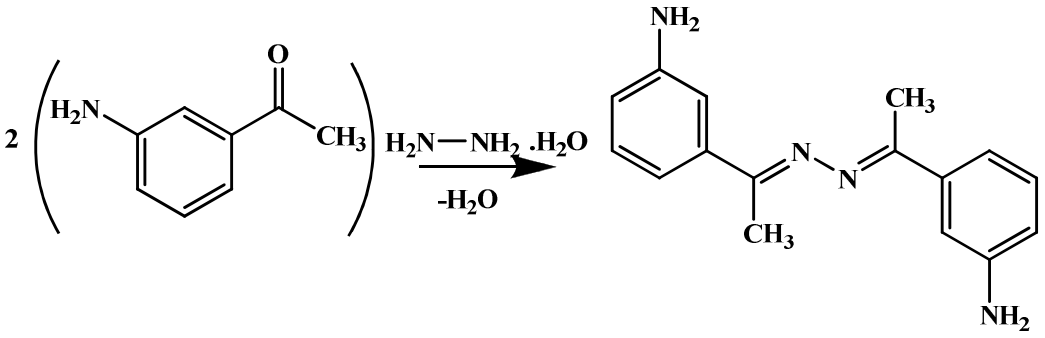

3-amino-acetophenone hydrazine hydrate (**PJ13**)

Compound **PJ13** was synthesized by condensation reaction, the solution of hydrazine hydrate (0.01 ml, 2 mmol) and 3-aminoacetophenone (0.49 ml, 4 mmol) in EtOH (20 ml). The resulting solution was refluxed for 4 hrs. The purity of the compounds was confirmed by thin-layer chromatography, yielding the yellow solution and purified by repeated recrystallization from CH_3COCH_3 to give a yellow crystal of compound **PJ13** (87% yield), mp. 142-143 °C, UV-Vis ($CHCl_3$) λ_{max} (nm) (ε x10^4): 240 (1.50). FT-IR (KBr) ν(cm^{-1}): 3494 (N-H stretching), 3041 (sp^2 C-H aromatic stretching), 2894 (C-H stretching), 1608 (C=N stretching), 1522 (C=C aromatic stretching), 1239 (C-N stretching). ^{1}H NMR (see **Table 30**).

2.3.14 (1*E*,2*E*)-1,2-bis(1-(3-nitrophenyl)ethylidene)hydrazine (PJ14)

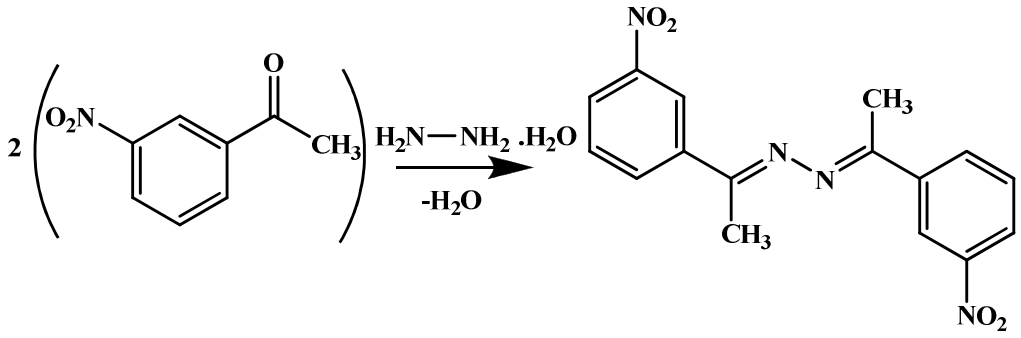

3-nitro-acetophenone | hydrazine hydrate | (**PJ14**)

Compound **PJ14** was synthesized by condensation reaction, the solution of hydrazine hydrate (0.01 ml, 2 mmol) and 3-nitroacetophenone (0.66g, 4 mmol) in EtOH (20 ml). The resulting solution was refluxed for 4 hrs. The purity of the compounds was confirmed by thin-layer chromatography, yielding the yellow solution and purified by repeated recrystallization from CH_3COCH_3 to give a yellow crystal of compound **PJ14** (85% yield), mp. 196-198 °C, UV-Vis ($CHCl_3$) λ_{max} (nm) (ε x10^4): 203 (3.70), 263 (2.00). FT-IR (KBr) ν(cm^{-1}): 2900-2960 (sp^2 C-H aromatic stretching), (C-H stretching), 1611 (C=N stretching), 1530 (N=O asymmetric stretching), 1347 (N=O symmetric stretching), 1268 (C-N stretching). ^{1}H NMR (see **Table 31**).

2.3.15 (1*E*,2*E*)-1,2-bis(1-(3-chlorophenyl)ethylidene)hydrazine (PJ15)

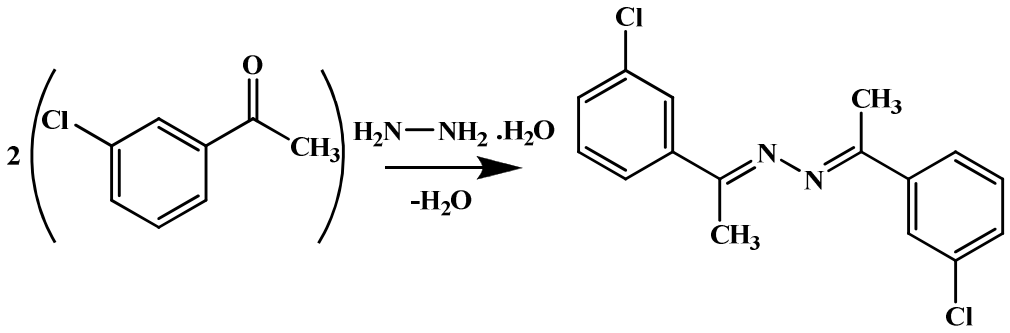

3-chloro-acetophenone | hydrazine hydrate | (**PJ15**)

Compound **PJ15** was synthesized by condensation reaction, the solution of hydrazine hydrate (0.01 ml, 2 mmol) and 3-chloroacetophenone (0.52 ml, 4 mmol) in EtOH (20 ml). The resulting solution was refluxed for 6 hrs. The purity of the compounds was confirmed by thin-layer chromatography, yielding the colorless solution and purified by repeated recrystallization from CH_3COCH_3 to give a yellow crystal of compound **PJ15** (84% yield), mp. 83-85 °C, UV-Vis ($CHCl_3$) λ_{max} (nm) (ε x10^4): 204 (6.00), 269 (2.60). FT-IR (KBr) ν(cm^{-1}): 2900-3000 (sp^2 C-H aromatic stretching), (C-H stretching), 1591 (C=N stretching), 1556 (C=C aromatic stretching), 1105 (C-N stretching), 795 (C-Cl stretching. ^{1}H NMR (see **Table 35**).

2.3.16 (1*E*,2*E*)-1,2-bis(1-(3-bromophenyl)ethylidene)hydrazine (PJ16)

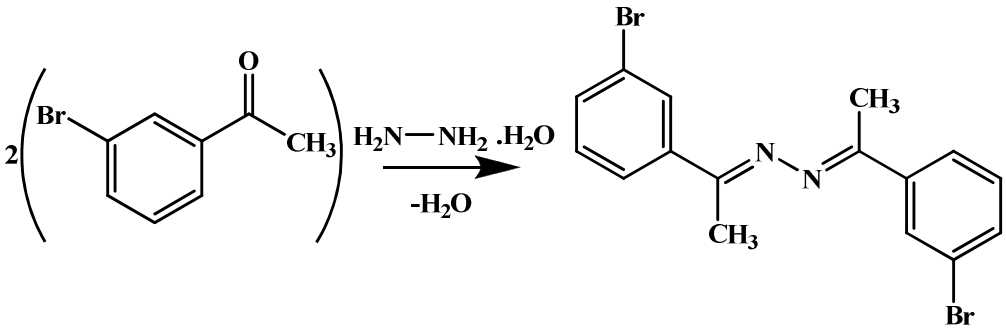

3-bromo-acetophenone | hydrazine hydrate | (**PJ16**)

Compound **PJ16** was synthesized by condensation reaction, the solution of hydrazine hydrate (0.01 ml, 2 mmol) and 3-bromoacetophenone (0.54 ml, 4 mmol) in EtOH (20 ml). The resulting solution was refluxed for 5 hrs. The purity of the compounds was confirmed by thin-layer chromatography, yielding the colorless solution and purified by repeated recrystallization from CH_3COCH_3 of compound **PJ16** (79% yield), mp. 85-86 °C, UV-Vis ($CHCl_3$) λ_{max} (nm) (ε x10^4): 209 (4.60), 269 (2.50). FT-IR (KBr) ν(cm^{-1}): 2997 (sp^2 C-H aromatic stretching), 2938 (C-H stretching), 1601 (C=N stretching), 1551 (C=C aromatic stretching), 641 (C-Br stretching). ^{1}H NMR (see **Table 39**).

2.3.17 (1*E*,2*E*)-1,2-bis(1-(3-fluorophenyl)ethylidene)hydrazine (PJ17)

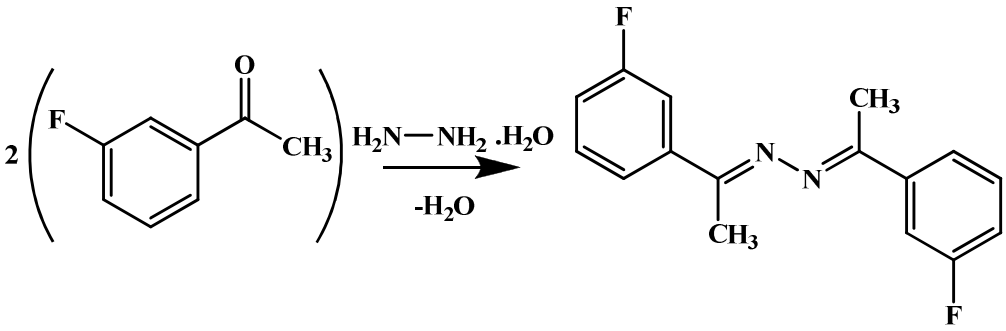

3-fluoro-acetophenone | hydrazine hydrate | (**PJ17**)

Compound **PJ17** was synthesized by condensation reaction, the solution of hydrazine hydrate (0.01 ml, 2 mmol) and 3-fluoroacetophenone (0.485 ml, 4 mmol) in EtOH (20 ml). The resulting solution was refluxed for 5 hrs. The purity of the compounds was confirmed by thin-layer chromatography, yielding the yellow solution and purified by repeated recrystallization from CH_3COCH_3 to give a yellow crystal of compound **PJ17** (80% yield), mp. 72-73 °C, UV-Vis ($CHCl_3$) λ_{max} (nm) (ε x10^4): 267 (2.38). FT-IR (KBr) ν(cm^{-1}): 3089 (sp^2 C-H aromatic stretching), 2962 (C-H stretching), 1691 (C=N stretching), 1578 (C=C aromatic stretching), 1267 (C-F stretching). ^{1}H NMR (see **Table 40**).

2.4 Absorption, excitation and emission spectral properties

2.4.1 UV-Vis spectral of hydrazone derivatives

The UV-Vis absorption spectral data of all hydrazone derivatives were collected in the range of 200-800 nm at room temperature. The concentrations of all compounds were prepared at 5 μM in $CHCl_3$.

2.4.2 Excitation and emission spectral of hydrazone derivatives

The fluorescence spectrum of all hydrazone derivatives were recorded in $CHCl_3$ at room temperature. The concentrations of all compounds were prepared at 5 μM in $CHCl_3$. For comparison of their emission, the excitation wavelength was fixed at 300 nm which is value in the range of maxima excitation wavelength of the seventeen (**PJ1**-**PJ17**) synthesized compounds. Their excitation spectra were also studied by fixing the emission wavelength at 420 nm.

2.5 Metal sensor

2.5.1 Scanning for metal sensor property of PJ1-PJ17 against various M^{2+} ions

The synthetic hydrazone derivatives (**PJ1**-**PJ17**) were scanned for metal chemosensor property with ten different chloride salts of metal ions which are Mg^{2+}, Ca^{2+}, Mn^{2+}, Fe^{2+}, Co^{2+}, Ni^{2+}, Cu^{2+}, Zn^{2+}, Hg^{2+} and Cd^{2+}, by observing the changing in color by naked-eyes. The stock solutions of **PJ1-PJ17** in the concentration of 1 mM were prepared in CH_3CN. The stock solution of each metal ion was prepared in the concentration of 10 mM in the mixed solvents of MeOH:H_2O (1:1 v/v). The method is as followings:

(1) A solution of each hydrazone derivatives (**PJ1-PJ17**) were contained into ten tubes (2.0 ml for each).

(2) 10 μl of ten different metal-chloride-salts stock solutions were then added to each tube.

(3) The color changed of solutions were observed by naked eyes.

2.5.2 Cu(I) and Cu(II) selective chemosensor property

From the scanning results for metal sensor property of **PJ1-PJ17** for ten chloride salts of M^{2+} ions (Experiment **2.5.1**), it was found that only **PJ7** with $CuCl_2$ solution was changed in color from yellow (370 nm) to yellow-brown (430 nm). So **PJ7** was then further investigated for Cu(I) and Cu(II) sensor.

The stock solutions (1 mM) of the different salts; CuBr, CuCl, CuI, $Cu(OAc)_2$, $CuCl_2$, $Cu(NO_3)_2$ and $CuSO_4$, in MeOH:H_2O (1:1 v/v) and **PJ7** solution (0.1 mM) in CH_3CN were prepared. Test solutions were prepared by placing 2.0 ml of **PJ7** solution in each of seven test tubes and then adding of each stock metal salts (10 μl). This experiment is carried out in order to see the effect caused by the counter ion, which are Cl^-, Br^- and so on, on the selective colorimetric chemosensor property for copper ions (Cu^+ or Cu^{2+}). To analyze the property, the absorbance of each solution was measured by UV-Vis spectrometer. The controlled sample for this test is the metal-free-derivative **PJ7**. Although the fluorescence emission intensity of **PJ7** in $CHCl_3$ is highest comparing to other solvents (**Scheme 13**), however $CHCl_3$ can not dissolve in mixed solvent (MeOH:H_2O) therefore the CH_3CN was chosen as a solvent for all chemosensor study. The fluorescence emission intensity of **PJ7** in various solvents as shown in **Scheme 13**.

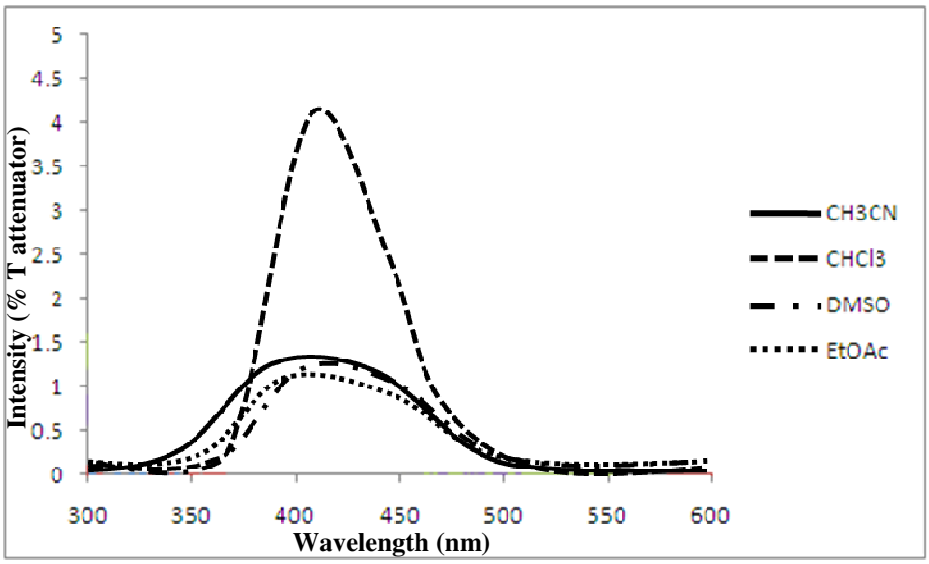

Scheme 13. Fluorescence emission spectra of **PJ7** in various solvent at room temperature in %T attenuator mode and slit 10:10.

2.5.3 Copper selective fluorescent sensor property

According to the previous Experiments (**2.5.2**), only $Cu(NO_3)_2$ and $CuCl_2$ exhibit a distinctive effect on the absorption wavelength (λ_{max}), compared to the metal-free **PJ7** (controlled sample). These copper containing **PJ7**'s are therefore studied for the fluorescent property. The emission spectra are recorded by the Perkin-Elmer LS 55 Luminescent spectrometer, mentioned earlier.

2.5.3 Detection limit of Cu^{2+}

The Cu^{2+}-**PJ7** mixture is tested for the detection limit. The varied concentrations of $CuCl_2$ and $Cu(NO_3)_2$ dropped in **PJ7** solution are 0.007, 0.008, 0.010, 0.050 and 0.10 mM. This is to find out the minimum trace of $CuCl_2$ and $Cu(NO_3)_2$ which can be detected.

CHAPTER 3
RESULTS AND DISCUSSION

3.1 Structural elucidations of hydrazones

3.1.1 (1*E*,2*E*)-1,2-bis(2,4,5-trimethoxybenzylidene)hydrazine (PJ1)

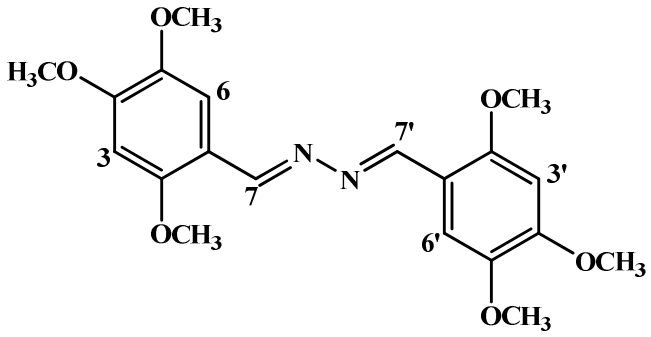

(PJ1)

Compound **PJ1** was obtained as a yellow solid (76% yield), mp. 250 °C (decompose). The UV-Vis absorption bands **(Figure 49)** were shown at 270 and 379 nm. The FT-IR spectrum of **PJ1** (**Figure 48**) revealed the stretching vibration of aromatic C-H at 2937 cm^{-1}. The strong peak of C=N stretching vibration was observed at 1608 cm^{-1} and C=C stretching vibration in aromatic ring at 1514 cm^{-1}. The C-O stretching vibration was observed at 1184 cm^{-1}.

The ^{1}H NMR spectrum of **PJ1** (**Figure 50**, see **Table 3**) showed *singlet* signals of protons H-2, H-2', H-4, H-4'and H-5, H-5'(-OCH_3) appeared at δ 3.88, δ 3.94 and δ 3.95 (18H). Two aromatic protons H-3, H-3'and H-6, H-6' showed the signals at δ 6.52 (2H) and δ 7.64 (2H) and *singlet* signals of protons H-7, H-7'appeared at δ 9.01 (2H). These spectroscopic data confirmed that **PJ1** is (1*E*,2*E*)-1,2-bis(2,4,5-trimethoxybenzylidene)hydrazine.

Table 3 ^{1}H NMR of compound **PJ1**

Position	**δ_H (ppm), *mult, J* (Hz)**
2, 2'& 4, 4'& 5,5' (-OCH_3)	3.88, 3.94, 3.95, *s*
3, 3'	6.52, *s*
6, 6'	7.64, *s*
7, 7'	9.01, *s*

The crystal structure and packing of **PJ1** are illustrated in **Figures 7** and **8**. The crystal and experiment data are given in **Table 4**. Bond lengths, angles and torsion angles are shown in **Table 5**. Hydrogen-bond geometry is shown in **Table 6**. The X-ray study shows that the **PJ1** crystallized out in monoclinic $P2_1/c$ space group.

The asymmetric unit of **PJ1** (**Figure 7**), contains one half-molecule and the complete molecule is generated by a crystallographic inversion centre -*x*, -*y*, 1 -*z*. The molecule of **PJ1** exists in an *E*, *E* configuration with respect to the two C═N double bonds [1.2870 (12) Å] and the torsion angle N1A–N1–C7–C1 = -178.99 (9)°. The molecule is nearly planar with the dihedral angle between the two benzene rings being 0.03 (4)°. Atoms C7/N1/N1A/C7A lie on a same plane [r.m.s 0.000 (1) Å]. This C/N/N/C plane makes a dihedral angle of 8.59 (7)° with each of its two adjacent benzene rings.

The three methoxy groups of the 2,4,5-trimethoxyphenyl unit have two different orientations: two methoxy groups at the ortho and meta positions (at atom C2 and C5 positions) are slightly twisted with the attached benzene ring with torsion angles C8–O1–C2–C3 = 7.23 (12)° and C10–O3–C5–C6 = 5.73 (13)° whereas the third one at para position (at atom C4) is co-planarly attached with the torsion angle C9–O2–C4–C3 = -2.02 (13)°.

In the crystal structure (**Figure 8**), the molecules are arranged into screw chains along the *c* axis and these chains stacked along the *a* direction. The molecules are consolidated by C—H···π (**Table 6**) and π–π interactions with the Cg1···Cg1 distances of 4.6314 (5) Å (symmetry code:-*x*, 1 - *y*, 1 - *z*) and 4.9695 (5) Å (symmetry code: 1 - *x*, 1 - *y*, 1 - *z*). Cg1 is the centriod of the C1-C6 ring. C···C [3.3411 (12)–3.3987 (12) Å] short contacts were observed.

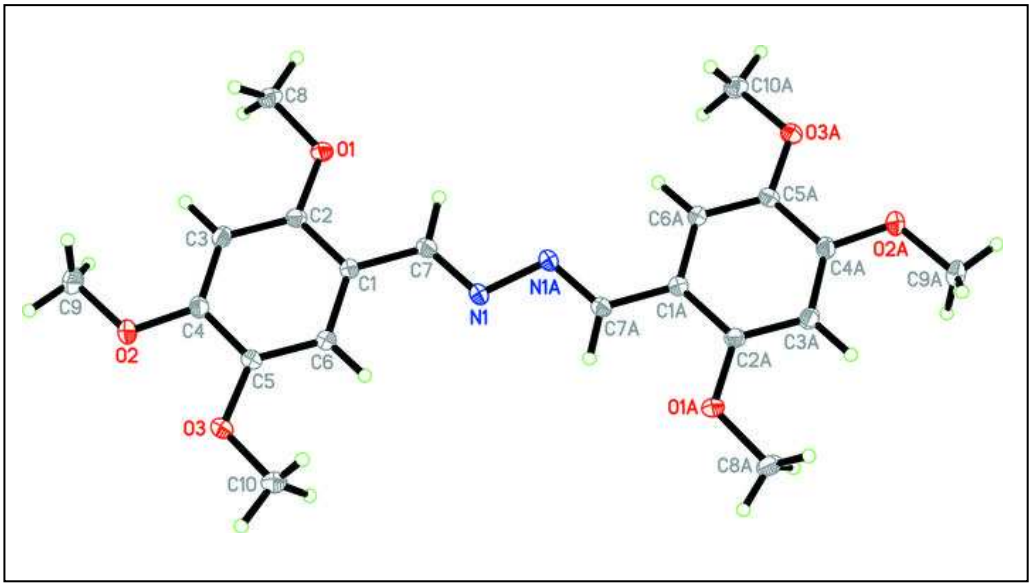

Figure 7 X-ray ORTEP diagram of the compound **PJ1**

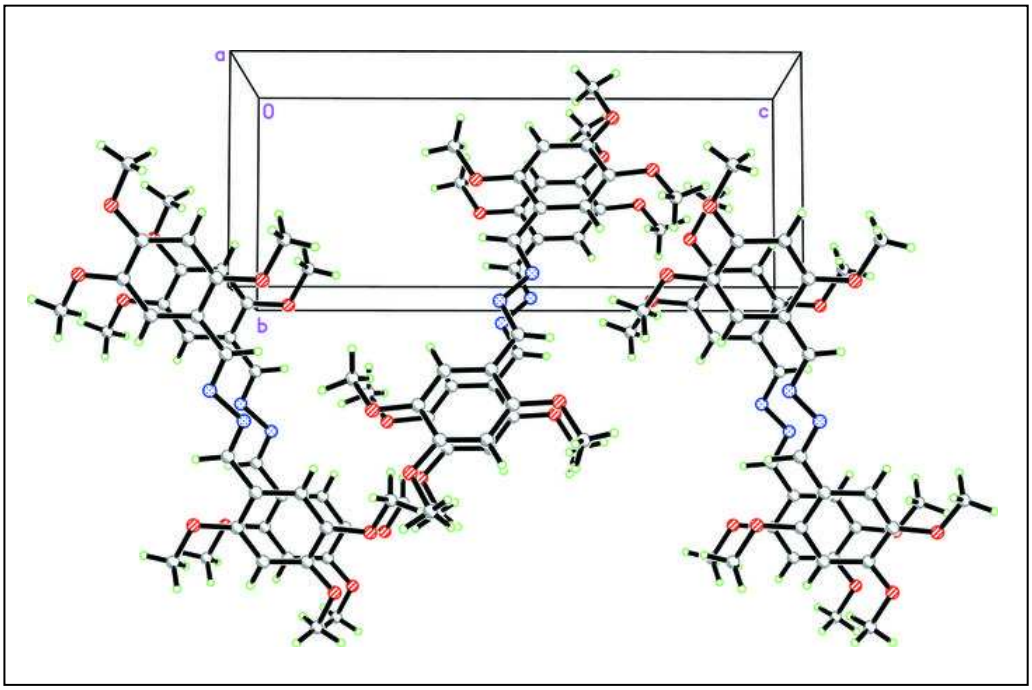

Figure 8 Packing diagram of **PJ1** viewed down the *a* axis.

Table 4 Crystal data and structure refinement for **PJ1**

.

Identification code	**PJ1**
Empirical formula	$C_{20}H_{24}N_2O_6$
Formula weight	388.41
Temperature	100.0(1) K
Wavelength	0.71073 Å
Crystal system, space group	Monoclinic, $P2_1/c$
Unit cell dimensions	a = 7.5056 (1) Å α = (90) ^{o} b = 7.2523 (1) Å β = 90.600 (1) ^{o} c = 17.4489 (2) Å γ = (90) ^{o}
Volume	949.74 (2) $Å^3$
Z, Calculated density	2, 1.358 Mg/m^3
Absorption coefficient	0.10 mm^{-1}
F(000)	412
Crystal size	0.47 × 0.29 × 0.10 mm
Theta range for data collection	2.3–30.0 °
Limiting indices	-10<=h<=10, -10<=k<=10, -24<=l<=24
Reflections collected / unique	18099/ 2778 [R(int) = 0.028]
Max. and min. transmission	0.990 and 0.954
Refinement method	Full-matrix least-squares on F^2
Data / restraints / parameters	2778 / 0 / 175
Final R indices [I>2σ(I)]	R1 = 0.038, wR2 = 0.113
Largest diff. peak and hole	0.45, −0.22 $e.A^{-3}$

Table 5 Bond lengths [Å], angles [°] and torsion angles [°] for **PJ1**

O1—C2	1.3664 (10)	C4—C5	1.4112 (12)
O1—C8	1.4301 (11)	C5—C6	1.3789 (12)
O2—C4	1.3624 (11)	C6—H6	0.970 (14)
O2—C9	1.4279 (12)	C7—H7	0.964 (13)
O3—C5	1.3681 (10)	C8—H8A	0.924 (13)
O3—C10	1.4257 (12)	C8—H8B	0.991 (14)
N1—C7	1.2870 (12)	C8—H8C	0.974 (13)
N1—N1^{i}	1.4103 (15)	C9—H9A	0.966 (15)
C1—C2	1.4031 (12)	C9—H9B	0.981 (14)
C1—C6	1.4102 (12)	C9—H9C	0.944 (14)
C1—C7	1.4544 (12)	C10—H10A	0.995 (12)
C2—C3	1.3987 (12)	C10—H10B	0.967 (16)
C3—C4	1.3906 (12)	C10—H10C	0.976 (15)
C3—H3	0.988 (13)		
C2—O1—C8	117.62 (7)	N1—C7—C1	122.08 (8)
C4—O2—C9	117.39 (7)	N1—C7—H7	119.0 (8)
C5—O3—C10	116.12 (7)	C1—C7—H7	118.9 (8)
C7—N1—N1^{i}	111.49 (9)	O1—C8—H8A	104.9 (8)
C2—C1—C6	118.95 (8)	O1—C8—H8B	111.1 (8)
C2—C1—C7	119.62 (8)	H8A—C8—H8B	110.6 (11)
C6—C1—C7	121.39 (8)	O1—C8—H8C	109.5 (8)
O1—C2—C3	123.51 (8)	H8A—C8—H8C	111.4 (11)
O1—C2—C1	116.21 (8)	H8B—C8—H8C	109.4 (11)
C3—C2—C1	120.28 (8)	O2—C9—H9A	108.9 (9)
C4—C3—C2	119.81 (8)	O2—C9—H9B	110.1 (9)
C4—C3—H3	119.7 (7)	H9A—C9—H9B	111.1 (12)
C2—C3—H3	120.5 (7)	O2—C9—H9C	101.2 (9)
O2—C4—C3	124.41 (8)	H9A—C9—H9C	112.6 (12)
O2—C4—C5	115.05 (8)	H9B—C9—H9C	112.4 (12)

Table 5 Bond lengths [Å], angles [°] and torsion angles [°] for **PJ1** (continued)

C3—C4—C5	120.54 (8)	O3—C10—H10A	108.7 (7)
O3—C5—C6	125.38 (8)	O3—C10—H10B	109.8 (9)
O3—C5—C4	115.40 (8)	H10A—C10—H10B	110.4 (12)
C6—C5—C4	119.22 (8)	O3—C10—H10C	104.5 (9)
C5—C6—C1	121.15 (8)	H10A—C10—H10C	110.3 (11)
C5—C6—H6	121.1 (8)	H10B—C10—H10C	112.8 (12)
C1—C6—H6	117.8 (8)	C8—O1—C2—C3	7.23 (12)
C10—O3—C5—C4	−173.90 (8)		
C8—O1—C2—C1	−173.26 (8)	O2—C4—C5—O3	−2.95 (12)
C6—C1—C2—O1	178.64 (7)	C3—C4—C5—O3	177.39 (8)
C7—C1—C2—O1	0.86 (12)	O2—C4—C5—C6	177.39 (8)
C6—C1—C2—C3	−1.84 (13)	C3—C4—C5—C6	−2.26 (13)
C7—C1—C2—C3	−179.61 (8)	O3—C5—C6—C1	−177.86 (8)
O1—C2—C3—C4	−179.16 (8)	C4—C5—C6—C1	1.76 (13)
C1—C2—C3—C4	1.34 (13)	C2—C1—C6—C5	0.27 (13)
C9—O2—C4—C3	−2.02 (13)	C7—C1—C6—C5	178.00 (8)
C9—O2—C4—C5	178.34 (8)	$N1^{i}$—N1—C7—C1	−178.99 (9)
C2—C3—C4—O2	−178.90 (8)	C2—C1—C7—N1	−173.65 (8)
C2—C3—C4—C5	0.72 (13)	C6—C1—C7—N1	8.63 (13)
C10—O3—C5—C6	5.73 (13)		

Symmetry code: (i) −*x*, −*y*, −*z*+1.

Table 6 Hydrogen-bond for **PJ1** (Å,°)

Cg1 is the centriod of the C1-C6 ring.

D—H···*A*	**D—H**	**H···*A***	**D···*A***	**D—H···*A***
C8—H8C···$Cg1^{ii}$	0.974 (13)	2.675 (14)	3.4837 (10)	140.7 (10)

Symmetry code: (ii) −*x*+1, −*y*+1, −*z*+1.

3.1.2 *(1E,2E)*-1,2-bis(2,4,6-trimethoxybenzylidene)hydrazine (PJ2)

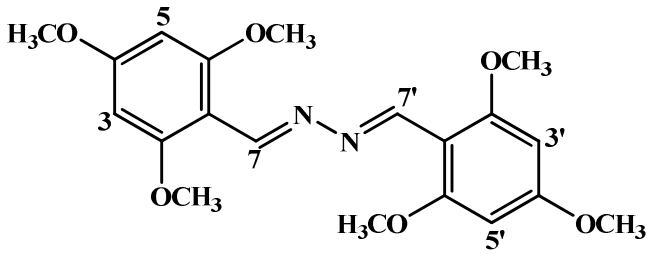

(PJ2)

Compound **PJ2** was obtained as a yellow solid (72% yield), mp. 211-213 °C. The UV-Vis absorption bands **(Figure 52)** were shown at 205 and 342 nm. The FT-IR spectrum of **PJ2** (**Figure 51**) revealed the stretching vibration of aromatic C-H at 2937 cm^{-1}. The strong peak of C=N stretching vibration was observed at 1547 cm^{-1} and C=C stretching vibration in aromatic ring at 1457 cm^{-1}. The C-O stretching vibration was observed at 1187 cm^{-1}.

The ^{1}H NMR spectrum of **PJ2** (**Figure 53**, see **Table 7**) showed *singlet* signals of protons H-2, H-2'(-OCH_3), H-4, H-4'and H-6, H-6'(-OCH_3) showed the signals at δ 3.88 and δ 3.86 (18H). Two equivalent aromatic protons H-3, H-3'and H-5, H-5' appeared at δ 6.15 (4H) and *singlet* signals of protons H-7, H-7'appeared at δ 9.10 (2H). These spectroscopic data confirmed that **PJ2** is (1*E*,2*E*)-1,2-bis(2,4,6-trimethoxy benzylidene)hydrazine.

Table 7 ^{1}H NMR of compound **PJ2**

Position	δ_H **(ppm),** ***mult, J*** **(Hz)**
2, 2'& 4, 4'& 6, 6' (-OCH_3)	3.86, 3.88, *s*
3, 3'	6.15, *s*
5, 5'	6.15, *s*
7, 7'	9.10, *s*

The crystal structure and packing of **PJ2** are illustrated in **Figures 9** and **10**. The crystal and experiment data are given in **Table 8**. Bond lengths, angles and torsion angles are shown in **Table 9**. Hydrogen-bond geometry is shown in **Table 10**. The X-ray study shows that the **PJ2** crystallized out in triclinic $\bar{P}1$ space group.

The asymmetric unit of **PJ2** (**Figure 9**), contains one half-molecule and the complete molecule is generated by an inversion centre (symmetry code -*x*, 2-*y*, 1-*z*). The mean plane through the C=N-N=C bridge forms a dihedral angle of 4.96 (9)° with the benzene rings. The methoxy groups attached to atoms C1 and C5 (positions 2 and 6) are approximately coplanar with the benzene ring whereas the one attached to atom C3 (position 4) is slightly twisted with respect to the benzene ring as described by the torsion angles of C8–O1–C1–C2 = 2.86 (15)°, C10–O3–C5–C4 = 3.58 (14)° and C9–O2–C3–C4 = 8.39 (15)°, respectively. The N-N bond length, 1.4117 (18) Å is comparable with 1.419 (3) Å and the C=N-N angle = 110.7 (2) °. The crystal structure is stabilized by weak C—H···N and C—H··π interactions (**Table 10**).

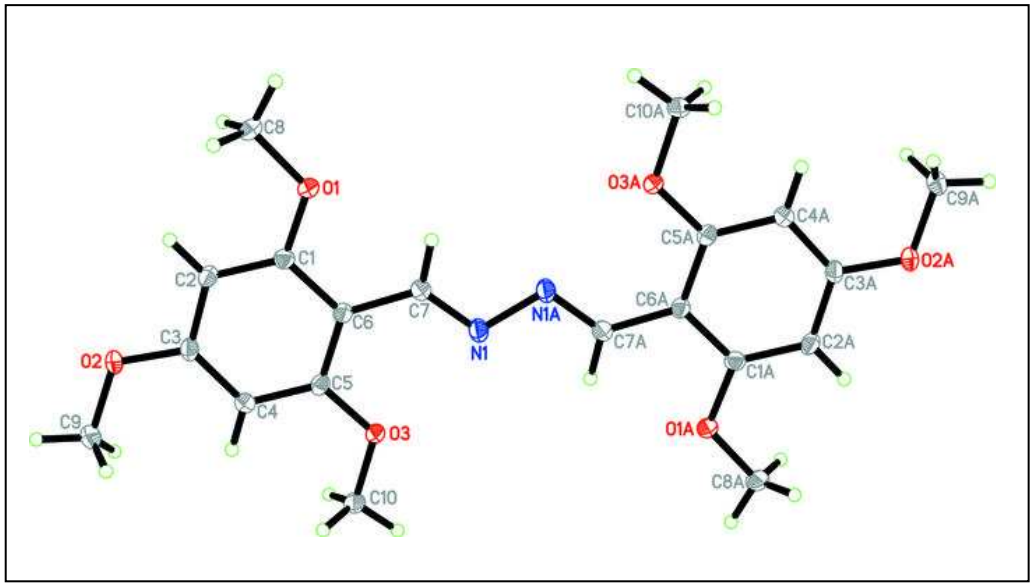

Figure 9 X-ray ORTEP diagram of the compound **PJ2**

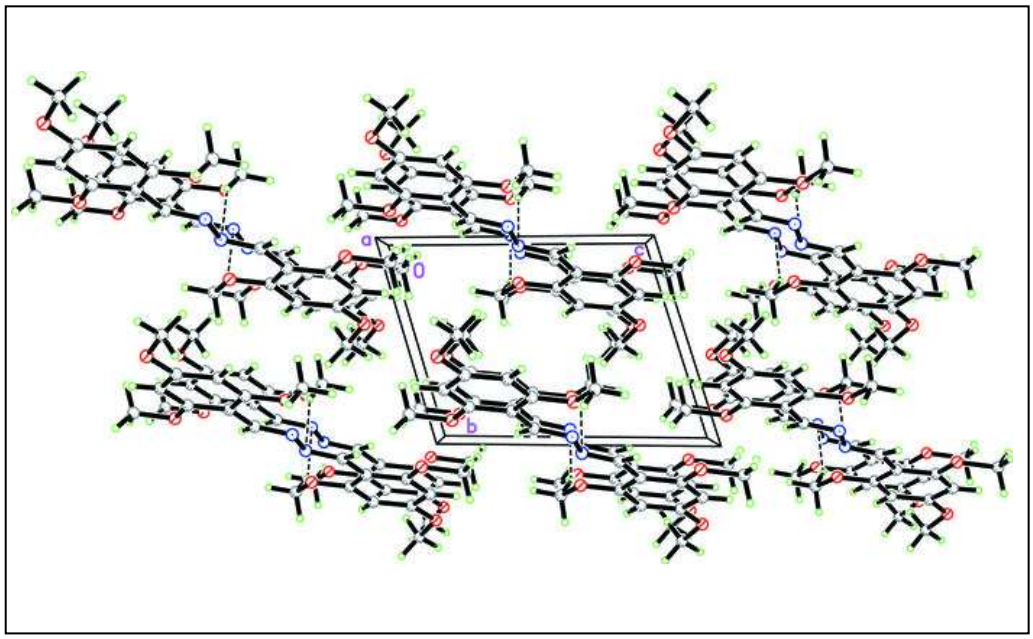

Figure 10 Packing diagram of **PJ2** viewed down the *a* axis with H-bonds shown as dashed lines.

Table 8 Crystal data and structure refinement for **PJ2**

.

Identification code	**PJ2**
Empirical formula	$C_{20}H_{24}N_2O_6$
Formula weight	388.41
Temperature	100.0(1) K
Wavelength	0.71073 Å
Crystal system, space group	Triclinic, $P\bar{1}$
Unit cell dimensions	a = 7.3851 (2) Å α = 71.412 (1) ° b = 7.4043 (2) Å β = 78.095 (1) ° c = 9.5440 (2) Å γ = 79.449 (1) °
Volume	480.13 (2) $Å^3$
Z, Calculated density	1, 1.343 Mg/m^3
Absorption coefficient	0.10 mm^{-1}
F(000)	206
Crystal size	0.29 × 0.14 × 0.08 mm
Theta range for data collection	2.3–30.0 °
Limiting indices	-10<=h<=10, -10<=k<=10, -13<=l<=13
Reflections collected / unique	11100 / 2791 [R(int) = 0.025]
Max. and min. transmission	0.992 and 0.972
Refinement method	Full-matrix least-squares on F^2
Data / restraints / parameters	2791 / 0 / 134
Final R indices [I>2σ(I)]	R1 = 0.040, wR2 = 0.115
Largest diff. peak and hole	0.42, -0.23 $e.A^{-3}$

Table 9 Bond lengths [Å], angles [°] and torsion angles [°] for **PJ2**

O1—C1	1.3632 (12)	C4—H4A	0.9300
O1—C8	1.4347 (12)	C5—C6	1.4135 (14)
O2—C3	1.3642 (12)	C6—C7	1.4564 (14)
O2—C9	1.4328 (13)	C7—H7	0.976 (14)
O3—C5	1.3528 (11)	C8—H8A	0.9600
O3—C10	1.4322 (12)	C8—H8B	0.9600
N1—C7	1.2882 (13)	C8—H8C	0.9600
N1—N1^{i}	1.4117 (18)	C9—H9A	0.9600
C1—C2	1.3866 (14)	C9—H9B	0.9600
C1—C6	1.4226 (13)	C9—H9C	0.9600
C2—C3	1.3944 (15)	C10—H10A	0.9600
C2—H2A	0.9300	C10—H10B	0.9600
C3—C4	1.3909 (13)	C10—H10C	0.9600
C4—C5	1.3974 (14)		
C1—O1—C8	118.01 (8)	N1—C7—C6	125.41 (9)
C3—O2—C9	117.79 (8)	N1—C7—H7	115.8 (8)
C5—O3—C10	117.61 (8)	C6—C7—H7	118.7 (8)
C7—N1—N1^{i}	110.66 (11)	O1—C8—H8A	109.5
O1—C1—C2	122.94 (9)	O1—C8—H8B	109.5
O1—C1—C6	115.10 (9)	H8A—C8—H8B	109.5
C2—C1—C6	121.95 (9)	O1—C8—H8C	109.5
C1—C2—C3	118.90 (9)	H8A—C8—H8C	109.5
C1—C2—H2A	120.5	H8B—C8—H8C	109.5
C3—C2—H2A	120.5	O2—C9—H9A	109.5
O2—C3—C4	123.44 (9)	O2—C9—H9B	109.5
O2—C3—C2	115.02 (9)	H9A—C9—H9B	109.5
C4—C3—C2	121.55 (9)	O2—C9—H9C	109.5
C3—C4—C5	118.99 (9)	H9A—C9—H9C	109.5

Table 9 Bond lengths [Å], angles [°] and torsion angles [°] for **PJ2** (continued)

C3—C4—H4A	120.5	H9B—C9—H9C	109.5
C5—C4—H4A	120.5	O3—C10—H10A	109.5
O3—C5—C4	122.15 (9)	O3—C10—H10B	109.5
O3—C5—C6	116.17 (9)	H10A—C10—H10B	109.5
C4—C5—C6	121.67 (9)	O3—C10—H10C	109.5
C5—C6—C1	116.93 (9)	H10A—C10—H10C	109.5
C5—C6—C7	124.92 (9)	H10B—C10—H10C	109.5
C1—C6—C7	118.15 (9)		
C8—O1—C1—C2	2.86 (15)	C3—C4—C5—C6	0.69 (15)
C8—O1—C1—C6	−176.61 (9)	O3—C5—C6—C1	179.70 (8)
O1—C1—C2—C3	−178.70 (9)	C4—C5—C6—C1	−1.27 (15)
C6—C1—C2—C3	0.74 (16)	O3—C5—C6—C7	−0.86 (15)
C9—O2—C3—C4	8.39 (15)	C4—C5—C6—C7	178.16 (9)
C9—O2—C3—C2	−171.46 (9)	O1—C1—C6—C5	−179.97 (8)
C1—C2—C3—O2	178.49 (9)	C2—C1—C6—C5	0.55 (15)
C1—C2—C3—C4	−1.37 (16)	O1—C1—C6—C7	0.55 (14)
O2—C3—C4—C5	−179.18 (9)	C2—C1—C6—C7	−178.93 (9)
C2—C3—C4—C5	0.67 (16)	$N1^{i}$—N1—C7—C6	179.28 (10)
C10—O3—C5—C4	3.58 (14)	C5—C6—C7—N1	5.52 (17)
C10—O3—C5—C6	−177.40 (8)	C1—C6—C7—N1	−175.05 (10)
C3—C4—C5—O3	179.66 (9)		

Symmetry code: (i) −x, −y+2, −z+1.

Table 10 Hydrogen-bond for **PJ2** (Å,°)

Cg is the centriod of the C1-C6 ring.

D—H···*A*	D—H	H···*A*	D···*A*	D—H···*A*
C7—H7···O1	0.977 (14)	2.332 (14)	2.6886 (12)	100.6 (10)
C10—H10B···N1^{ii}	0.96	2.49	3.3876 (15)	155
C8—H8C···Cg^{iii}	0.97	2.79	3.6678 (13)	152
C10—H10C···Cg^{iv}	0.97	2.63	3.4385 (13)	142

Symmetry code: (ii) −*x*+1, −*y*+2, −*z*+1; (iii) −*x*+1, −*y*+2, −*z*; (iv) −*x*+1, −*y*+1, −*z*+1.

3.13 *(1E,2E)*-1,2-bis(3,4,5-trimethoxybenzylidene)hydrazine (PJ3)

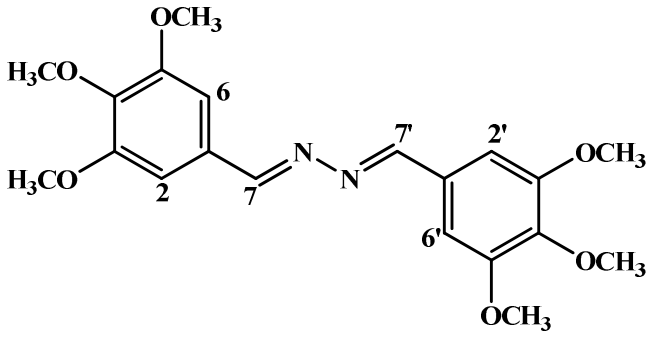

(PJ3)

Compound **PJ3** was obtained as a yellow solid (73% yield), mp. 190-192 °C. The UV-Vis absorption bands **(Figure 55)** were shown at 211 and 335 nm. The FT-IR spectrum of **PJ3** (**Figure 54**) revealed the stretching vibration of aromatic C-H at 2936 cm^{-1}. The strong peak of C=N stretching vibration was observed at 1616 cm^{-1}, C=C stretching vibration in aromatic ring at 1581 $cm^{-1}$and The C-O stretching was observed at 1182 cm^{-1}.

The ^{1}H NMR spectrum of **PJ3** (**Figure 56**, see **Table 11**) showed *singlet* signals of protons H-3, H-3'(-OCH_3), H-4, H-4'(-OCH_3) and H-5, H-5' (-OCH_3) appeared at δ 3.96 and δ 3.93 (18H). Two equivalent aromatic protons H-2, H-2' and H-6, H-6'showed the signals at δ 7.11 (4H) and *singlet* signals of protons H-7, H-7' appeared at δ 8.59 (2H). These spectroscopic data confirmed that **PJ3** is *(*1*E*,2*E*)-1,2-bis(3,4,5-trimethoxybenzylidene)hydrazine.

Table 11 ^{1}H NMR of compound **PJ3**

Position	**δ_H (ppm), *mult*, *J* (Hz)**
2, 2'	7.11, *s*
3, 3' (-OCH_3)	3.96, *s*
4, 4' (-OCH_3)	3.93, *s*
5, 5' (-OCH_3)	3.96, *s*
6, 6'	7.11, *s*
7, 7'	8.59, *s*

3.1.4 *(1E,2E)*-1, 2-bis(3-hydroxy-4-nitrobenzylidene)hydrazine (PJ4)

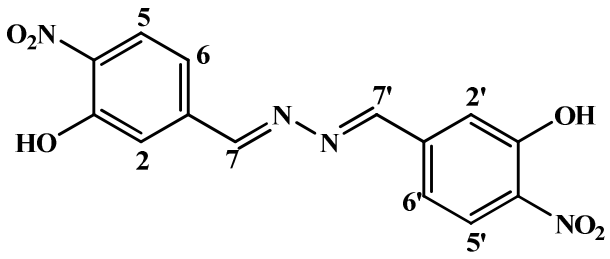

(PJ4)

Compound **PJ4** was obtained as an orange solid (82% yield), mp. 156-158 °C. The UV-Vis absorption bands **(Figure 58)** were shown at 227 and 371 nm. The FT-IR spectrum of **PJ4** (**Figure 57**) revealed the stretching vibration of aromatic C-H at 3038 cm^{-1}. The strong peak of C=N stretching vibration was observed at 1614 cm^{-1}, N=O asymmetric stretching vibration in aromatic ring at 1557 cm^{-1} and N=O symmetric stretching vibration in aromatic ring at 1327 cm^{-1}. The C-O stretching was observed at 1259 $cm^{-1}$and C-N stretching was observed at 1152 cm^{-1}.

The ^{1}H NMR spectrum of **PJ4** (**Figure 59**, see **Table 12**) showed *singlet* signals of protons H-7, H-7' appeared at δ 8.69 (2H). Three equivalent aromatic protons (H-2, H-2'), (H-5, H-5') and (H-6, H-6') showed the *doublet* signals at δ 7.47 (2H, J = 1.2 Hz), δ 7.98 (2H, J = 8.7 Hz) and *doublet* of *doublet* signals at δ 7.63 (2H, J = 1.2, 8.7 Hz). These spectroscopic data confirmed that **PJ4** is (1*E*,2*E*)-1,2-bis(3-hydroxy-4-nitrobenzylidene)hydrazine.

Table 12 ^{1}H NMR of compound **PJ4**

Position	**δ_H (ppm), *mult, J* (Hz)**
2, 2’	7.63, *d*,1.2
5, 5’	7.98, *d*, 8.7
6, 6’	7.47, *dd*, 1.2, 8.4
7, 7’	8.69, *s*

3.1.5 *(1E,2E)*-1, 2-bis(4-hydroxy-3-nitrobenzylidene)hydrazine (PJ5)

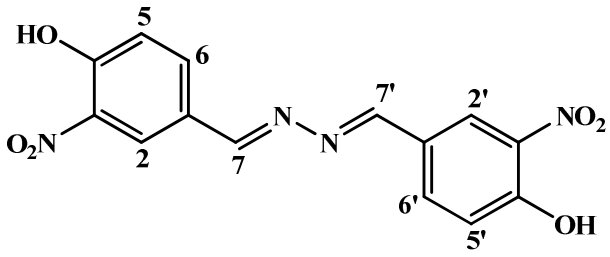

(PJ5)

Compound **PJ5** was obtained as an orange solid (81% yield), mp. 250 °C (decompose). The UV-Vis absorption bands **(Figure 61)** were shown at 206, 264 and 369 nm. The FT-IR spectrum of **PJ5** (**Figure 60**) revealed the stretching vibration of aromatic C-H at 3057 cm^{-1}. The strong peak of C=N stretching vibration was observed at 1610 cm^{-1}, N=O asymmetric stretching at 1507 cm^{-1} and N=O symmetric stretching at 1327 cm^{-1}. The C-O stretching was observed at 1210 cm^{-1} and C-N stretching was observed at 1165 cm^{-1}.

The ^{1}H NMR spectrum of **PJ5** (**Figure 62**, see **Table 13**) showed *singlet* signals of protons H-7, H-7' appeared at δ 8.69 (2H). Three equivalent aromatic protons (H-2, H-2'), (H-5, H-5') and (H-6, H-6') showed the *doublet* signals at δ 8.27 (2H, J = 1.2 Hz), δ 8.04 (2H, J = 1.8 Hz) and *doublet* of *doublet* signals at δ 8.00 (2H, J = 2.2, 8.7 Hz). These spectroscopic data confirmed that **PJ5** is *(1E,2E)*-1,2-bis(4-hydroxy-3-nitrobenzylidene)hydrazine.

Table 13 ^{1}H NMR of compound **PJ5**

Position	**δ_H (ppm), *mult*, *J* (Hz)**
2, 2’	8.27, *d*,1.2
5, 5’	8.04, *d*, 1.8
6, 6’	8.00, *dd*, 2.2, 8.7
7, 7’	8.69, *s*

3.1.6 (1*E*,2*E*)-1,2-bis(1-(2-methoxyphenyl)ethylidene)hydrazine (PJ6)

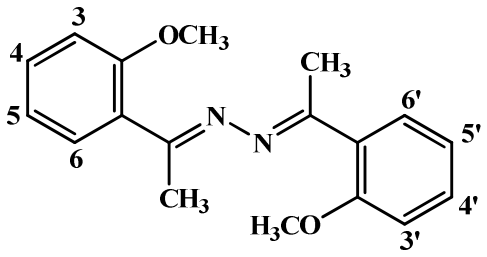

(PJ6)

Compound **PJ6** was obtained as a pale brown solid (79% yield), mp. >300 °C. The UV-Vis absorption bands **(Figure 64)** were shown at 248 and 287 nm. The FT-IR spectrum of **PJ6** (**Figure 63**) revealed the stretching vibration of aromatic C-H at 3069 cm^{-1}. The strong peak of C-H stretching was observed at 2967 cm^{-1} and C=N stretching vibration was observed at 1602 cm^{-1}. The C=C stretching vibration in aromatic ring at 1492 cm^{-1} and C-O stretching was observed at 1240 cm^{-1}.

The ^{1}H NMR spectrum of **PJ6** (**Figure 65**, see **Table 14**) showed *singlet* signals of protons H-2, H-2'(-OCH_3) and H-7, H-7'(-CH_3) appeared at δ 3.84 (6H) and δ 2.12 (6H). Two aromatic protons *doublet* of *triplet* signals of equivalent protons H-4, H-4'and H-5, H-5'(4H, J = 2.1, 7.8 Hz) at δ 7.00 and δ 7.41. Two aromatic protons *doublet* of *doublet* signals of equivalent protons H-3, H-3'and H-6, H-6'(2H, J = 8.1 Hz) at δ 7.01 and δ 7.42. These spectroscopic data confirmed that **PJ6** is (1*E*,2*E*)-1,2-bis(1-(2-methoxyphenyl)ethylidene) hydrazine.

Table 14 ^{1}H NMR of compound **PJ6**

Position	**δ_H (ppm), *mult*, *J* (Hz)**
2, 2'(-OCH_3)	3.84, *s*
3, 3'	7.01, *dd*, 8.1
4, 4'	7.00, *dt*, 2.1, 7.8
5, 5'	7.41, *dt*, 2.1, 7.8
6, 6'	7.42, *dd*, 8.1
7, 7'(-CH_3)	2.12, *s*

The crystal structure and packing of **PJ6** are illustrated in **Figures 11** and **12**. The crystal and experiment data are given in **Table 15**. Bond lengths, angles and torsion angles are shown in **Table 16**. Hydrogen-bond geometry is shown in **Table 17**. The X-ray study shows that the **PJ6** crystallized out in triclinic $P\bar{1}$ space group.

There are two molecules (A and B) in an asymmetric unit of **PJ6** (**Figure 11**). The two molecules have slightly different bond angles but exist in the same configuration which is *E*,*E* configuration with respect to the C7═N1 and C8═N2 double bonds[1.2835 (14) and 1.2821 (14) Å, respectively in molecule A, and 1.2877 (14) and 1,2837 (13) Å in molecule B] and with torsion angles N2–N1–C7–C6 = 169.23 (9)° and N1–N2–C8–C9 = 167.25 (19)° in molecule A [-166.13 (9) and -166.24 (9)° in molecule B]. The dihedral angle between the two benzene rings is 16.89 (6)° in molecule A [18.84 (6)° in molecule B]. The two methoxy groups are co-planar with each attached benzene ring with the dihedral angles of C15–O1–C1–C2 = -3.00 (17)° and C18–O2–C14–C13 = 1.85 (15)° in molecule A [the corresponding values are 0.99 (16) and -1.54 (18)° in molecule B]. The two methyl groups are twisted from the plane of benzene rings and their orientations can be indicated by the torsion angles C1–C6–C7–C16 = -48.69 (14)° and C17–C8–C9–C14 = -49.33 (16)° in

molecule A [the correspondibng values are 44.04 (16) and 53.67 (15)° in molecule B]. In molecule B, the intramolecular C17B—H17F···O2B weak interaction (**Table 17**).

In the crystal structure (**Figure 12**), the molecules are arranged into ribbons along the *c* axis. These ribbons are further stacked along the *a* axis. The molecules are consolidated by C···N [3.306 (2)–3.427 (2) Å] and C···O [3.3284 (16)–3.3863 (15) Å] short contacts. C—H··π interactions were also observed (**Table 17**).

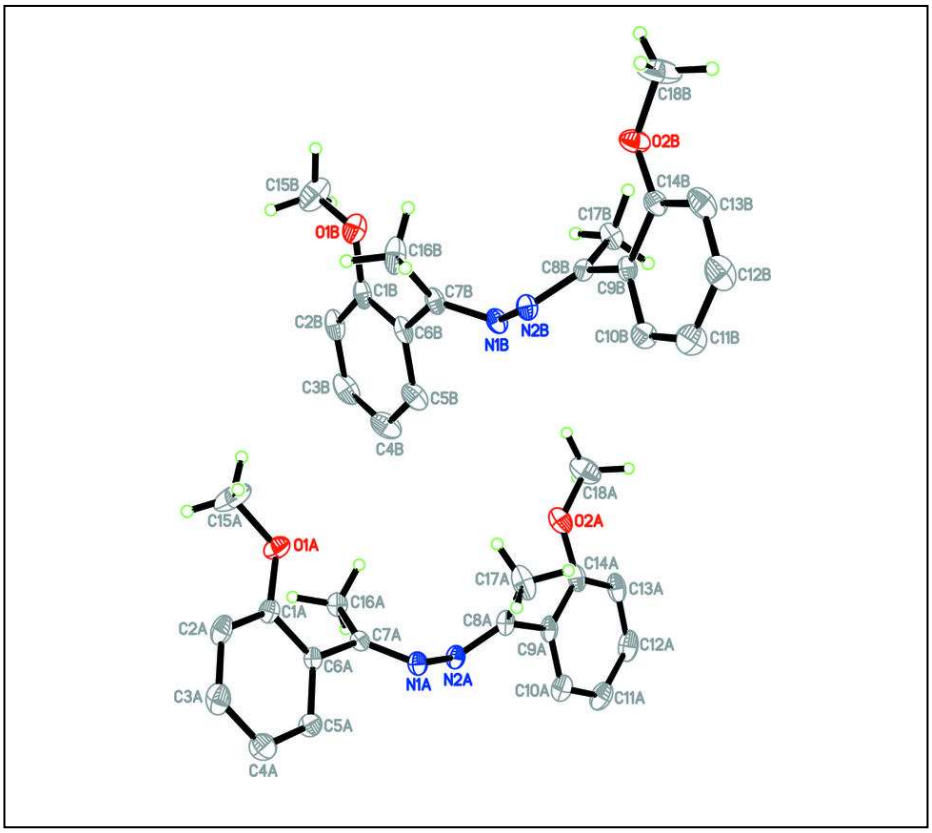

Figure 11 X-ray ORTEP diagram of the compound **PJ6**

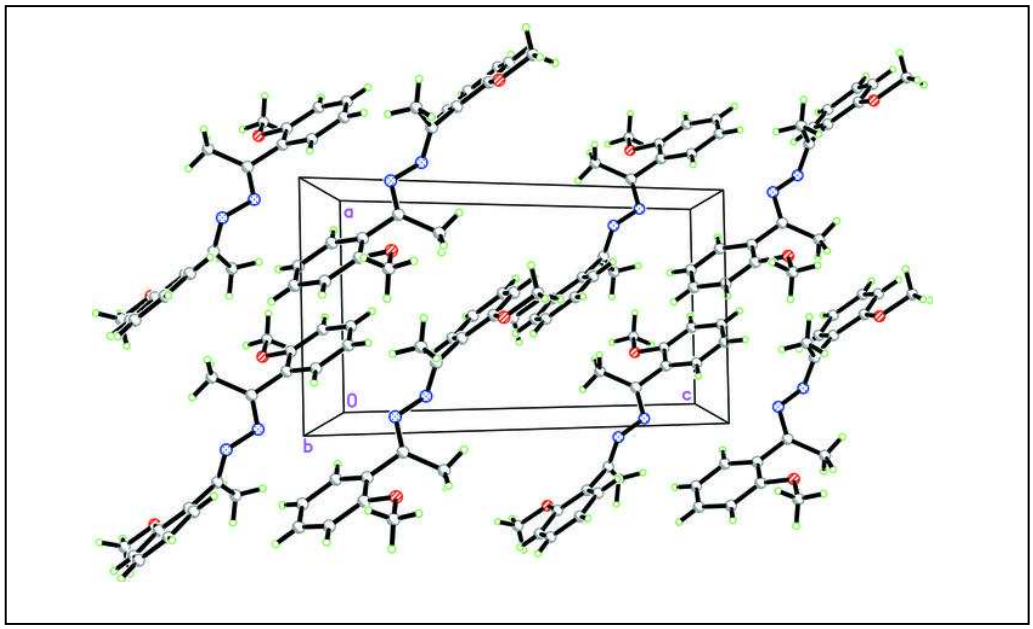

Figure 12 Packing diagram of **PJ6** viewed down the *b* axis.

Table 15 Crystal data and structure refinement for **PJ6**

.

Identification code	**PJ6**
Empirical formula	$C_{18}H_{20}N_2O_2$
Formula weight	296.36
Temperature	100.0(1) K
Wavelength	0.71073 Å
Crystal system, space group	Triclinic, $P\bar{1}$
Unit cell dimensions	a = 7.9695 (2) Å α = 117.909 (1) ° b = 14.8028 (4) Å β = 90.151 (1) ° c = 15.4704 (4) Å γ = 91.979 (1) °
Volume	1611.46 (7) $Å^3$
Z, Calculated density	4, 1.222 Mg/m^3
Absorption coefficient	0.08 mm^{-1}
F(000)	632
Crystal size	0.55 × 0.37 × 0.20 mm
Theta range for data collection	1.5–30.0 °
Limiting indices	-10<=h<=10, -20<=k<=20, -21<=l<=21
Reflections collected / unique	39016 / 9367 [R(int) = 0.028]
Max. and min. transmission	0.984 and 0.957
Refinement method	Full-matrix least-squares on F^2
Data / restraints / parameters	9367 / 0 / 405
Final R indices [I>2σ(I)]	R1 = 0.046, wR2 = 0.123
Largest diff. peak and hole	0.37, -0.24 $e.A^{-3}$

Table 16 Bond lengths [Å], angles [°] and torsion angles [°] for **PJ6**

O1A—C1A	1.3673 (14)	O1B—C1B	1.3619 (15)
O1A—C15A	1.4237 (16)	O1B—C15B	1.4366 (16)
O2A—C14A	1.3656 (15)	O2B—C14B	1.3670 (14)
O2A—C18A	1.4325 (15)	O2B—C18B	1.4255 (15)
N1A—C7A	1.2835 (14)	N1B—C7B	1.2877 (14)
N1A—N2A	1.3954 (12)	N1B—N2B	1.3938 (12)
N2A—C8A	1.2821 (14)	N2B—C8B	1.2837 (13)
C1A—C2A	1.3935 (15)	C1B—C2B	1.4004 (15)
C1A—C6A	1.4053 (15)	C1B—C6B	1.4086 (16)
C2A—C3A	1.3875 (18)	C2B—C3B	1.382 (2)
C2A—H2AA	0.9300	C2B—H2BA	0.9300
C3A—C4A	1.3828 (19)	C3B—C4B	1.385 (2)
C3A—H3AA	0.9300	C3B—H3BA	0.9300
C4A—C5A	1.3904 (16)	C4B—C5B	1.3926 (16)
C4A—H4AA	0.9300	C4B—H4BA	0.9300
C5A—C6A	1.3906 (15)	C5B—C6B	1.3946 (18)
C5A—H5AA	0.9300	C5B—H5BA	0.9300
C6A—C7A	1.4876 (14)	C6B—C7B	1.4935 (14)
C7A—C16A	1.5044 (14)	C7B—C16B	1.4977 (17)
C8A—C9A	1.4929 (15)	C8B—C9B	1.4917 (13)
C8A—C17A	1.5013 (16)	C8B—C17B	1.5018 (14)
C9A—C10A	1.3935 (17)	C9B—C10B	1.3907 (15)
C9A—C14A	1.4052 (16)	C9B—C14B	1.4052 (15)
C10A—C11A	1.3936 (17)	C10B—C11B	1.3924 (15)
C10A—H10A	0.9300	C10B—H10B	0.9300
C11A—C12A	1.3858 (19)	C11B—C12B	1.3876 (18)
C11A—H11A	0.9300	C11B—H11B	0.9300
C12A—C13A	1.388 (2)	C12B—C13B	1.3870 (18)

Table 16 Bond lengths [Å], angles [°] and torsion angles [°] for **PJ6** (continued)

C12A—H12A	0.9300	C12B—H12B	0.9300
C13A—C14A	1.3990 (16)	C13B—C14B	1.3948 (15)
C13A—H13A	0.9300	C13B—H13B	0.9300
C15A—H15A	0.9600	C15B—H15D	0.9600
C15A—H15B	0.9600	C15B—H15E	0.9600
C15A—H15C	0.9600	C15B—H15F	0.9600
C16A—H16A	0.9600	C16B—H16D	0.9600
C16A—H16B	0.9600	C16B—H16E	0.9600
C16A—H16C	0.9600	C16B—H16F	0.9600
C17A—H17A	0.9600	C17B—H17D	0.9600
C17A—H17B	0.9600	C17B—H17E	0.9600
C17A—H17C	0.9600	C17B—H17F	0.9600
C18A—H18A	0.9600	C18B—H18D	0.9600
C18A—H18B	0.9600	C18B—H18E	0.9600
C18A—H18C	0.9600	C18B—H18F	0.9600
C1A—O1A—C15A	117.43 (10)	C1B—O1B—C15B	116.31 (10)
C14A—O2A—C18A	116.57 (10)	C14B—O2B—C18B	117.64 (10)
C7A—N1A—N2A	116.67 (9)	C7B—N1B—N2B	116.99 (9)
C8A—N2A—N1A	116.75 (9)	C8B—N2B—N1B	117.11 (9)
O1A—C1A—C2A	124.13 (10)	O1B—C1B—C2B	123.31 (11)
O1A—C1A—C6A	115.45 (9)	O1B—C1B—C6B	116.88 (9)
C2A—C1A—C6A	120.40 (10)	C2B—C1B—C6B	119.79 (12)
C3A—C2A—C1A	119.57 (11)	C3B—C2B—C1B	120.34 (12)
C3A—C2A—H2AA	120.2	C3B—C2B—H2BA	119.8
C1A—C2A—H2AA	120.2	C1B—C2B—H2BA	119.8
C4A—C3A—C2A	120.79 (11)	C2B—C3B—C4B	120.68 (11)
C4A—C3A—H3AA	119.6	C2B—C3B—H3BA	119.7
C2A—C3A—H3AA	119.6	C4B—C3B—H3BA	119.7

Table 16 Bond lengths [Å], angles [°] and torsion angles [°] for **PJ6** (continued)

C3A—C4A—C5A	119.47 (11)	C3B—C4B—C5B	119.11 (13)
C3A—C4A—H4AA	120.3	C3B—C4B—H4BA	120.4
C5A—C4A—H4AA	120.3	C5B—C4B—H4BA	120.4
C4A—C5A—C6A	121.10 (11)	C4B—C5B—C6B	121.66 (12)
C4A—C5A—H5AA	119.4	C4B—C5B—H5BA	119.2
C6A—C5A—H5AA	119.4	C6B—C5B—H5BA	119.2
C5A—C6A—C1A	118.64 (10)	C5B—C6B—C1B	118.39 (10)
C5A—C6A—C7A	119.18 (10)	C5B—C6B—C7B	118.06 (10)
C1A—C6A—C7A	122.16 (9)	C1B—C6B—C7B	123.53 (11)
N1A—C7A—C6A	115.93 (9)	N1B—C7B—C6B	114.65 (10)
N1A—C7A—C16A	123.32 (9)	N1B—C7B—C16B	123.60 (9)
C6A—C7A—C16A	120.57 (9)	C6B—C7B—C16B	121.53 (9)
N2A—C8A—C9A	115.31 (10)	N2B—C8B—C9B	115.69 (9)
N2A—C8A—C17A	123.59 (10)	N2B—C8B—C17B	124.37 (9)
C9A—C8A—C17A	120.83 (9)	C9B—C8B—C17B	119.59 (9)
C10A—C9A—C14A	118.35 (10)	C10B—C9B—C14B	118.76 (9)
C10A—C9A—C8A	118.65 (10)	C10B—C9B—C8B	118.58 (9)
C14A—C9A—C8A	123.00 (11)	C14B—C9B—C8B	122.64 (10)
C9A—C10A—C11A	121.69 (12)	C9B—C10B—C11B	121.21 (11)
C9A—C10A—H10A	119.2	C9B—C10B—H10B	119.4
C11A—C10A—H10A	119.2	C11B—C10B—H10B	119.4
C12A—C11A—C10A	119.09 (13)	C12B—C11B—C10B	119.19 (11)
C12A—C11A—H11A	120.5	C12B—C11B—H11B	120.4
C10A—C11A—H11A	120.5	C10B—C11B—H11B	120.4
C11A—C12A—C13A	120.65 (11)	C13B—C12B—C11B	120.86 (11)
C11A—C12A—H12A	119.7	C13B—C12B—H12B	119.6
C13A—C12A—H12A	119.7	C11B—C12B—H12B	119.6
C12A—C13A—C14A	120.00 (11)	C12B—C13B—C14B	119.64 (11)

Table 16 Bond lengths [Å], angles [°] and torsion angles [°] for **PJ6** (continued)

C12A—C13A—H13A	120.0	C12B—C13B—H13B	120.2
C14A—C13A—H13A	120.0	C14B—C13B—H13B	120.2
O2A—C14A—C13A	123.34 (11)	O2B—C14B—C13B	123.88 (10)
O2A—C14A—C9A	116.44 (10)	O2B—C14B—C9B	115.77 (9)
C13A—C14A—C9A	120.19 (12)	C13B—C14B—C9B	120.31 (11)
O1A—C15A—H15A	109.5	O1B—C15B—H15D	109.5
O1A—C15A—H15B	109.5	O1B—C15B—H15E	109.5
H15A—C15A—H15B	109.5	H15D—C15B—H15E	109.5
O1A—C15A—H15C	109.5	O1B—C15B—H15F	109.5
H15A—C15A—H15C	109.5	H15D—C15B—H15F	109.5
H15B—C15A—H15C	109.5	H15E—C15B—H15F	109.5
C7A—C16A—H16A	109.5	C7B—C16B—H16D	109.5
C7A—C16A—H16B	109.5	C7B—C16B—H16E	109.5
H16A—C16A—H16B	109.5	H16D—C16B—H16E	109.5
C7A—C16A—H16C	109.5	C7B—C16B—H16F	109.5
H16A—C16A—H16C	109.5	H16D—C16B—H16F	109.5
H16B—C16A—H16C	109.5	H16E—C16B—H16F	109.5
C8A—C17A—H17A	109.5	C8B—C17B—H17D	109.5
C8A—C17A—H17B	109.5	C8B—C17B—H17E	109.5
H17A—C17A—H17B	109.5	H17D—C17B—H17E	109.5
C8A—C17A—H17C	109.5	C8B—C17B—H17F	109.5
H17A—C17A—H17C	109.5	H17D—C17B—H17F	109.5
H17B—C17A—H17C	109.5	H17E—C17B—H17F	109.5
O2A—C18A—H18A	109.5	O2B—C18B—H18D	109.5
O2A—C18A—H18B	109.5	O2B—C18B—H18E	109.5
H18A—C18A—H18B	109.5	H18D—C18B—H18E	109.5
O2A—C18A—H18C	109.5	O2B—C18B—H18F	109.5
H18A—C18A—H18C	109.5	H18D—C18B—H18F	109.5

Table 16 Bond lengths [Å], angles [°] and torsion angles [°] for **PJ6** (continued)

H18B—C18A—H18C	109.5	H18E—C18B—H18F	109.5
C7A—N1A—N2A—C8A	117.39 (11)	C7B—N1B—N2B—C8B	−121.46 (11)
C15A—O1A—C1A—C2A	−3.00 (17)	C15B—O1B—C1B—C2B	0.99 (16)
C15A—O1A—C1A—C6A	178.73 (12)	C15B—O1B—C1B—C6B	179.48 (11)
O1A—C1A—C2A—C3A	−179.01 (11)	O1B—C1B—C2B—C3B	177.84 (11)
C6A—C1A—C2A—C3A	−0.82 (17)	C6B—C1B—C2B—C3B	−0.61 (16)
C1A—C2A—C3A—C4A	0.69 (19)	C1B—C2B—C3B—C4B	−0.64 (18)
C2A—C3A—C4A—C5A	0.6 (2)	C2B—C3B—C4B—C5B	0.9 (2)
C3A—C4A—C5A—C6A	−1.75 (19)	C3B—C4B—C5B—C6B	0.11 (19)
C4A—C5A—C6A—C1A	1.61 (16)	C4B—C5B—C6B—C1B	−1.33 (17)
C4A—C5A—C6A—C7A	−177.40 (10)	C4B—C5B—C6B—C7B	177.19 (11)
O1A—C1A—C6A—C5A	178.03 (9)	O1B—C1B—C6B—C5B	−176.99(10)
C2A—C1A—C6A—C5A	−0.31 (15)	C2B—C1B—C6B—C5B	1.56 (16)
O1A—C1A—C6A—C7A	−2.99 (14)	O1B—C1B—C6B—C7B	4.58 (15)
C2A—C1A—C6A—C7A	178.67 (10)	C2B—C1B—C6B—C7B	−176.86(10)
N2A—N1A—C7A—C6A	169.23 (9)	N2B—N1B—C7B—C6B	−166.13 (9)
N2A—N1A—C7A—C16A	−5.92 (15)	N2B—N1B—C7B—C16B	8.60 (16)
C5A—C6A—C7A—N1A	−45.02 (14)	C5B—C6B—C7B—N1B	40.45 (14)
C1A—C6A—C7A—N1A	136.01 (11)	C1B—C6B—C7B—N1B	−141.12(11)
C5A—C6A—C7A—C16A	130.28 (11)	C5B—C6B—C7B—C16B	−134.40(12)
C1A—C6A—C7A—C16A	−48.69 (14)	C1B—C6B—C7B—C16B	44.04 (16)
N1A—N2A—C8A—C9A	167.25 (9)	N1B—N2B—C8B—C9B	−166.24 (9)
N1A—N2A—C8A—C17A	−6.81 (17)	N1B—N2B—C8B—C17B	6.97 (16)
N2A—C8A—C9A—C10A	−43.91 (14)	N2B—C8B—C9B—C10B	48.84 (14)
C17A—C8A—C9A—C10A	130.33 (12)	C17B—C8B—C9B—C10B	−124.72(11)
N2A—C8A—C9A—C14A	136.44 (11)	N2B—C8B—C9B—C14B	−132.77(11)
C17A—C8A—C9A—C14A	−49.33 (16)	C17B—C8B—C9B—C14B	53.67 (15)
C14A—C9A—C10A—C11A	1.51 (16)	C14B—C9B—C10B—C11B	−1.41 (17)

Table 16 Bond lengths [Å], angles [°] and torsion angles [°] for **PJ6** (continued)

C8A—C9A—C10A—C11A −178.16 (10)	C8B—C9B—C10B—C11B 177.04 (11)
C9A—C10A—C11A—C12A 0.19 (18)	C9B—C10B—C11B—C12B 1.50 (19)
C10A—C11A—C12A—C13A −1.31 (18)	C10B—C11B—C12B—C13B −0.5 (2)
C11A—C12A—C13A—C14A 0.68 (18)	C11B—C12B—C13B—C14B −0.6 (2)
C18A—O2A—C14A—C13A 1.85 (15)	C18B—O2B—C14B—C13B −1.54 (18)
C18A—O2A—C14A—C9A −176.08 (10)	C18B—O2B—C14B—C9B 176.41 (12)
C12A—C13A—C14A—O2A −176.79 (10)	C12B—C13B—C14B—O2B 178.53 (12)
C12A—C13A—C14A—C9A 1.07 (16)	C12B—C13B—C14B—C9B 0.67 (18)
C10A—C9A—C14A—O2A 175.87 (9)	C10B—C9B—C14B—O2B −177.71 (10)
C8A—C9A—C14A—O2A −4.47 (15)	C8B—C9B—C14B—O2B 3.90 (15)
C10A—C9A—C14A—C13A −2.13 (15)	C10B—C9B—C14B—C13B 0.32 (16)
C8A—C9A—C14A—C13A 177.52 (10)	C8B—C9B—C14B—C13B −178.07 (10)

Table 17 Hydrogen-bond for **PJ6** (Å,°)

Cg1 and Cg2 are the centroids of C9A–C14A and C1B–C6B rings.

D—H···*A*	**D—H**	**H···*A***	**D···*A***	**D—H···*A***
C17B—H17F···O2B	0.96	2.36	2.9918 (17)	123
C15B—H15E···Cg1^{i}	0.96	2.83	3.5974 (17)	138
C18A—H18C···Cg2^{ii}	0.96	2.90	3.6976 (17)	141

Symmetry code: (i) −*x*+1, −*y*+1, −*z*+1; (ii) −*x*, −*y*+1, −*z*+1.

3.1.7 (1*E*,2*E*)-1,2-bis(1-(2-aminophenyl)ethylidene)hydrazine (PJ7)

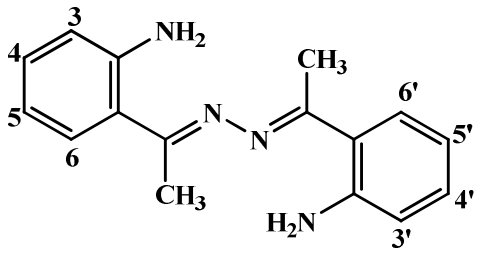

(PJ7)

Compound **PJ7** was obtained as a yellow solid (84% yield), mp. 179-180 °C. The UV-Vis absorption bands **(Figure 67)** were shown at 238 and 379 nm. The FT-IR spectrum of **PJ7** (**Figure 66**) revealed the stretching vibration of N-H stretching vibration was observed at 3348 $cm^{-1}$and the stretching vibration of aromatic C-H at 3187 cm^{-1}. The strong peak of C-H stretching was observed at 2961 cm^{-1} and the strong peak of C=N stretching vibration was observed at 1609 cm^{-1}. The C=C stretching vibration in aromatic ring at 1546 cm^{-1} and the C-N stretching was observed at 1293 cm^{-1}.

The ^{1}H NMR spectrum of **PJ7** (**Figure 68**, see **Table 18**) showed *singlet* signals of protons H-2, H-2'(-NH_2) and H-7, H-7'(-CH_3) appeared at δ 7.06 (4H) and δ 2.38 (6H). Two aromatic protons *doublet* signals of equivalent protons H-3, H-3'and H-6, H-6' (2H, J = 7.8 Hz) at δ 6.77 and δ 7.52. Two aromatic protons *triplet* signals of equivalent protons H-4, H-4'and H-5, H-5' (2H, J = 7.8 Hz) at δ 7.11 and δ 6.59. These spectroscopic data confirmed that **PJ7** is (1*E*,2*E*)-1,2-bis(1-(2-aminophenyl)ethylidene)hydrazine.

Table 18 ^{1}H NMR of compound **PJ7**

Position	**δ_H (ppm), *mult, J* (Hz)**
2, 2'(-NH_2)	7.06, *s*
3, 3'	6.77, *d*, 7.8
4, 4'	7.11, *t*, 7.8
5, 5'	6.59, *t*, 7.8
6, 6'	7.52, *d*, 7.8
7, 7'(-CH_3)	2.38, *s*

3.1.8 (1*E*,2*E*)-1,2-bis(1-(2-nitrophenyl)ethylidene)hydrazine (PJ8)

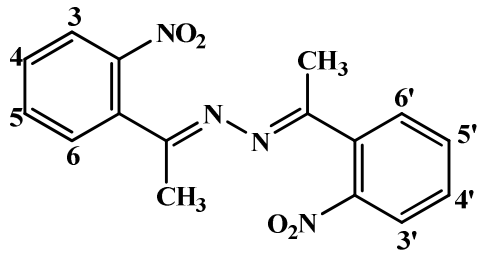

(PJ8)

Compound **PJ8** was obtained as a yellow solid (78% yield), mp. 171-173 °C. The UV-Vis absorption bands **(Figure 70)** were shown at 235 nm. The FT-IR spectrum of **PJ8** (**Figure 69**) revealed the stretching vibration of aromatic C-H at 3063 cm^{-1}. The strong peak of C-H stretching vibration was observed at 2861 cm^{-1} and C=N stretching vibration was observed at 1623 cm^{-1}. The N=O asymmetric stretching vibration in aromatic ring at 1545 cm^{-1} and N=O symmetric stretching was observed at 1358 cm^{-1}.

The ^{1}H NMR spectrum of **PJ8** (**Figure 71**, see **Table 19**) showed *singlet* signals of protons H-7, H-7'(-CH_3) appeared at δ 2.58 (6H). Two aromatic protons *doublet* signals of equivalent protons H-3, H-3' and H-6, H-6' at δ 8.08 and δ 7.85 (4H, J = 7.8 Hz). Two aromatic protons *triplet* signals of equivalent protons H-4, H-4'and H-5, H-5' appeared at δ 7.80 and δ 7.78 (4H, J = 7.8 Hz). These spectroscopic data confirmed that **PJ8** is (1*E*,2*E*)-1,2-bis(1-(2-nitrophenyl)-ethylidene)hydrazine.

Table 19 ^{1}H NMR of compound **PJ8**

Position	**δ_H (ppm), *mult*, *J* (Hz)**
3, 3’	8.08, *d*, 7.8
4, 4’	7.80, *t*, 7.8
5, 5’	7.78, *t*, 7.8
6, 6’	7.85, *d*, 7.8
7, 7’(-CH_3)	2.58, *s*

3.1.9 (1*E*,2*E*)-1,2-bis(1-(2-chlorophenyl)ethylidene)hydrazine (PJ9)

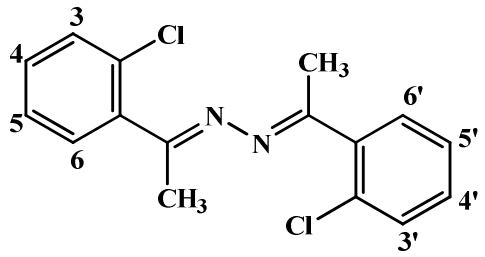

(PJ9)

Compound **PJ9** was obtained as a yellow solid (67% yield), mp. 92-93 °C. The UV-Vis absorption bands **(Figure 73)** were shown at 242 nm. The FT-IR spectrum of **PJ9** (**Figure 72**) revealed the stretching vibration of aromatic C-H at 3045 cm^{-1}. The strong peak of C-H stretching was observed at 2995 cm^{-1} and the strong peak of C=N stretching vibration was observed at 1612 cm^{-1}. The C=C stretching vibration in aromatic ring at 1431 cm^{-1} and the C-Cl stretching was observed at 737 cm^{-1}.

The ^{1}H NMR spectrum of **PJ9** (**Figure 74**, see **Table 20**) showed *singlet* signals of protons H-7, H-7'(-CH_3) appeared at δ 2.18 (6H). Two aromatic protons *multiplet* signals of equivalent protons H-3, H-3' and H-6, H-6' at δ 7.52-7.58 (4H). Two aromatic protons *triplet* signals of equivalent protons H-4, H-4'and H-5, H-5'appeared at δ 7.46 and δ 7.45 (4H, J = 3.9 Hz). These spectroscopic data confirmed that **PJ9** is (1*E*,2*E*)-1,2-bis(1-(2-chlorophenyl)ethylidene)hydrazine.

Table 20 ^{1}H NMR of compound **PJ9**

Position	δ_H **(ppm),** ***mult, J*** **(Hz)**
3, 3’	7.52-7.58, *m*
4, 4’	7.46, *t*, 3.9
5, 5’	7.45, *t*, 3.9
6, 6’	7.52-7.58, *m*
7, 7’(-CH_3)	2.18, *s*

3.1.10 (1*E*,2*E*)-1,2-bis(1-(2-bromophenyl)ethylidene)hydrazine (PJ10)

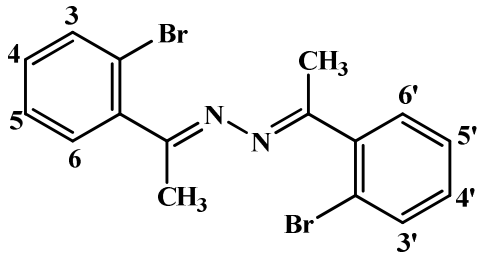

(PJ10)

Compound **PJ10** was obtained as a white solid (89% yield), mp.114-116 °C. The UV-Vis absorption bands **(Figure 76)** were shown at 207 nm. The FT-IR spectrum of **PJ10** (**Figure 75**) revealed the stretching vibration of aromatic C-H at 3058 cm^{-1}. The strong peak of C-H stretching vibration was observed at 2994 cm^{-1} and C=N stretching vibration was observed at 1615 cm^{-1}. The C=C stretching vibration in aromatic ring at 1559 cm^{-1} and C-Br stretching vibration was observed at 575 cm^{-1}.

The ^{1}H NMR spectrum of **PJ10** (**Figure 77**, see **Table 21**) showed *singlet* signals of protons H-7, H-7'(-CH_3) appeared at δ 2.18 (6H). Two aromatic protons *multiplet* signals of protons H-5, H-5' and H-6, H-6' at δ 7.34-7.41 (4H). Two aromatic protons *doublet* and *triplet* signals of protons H-3, H-3'and H-4, H-4' appeared at δ 7.71 (2H, J = 7.8 Hz) and δ 7.48 (2H, J = 5.7 Hz). These spectroscopic data confirmed that **PJ10** is (1*E*,2*E*)-1,2-bis(1-(2-bromophenyl) ethylidene)hydrazine.

Table 21 ^{1}H NMR of compound **PJ10**

Position	δ_H **(ppm),** ***mult, J*** **(Hz)**
3, 3’	7.71, *d*, 7.8
4, 4’	7.48, *t*, 5.7
5, 5’	7.34-7.41, *m*
6, 6’	7.34-7.41, *m*
7, 7’(-CH_3)	2.18, *s*

The crystal structure and packing of **PJ10** are illustrated in **Figures 13** and **14**. The crystal and experiment data are given in **Table 22**. Bond lengths, angles and torsion angles are shown in **Table 23**. Hydrogen-bond geometry is shown in **Table 24**. The X-ray study shows that the **PJ10** crystallized out in monoclinic $P2_1/c$ space group.

The asymmetric unit of **PJ10** (**Figure 13**), contains one half-molecule and the complete molecule is generated by a crystallographic symmetry centre 1 - *x*, *y*, 1/2 - *z*. The molecule of **PJ10** exists in an *E* configuration with respect to the C7═N1 double bond [1.2812 (19) Å] and the torsion angle N1A–N1–C7–C6 = -173.12 (13)°. The dihedral angle between the two benzene rings is 35.28 (8)°. Atoms C7/C8/ N1/N1A lie on a same plane [r.m.s 0.0116 (2) Å] and the torsion angle N1A–N1–C7–C8 = 3.8 (2)°. The dihedral angle between this plane and its symmetry related plane (C7A/C8A/N1/N1A) is 87.67 (11)°. Each of these two middle C/C/N/N planes makes a dihedral angle of 63.81 (10)° with its adjacent benzene ring.

In the crystal structure (**Figure 14**), the molecules are arranged into zigzag chains along the *a* axis and these chains stacked along the *c* direction. The molecules are consolidated by C···Br [3.4032 (18)–35969 (19) Å] short contacts. C—H··π interactions were also observed (**Table 24**).

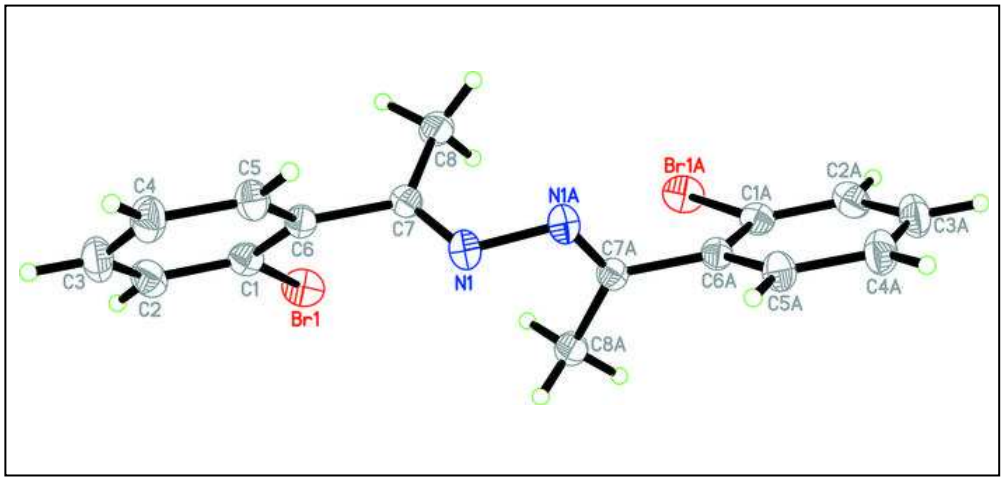

Figure 13 X-ray ORTEP diagram of the compound **PJ10**

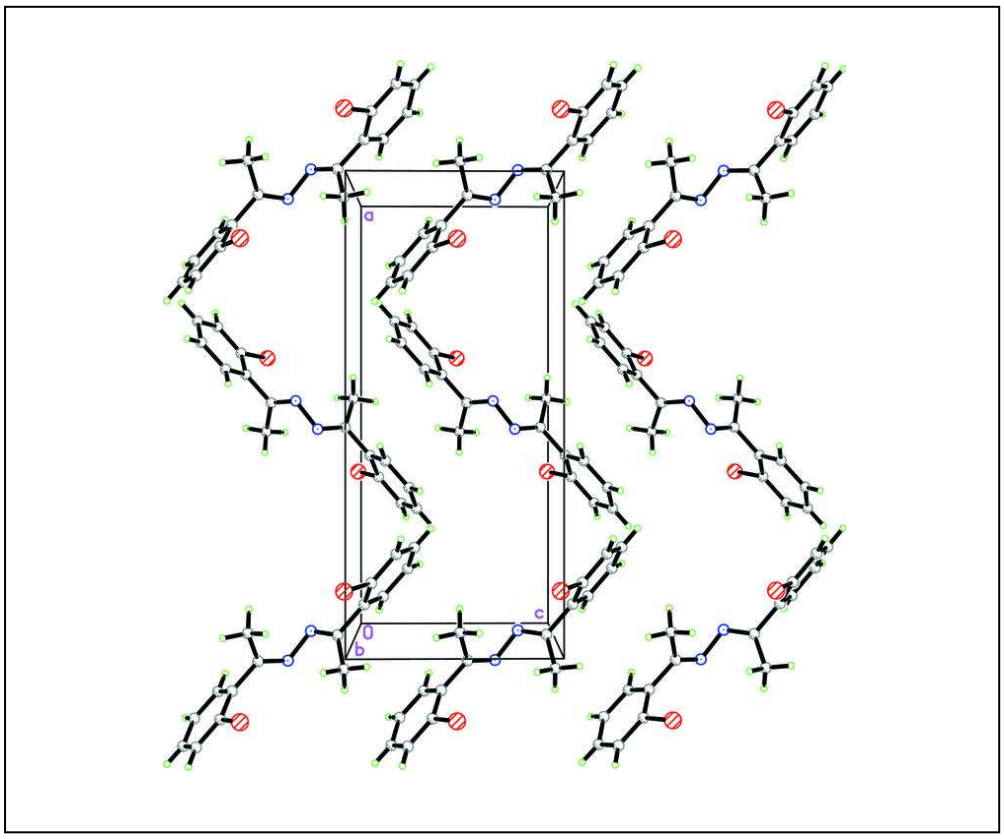

Figure 14 Packing diagram of **PJ10** viewed down the *b* axis.

Table 22 Crystal data and structure refinement for **PJ10**

.

Identification code	**PJ10**
Empirical formula	$C_{16}H_{14}Br_2N_2$
Formula weight	394.11
Temperature	100.0(1) K
Wavelength	0.71073 Å
Crystal system, space group	Monoclinic, $P2_1/c$
Unit cell dimensions	a = 17.2162 (3) Å α = (90) ° b = 11.8414 (3) Å β = (90) ° c = 11.8414 (3) Å γ = (90) °
Volume	734.62 (2) $Å^3$
Z, Calculated density	2, 1.376 Mg/m^3
Absorption coefficient	0.10 mm^{-1}
F(000)	324
Crystal size	0.35 × 0.26 × 0.22 mm
Theta range for data collection	2.4–30.0 °
Limiting indices	-27<=h<=27, -19<=k<=17, -12<=l<=12
Reflections collected / unique	18529 / 3458 [R(int) = 0.042]
Max. and min. transmission	0.979 and 0.966
Refinement method	Full-matrix least-squares on F^2
Data / restraints / parameters	3458 / 0 / 92
Final R indices [I>2σ(I)]	R1 = 0.031, wR2 = 0.081
Largest diff. peak and hole	0.75, -0.40 $e.A^{-3}$

Table 23 Bond lengths [Å], angles [°] and torsion angles [°] for **PJ10**

O1—C4	1.3644 (11)	C4—C5	1.3971 (14)
O1—H1O1	0.8256	C5—C6	1.3854 (13)
N1—C7	1.2985 (13)	C5—H5A	0.9300
N1—N1^{i}	1.4050 (16)	C6—H6A	0.9300
C1—C2	1.4016 (14)	C7—C8	1.5010 (14)
C1—C6	1.4056 (14)	C8—H8A	0.9600
C1—C7	1.4814 (13)	C8—H8B	0.9600
C2—C3	1.3934 (13)	C8—H8C	0.9600
C2—H2A	0.9300	O1W—H1W	0.8598
C3—C4	1.3913 (14)	O1W—H2W	0.8601
C3—H3A	0.9300		
C4—O1—H1O1	111.9	C6—C5—H5A	120.1
C7—N1—N1^{i}	114.55 (10)	C4—C5—H5A	120.1
C2—C1—C6	118.04 (9)	C5—C6—C1	121.28 (9)
C2—C1—C7	121.45 (9)	C5—C6—H6A	119.4
C6—C1—C7	120.50 (9)	C1—C6—H6A	119.4
C3—C2—C1	121.04 (9)	N1—C7—C1	116.07 (9)
C3—C2—H2A	119.5	N1—C7—C8	125.01 (9)
C1—C2—H2A	119.5	C1—C7—C8	118.92 (9)
C4—C3—C2	119.82 (9)	C7—C8—H8A	109.5
C4—C3—H3A	120.1	C7—C8—H8B	109.5
C2—C3—H3A	120.1	H8A—C8—H8B	109.5
O1—C4—C3	119.26 (9)	C7—C8—H8C	109.5
O1—C4—C5	120.65 (9)	H8A—C8—H8C	109.5
C3—C4—C5	120.09 (9)	H8B—C8—H8C	109.5
C6—C5—C4	119.72 (9)	H1W—O1W—H2W	110.1
C6—C1—C2—C3	0.95 (16)	C2—C1—C6—C5	−0.70 (15)
C7—C1—C2—C3	−179.93 (9)	C7—C1—C6—C5	−179.83 (9)
C1—C2—C3—C4	−0.37 (16)	N1^{i}—N1—C7—C1	177.76 (10)

Table 23 Bond lengths [Å], angles [°] and torsion angles [°] for **PJ10** (continued)

C2—C3—C4—O1	179.26 (9)	N1^{i}—N1—C7—C8	−2.78 (17)
C2—C3—C4—C5	−0.48 (16)	C2—C1—C7—N1	171.18 (10)
O1—C4—C5—C6	−179.01 (9)	C6—C1—C7—N1	−9.72 (14)
C3—C4—C5—C6	0.72 (15)	C2—C1—C7—C8	−8.31 (15)
C4—C5—C6—C1	−0.12 (16)	C6—C1—C7—C8	170.78 (10)

Symmetry code: (i) −x+1, −y+1, −z+1.

Table 24 Hydrogen-bond for **PJ10** (Å,°)

Cg1 is the centriod of the C1-C6 ring.

D—H···*A*	**D—H**	**H···*A***	**D···*A***	**D—H···*A***
O1—H1O1···O1W^{ii}	0.83	1.86	2.6747 (12)	171
O1W—H1W···O1^{iii}	0.86	2.07	2.8429 (12)	149
O1W—H2W···N1^{i}	0.86	2.17	3.0132 (14)	166
C5—H5A···Cg1^{iv}	0.93	2.80	3.5046 (12)	134

Symmetry code: (ii) *x*+1, −*y*+1/2, *z*+1/2; (iii) −*x*+1, *y*−1/2, −*z*+3/2; (i) −*x*+1, −*y*+1, −*z*+1; (iv) −*x*+2, *y*−1/2, −*z*+3/2.

3.1.11 (1*E*,2*E*)-1,2-bis(1-(4-hydroxyphenyl)ethylidene)hydrazine (PJ11)

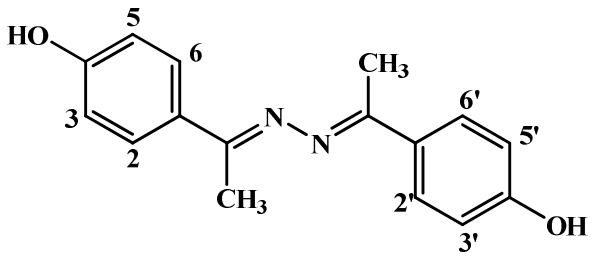

(PJ11)

Compound **PJ11** was obtained as a brown solid (82% yield), mp. 210-212 °C. The UV-Vis absorption bands **(Figure 79)** 223 and 306 nm. The FT-IR spectrum of **PJ11** (**Figure 78**) revealed the stretching vibration of aromatic C-H and the stretching vibration of O-H and C-H at 2900-3400 cm^{-1}. The strong peak of C=N stretching vibration was observed at 1666 cm^{-1} and C=C stretching vibration in aromatic ring at 1595 cm^{-1}. The C-O stretching vibration was observed at 1225 cm^{-1}.

The ^{1}H NMR spectrum of **PJ11** (**Figure 80**, see **Table 25**) showed *singlet* signals of protons H-7, H-7'(-CH_3) and 4, 4'(-OH) appeared at δ 2.24 (6H) and δ 10.22 (2H). Two equivalent aromatic protons *doublet* signals of protons H-2, H-2' and H-6, H-6' (4H, J = 8.7 Hz) at δ 7.83. Two equivalent aromatic protons *doublet* signals of protons H-3, H-3' and H-5, H-5' appeared at (4H, J = 8.7 Hz) at δ 7.76. These spectroscopic data confirmed that **PJ11** is (1*E*,2*E*)-1,2-bis(1-(4-hydroxy phenyl)ethylidene) hydrazine.

Table 25 ^{1}H NMR of compound **PJ11**

Position	**δ_H (ppm), *mult*, *J* (Hz)**
2, 2’	7.83, *d*, 8.7
3, 3’	7.76, *d*, 8.7
4, 4’(-OH)	10.22, *s*
5, 5’	7.76, *d*, 8.7
6, 6’	7.83, *d*, 8.7
7, 7’(-CH_3)	2.24, *s*

The crystal structure and packing of **PJ11** are illustrated in **Figures 15** and **16**. The crystal and experiment data are given in **Table 26**. Bond lengths, angles and torsion angles are shown in **Table 27**. Hydrogen-bond geometry is shown in **Table 28**. The X-ray study shows that the **PJ11** crystallized out in monoclinic $P2_1/c$ space group.

The asymmetric unit of **PJ11** (**Figure 15**), contains one half-molecule of diphenol and the complete molecule is generated by a crystallographic inversion centre 1 - *x*, 1 - *y*, 1 - *z*. The molecule of **PJ11** exists in an *E*,*E* configuration with respect to the two C═N double bonds [1.2985 (13) Å] and the torsion angle N1A–N1–C7–C1 = 177.76 (10)°. The diethylidenehydrazine moiety (C7/C8/N1/N1A/C7A /C8A) is planar with an r.m.s deviation of 0.0084 (1) Å. This C/C/N/N/C/C plane makes a dihedral angle of 8.88 (6)° with its both adjacent benzene rings. Each hydroxy group is co-planarly attached with the benzene ring with the r.m.s. of 0.0056 (1) Å for the seven non H atoms.

In the crystal structure (**Figure 16**), the molecules are linked into three dimensional network by O—H···N and O—H···O hydrogen bonds (**Table 28**). C—H··π interaction was also observed (**Table 28**).

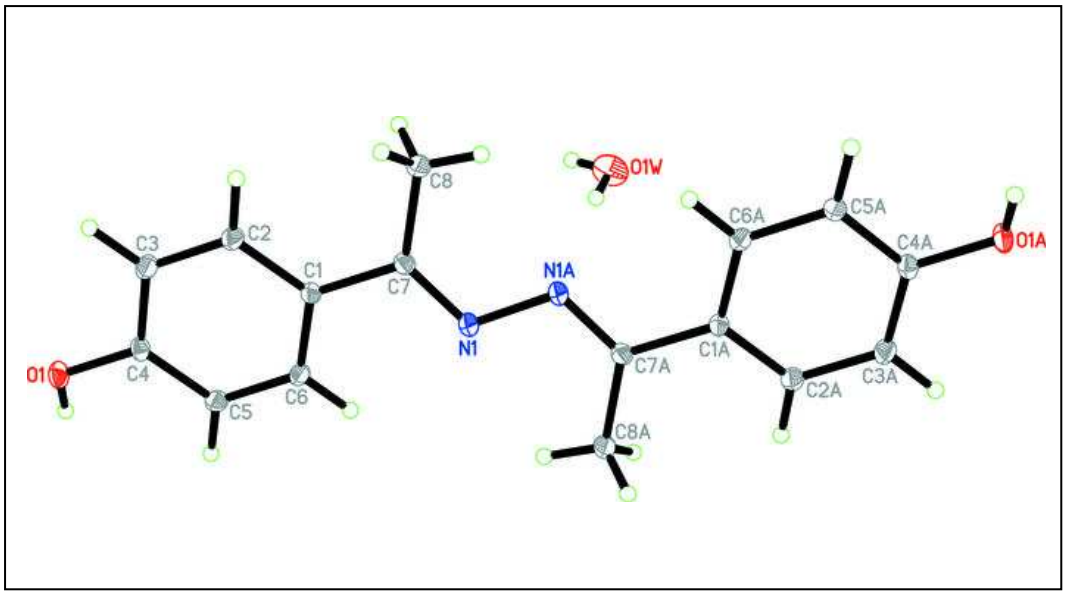

Figure 15 X-ray ORTEP diagram of the compound **PJ11**

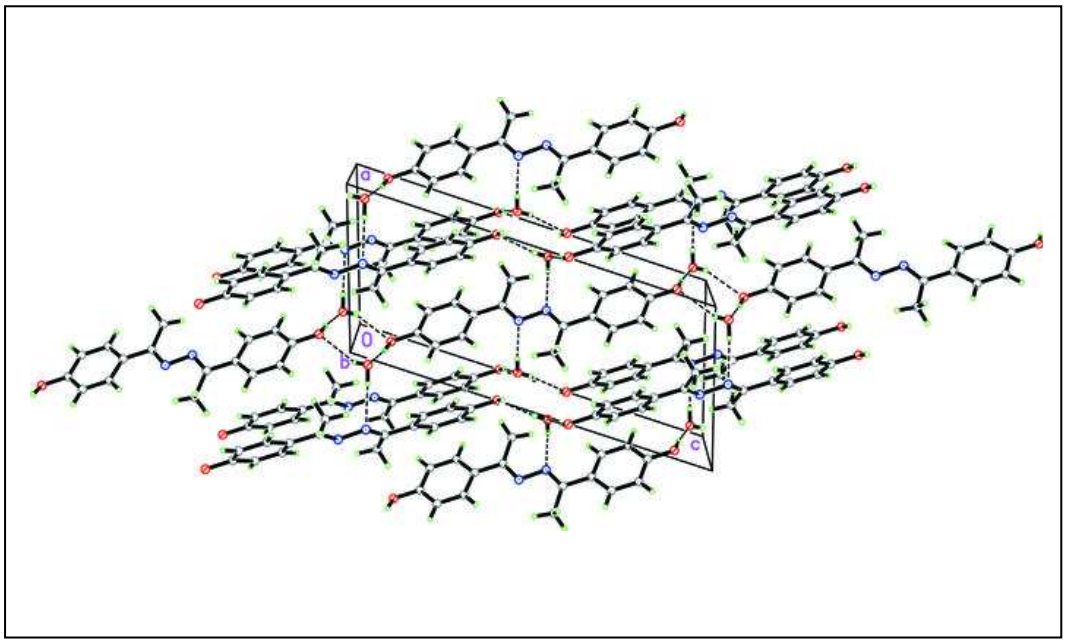

Figure 16 Packing diagram of **PJ11** viewed down the *b* axis with H-bonds shown as dashed lines.

Table 26 Crystal data and structure refinement for **PJ11**

.

Identification code	**PJ11**
Empirical formula	$C_{16}H_{16}N_2O_2 \cdot 2H_2O$
Formula weight	304.34
Temperature	100.0(1) K
Wavelength	0.71073 Å
Crystal system, space group	Monoclinic, $P2_1/c$
Unit cell dimensions	a = 7.8522 (1) Å α = (90) ° b = 5.5151 (1) Å β = 108.536 (1) ° c = 17.8918 (3) Å γ = (90) °
Volume	734.62 (2) $Å^3$
Z, Calculated density	2, 1.376 Mg/m^3
Absorption coefficient	0.10 mm^{-1}
F(000)	324
Crystal size	0.35 × 0.26 × 0.22 mm
Theta range for data collection	2.4–30.0 °
Limiting indices	-10<=h<=11, -7<=k<=7, -24<=l<=24
Reflections collected / unique	8010 / 2129 [R(int) = 0.021]
Max. and min. transmission	0.979 and 0.966
Refinement method	Full-matrix least-squares on F^2
Data / restraints / parameters	2129 / 0 / 101
Final R indices [I>2σ(I)]	R1 = 0.046, wR2 = 0.125
Largest diff. peak and hole	0.39, -0.34 $e.A^{-3}$

Table 27 Bond lengths [Å], angles [°] and torsion angles [°] for **PJ11**

O1—C4	1.3644 (11)	C4—C5	1.3971 (14)
O1—H1O1	0.8256	C5—C6	1.3854 (13)
N1—C7	1.2985 (13)	C5—H5A	0.9300
N1—N1^{i}	1.4050 (16)	C6—H6A	0.9300
C1—C2	1.4016 (14)	C7—C8	1.5010 (14)
C1—C6	1.4056 (14)	C8—H8A	0.9600
C1—C7	1.4814 (13)	C8—H8B	0.9600
C2—C3	1.3934 (13)	C8—H8C	0.9600
C2—H2A	0.9300	O1W—H1W	0.8598
C3—C4	1.3913 (14)	O1W—H2W	0.8601
C3—H3A	0.9300		
C4—O1—H1O1	111.9	C6—C5—H5A	120.1
C7—N1—N1^{i}	114.55 (10)	C4—C5—H5A	120.1
C2—C1—C6	118.04 (9)	C5—C6—C1	121.28 (9)
C2—C1—C7	121.45 (9)	C5—C6—H6A	119.4
C6—C1—C7	120.50 (9)	C1—C6—H6A	119.4
C3—C2—C1	121.04 (9)	N1—C7—C1	116.07 (9)
C3—C2—H2A	119.5	N1—C7—C8	125.01 (9)
C1—C2—H2A	119.5	C1—C7—C8	118.92 (9)
C4—C3—C2	119.82 (9)	C7—C8—H8A	109.5
C4—C3—H3A	120.1	C7—C8—H8B	109.5
C2—C3—H3A	120.1	H8A—C8—H8B	109.5
O1—C4—C3	119.26 (9)	C7—C8—H8C	109.5
O1—C4—C5	120.65 (9)	H8A—C8—H8C	109.5
C3—C4—C5	120.09 (9)	H8B—C8—H8C	109.5
C6—C5—C4	119.72 (9)	H1W—O1W—H2W	110.1
C6—C1—C2—C3	0.95 (16)	C2—C1—C6—C5	−0.70 (15)
C7—C1—C2—C3	−179.93 (9)	C7—C1—C6—C5	−179.83 (9)
C1—C2—C3—C4	−0.37 (16)	N1^{i}—N1—C7—C1	177.76 (10)

Table 27 Bond lengths [Å], angles [°] and torsion angles [°] for **PJ11** (continued)

C2—C3—C4—O1	179.26 (9)	N1^{i}—N1—C7—C8	−2.78 (17)
C2—C3—C4—C5	−0.48 (16)	C2—C1—C7—N1	171.18 (10)
O1—C4—C5—C6	−179.01 (9)	C6—C1—C7—N1	−9.72 (14)
C3—C4—C5—C6	0.72 (15)	C2—C1—C7—C8	−8.31 (15)
C4—C5—C6—C1	−0.12 (16)	C6—C1—C7—C8	170.78 (10)

Symmetry code: (i) −x+1, −y+1, −z+1.

Table 28 Hydrogen-bond for **PJ11** (Å,°)

Cg1 is the centriod of the C1-C6 ring.

D—H···*A*	**D—H**	**H···*A***	**D···*A***	**D—H···*A***
O1—H1O1···O1W^{ii}	0.83	1.86	2.6747 (12)	171
O1W—H1W···O1^{iii}	0.86	2.07	2.8429 (12)	149
O1W—H2W···N1^{i}	0.86	2.17	3.0132 (14)	166
C5—H5A···Cg1^{iv}	0.93	2.80	3.5046 (12)	134

Symmetry code: (ii) *x*+1, −*y*+1/2, *z*+1/2; (iii) −*x*+1, *y*−1/2, −*z*+3/2; (i) −*x*+1, −*y*+1, −*z*+1; (iv) −*x*+2, *y*−1/2, −*z*+3/2.

3.1.12 (1*E*,2*E*)-1,2-bis(1-(3-methoxyphenyl)ethylidene)hydrazine (PJ12)

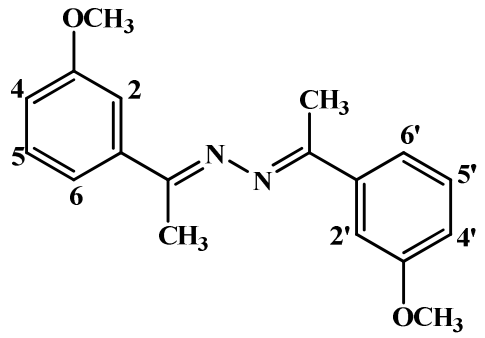

(PJ12)

Compound **PJ12** was obtained as a yellow solid (81% yield), mp. 95-97°C. The UV-Vis absorption bands (**Figure 82**) were shown at 222 and 267 nm. The FT-IR spectrum of **PJ12** (**Figure 81**) revealed the stretching vibration of aromatic C-H at 3104 cm^{-1}. The strong peak of C-H stretching vibration was observed at 2954 cm^{-1} and C=C stretching vibration in aromatic ring at 1575 cm^{-1}. The C-O stretching vibration was observed at 1218 cm^{-1}.

The ^{1}H NMR spectrum of **PJ12** (**Figure 83**, see **Table 29**) showed *singlet* signals of protons (H-2, H-2'), (H-4, H-4') (-OCH_3) and (H-7, H-7') (-CH_3) appeared at δ 7.45 (2H), δ 3.82 (6H) and δ 2.25 (6H), respectively. Aromatic protons *triplet* of *doublet* signals of protons H-4, H-4' (2H, J = 4.2, 8.1 Hz) at δ 7.04. Two aromatic protons *triplet* signals of protons H-5, H-5' (2H, J = 7.8 Hz) at δ 7.38 and *doublet* signals of protons H-6, H-6' (2H, J = 7.8 Hz) at δ 7.38. These spectroscopic data confirmed that **PJ12** is (1*E*,2*E*)-1,2-bis(1-(3-methoxyphenyl)ethylidene)-hydrazine.

Table 29 ^{1}H NMR of compound **PJ12**

Position	**δ_H (ppm), *mult, J* (Hz)**
2, 2’	7.45, *s*
3, 3’(-OCH_3)	3.82, *s*
4, 4’	7.04, *td*, 4.2,8.1
5, 5’	7.38, *t*, 7.8
6, 6’	7.47, *d*, 7.8
7, 7’(-CH_3)	2.25, *s*

3.1.13 (1*E*,2*E*)-1,2-bis(1-(3-aminophenyl)ethylidene)hydrazine (PJ13)

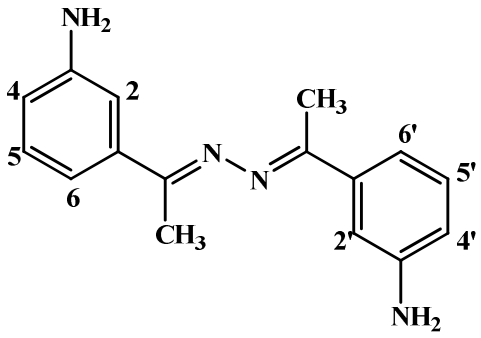

(PJ13)

Compound **PJ13** was obtained as a yellow solid (87% yield), mp. 142-143 °C. The UV-Vis absorption bands **(Figure 85)** were shown at 240 nm. The FT-IR spectrum of **PJ13** (**Figure 84**) revealed the stretching vibration of N-H stretching at 3494 cm^{-1} and the stretching vibration of aromatic C-H at 3041 cm^{-1}. The strong peak of C-H stretching vibration was observed at 2894 $cm^{-1}$and C=C stretching vibration in aromatic ring at 1522 cm^{-1}. The C-N stretching vibration was observed at 1239 cm^{-1}.

The ^{1}H NMR spectrum of **PJ13** (**Figure 86**, see **Table 30**) showed *singlet* signals of protons H-2, H-2'and H-7, H-7'(-CH_3) appeared at δ 7.24 (2H) and 2.27 (6H). Three equivalent aromatic protons *multiplet* signals of protons H-4, H-4'(2H, *J* = 7.8 Hz), *triplet* signals of protons H-5, H-5'(2H, *J* = 4.5 Hz) and *doublet* signals of protons H-6, H-6' (2H, *J* = 1.8 Hz) at δ 6.74-6.89, δ 7.22 and δ 7.30, respectively. These spectroscopic data confirmed that **PJ13** is (1*E*,2*E*)-1,2-bis(1-(3-aminophenyl)ethylidene)hydrazine.

Table 30 ^{1}H NMR of compound **PJ13**

Position	**δ_H (ppm), *mult, J* (Hz)**
2, 2’	7.24, *s*
4, 4’	6.74-6.89, *m*
5, 5’	7.22, *t*, 4.5
6, 6’	7.30, *d*,1.8
7, 7’(-CH_3)	2.27, *s*

3.1.14 (1*E*,2*E*)-1,2-bis(1-(3-nitrophenyl)ethylidene)hydrazine (PJ14)

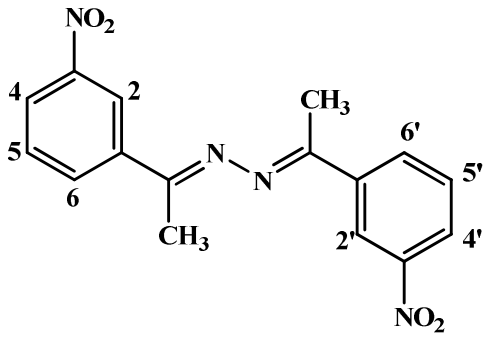

(PJ14)

Compound **PJ14** was obtained as a yellow solid (85% yield), mp. 196-198 °C. The UV-Vis absorption bands **(Figure 88)** were shown at 203 and 263 nm. The FT-IR spectrum of **PJ14** (**Figure 87**) revealed the stretching vibration of aromatic C-H and the strong peak of C-H stretching vibration was observed at 2900-2960 cm^{-1}. The strong peak of C=N stretching vibration was observed at 1611 cm^{-1}, N=O asymmetric stretching vibration at 1530 cm^{-1} and N=O symmetric stretching vibration at 1347 cm^{-1}. The C-N stretching vibration was observed at 1268 cm^{-1}.

The ^{1}H NMR spectrum of **PJ14** (**Figure 89**, see **Table 31**) showed *singlet* signals of protons H-2, H-2'and H-7, H-7'(-CH_3) appeared at δ 8.69 (2H), δ 2.37 (6H). Two equivalent aromatic protons *doublet* of *doublet* signals of protons H-4, H-4' and H-6, H-6' (4H, J = 2.1, 7.8 Hz) at δ 8.36 and δ 8.32 and *triplet* signals of protons H-5, H-5' (2H, J = 7.8 Hz) at δ 7.79. These spectroscopic data confirmed that **PJ14** is (1*E*,2*E*)-1,2-bis(1-(3-nitrophenyl)ethylidene)hydrazine.

Table 31 ^{1}H NMR of compound **PJ14**

Position	**δ_H (ppm), *mult*, *J* (Hz)**
2, 2’	8.69, *s*
4, 4’	8.36, *dd*, 2.1, 7.8
5, 5’	7.79, *t*, 7.8
6, 6’	8.32, *dd*, 2.1, 7.8
7, 7’(-CH_3)	2.37, *s*

The crystal structure and packing of **PJ14** are illustrated in **Figures 17** and **18**. The crystal and experiment data are given in **Table 32**. Bond lengths, angles and torsion angles are shown in **Table 33**. Hydrogen-bond geometry is shown in **Table 34**. The X-ray study shows that the **PJ14** crystallized out in monoclinic $P2_1/c$ space group.

The asymmetric unit of **PJ14** (**Figure 17**), contains one half-molecule of (nitrophenyl)ethanimine and the complete molecule is generated by a crystallographic inversion centre (-*x*,-*y* + 1,-*z*). The molecule is **PJ14** in an *E* configuration with respect to C7═N1 double bond [1.2803 (17) Å] with the torsion angle N1A—N1—C7—C1 = 179.92 (10)°. The methyl groups are twisted from the planes of benzene (C1–C6 and C1A–C6A) rings and their orientations can be indicated by the torsion angles (C1—C6—C7—C8 and C1A—C6A—C7A—C8A) = 24.91 (19)°. In the crystal structure (**Figure 18**), the C3—H3A···O1 interaction links the molecules into two-dimensional layers parallel to the (1 0 4) plane.

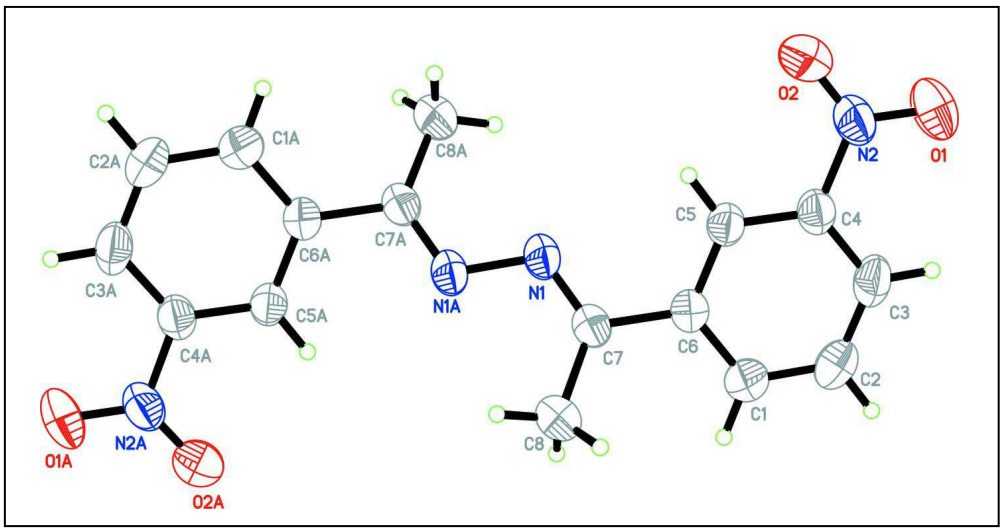

Figure 17 X-ray ORTEP diagram of the compound **PJ14**

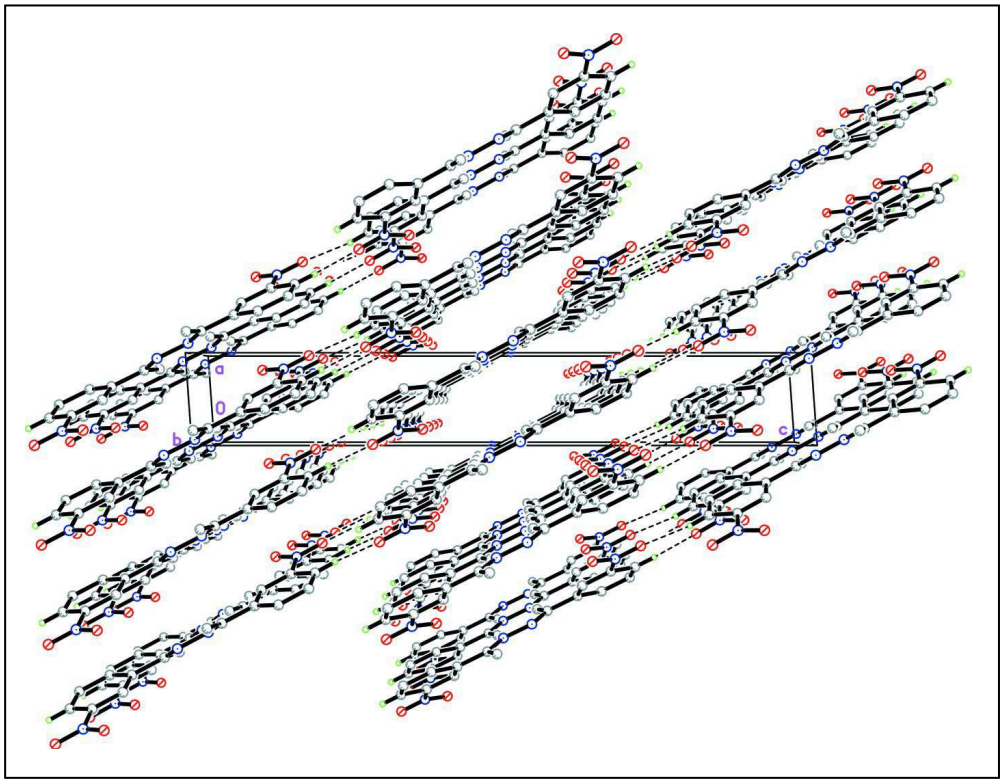

Figure 18 Packing diagram of **PJ14** viewed down the *b* axis with H-bonds shown as dashed lines.

Table 32 Crystal data of **PJ14**.

Identification code	**PJ14**
Empirical formula	$C_{16}H_{14}N_4O_4$
Formula weight	326.31
Temperature	100.0(1) K
Wavelength	0.71073 Å
Crystal system, space group	Monoclinic, $P2_1/c$
Unit cell dimensions	a = 10.7796 (18) Å α = (90)^o b = 5.2725 (9) Å β = 94.022 (1)^o c = 15.3427 (18) Å γ = (90)^o
Volume	770.37 (10) Å^3
Z, Calculated density	2, 1.407 Mg/m^3
Absorption coefficient	0.10 mm^{-1}
F(000)	340
Crystal size	0.34 × 0.17 × 0.10 mm
Theta range for data collection	2.8–28.3 ^{o}
Limiting indices	-5<=h<=5, -10<=k<=10, -37<=l<=37
Reflections collected / unique	15392 / 2254 [R(int) = 0.028]
Max. and min. transmission	0.990 and 0.966
Refinement method	Full-matrix least-squares on F^2
Data / restraints / parameters	2254 / 0 / 110
Final R indices [I>2σ(I)]	R1 = 0.047, wR2 = 0.146
Largest diff. peak and hole	0.21, -0.18 e.A^{-3}

Table 33 Bond lengths [Å], angles [°] and torsion angles [°] for **PJ14**

O1—N2	1.2121 (16)	C3—C4	1.3808 (19)
O2—N2	1.2105 (19)	C3—H3A	0.9300
N1—C7	1.2803 (17)	C4—C5	1.3756 (17)
N1—N1^{i}	1.406 (2)	C5—C6	1.3916 (18)
N2—C4	1.4663 (19)	C5—H5A	0.9300
C1—C2	1.387 (2)	C6—C7	1.4867 (17)
C1—C6	1.3930 (19)	C7—C8	1.489 (2)
C1—H1A	0.9300	C8—H8A	0.9600
C2—C3	1.374 (2)	C8—H8B	0.9600
C2—H2A	0.9300	C8—H8C	0.9600
C7—N1—N1^{i}	113.69 (14)	C4—C5—C6	119.02 (12)
O2—N2—O1	122.84 (15)	C4—C5—H5A	120.5
O2—N2—C4	118.75 (12)	C6—C5—H5A	120.5
O1—N2—C4	118.38 (14)	C5—C6—C1	118.67 (11)
C2—C1—C6	120.76 (14)	C5—C6—C7	119.49 (11)
C2—C1—H1A	119.6	C1—C6—C7	121.84 (12)
C6—C1—H1A	119.6	N1—C7—C6	115.05 (11)
C3—C2—C1	120.81 (14)	N1—C7—C8	125.53 (12)
C3—C2—H2A	119.6	C6—C7—C8	119.41 (12)
C1—C2—H2A	119.6	C7—C8—H8A	109.5
C2—C3—C4	117.74 (12)	C7—C8—H8B	109.5
C2—C3—H3A	121.1	H8A—C8—H8B	109.5
C4—C3—H3A	121.1	C7—C8—H8C	109.5
C5—C4—C3	122.99 (13)	H8A—C8—H8C	109.5
C5—C4—N2	118.04 (12)	H8B—C8—H8C	109.5
C3—C4—N2	118.94 (12)		

Table 33 Bond lengths [Å], angles [°] and torsion angles [°] for **PJ14** (continued)

C6—C1—C2—C3	1.1 (2)	C4—C5—C6—C1	0.12 (19)
C1—C2—C3—C4	−0.5 (2)	C4—C5—C6—C7	179.49 (11)
C2—C3—C4—C5	−0.3 (2)	C2—C1—C6—C5	−0.9 (2)
C2—C3—C4—N2	177.71 (14)	C2—C1—C6—C7	179.72 (13)
O2—N2—C4—C5	1.6 (2)	N1^{i}—N1—C7—C6	−179.90 (13)
O1—N2—C4—C5	179.73 (15)	N1^{i}—N1—C7—C8	−0.7 (2)
O2—N2—C4—C3	−176.58 (16)	C5—C6—C7—N1	24.84 (17)
O1—N2—C4—C3	1.6 (2)	C1—C6—C7—N1	−155.80 (13)
C3—C4—C5—C6	0.5 (2)	C5—C6—C7—C8	−154.43 (14)
N2—C4—C5—C6	−177.55 (11)	C1—C6—C7—C8	24.9 (2)

Symmetry code: (i) −*x*, −*y*+1, −*z*.

Table 34 Hydrogen-bond for **PJ14** (Å,°)

D—H···*A*	**D—H**	**H···*A***	**D···*A***	**D—H···*A***
C3—H3A···O1^{ii}	0.93	2.57	3.239 (2)	129

Symmetry code: (ii) −*x*+2, *y*+1/2, −*z*+1/2.

3.1.15 (1*E*,2*E*)-1,2-bis(1-(3-chlorophenyl)ethylidene)hydrazine (PJ15)

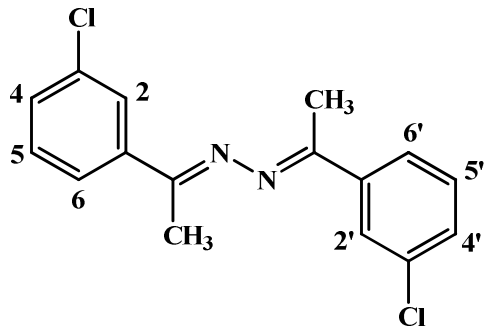

(PJ15)

Compound **PJ15** was obtained as a yellow solid (84% yield), mp. 83-85 °C. The UV-Vis absorption bands **(Figure 91)** were shown at 204 and 269 nm. The FT-IR spectrum of **PJ15** (**Figure 90**) revealed the stretching vibration of aromatic C-H and the strong peak of C-H stretching vibration was observed at 2900-3000 cm^{-1}. The strong peak of C=N stretching vibration was observed at 1591 $cm^{-1}$and C=C stretching vibration in aromatic ring at 1556 cm^{-1}. The C-N stretching vibration was observed at 1105 $cm^{-1}$and C-Cl stretching vibration in aromatic ring at 795 cm^{-1}.

The ^{1}H NMR spectrum of **PJ15** (**Figure 92**, see **Table 35**) showed *singlet* signals of protons H-7, H-7'(-CH_3) appeared at δ 2.32 (6H). Four aromatic protons *triplet* signals of protons H-2, H-2'(2H, J = 2.1 Hz), *doublet* signals of protons H-4, H-4'(2H, J = 7.2 Hz), *triplet* signals of protons H-5, H-5'(2H, J = 7.2 Hz) and *triplet* signals of protons H-6, H-6'(2H, J = 7.2 Hz) at δ 7.93, δ 7.79, δ 7.37 and δ 7.41, respectively. These spectroscopic data confirmed that **PJ15** is (1*E*,2*E*)-1,2-bis(1-(3-chlorophenyl)ethylidene)hydrazine.

Table 35 ^{1}H NMR of compound **PJ15**

Position	**δ_H (ppm), *mult*, *J* (Hz)**
2, 2’	7.93, *t*, 2.1
4, 4’	7.79, *d*, 7.2
5, 5’	7.37, *t*, 7.2
6, 6’	7.41, *t*, 7.2
7, 7’(-CH_3)	2.32, *s*

The crystal structure and packing of **PJ15** are illustrated in **Figures 19** and **20**. The crystal and experiment data are given in **Table 36**. Bond lengths, angles and torsion angles are shown in **Table 37**. Hydrogen-bond geometry is shown in **Table 38**. The X-ray study shows that the **PJ15** crystallized out in monoclinic $P2_1/c$ space group.

The molecular structure of **PJ15** is shown in **Figure 19**. The asymmetric unit contains half a molecule and the complete molecule is generated by a crystallographic inversion center at -*x*, 1-*y*, 2-*z*. The molecule exists in an *E*,*E* configuration with respect to the two ethylidene C═N bonds [1.279 (3) Å] and the torsion angle N1A–N1–C7–C1 = 179.8 (2)°. The molecule is essentially planar with the dihedral angle between the two benzene rings of 0.02 (11)°. The diethylidene-hydrazine moiety (C7/C8/N1/N1A/C7A/C8A) is planar with the r.m.s of 0.0015 (2) Å. This central C(methyl)—C═N—N═C—C(methyl) mean plane makes the dihedral angle of 5.57 (12)° with the adjacent benzene rings. Although no clasical hydrogen bonds or weak interactions were observed in the crystal structure, the crystal packing is shown in **Figure 20.**

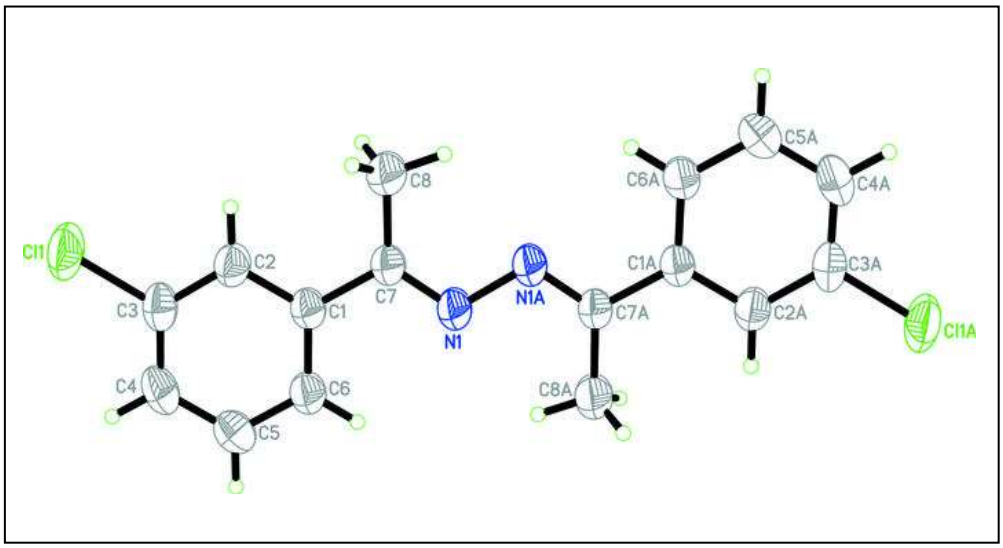

Figure 19 X-ray ORTEP diagram of the compound **PJ15**

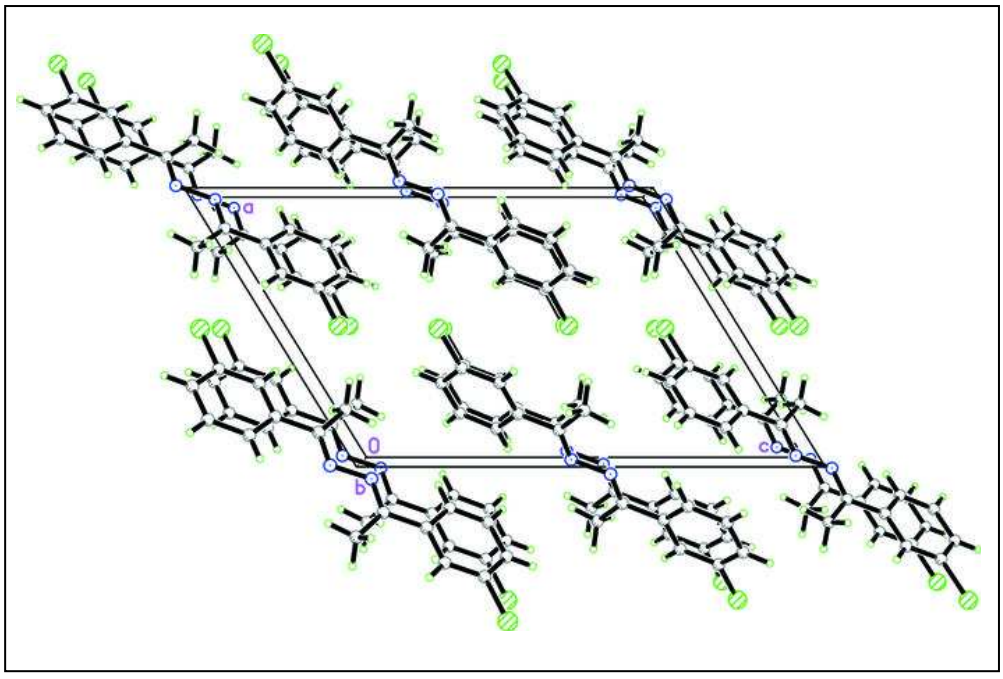

Figure 20 Packing diagram of **PJ15** viewed down the *b* axis.

Table 36 Crystal data of **PJ15**.

Identification code	**PJ15**
Empirical formula	$C_{16}H_{14}C_{l2}N_2$
Formula weight	305.19
Temperature	100.0(1) K
Wavelength	0.71073 Å
Crystal system, space group	Monoclinic, $P2_1/c$
Unit cell dimensions	a = 10.7796 (18) Å α = (90)^o b = 5.2725 (9) Å β = 121.540 (8)^o c = 15.3427 (18) Å γ = (90)^o
Volume	743.2 (2) Å^3
Z, Calculated density	2, 1.364 Mg/m^3
Absorption coefficient	0.43 mm^{-1}
F(000)	316
Crystal size	0.31 × 0.15 × 0.11 mm
Theta range for data collection	2.2–29.0 ^{o}
Limiting indices	-14<=h<=14, -7<=k<=6, -20<=l<=20
Reflections collected / unique	7616 / 1970 [R(int) = 0.028]
Max. and min. transmission	0.957 and 0.880
Refinement method	Full-matrix least-squares on F^2
Data / restraints / parameters	7616 / 0 / 202
Final R indices [I>2σ(I)]	R1 = 0.051, wR2 = 0.180
Largest diff. peak and hole	0.46, -0.41 e.A^{-3}

Table 37 Bond lengths [Å], angles [°] and torsion angles [°] for **PJ15**

Cl1—C3	1.743 (2)	C4—C5	1.380 (3)
N1—C7	1.279 (3)	C4—H4A	0.9300
N1—N1^{i}	1.406 (3)	C5—C6	1.383 (3)
C1—C2	1.395 (3)	C5—H5A	0.9300
C1—C6	1.399 (3)	C6—H6A	0.9300
C1—C7	1.486 (3)	C7—C8	1.491 (3)
C2—C3	1.382 (3)	C8—H8A	0.9600
C2—H2A	0.9300	C8—H8B	0.9600
C3—C4	1.380 (3)	C8—H8C	0.9600
C7—N1—N1^{i}	113.9 (2)	C4—C5—H5A	119.6
C2—C1—C6	118.78 (18)	C6—C5—H5A	119.6
C2—C1—C7	120.47 (19)	C5—C6—C1	120.5 (2)
C6—C1—C7	120.74 (18)	C5—C6—H6A	119.8
C3—C2—C1	119.3 (2)	C1—C6—H6A	119.8
C3—C2—H2A	120.3	N1—C7—C1	115.82 (18)
C1—C2—H2A	120.3	N1—C7—C8	124.68 (19)
C4—C3—C2	122.2 (2)	C1—C7—C8	119.49 (18)
C4—C3—Cl1	119.20 (16)	C7—C8—H8A	109.5
C2—C3—Cl1	118.63 (18)	C7—C8—H8B	109.5
C5—C4—C3	118.4 (2)	H8A—C8—H8B	109.5
C5—C4—H4A	120.8	C7—C8—H8C	109.5
C3—C4—H4A	120.8	H8A—C8—H8C	109.5
C4—C5—C6	120.9 (2)	H8B—C8—H8C	109.5
C6—C1—C2—C3	0.3 (3)	C2—C1—C6—C5	−0.6 (3)
C7—C1—C2—C3	−178.95 (19)	C7—C1—C6—C5	178.6 (2)
C1—C2—C3—C4	0.2 (3)	N1^{i}—N1—C7—C1	179.8 (2)
C1—C2—C3—Cl1	−179.32 (16)	N1^{i}—N1—C7—C8	−0.5 (4)

Table 37 Bond lengths [Å], angles [°] and torsion angles [°] for **PJ15** (continued)

C2—C3—C4—C5	−0.4 (3)	C2—C1—C7—N1	−175.2 (2)
Cl1—C3—C4—C5	179.15 (17)	C6—C1—C7—N1	5.6 (3)
C3—C4—C5—C6	0.0 (4)	C2—C1—C7—C8	5.1 (3)
C4—C5—C6—C1	0.5 (4)	C6—C1—C7—C8	−174.1 (2)

Symmetry code: (i) −x, −y+1, −z+2.

3.1.17 (1*E*,2*E*)-1,2-bis(1-(3-bromophenyl)ethylidene)hydrazine (PJ16)

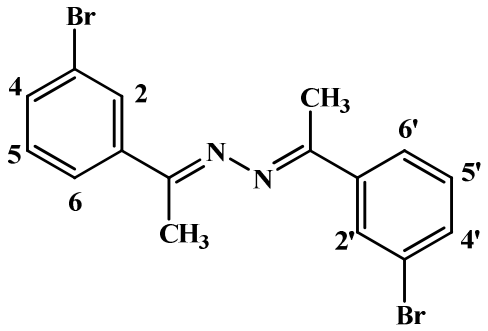

(PJ16)

Compound **PJ16** was obtained as a white solid (79% yield), mp. 85-86 °C. The UV-Vis absorption bands (**Figure 94**) were shown at 209 and 269 nm. The FT-IR spectrum of **PJ16** (**Figure 93**) revealed the stretching vibration of aromatic C-H at 2997 cm^{-1} and the strong peak of C-H stretching vibration was observed at 2938 cm^{-1}. The strong peak of C=N stretching vibration was observed at 1601 $cm^{-1}$and C=C stretching vibration in aromatic ring at 1551 cm^{-1}. The C-Br stretching vibration was observed at 641 cm^{-1}.

The ^{1}H NMR spectrum of **PJ16** (**Figure 95**, see **Table 39**) showed *singlet* signals of protons H-7, H-7'(-CH_3) appeared at δ 2.25 (6H) and aromatic protons *triplet* signals of protons H-2, H-2'(2H, J = 1.8 Hz), *doublet* signals of protons H-4, H-4'(2H, J = 8.1 Hz), *triplet* signals of protons H-5, H-5'(2H, J = 8.1 Hz) and *doublet* signals of protons H-6, H-6'(2H, J = 8.1 Hz) at δ8.06, δ7.90, δ7.44 and δ7.67, respectively. These spectroscopic data confirmed that **PJ16** is (1*E*,2*E*)-1,2-bis(1-(3-bromophenyl) ethylidene)hydrazine**.**

Table 38 ^{1}H NMR of compound **PJ16**

Position	**δ_H (ppm), *mult*, *J* (Hz)**
2, 2'	8.06, *t*, 1.8
4, 4'	7.90, *d*, 8.1
5, 5'	7.44, *t*, 8.1
6, 6'	7.67, *d*, 8.1
7, 7'(-CH_3)	2.25, *s*

3.1.17 (1*E*,2*E*)-1,2-bis(1-(3-fluorophenyl)ethylidene)hydrazine (PJ17)

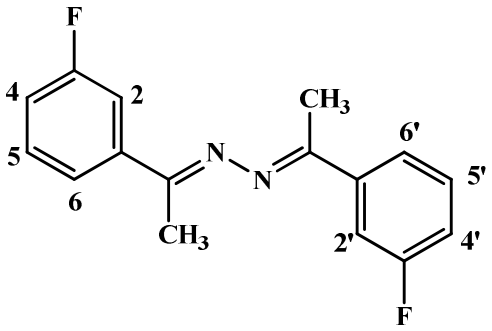

(PJ17)

Compound **PJ17** was obtained as a yellow solid (80% yield), mp. 72-73 °C. The UV-Vis absorption bands **(Figure 97)** were shown at 267 nm. The FT-IR spectrum of **PJ17** (**Figure 96**) revealed the stretching vibration of aromatic C-H at 3089 cm^{-1} and the strong peak of C-H stretching vibration was observed at 2962 cm^{-1}. The strong peak of C=N stretching vibration was observed at 1691 $cm^{-1}$and C=C stretching vibration in aromatic ring at 1578 cm^{-1}. The C-F stretching vibration was observed at 1267 cm^{-1}.

The ^{1}H NMR spectrum of **PJ17** (**Figure 98**, see **Table 40**) showed *singlet* signals of protons H-2, H-2' and H-7, H-7'(-CH_3) appeared at δ 7.52 (2H) and 2.16 (6H) and aromatic protons *doublet* signals of protons H-4, H-4' (2H, J = 8.4 Hz), *multiplet* signals of protons H-5, H-5'(2H) and H-6, H-6' (2H) at δ 7.49, δ 7.20-7.28 and δ 6.88-7.10, respectively. These spectroscopic data confirmed that **PJ17** is (1*E*,2*E*)-1,2-bis(1-(3-fluorophenyl)ethylidene)hydrazine.

Table 39 ^{1}H NMR of compound **PJ17**

Position	**δ_H (ppm), *mult*, *J* (Hz)**
2, 2’	7.52, *s*
4, 4’	7.49, *d*, 8.4
5, 5’	7.20-7.28, *m*
6, 6’	6.88-7.10, *m*
7, 7’(-CH_3)	2.16, *s*

3.2 Absorption spectra and fluorescence properties of hydrazone derivatives

3.2.1 Absorption spectra of hydrazone derivatives

Absorption maxima of hydrazones were showed in **Figure 49** (**PJ1**), **52** (**PJ2**), **55** (**PJ3**), **58** (**PJ4**), **61** (**PJ5**), **64**, (**PJ6**), **67** (**PJ7**), **70** (**PJ8**), **73** (**PJ9**), **76** (**PJ10**), **79** (**PJ11**), **82** (**PJ12)**, **85** (**PJ13**), **88** (**PJ14**), **91** (**PJ15**)**, 94** (**PJ16**), **97** (**PJ17)**. The summarized of maxima absorption wavelength (λ_{max}) of hydrazones were showed in **Table 40**. The absorption spectra of compounds have been recorded in $CHCl_3$ with the concentration of 5 μM. Several absorption peaks could be observed in the wavelength range from 200-455 nm. It can be seen that the spectral shapes are similar due to their similar structures.

Table 40 Absorption maxima of hydrazone derivatives

Compound	**Absorption maxima, λ_{max} (nm)**
PJ1	270, 379
PJ2	205, 342
PJ3	211, 335
PJ4	227, 371
PJ5	206, 264, 369
PJ6	248, 287
PJ7	238, 379
PJ8	235
PJ9	242
PJ10	207
PJ11	223, 306
PJ12	222, 267
PJ13	240
PJ14	203, 263
PJ15	267
PJ16	204, 269
PJ17	209, 269

3.2.2 Emission spectra of hydrazone derivatives

In the preliminary method to study the fluorescent properties, the emission in fluorescence determination was selected to find the compounds which show the considerable fluorescent property.

3.2.2.1 (1*E*,2*E*)-1,2-bis(2,4,5-trimethoxybenzylidene)hydrazine (PJ1)

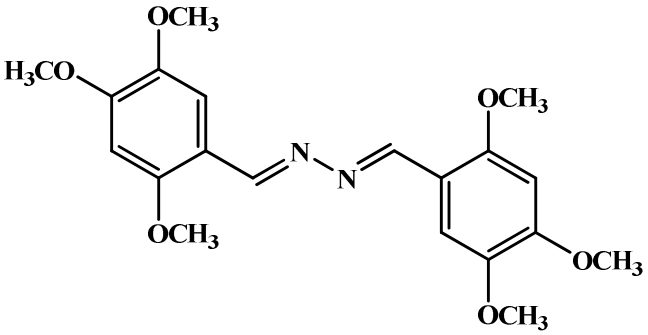

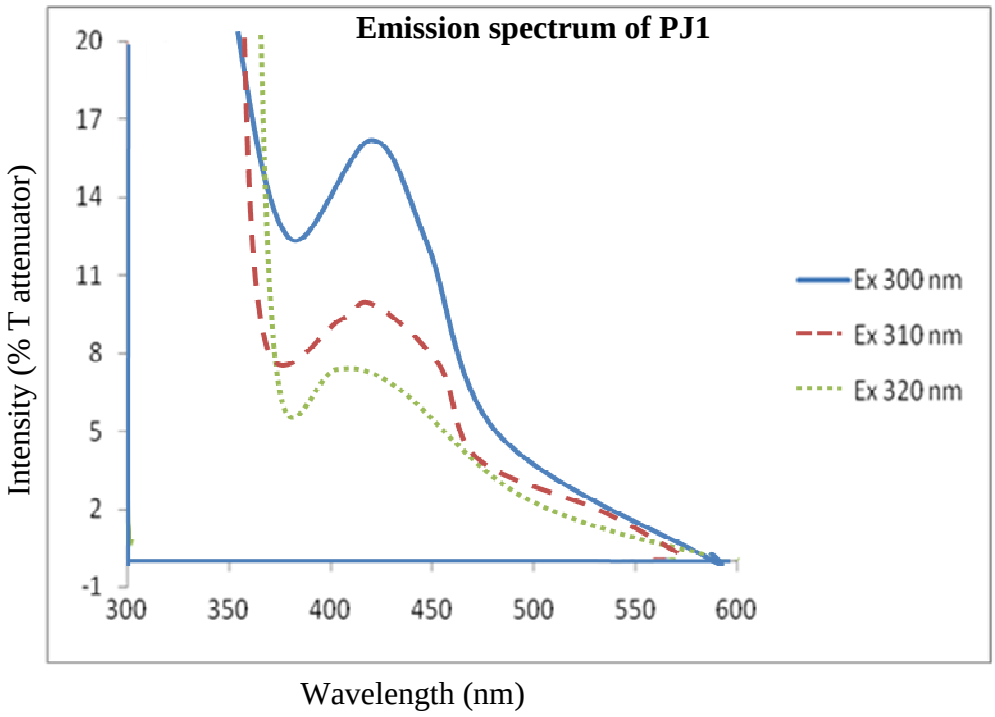

Figure 21 Emission spectrum of 5 μM **PJ1** in $CHCl_3$ at room temperature in %T attenuator mode and slit 10:10.

The emission fluorescence spectrum of **PJ1** was shown in **Figure 21**. Compound **PJ1** shows the fluorescent property which clearly seen in the appearance of fluorescence emission spectrum. The emission spectrum of **PJ1** was observed in the range of 370-570 nm. It was found that **PJ1** exhibits fluorescence with the maximum emission at 413 nm when was excited at 300 nm in $CHCl_3$.

3.2.2.2 *(1E,2E)*-1,2-bis(2,4,6-trimethoxybenzylidene)hydrazine (PJ2)

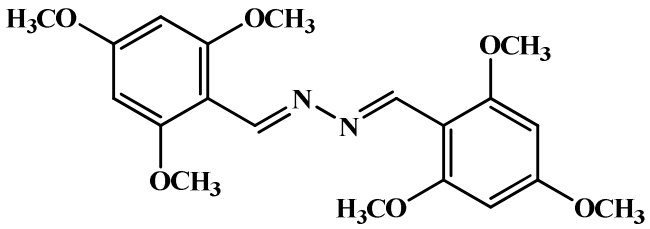

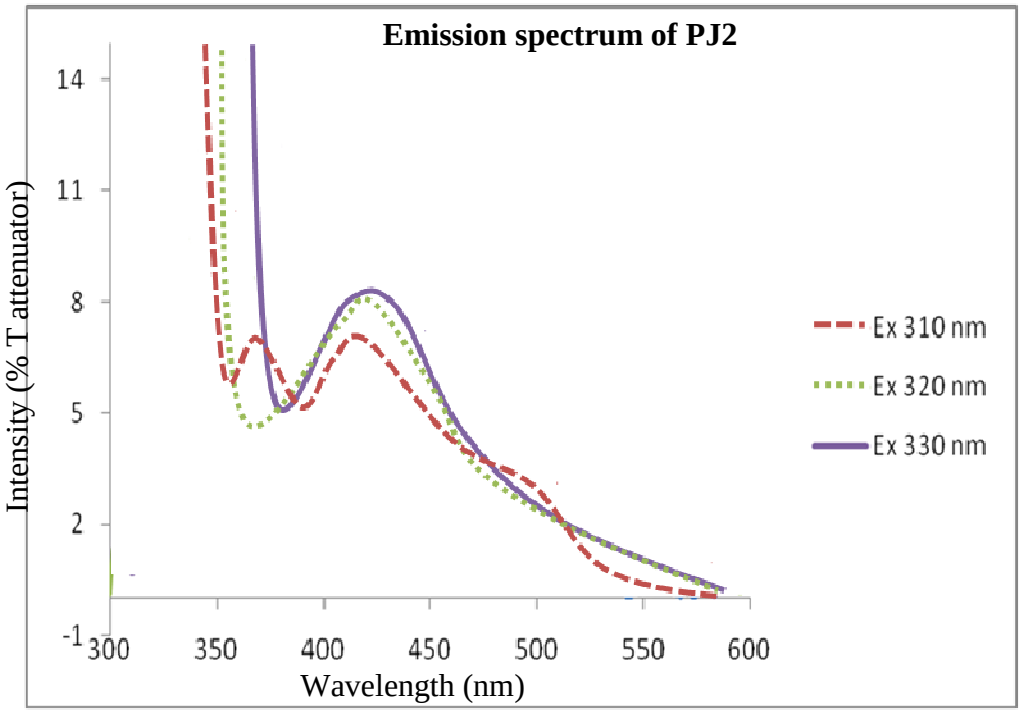

Figure 22 Emission spectrum of 5 μM **PJ2** in $CHCl_3$ at room temperature in %T attenuator mode and slit 10:10.

The emission fluorescence spectrum of **PJ2** was shown in **Figure 22**. Compound **PJ2** shows the fluorescent property which seen in the appearance of fluorescence emission spectrum. The emission spectrum of **PJ2** was observed in the range of 360-570 nm. It was found that **PJ2** exhibits fluorescence with the maximum emission at 412 nm when was excited at 330 nm in $CHCl_3$.

. **3.2.2.3 *(1E,2E)*-1,2-bis(3,4,5-trimethoxybenzylidene)hydrazine (PJ3)**

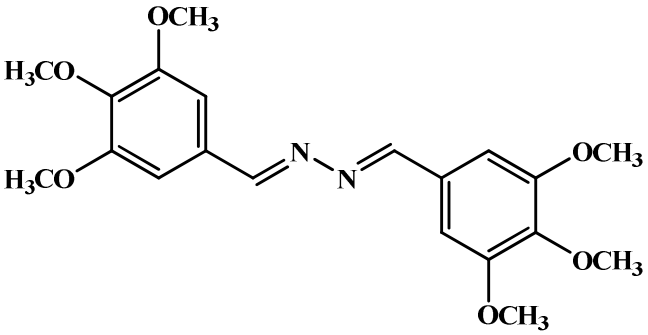

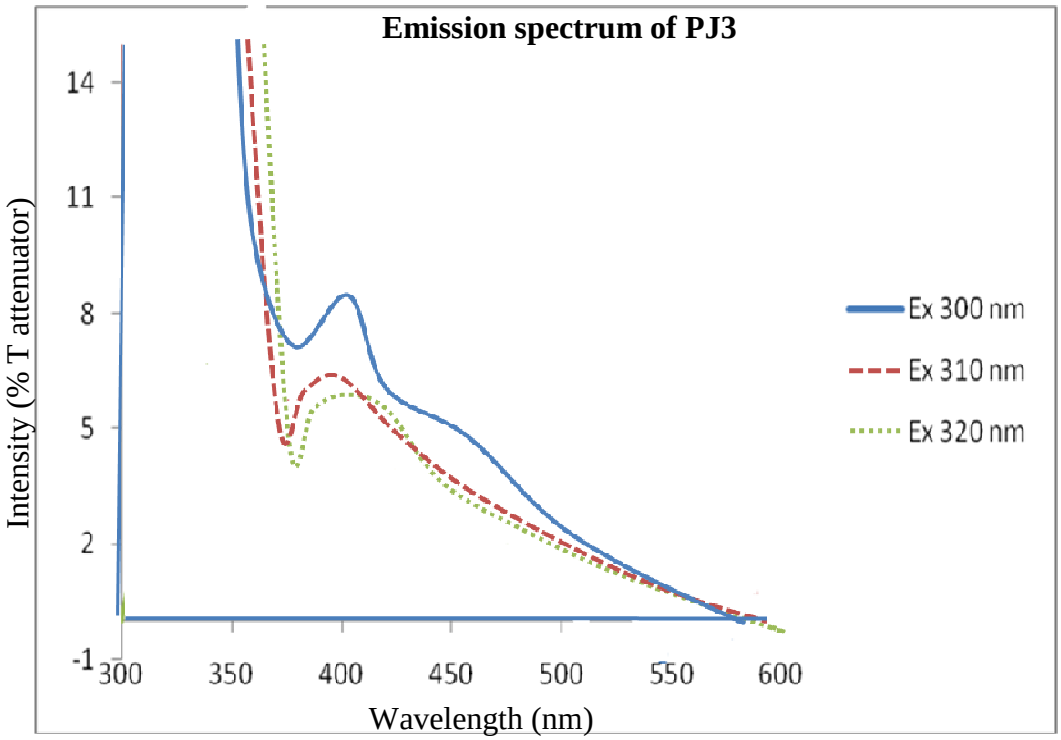

Figure 23 Emission spectrum of 5 μM **PJ3** in $CHCl_3$ at room temperature in %T attenuator mode and slit 10:10.

The emission fluorescence spectrum of **PJ3** was shown in **Figure 23**. Compound **PJ5** shows the fluorescent property which clearly seen in the appearance of fluorescence emission spectrum. The emission spectrum of **PJ3** was observed in

the range of 370-570 nm. It was found that **PJ3** exhibits fluorescence with the maximum emission at 411 nm when was excited at 300 nm in $CHCl_3$.

3.2.2.4 *(1E,2E)*-1,2-bis(3-hydroxy-4-nitrobenzylidene)hydrazine (PJ4)

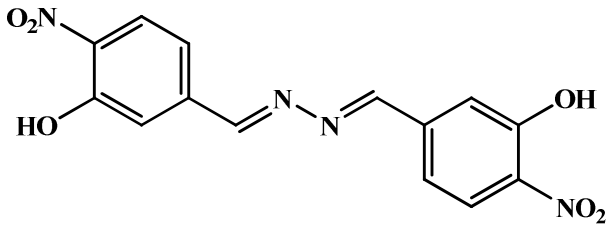

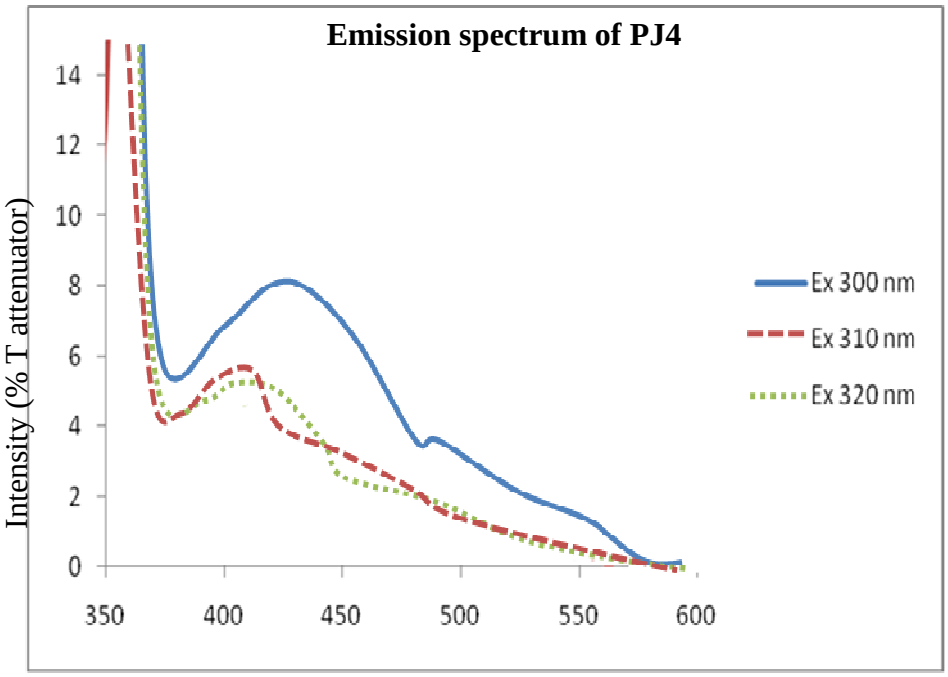

Figure 24 Emission spectrum of 5 μM **PJ4** in $CHCl_3$ at room temperature in %T attenuator mode and slit 10:10.

The emission fluorescence spectrum of **PJ4** was shown in **Figure 24**. Compound **PJ4** shows the fluorescent property which clearly seen in the appearance of fluorescence emission spectrum. The emission spectrum of **PJ4** was observed in the range of 370-590 nm. It was found that **PJ4** exhibits fluorescence with the emission at 400-430 nm when was excited at 300-320 nm in $CHCl_3$.

3.2.2.5 *(1E,2E)*-1,2-bis(4-hydroxy-3-nitrobenzylidene)hydrazine (PJ5)

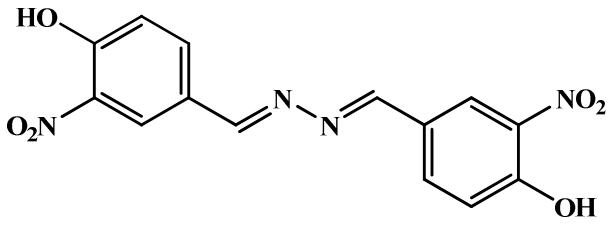

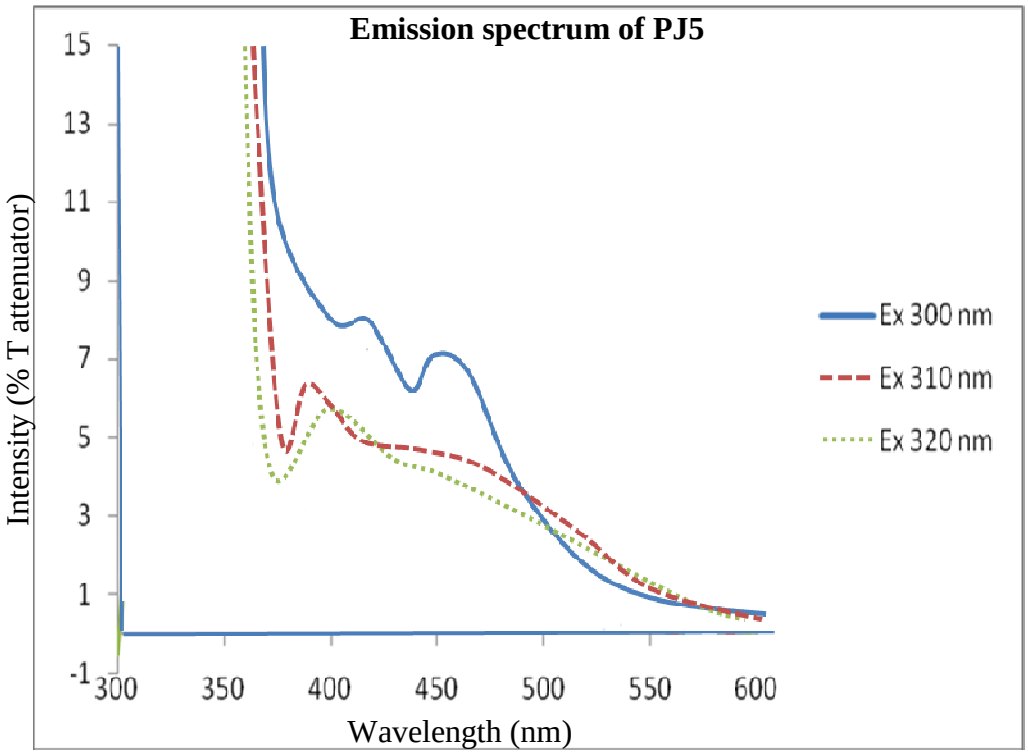

Figure 25 Emission spectrum of 5 μM **PJ5** in $CHCl_3$ at room temperature in %T attenuator mode and slit 10:10.

The pre-scan of excitation and emission fluorescence spectrum of **PJ5** was shown in **Figure 25**. Compound **PJ5** shows the fluorescent property which clearly seen in the appearance of fluorescence emission spectrum. The emission spectrum of **PJ5** was observed in the range of 360-580 nm. It was found that **PJ5**

exhibits fluorescence with the emission at 400-450 nm when was excited at 300-320 nm in $CHCl_3$.

3.2.2.6 (1*E*,2*E*)-1,2-bis(1-(2-methoxyphenyl)ethylidene)hydrazine (PJ6)

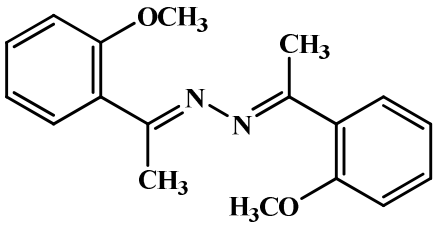

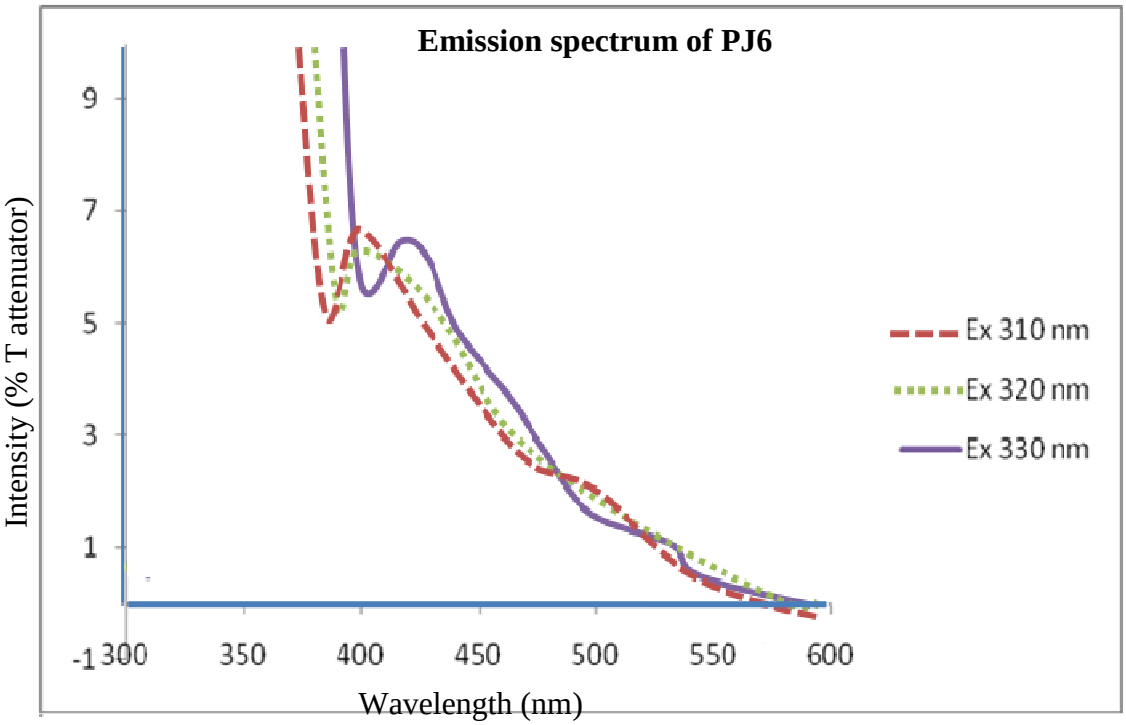

Figure 26 Emission spectrum of 5 μM **PJ6** in $CHCl_3$ at room temperature in %T attenuator mode and slit 10:10**.**

The emission fluorescence spectrum of **PJ6** was shown in **Figure 26**. Compound **PJ6** shows the fluorescent property which clearly seen in the appearance of fluorescence emission spectrum. The emission spectrum of **PJ6** was observed in

the range of 370-570 nm. It was found that **PJ6** exhibits fluorescence with the emission at 390-420 nm when was excited at 310-330 nm in $CHCl_3$.

3.2.2.7 (1*E*,2*E*)-1,2-bis(1-(2-aminophenyl)ethylidene)hydrazine (PJ7)

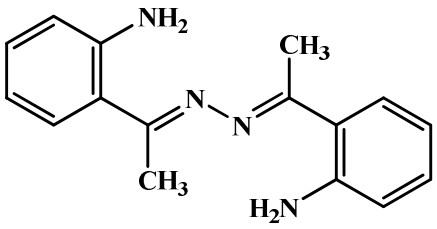

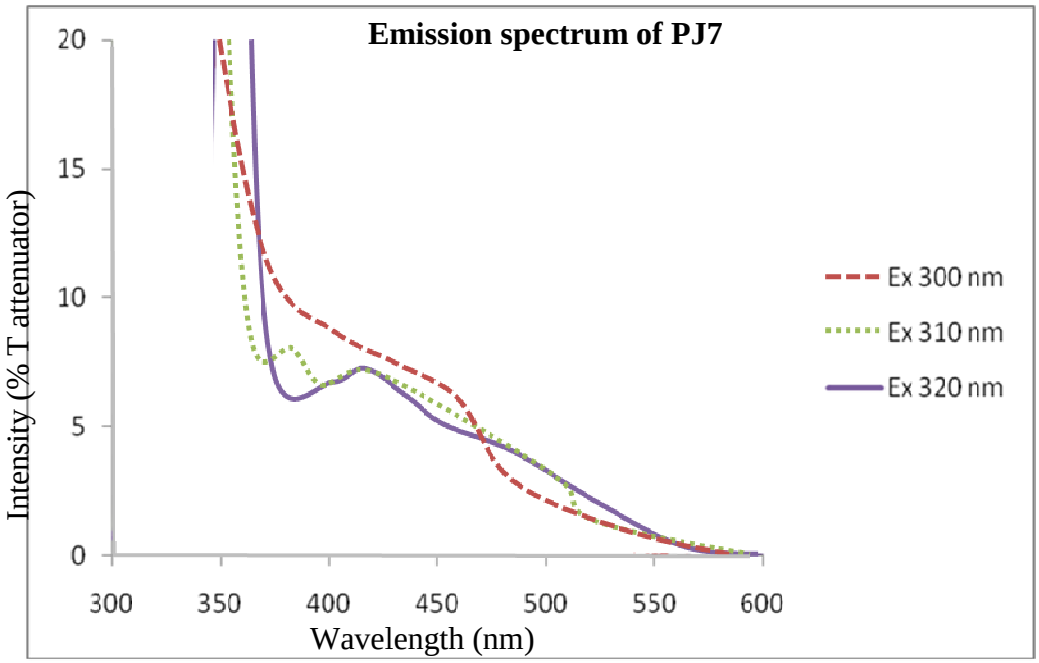

Figure 27 Emission spectrum of 5 μM **PJ7** in $CHCl_3$ at room temperature in %T attenuator mode and slit 10:10.

The emission fluorescence spectrum of **PJ7** was shown in **Figure 27**. Compound **PJ7** shows the fluorescent property which clearly seen in the appearance of fluorescence emission spectrum. The emission spectrum of **PJ7** was observed in

the range of 370-570 nm. It was found that **PJ7** exhibits fluorescence with the emission at 390-420 nm when was excited at 300-320 nm in $CHCl_3$.

3.2.2.8 (1*E*,2*E*)-1,2-bis(1-(2-nitrophenyl)ethylidene)hydrazine (PJ8)

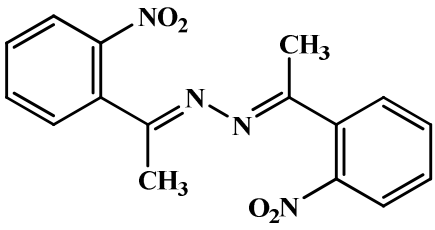

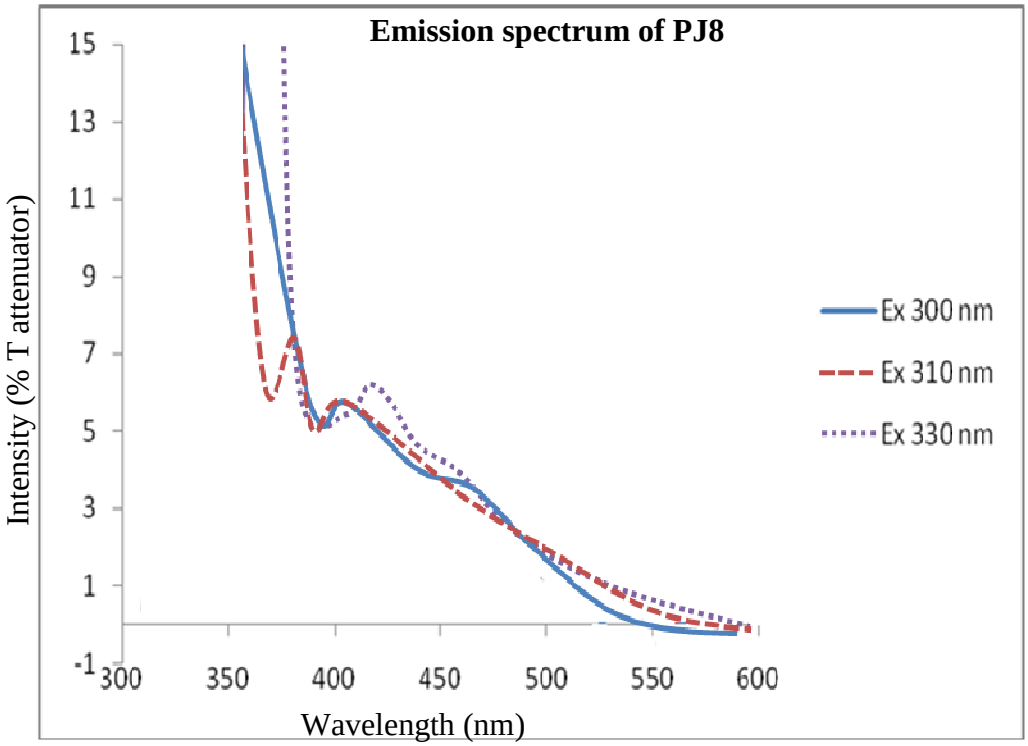

Figure 28 Emission spectrum of 5 μM **PJ8** in $CHCl_3$ at room temperature in %T attenuator mode and slit 10:10.

The emission fluorescence spectrum of **PJ8** was shown in **Figure 28**. Compound **PJ8** shows the fluorescent property which clearly seen in the appearance

of fluorescence emission spectrum. The emission spectrum of **PJ8** was observed in the range of 380-570 nm. It was found that **PJ8** exhibits fluorescence with the emission at 390-420 nm when was excited at 300-330 nm in $CHCl_3$.

3.2.2.9 (1*E*,2*E*)-1,2-bis(1-(2-chlorophenyl)ethylidene)hydrazine (PJ9)

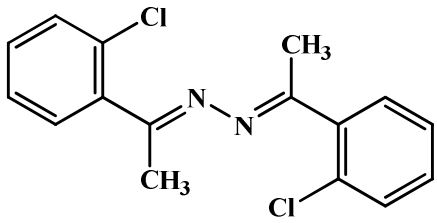

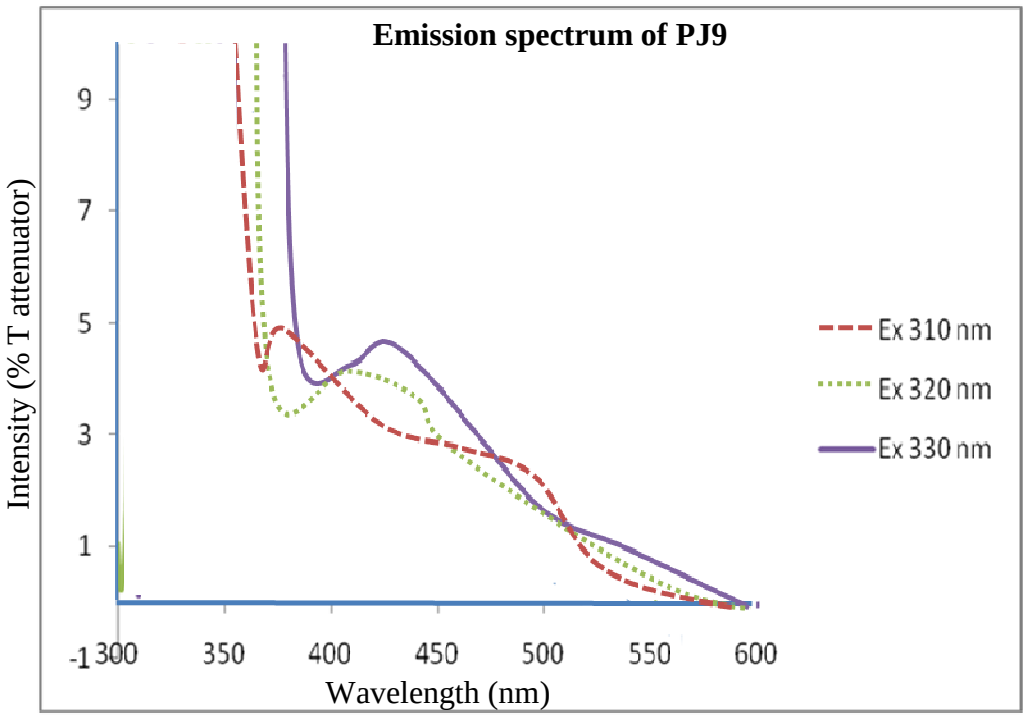

Figure 29 Emission spectrum of 5 μM **PJ9** in $CHCl_3$ at room temperature in %T attenuator mode and slit 10:10.

The emission fluorescence spectrum of **PJ9** was shown in **Figure 29**. Compound **PJ9** shows the fluorescent property which clearly seen in the appearance

of fluorescence emission spectrum. The emission spectrum of **PJ9** was observed in the range of 370-570 nm. It was found that **PJ9** exhibits fluorescence with the emission at 390-420 nm when was excited at 310-330 nm in $CHCl_3$.

3.2.2.10 (1*E*,2*E*)-1,2-bis(1-(2-bromophenyl)ethylidene)hydrazine (PJ10)

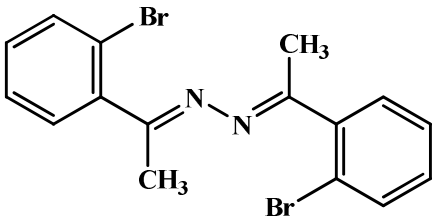

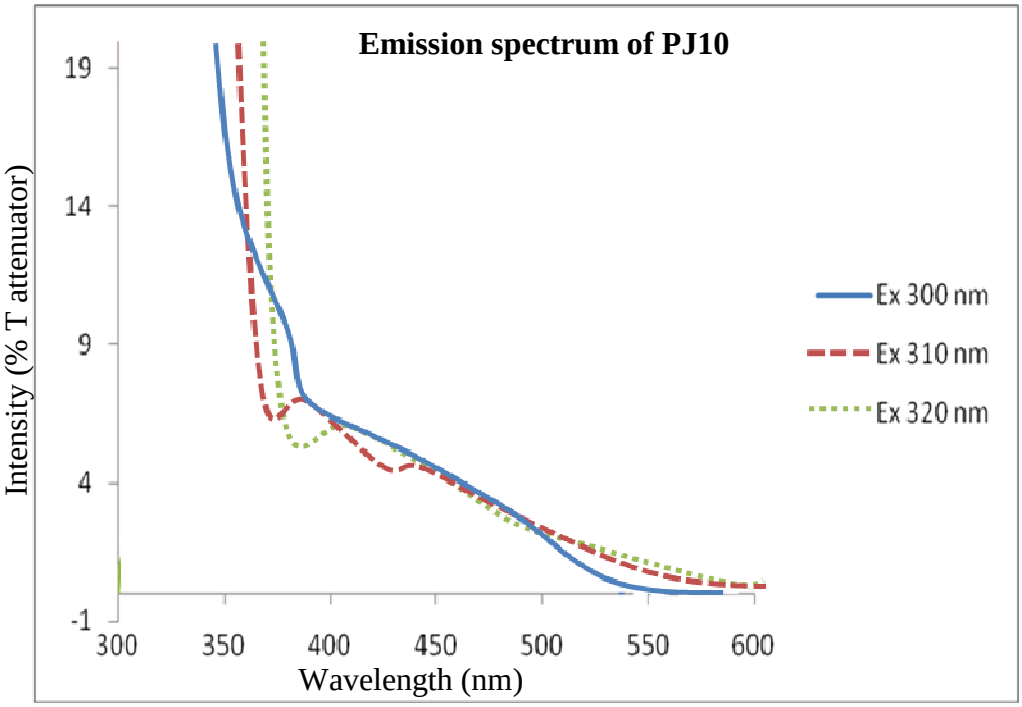

Figure 30 Emission spectrum of 5 μM **PJ10** in $CHCl_3$ at room temperature in %T attenuator mode and slit 10:10.

The emission fluorescence spectrum of **PJ10** was shown in **Figure 30**. Compound **PJ10** shows the fluorescent property which clearly seen in the appearance

of fluorescence emission spectrum. The emission spectrum of **PJ10** was observed in the range of 370-560 nm. It was found that **PJ10** exhibits fluorescence with the emission at 390-410 nm when was excited at 300-320 nm in $CHCl_3$.

3.2.2.11 (1*E*,2*E*)-1,2-bis(1-(4-hydroxyphenyl)ethylidene)hydrazine (PJ11)

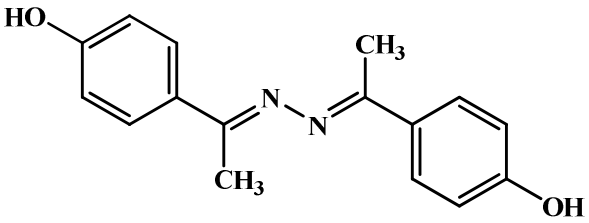

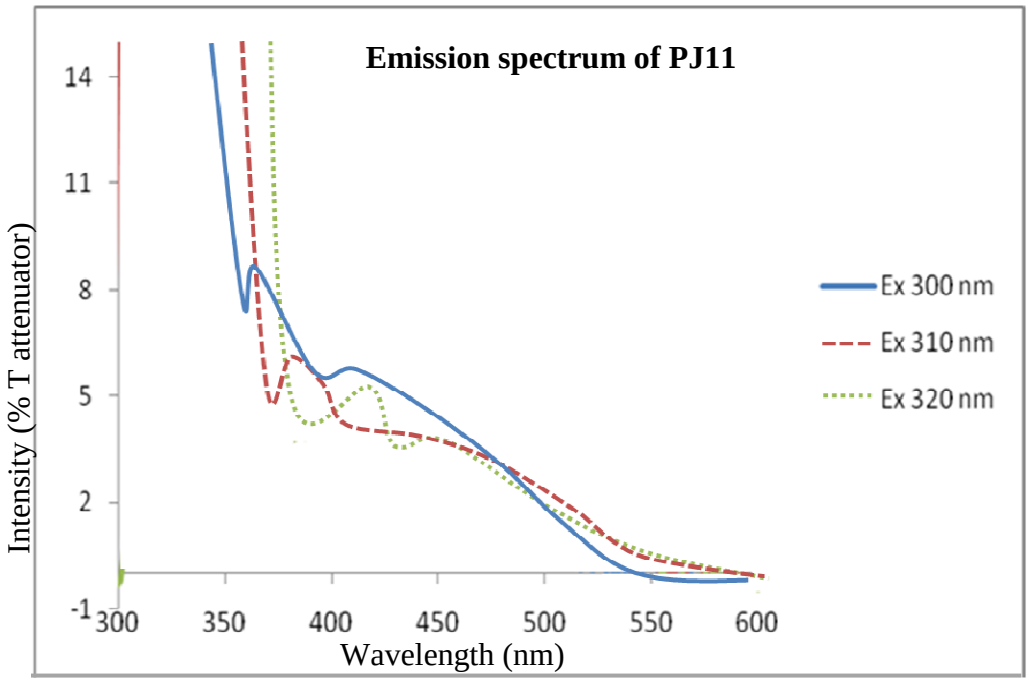

Figure 31 Emission spectrum of 5 µM **PJ11** in $CHCl_3$ at room temperature in %T attenuator mode and slit 10:10.

The emission fluorescence spectrum of **PJ11** was shown in **Figure 31**. Compound **PJ11** shows the fluorescent property which clearly seen in the appearance

of fluorescence emission spectrum. The emission spectrum of **PJ11** was observed in the range of 360-570 nm. It was found that **PJ11** exhibits fluorescence with the emission at 380-410 nm when was excited at 300-320 nm in $CHCl_3$.

3.2.2.12 (1*E*,2*E*)-1,2-bis(1-(3-methoxyphenyl)ethylidene)hydrazine (PJ12)

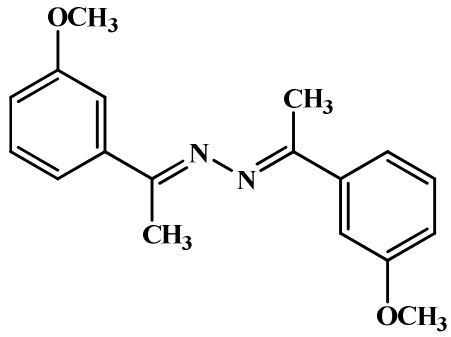

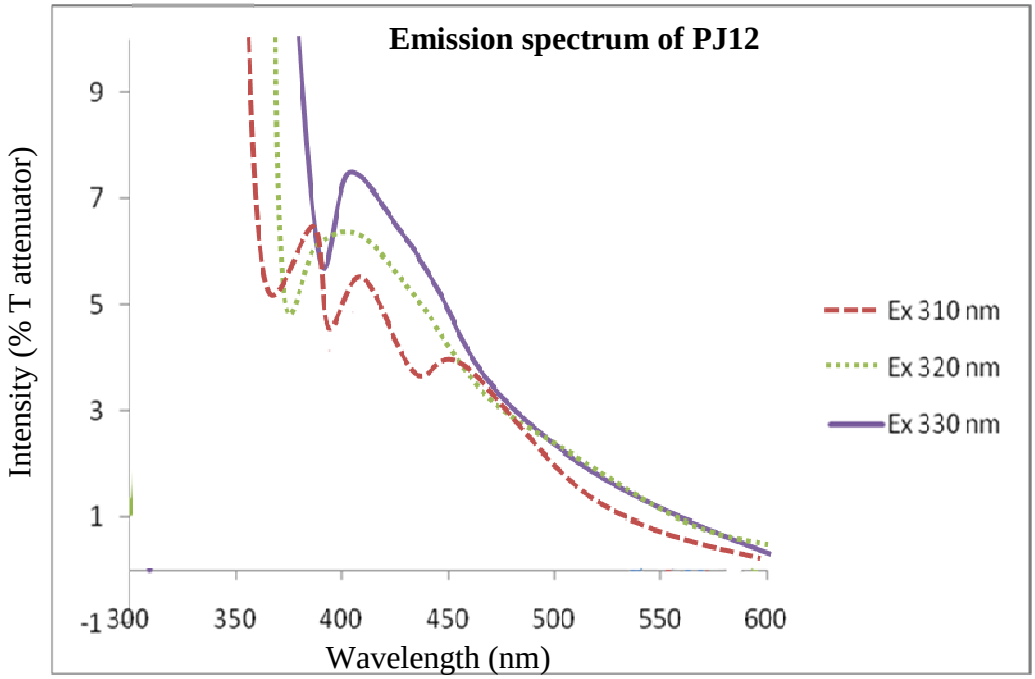

Figure 32 Emission spectrum of 5 μM **PJ12** in $CHCl_3$ at room temperature in %T attenuator mode and slit 10:10.

The emission fluorescence spectrum of **PJ12** was shown in **Figure 32**. Compound **PJ12** the fluorescent property which clearly seen in the appearance of fluorescence emission spectrum. The emission spectrum of **PJ12** was observed in the range of 370-590 nm. It was found that **PJ12** exhibits fluorescence with the emission at 380-410 nm when was excited at 310-330 nm in $CHCl_3$.

3.2.2.13 (1*E*,2*E*)-1,2-bis(1-(3-aminophenyl)ethylidene)hydrazine (PJ13)

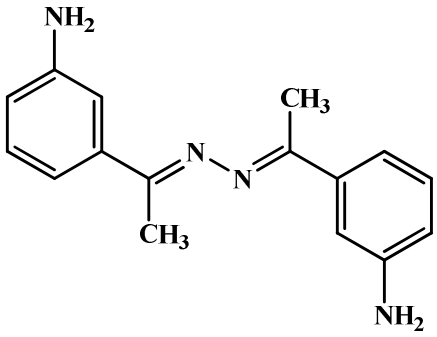

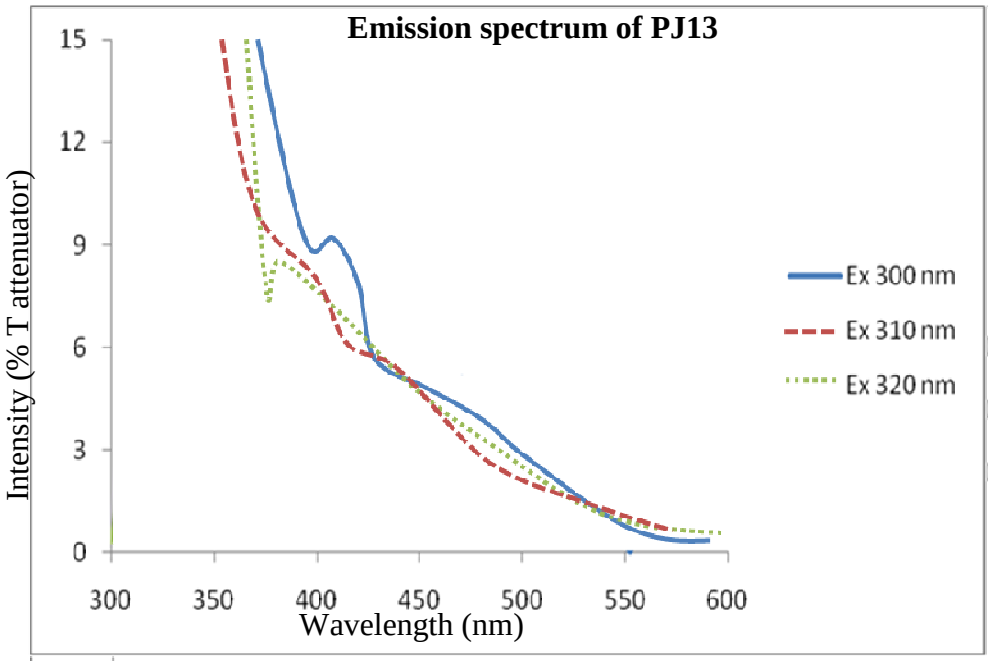

Figure 33 Emission spectrum of 5 µM **PJ13** in $CHCl_3$ at room temperature in %T attenuator mode and slit 10:10.

The emission fluorescence spectrum of **PJ13** was shown in **Figure 33**. Compound **PJ13** shows the fluorescent property which clearly seen in the appearance of fluorescence emission spectrum. The emission spectrum of **PJ13** was observed in the range of 380-560 nm. It was found that **PJ13** exhibits fluorescence with the emission at 390-420 nm when was excited at 300-320 nm in $CHCl_3$.

3.2.2.14 (1*E*,2*E*)-1,2-bis(1-(3-nitrophenyl)ethylidene)hydrazine (PJ14)

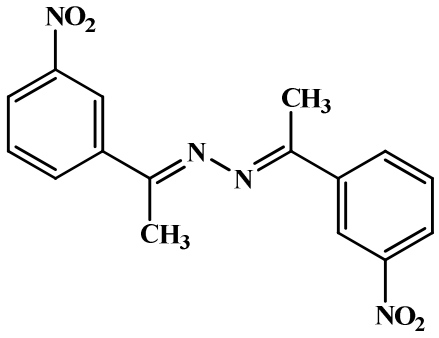

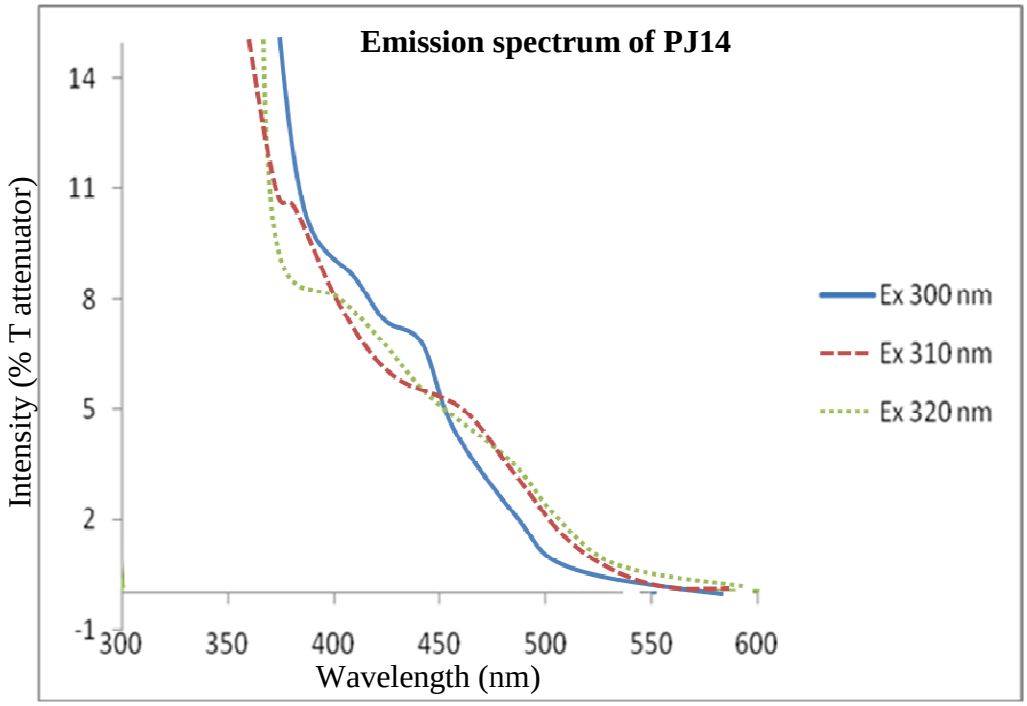

Figure 34 Emission spectrum of 5 µM **PJ14** in $CHCl_3$ at room temperature in %T attenuator mode and slit 10:10.

The emission fluorescence spectrum of **PJ14** was shown in **Figure 34**. Compound **PJ14** shows the fluorescent property which clearly seen in the appearance of fluorescence emission spectrum. The emission spectrum of **PJ14** was observed in the range of 370-580 nm. It was found that **PJ14** exhibits fluorescence with the emission at 370-400 nm when was excited at 300-320 nm in $CHCl_3$.

3.2.2.15 (1*E*,2*E*)-1,2-bis(1-(3-chlorophenyl)ethylidene)hydrazine (PJ15)

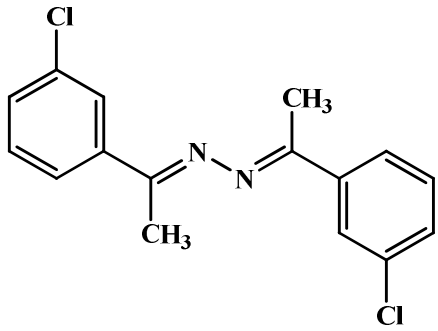

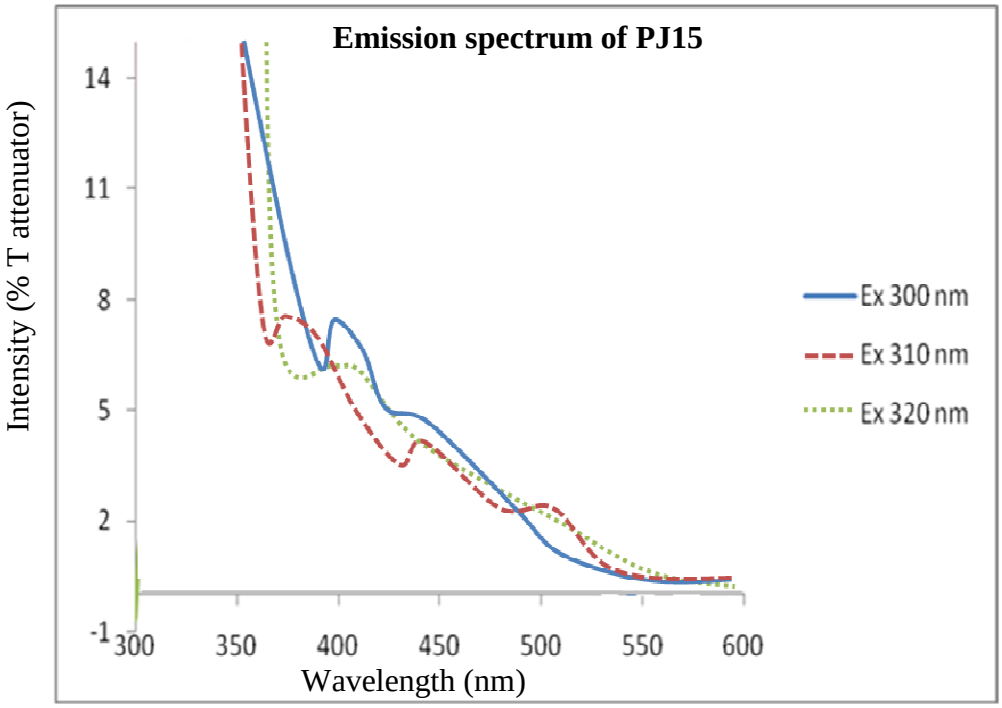

Figure 35 Emission spectrum of 5 μM **PJ15** in $CHCl_3$ at room temperature in %T attenuator mode and slit 10:10.

The emission fluorescence spectrum of **PJ15** was shown in **Figure 36**. Compound **PJ15** shows the fluorescent property which clearly seen in the appearance of fluorescence emission spectrum. The emission spectrum of **PJ15** was observed in the range of 370-570 nm. It was found that **PJ15** exhibits fluorescence with the emission at 390-420 nm when was excited at 300-320 nm in $CHCl_3$.

3.2.2.16 (1*E*,2*E*)-1,2-bis(1-(3-bromophenyl)ethylidene)hydrazine (PJ16)

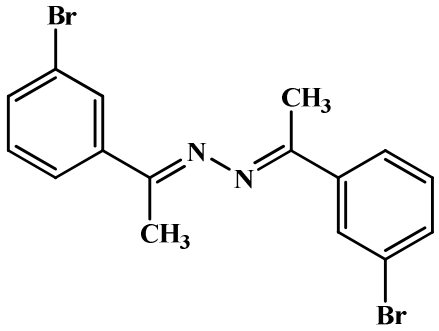

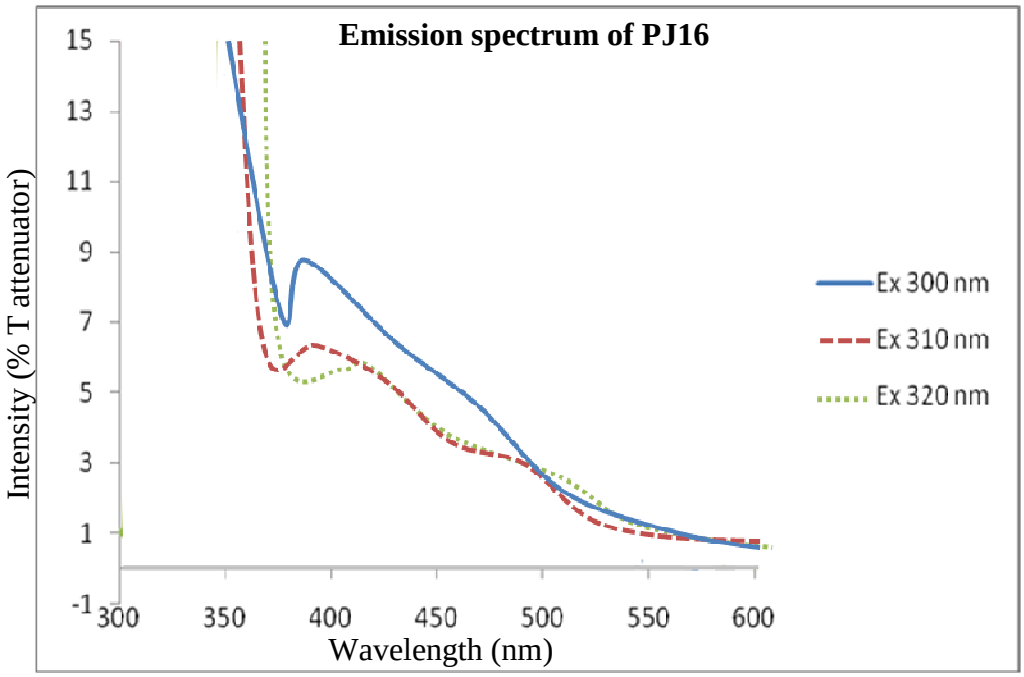

Figure 36 Emission spectrum of 5 μM **PJ16** in $CHCl_3$ at room temperature in %T attenuator mode and slit 10:10.

The emission fluorescence spectrum of **PJ16** was shown in **Figure 36**. Compound **PJ16** shows the fluorescent property which clearly seen in the appearance of fluorescence emission spectrum. The emission spectrum of **PJ16** was observed in the range of 360-570 nm. It was found that **PJ16** exhibits fluorescence with the emission at 390-420 nm when was excited at 300-320 nm in $CHCl_3$.

3.2.2.17 (1*E*,2*E*)-1,2-bis(1-(3-fluorophenyl)ethylidene)hydrazine (PJ17)

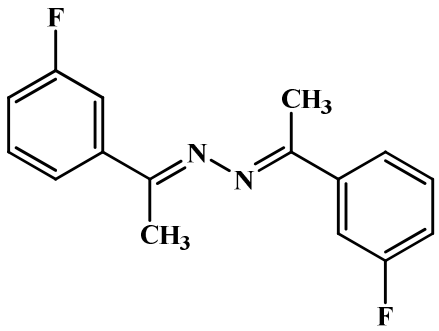

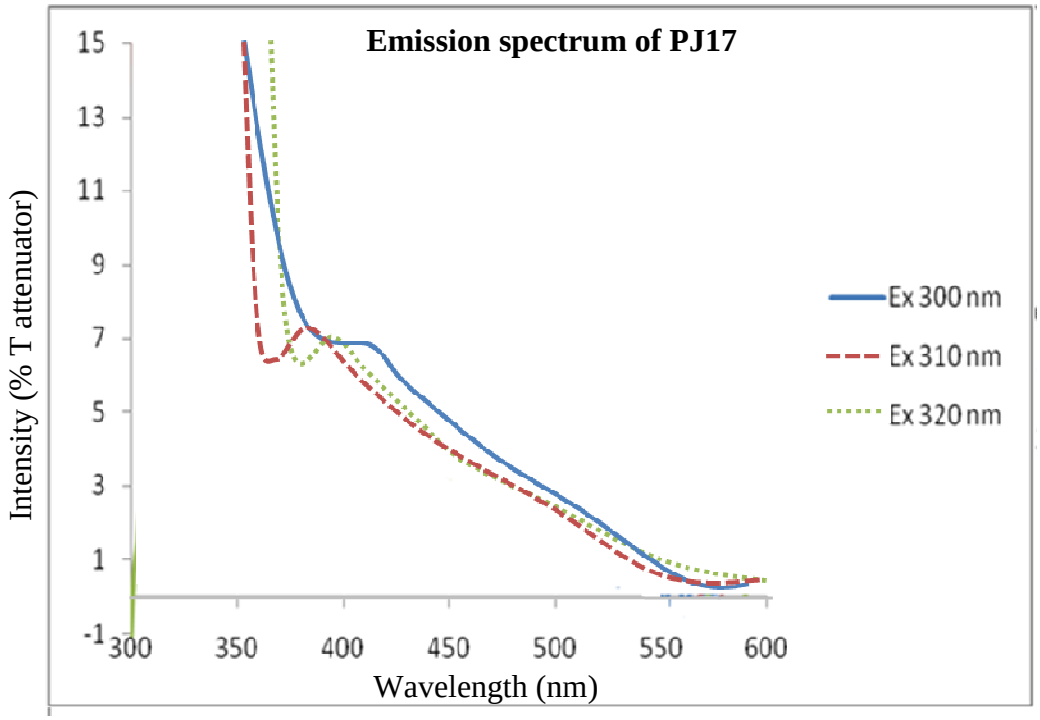

Figure 37 Emission spectrum of 5 µM **PJ17** in $CHCl_3$ at room temperature in %T attenuator mode and slit 10:10.

The emission fluorescence spectrum of **PJ17** was shown in **Figure 37**. Compound **PJ17** shows the fluorescent property which clearly seen in the appearance of fluorescence emission spectrum. The emission spectrum of **PJ17** was observed in the range of 380-580 nm. It was found that **PJ17** exhibits fluorescence with the emission at 380-420 nm when was excited at 300-320 nm in $CHCl_3$.

From **Figures 21-37**, it was found that compounds **PJ1-PJ17** exhibit fluorescent properties.

3.2.3 Comparison of fluorescent spectra

The emission spectra of compounds **PJ1-PJ5** in $CHCl_3$ (5 μM) are shown in **Figure 38**. Compounds **PJ1-PJ3** show the maxima wavelength at 413, 412 and 411 nm, respectively. Compounds **PJ4** and **PJ5** show the maxima wavelength at 400-450 nm. It was found that **PJ1-PJ3** which contains methoxy moieties showed high fluorescent emission intensity.

The emission spectra of compounds **PJ6-PJ17** in $CHCl_3$ (5 μM) are shown in **Figure 39**. It can be explained that maxima wavelength are ambiguous due to the weak fluorescent properties.

The excitation spectra of compounds **PJ1-PJ5** in $CHCl_3$ (5 μM) are shown in **Figure 40**. Compounds **PJ1-PJ5** show the maxima wavelength at 296, 300, 293, 298 and 294 nm, respectively. The highest intensity was observed for **PJ1**. The stokes shift of hydrazone derivatives (**PJ1-PJ17**) in $CHCl_3$ when the absorption wavelength was set at 300 nm for emission spectra studied are shown in **Table 41** and **Table 42**. Moreover, the Stoke shift of **PJ3** was larger than the other compounds which shown in **Table 41** and excitation spectra of compounds **PJ6-PJ17** in $CHCl_3$ (5 μM) are shown in **Figure 41**. Compounds show the maxima wavelength at 302, 304, 298, 302, 299, 298, 303, 298, 300, 299, 302 and 302 nm, respectively. Moreover, the Stoke shift of **PJ10** was larger than the other compounds which shown in **Table 42**.

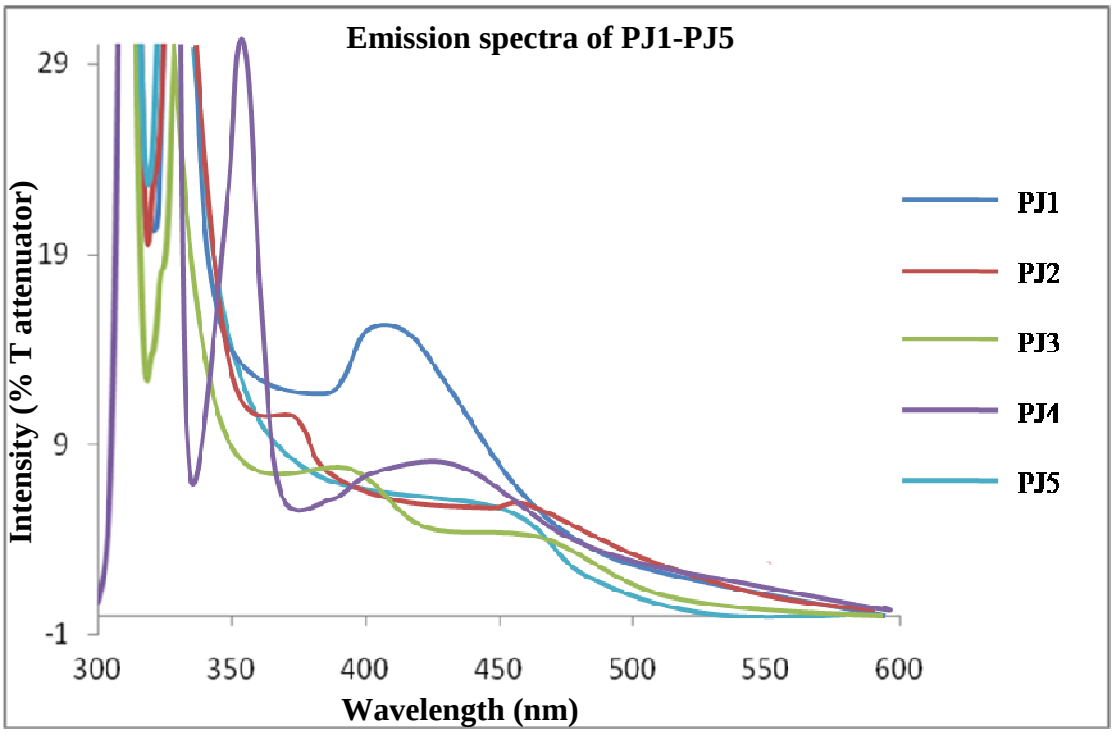

Figure 38 Emission spectra (excited at 300 nm) of 5μM **PJ1-PJ5** in $CHCl_3$ at room temperature (slit 10:10).

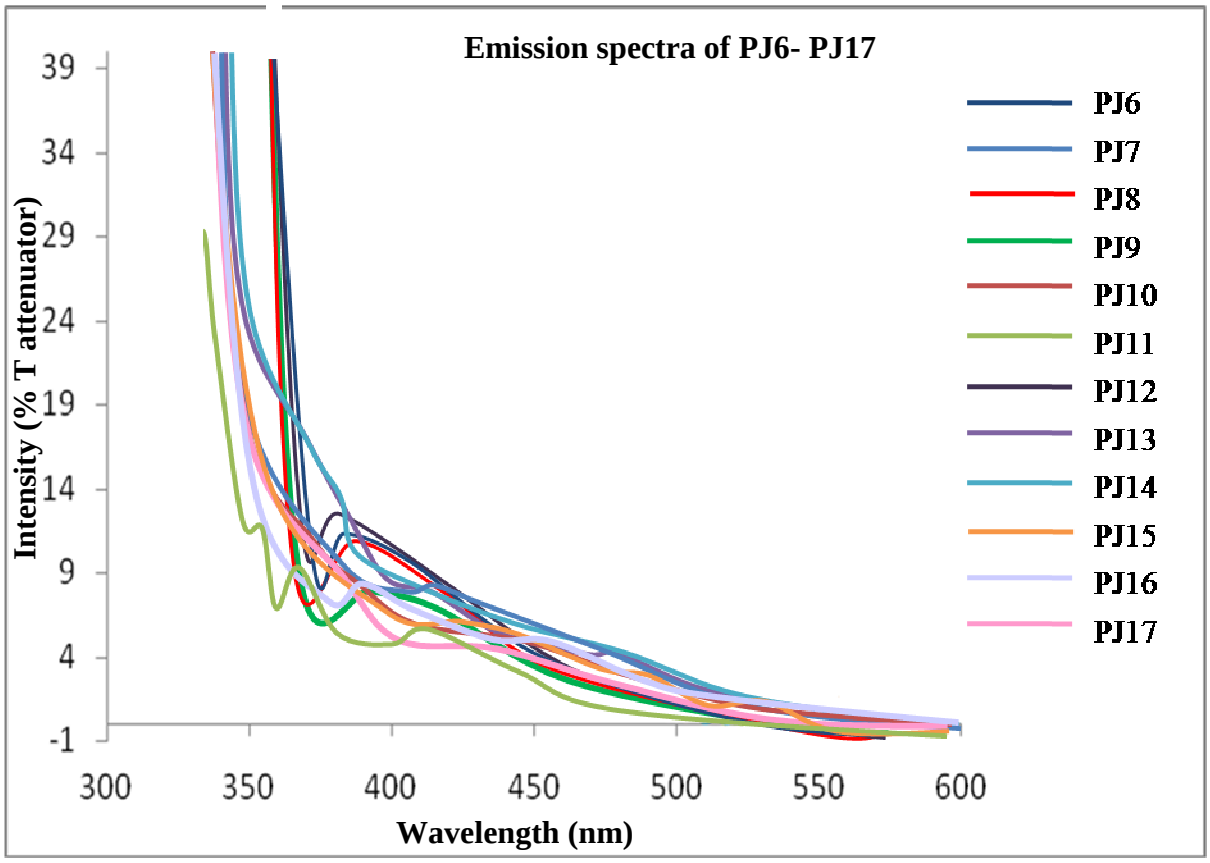

Figure 39 Emission spectra (excited at 300 nm) of 5μM **PJ6-PJ17** in $CHCl_3$ at room temperature (slit 10:10).

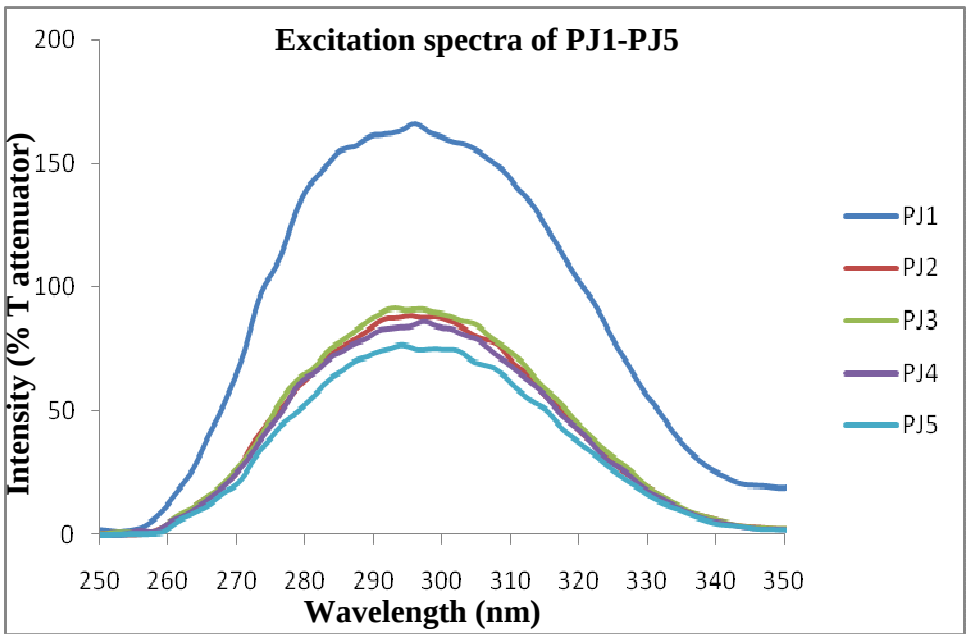

Figure 40 Excitation spectra (emitted at 420 nm) of 5μM **PJ1-PJ5** in $CHCl_3$ at room temperature (slit 10:10).

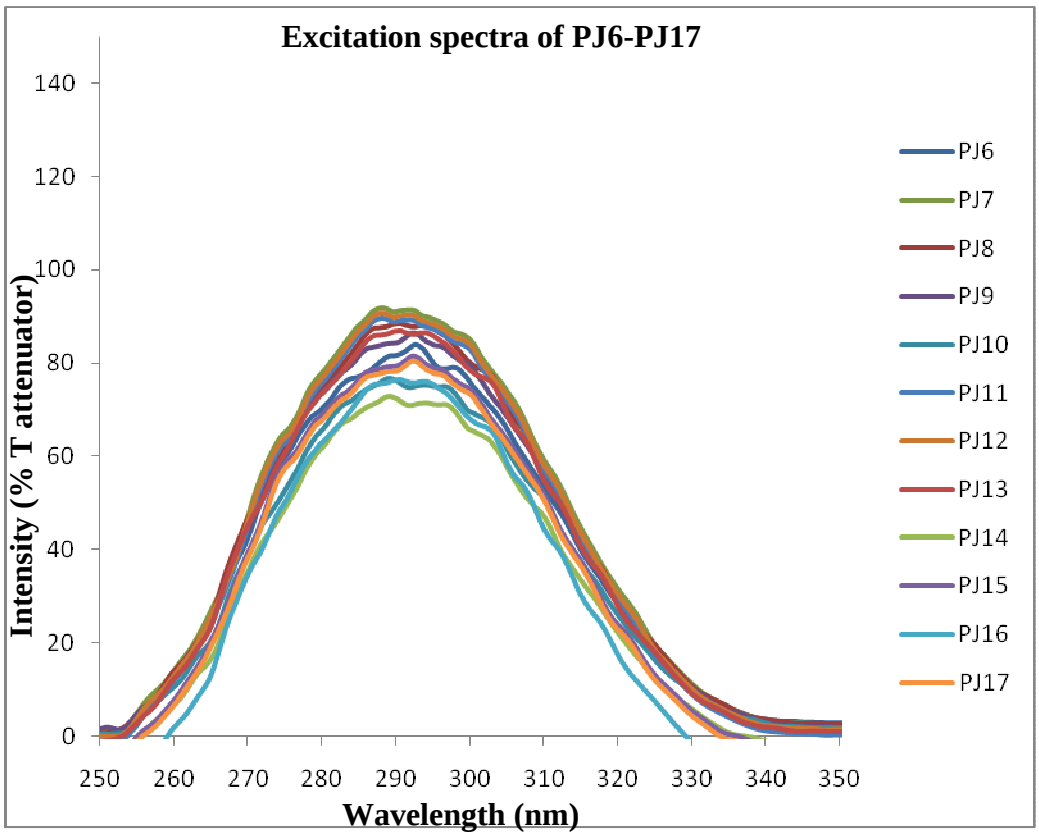

Figure 41 Excitation spectra (emitted at 420 nm) of 5μM **PJ6-PJ17** in $CHCl_3$ at room temperature (slit 10:10).

Table 41 Fluorescence spectra data and stokes shift of hydrazone derivatives (**PJ1-PJ5**) in $CHCl_3$.

Compounds	Absorption maxima, λ_{abs} (nm)	Emission maxima, λ_{em} (nm)	Stoke shift (nm)
PJ1	379	413	34
PJ2	342	412	70
PJ3	335	411	76
PJ4	371	406	35
PJ5	369	404	35

Table 42 Fluorescence spectra data and stokes shift of hydrazone derivatives (**PJ6-PJ17**) in $CHCl_3$.

Compounds	Absorption maxima, λ_{abs} (nm)	Emission maxima, λ_{em} (nm)	Stoke shift (nm)
PJ6	287	410	123
PJ7	379	412	33
PJ8	235	407	172
PJ9	242	408	166
PJ10	207	409	202
PJ11	306	409	103
PJ12	267	404	137
PJ13	240	412	172
PJ14	263	405	142
PJ15	267	404	137
PJ16	269	410	141
PJ17	269	404	135

Compounds **PJ1-PJ3** which are the compounds containing trimethoxy groups show higher fluorescent properties than both compounds **PJ4** and **PJ5** which containing hydroxyl and nitro groups. These results may be due to the effect of the π electrons donating groups in compounds **PJ1-PJ3** but electron withdrawing groups in compounds **PJ4** and **PJ5**. Compounds **PJ6-PJ17** may be affected by the steric effect of the two methyl groups in the molecules which cause the decreasing of the fluorescence. However, the fluorescence quantum yield (Φ_f) of all the hydrazone derivatives can not be calculated due to the relatively low emission intensity.

3.2.4 Studies for metal sensor based on hydrazones

The **PJ1-PJ17** were treated for surveyed chemosensor property with ten different metal ions which are Mg^{2+}, Ca^{2+}, Mn^{2+}, Fe^{2+}, Co^{2+}, Ni^{2+}, Cu^{2+}, Zn^{2+}, Hg^{2+} and Cd^{2+} (10 mM) in CH_3CN. It was found that the color changed was observed by naked-eyes only for **PJ7** with Cu^{2+} solution from pale yellow to yellow-brown as shown in **Figure 42**.

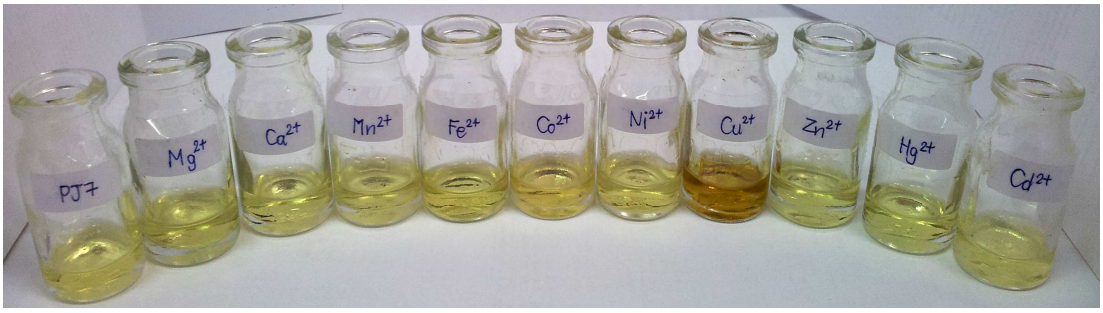

Figure 42 PJ7 in the presence of different salts of Mg^{2+}, Ca^{2+}, Mn^{2+}, Fe^{2+}, Co^{2+}, Ni^{2+}, Cu^{2+}, Zn^{2+} , Hg^{2+} and Cd^{2+} (10 mM) in CH_3CN at room temperature.

These studies suggested that **PJ7** could be served as reversible naked-eye Cu^{+} and Cu^{2+}-specific chemosensors in neutral solution media as shown in **Figure 43**.

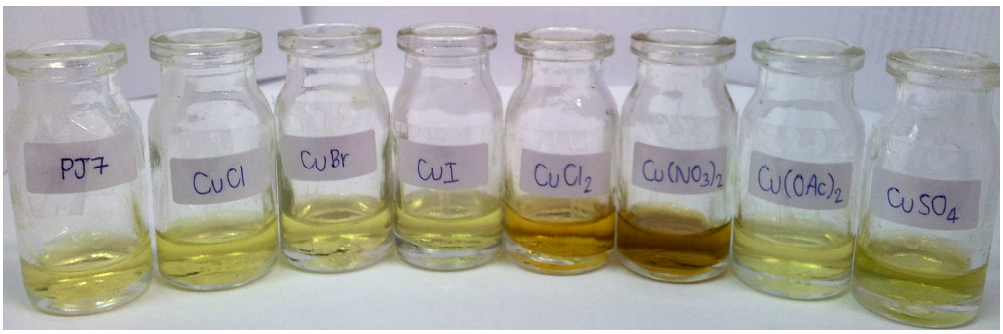

Figure 43 PJ7 in the presence of different salts of Cu^{+} and Cu^{2+} (10 mM) in CH_3CN at room temperature.

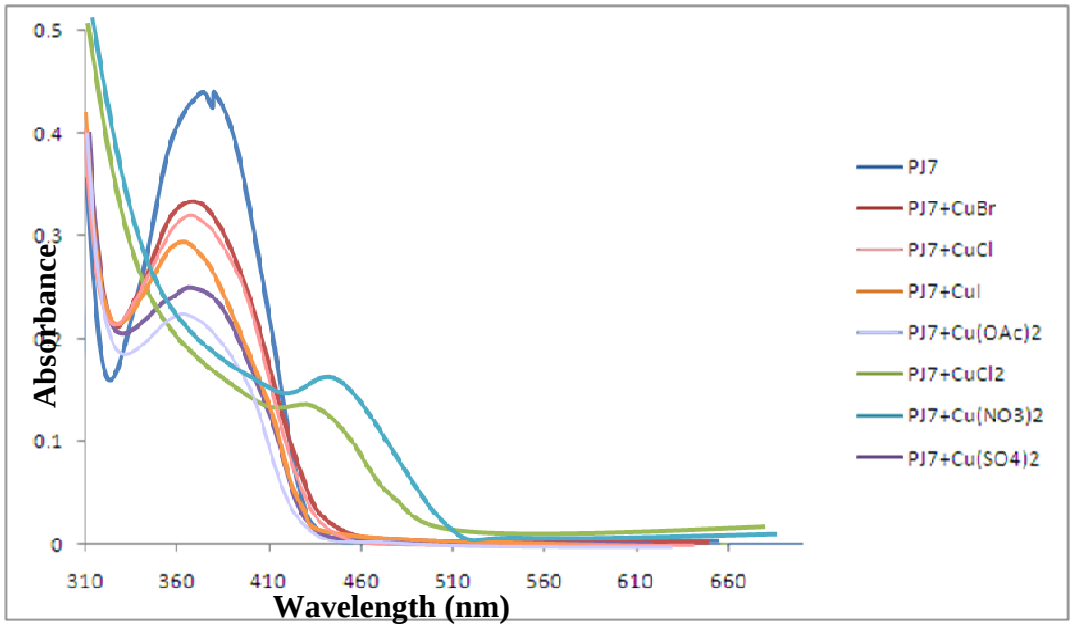

Figure 44 Absorption spectra of **PJ7** in the presence of different salts of Cu^{+} and Cu^{2+} (1 mM) at room temperature.

Table 43 Absorption spectra data of **PJ7** and **PJ7** with Cu^{+} and Cu^{2+} (1 mM) in CH_3CN at room temperature.

Compound	Absorption, λ_{max} (nm)
PJ7	370
PJ7+CuBr	368
PJ7+CuCl	368
PJ7+CuI	363
PJ7+$Cu(OAc)_2$	364
PJ7+$CuCl_2$	430
PJ7+$Cu(NO_3)_2$	452
PJ7+$CuSO_4$	365

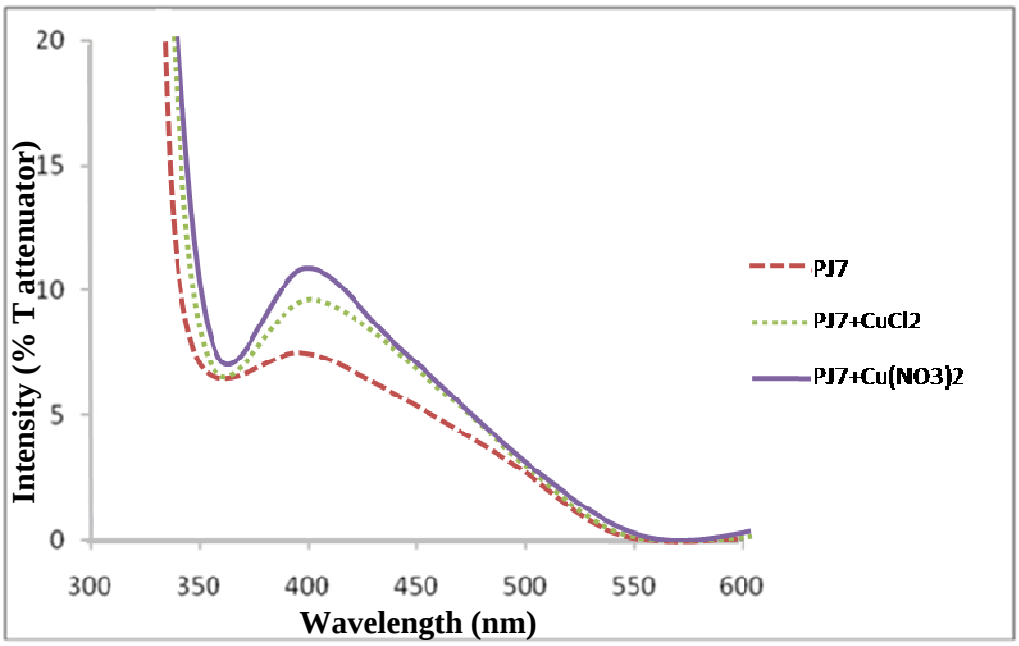

Figure 45 Fluorescence emission spectra of **PJ7** and that after addition of $CuCl_2$ and $Cu(NO_3)_2$ in CH_3CN at room temperature in %T attenuator mode and slit 10:10.

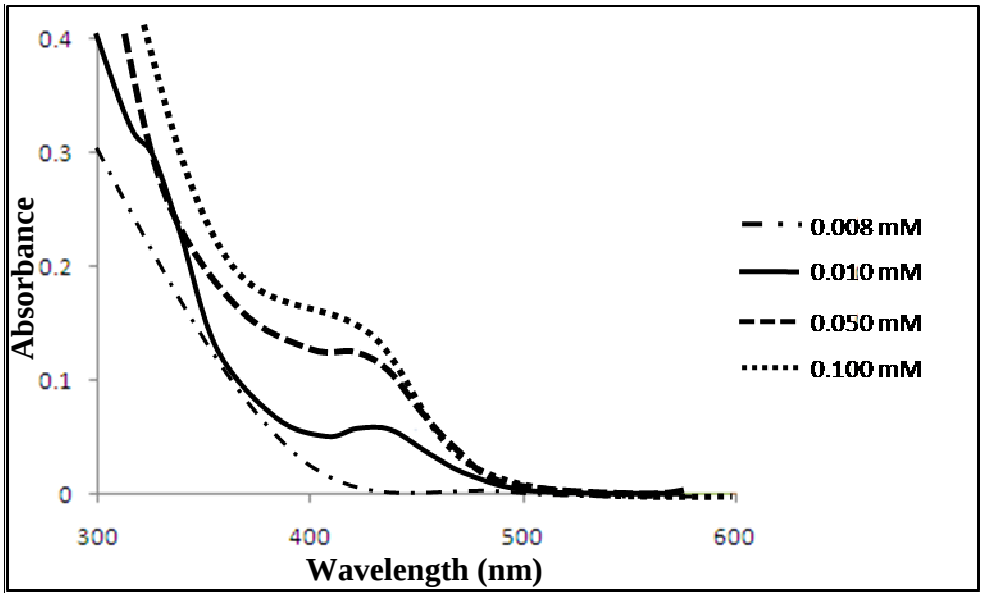

Figure 46 Absorption spectra of **PJ7** in the presence of different concentration of $CuCl_2$ at room temperature.

Table 44 Absorbance of **PJ7** in various concentrations of $CuCl_2$ in CH_3CN at room temperature (at 430 nm).

PJ7+$CuCl_2$ (mM)	**Absorbance**
0.008	0.00
0.010	0.07
0.050	0.12
0.100	0.14

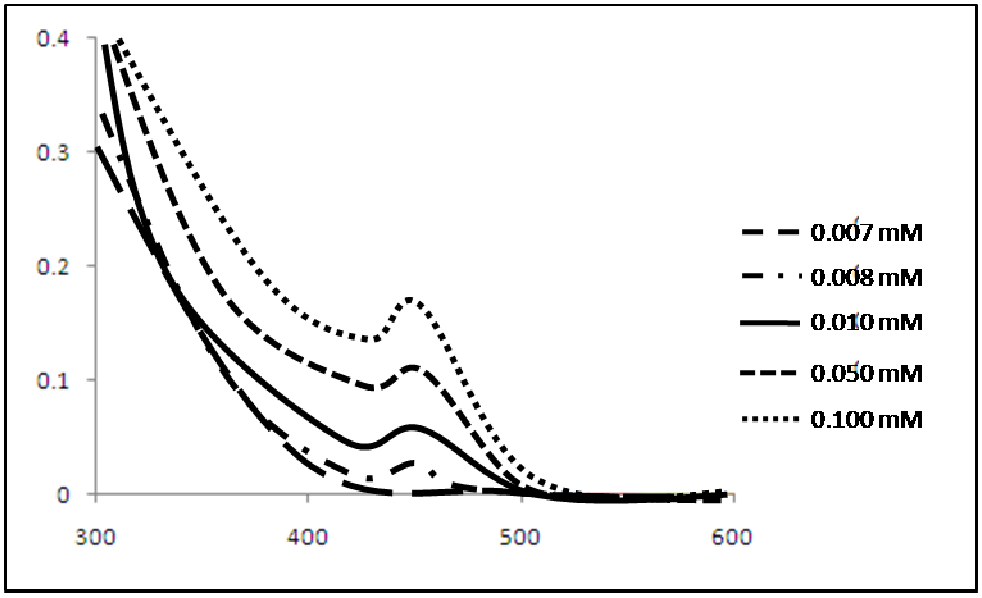

Figure 47 Absorption spectra of **PJ7** in the presence of different concentration of $Cu(NO_3)_2$ at room temperature.

Table 45 Absorbance of **PJ7** in various concentrations of $Cu(NO_3)_2$ in CH_3CN at room temperature (at 452 nm).

PJ7+ $Cu(NO_3)_2$ (mM)	**Absorbance**
0.007	0.00
0.008	0.02
0.010	0.06
0.050	0.12
0.100	0.17

From **Figure 44** and **Table 43**, it can be summarized that the complexation studies of **PJ7** with metal salts of Cu^{+} and Cu^{2+} can be considered from absorbance spectra. The chemosensor property of **PJ7** was also measured by the addition of CuBr, CuCl, CuI, $Cu(OAc)_2$, $CuCl_2$, $Cu(NO_3)_2$ and $CuSO_4$ in **PJ7** solution (CH_3CN) to study of the effect of counter ions on sensitivity of Cu^{+} and Cu^{2+}. The color of **PJ7** solution remained pale yellow and present the maxima absorption wavelength (λ_{max}) at 370 nm. From **Figure 43**, it can be obviously seen that **PJ7** with $CuCl_2$ and $Cu(NO_3)_2$ show considerable and simultaneous color changed from pale yellow to yellow-brown and the absorption spectra were red shifted to 430 and 452 nm, respectively. For the additions of Cu^{+} and Cu^{2+} with the other counter ions to **PJ7** solutions, the absorbance was slightly decreased and the λ_{max} was also slightly changed. Therefore, **PJ7** could be considered to use as receptor in the sensing for Cu^{2+} which are $CuCl_2$ and $Cu(NO_3)_2$. The decreasing of intensity the maxima wavelength was observed when decreasing the concentration of $CuCl_2$ (**Figure 46** and **Table 44**) and $Cu(NO_3)_2$ (**Figure 47** and **Table 45**) solution. The detection limit of $CuCl_2$ is 0.010 mM (**Figure 46** and **Table 44**) and 0.008 mM for $Cu(NO_3)_2$ (**Figure 47** and **Table 45**).

Fluorescence emission intensity of **PJ7** with $CuCl_2$ and $Cu(NO_3)_2$ in CH_3CN were slightly increased (**Figure 45**) and show emission maxima wavelength at 413, 416 and 418 nm respectively for **PJ7**, **PJ7+**$CuCl_2$ and **PJ7+** $Cu(NO_3)_2$. The **PJ7** can be served as Cu^{2+} chemosensor which may be due to the containg NH_2 group at ortho position which leading to the chelation with Cu^{2+}.

CHAPTER 4
CONCLUSION

Seventeen hydrazone derivatives were successfully synthesized. Their structures were elucidated by spectroscopic techniques. Seventeen of these compounds are

(1*E*,2*E*)-1,2-bis(2,4,5-trimethoxybenzylidene)hydrazine (**PJ1**),
(1*E*,2*E*)-1,2-bis(2,4,6-trimethoxybenzylidene)hydrazine (**PJ2**),
(1*E*,2*E*)-1,2-bis(3,4,5-trimethoxybenzylidene)hydrazine (**PJ3**),
(1*E*,2*E*)-1,2-bis(3-hydroxy-4-nitrobenzylidene)hydrazine (**PJ4**),
(1*E*,2*E*)-1,2-bis(4-hydroxy-3-nitrobenzylidene)hydrazine (**PJ5**),
(1*E*,2*E*)-1,2-bis(1-(2-methoxyphenyl)ethylidene)hydrazine (**PJ6**),
(1*E*,2*E*)-1,2-bis(1-(2-aminophenyl)ethylidene)hydrazine (**PJ7**),
(1*E*,2*E*)-1,2-bis(1-(2-nitrophenyl)ethylidene)hydrazine (**PJ8**),
(1*E*,2*E*)-1,2-bis(1-(2-chlorophenyl)ethylidene)hydrazine (**PJ9**),
(1*E*,2*E*)-1,2-bis(1-(2-bromophenyl)ethylidene)hydrazine (**PJ10**),
(1*E*,2*E*)-1,2-bis(1-(4-hydroxyphenyl)ethylidene)hydrazine (**PJ11**),
(1*E*,2*E*)-1,2-bis(1-(3-methoxyphenyl)ethylidene)hydrazine (**PJ12**),
(1*E*,2*E*)-1,2-bis(1-(3-aminophenyl)ethylidene)hydrazine (**PJ13**),
(1*E*,2*E*)-1,2-bis(1-(3-nitrophenyl)ethylidene)hydrazine (**PJ14**),
(1*E*,2*E*)-1,2-bis(1-(3-fluorophenyl)ethylidene)hydrazine (**PJ15**),
(1*E*,2*E*)-1,2-bis(1-(3-chlorophenyl)ethylidene)hydrazine (**PJ16**) and
(1*E*,2*E*)-1,2-bis(1-(3-bromophenyl)ethylidene)hydrazine (**PJ17**)

Their fluorescent properties were studied in $CHCl_3$ at room temperature. It was found that the seventeen compounds in **PJ** series exhibited fluorescent properties. These compounds which are **PJ1-PJ17** show emission spectra in the range of 403-413 nm and their emission spectra pattern are similar and **PJ1-PJ17** present maxima wavelength at 413, 412, 411, 406, 404, 410, 412, 407, 408, 409, 409, 404, 412, 405, 404, 410 and 404 nm present maxima wavelength at 390-420

nm. The excitation spectra of these compounds show excitation spectra in the range of 250-350 nm and present maxima wavelength at 296, 300, 293, 298, 294, 302, 304, 298, 302, 299, 298, 298, 300, 299, 302, 300 and 302 nm. The fluorescent properties of the compounds (**PJ6-PJ17**) which containing -CH_3 group in the middle >C=N-N=C< are lower than that of compounds (**PJ1-PJ5**) which containing -H in the middle >C=N-N=C< because of the steric effects of -CH_3 groups. However, the fluorescence quantum yield (Φ_f) of all hydrazone derivatives can not be calculated because of their relatively low of the emission.

Metal sensor for Cu^{+}, Cu^{2+} (0.10 M) based on the **PJ7** was studied in CH_3CN at room temperature. It was found that the **PJ7** with anions of Cu^{2+} are Cl^{-} and NO_3^{-} show absorption spectra changed to red shift from λ_{max} 370 to 430 and 452 nm, respectively, and a simultaneous color changed was also found (from pale yellow to yellow-brown). The concentration detecting limit of $CuCl_2$ at 0.010 mM and $Cu(NO_3)_2$ at 0.008 mM. The selectivity for $CuCl_2$ and $Cu(NO_3)_2$ than other salts such as CuBr, CuCl, CuI, $Cu(OAc)_2$ and $CuSO_4$.

In addition, compounds **PJ1**, **PJ10**, **PJ11**, **PJ14** and **PJ15** were recrystallized from CH_3COCH_3 and all crystallized out in monoclinic $P2_1/c$ space group and **PJ2**, **PJ6** were recrystallized from CH_3COCH_3/EtOH and crystallized out in triclinic $P\bar{1}$ space group.

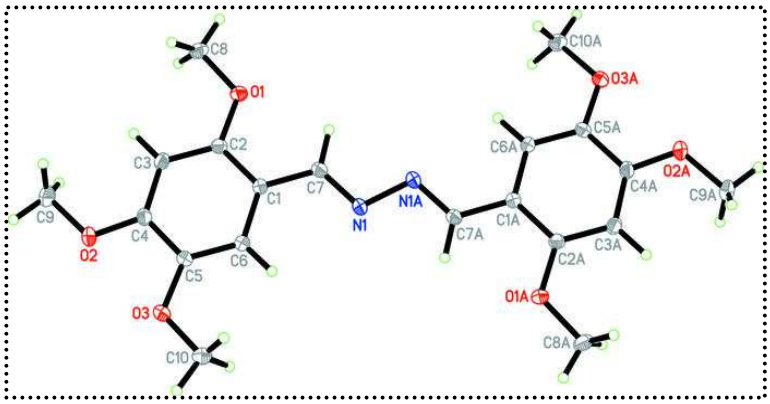

(1*E*,2*E*)-1,2-bis(2,4,5-trimethoxybenzylidene)hydrazine (**PJ1**)

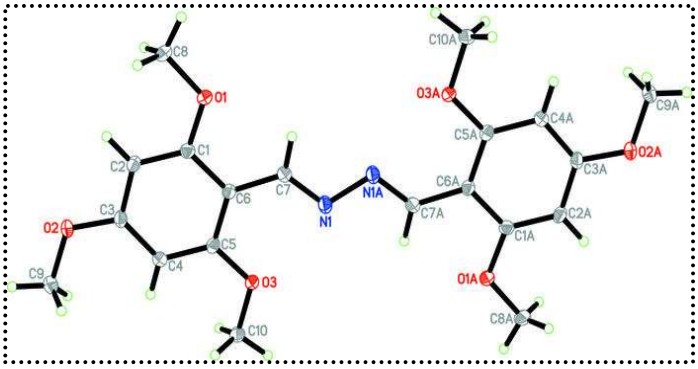

(1*E*,2*E*)-1,2-bis(2,4,6-trimethoxybenzylidene)hydrazine (**PJ2**)

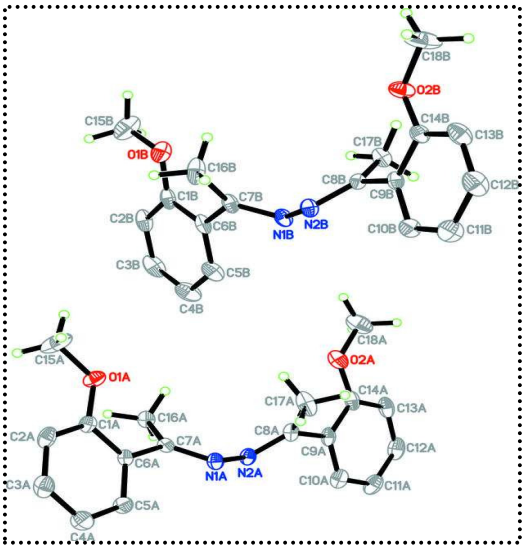

(1*E*,2*E*)-1,2-bis(1-(2-methoxyphenyl)ethylidene)hydrazine (**PJ6**)

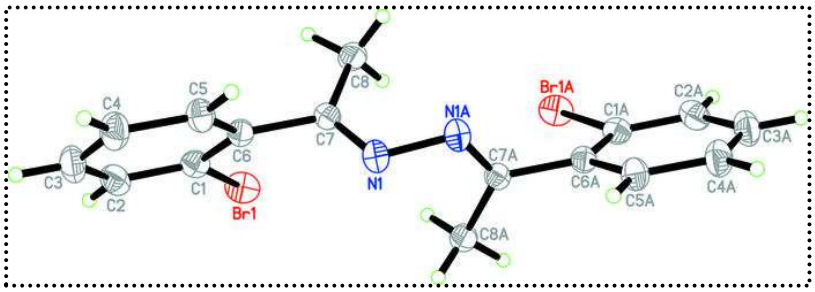

(1*E*,2*E*)-1,2-bis(1-(2-bromophenyl)ethylidene)hydrazine (**PJ10**)

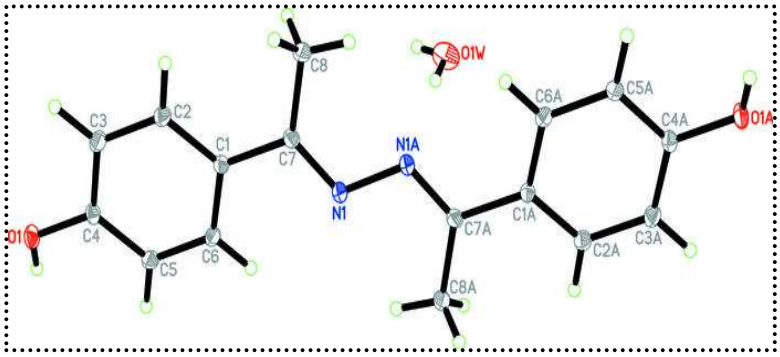

(1*E*,2*E*)-1,2-bis(1-(4-hydroxyphenyl)ethylidene)hydrazine (**PJ11**)

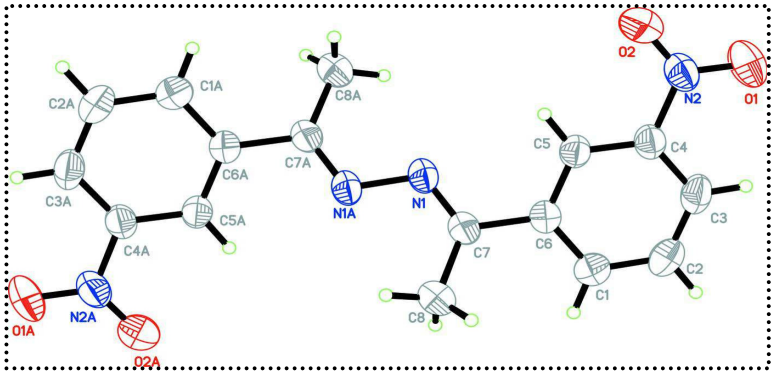

(1*E*,2*E*)-1,2-bis(1-(3-nitrophenyl)ethylidene)hydrazine (**PJ14**)

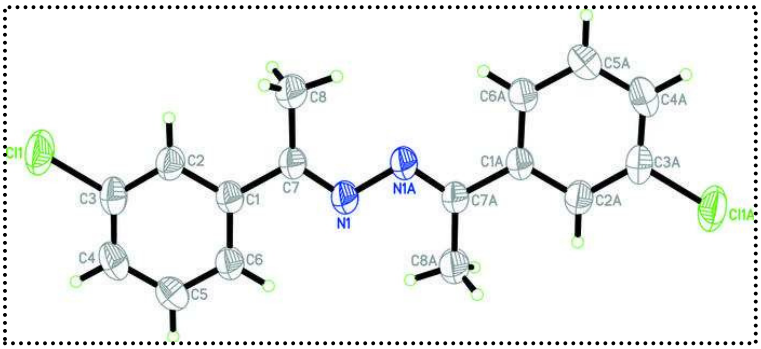

(1*E*,2*E*)-1,2-bis(1-(3-fluorophenyl)ethylidene)hydrazine (**PJ15**)

Scheme 13. Crystal structure of the hydrazone derivatives

REFERENCES

Arun, V., Robinson, P.P., Manju, S., Leeju, P., Varsha, G., Digna, V., Yusuff, K.K.M. (2009) "A novel fluorescent bisazomethine dye derived from 3-hydroxy quinoxaline-2-carboxaldehyde and 2,3-diaminomaleonitrile", *Dyes Pigments*, **82**, 268–275.

Avaji, P.G., Kumar, C.H.V., Patil, S.A., Shivananda, K.N., Nagaraju, C. (2009) "Synthesis, spectral characterization, in-vitro microbiological evaluation and cytotoxic activities of novel macrocyclic bis hydrazone", *Eur. J. Med. Chem*., **44**, 3552–3559.

Chen, X., Jou, M.J., Lee, H., Kou, S., Lim, J., Nam, S.-W., Park, S., Kim, K.-M., Yoon, J. (2009) "New fluorescent and colorimetric chemosensors bearing rhodamine and binaphthyl groups for the detection of Cu^{2+}", *Sensor Actuat. B-Chem*., **137**, 597–602.

Dang, D., Gao, H., Bai, Y., Pan, X., Shang, W. (2010) "Self-assembly of one Ag(I) 2D metallacrown polymer with bis-bidentate Schiff-base ligand *N*,*N*'- bis (furan-2-ylmethylene)hydrazine: Synthesis, crystal structures and luminescent properties", *J. Mol. Struct*., **969**, 120–125.

Dilek, Ö., Bane, S.L. (2008) “Synthesis of boron dipyrromethene fluorescent probes for bioorthogonal labeling”, *Tetrahedron Lett.*, **49**, 1413–1416.

El-Sherif, A.A. (2009) “Synthesis, spectroscopic characterization and biological activity on newly synthesized copper(II) and nickel(II) complexes incorporating bidentate oxygen–nitrogen hydrazone ligands”, *Inorg. Chim. Acta*, **362**, 4991–5000.

El-Tabl, A.S., El-Saied, F.A., Plass, W., Al-Hakimi, A.N. (2008) “Synthesis, spectroscopic characterization and biological activity of the metal complexes of the Schiff base derived from phenylaminoacetohydrazide and dibenzoyl methane”, *Spectrochim. Acta A*, **71**, 90–99.

Han, F., Bao, Y., Yang, Z., Fyles, T.M., Zhao, J., Peng, X., Fan, J., Wu, Y., Sun, S. (2007) “Simple Bisthiocarbonohydrazones as Sensitive, Selective, Colorimetric, and Switch-On Fluorescent Chemosensors for Fluoride Anions”, *Chem. Eur. J.*, **13**, 2880 –2892.

Houdier, S., Legrand, M., Boturyn, D., Croze, S., Defrancq, E., Lhomme, J. (1999) “A new fluorescent probe for sensitive detection of carbonyl compounds”, *Anal. Chim. Acta*, **382**, 253-263.

Huh, H.S., Kim, S.H., Yun, S.Y., Lee, S.W. (2008) “Silver coordination polymers and networks based on *O*-or *S*-heterocyclic linking ligands: $[AgL^1_2](PF_6)$, $[Ag_2L^2_3](PF_6)_2$, $[Ag_2L^2_3](ClO_4)_2$, $[Ag_2L^2_2](BF_4)_2$, and $[Ag_2L^2(NO_3)_2]$ (L^1 = 1,2-bis(thiophen-2-ylmethylene)hydrazine; L^2 = 1,2-bis(furan-2-yl methylene)hydrazine)”, *Polyhedron*, **27**, 1229–1237.

Jiménez-Pulido, S.B., Linares-Ordóñez, F.M., Moreno-Carretero, M.N. (2009) “Novel coordination behavior of a pteridine-benzoylhydrazone ligand (BZLMH): Theoretical calculations, XRD structures and luminescence studies”, *Polyhedron*, **28**, 2641–2648.

Lakowicz, J.R. (1999) “Principles of Fluorescence Spectroscopy (2nd ed^n)”, Kluwer Academic/Plenum Publishers, New York, London, Moscow, Dordrecht.

Li, J., Dasgupta, P.K., Luke, W. (2005) “Measurement of gaseous and aqueous trace formaldehyde Revisiting the pentanedione reaction and field applications”, *Anal. Chim. Acta*, **531**, 51–68.

Liu, F., Zhang, W.P., He, S.Y. (2010) “Crystal Structure, DNA-Binding, and Fluorescence Properties of Cadmium(II) Complex with *N*-(2-Acetic Acid) Salicyloyl Hydrazone and Imidazole”, *Russ. J. Coord. Chem.*, **36**, 105–112.

Lu, J., Zhang, L., Liu, L., Liu, G., Jia, D., Wu, D., Xu, G. (2008) "Study of fluorescence properties of several 4-acyl pyrazolone derivatives and their Zn(II) complexes", *Spectrochim. Acta A*, **71**, 1036–1041.

Mashraqui, S. H., Chandiramani, M., Betkar, R., Ghorpade, S. (2010) "An easily accessible internal charge transfer chemosensor exhibiting dual colorimetric and luminescence switch on responses for targeting Cu^{2+}", *Sensor. Actuat. B*, **150**, 574–578.

Melnyk, P., Leroux V., Sergheraert, C., Grellier, P. (2006) "Synthesis and in vitro antimalarial activity of an acylhydrazone library", *Bioorg. Med. Chem. Lett.*, **16**, 31–35.

Patole, J., Sandbhor, U., Padhye, S., Deobagkar, D.N., Anson, C.E., Powell, A.K. (2003) "Structural chemistry and in-vitro antitubercular activity of acetylpyridine benzoyl hydrazone and its copper complex against Mycobacterium smegmatis", *Bioorg. Med. Chem. Lett.*, **13**, 51-55.

Qin, D.-D., Yang, Z.-Y., Qi G.-F. (2009) "Synthesis, fluorescence study and biological evaluation of three Zn(II) complexes with Paeonol Schiff base", *Spectrochim. Acta A*, **74**, 415–420.

Stokes G.G. (1852) “On the change of refrangibility of light”, *Phil. Trans. R. Soc. Lond.*, **142**, 463–562.

Valeur, B. (2002) “Molecular Fluorescence: Principles and Applications”, Wiley-VCH, Weinheim.

Wang, Q., Yang, Z.-Y., Qi, G.-F., Qin, D.-D. (2009) “Synthesis, crystal structure, antioxidant activities and DNA-binding studies of the Ln(III) complexes with 7-methoxychromone-3-carbaldehyde-(40-hydroxy)benzoyl hydrazone”, *Eur. J. Med. Chem.*, **44**, 2425–2433.

APPENDIX

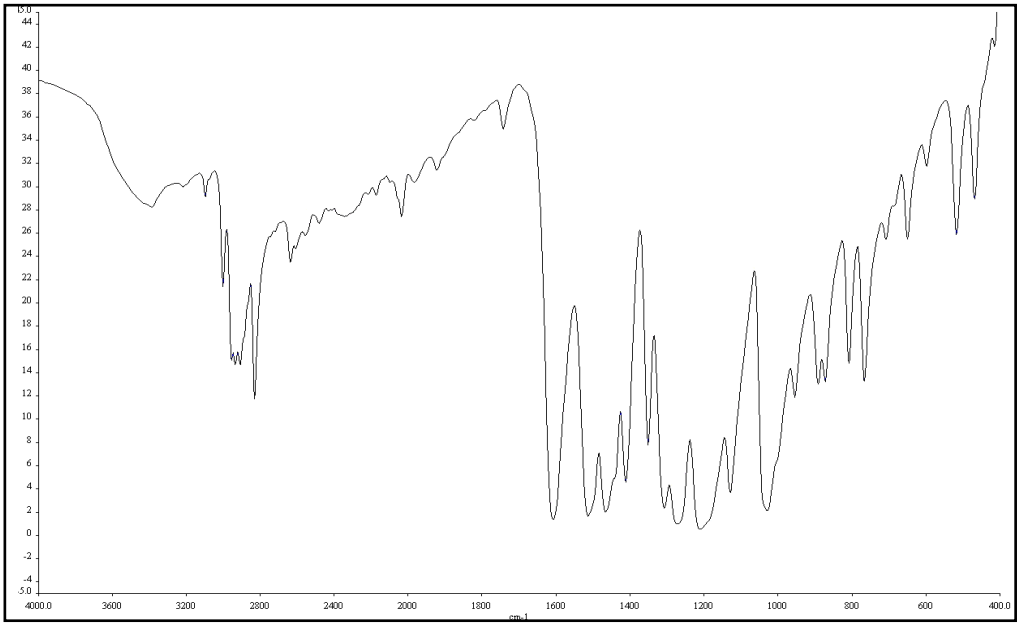

Figure 48 FT-IR (KBr) spectrum of compound **PJ1**

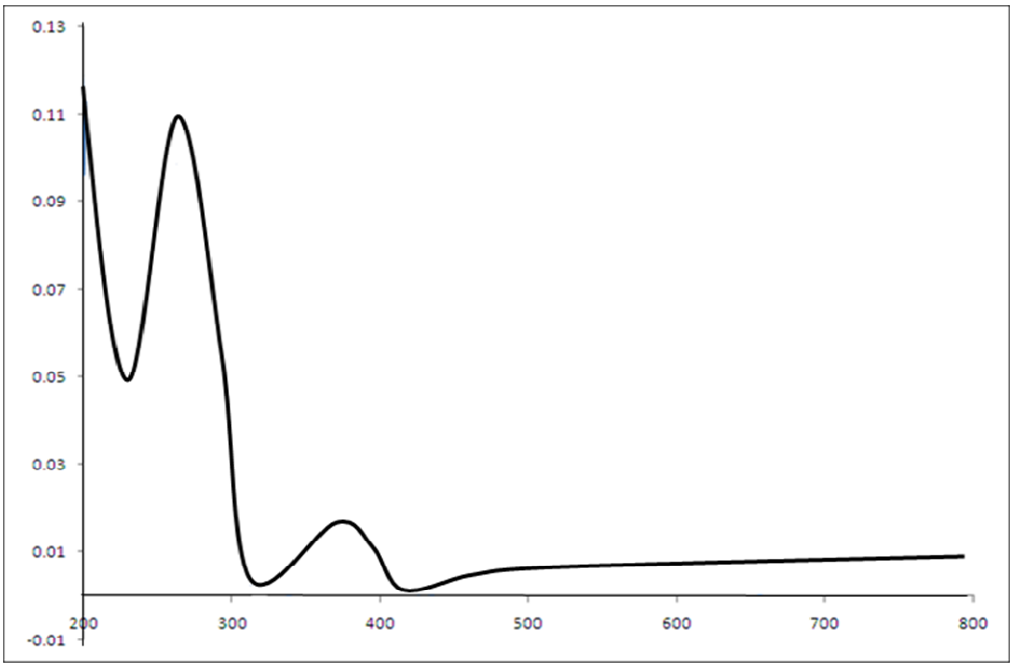

Figure 49 UV-Vis ($CHCl_3$) spectrum of compound **PJ1**

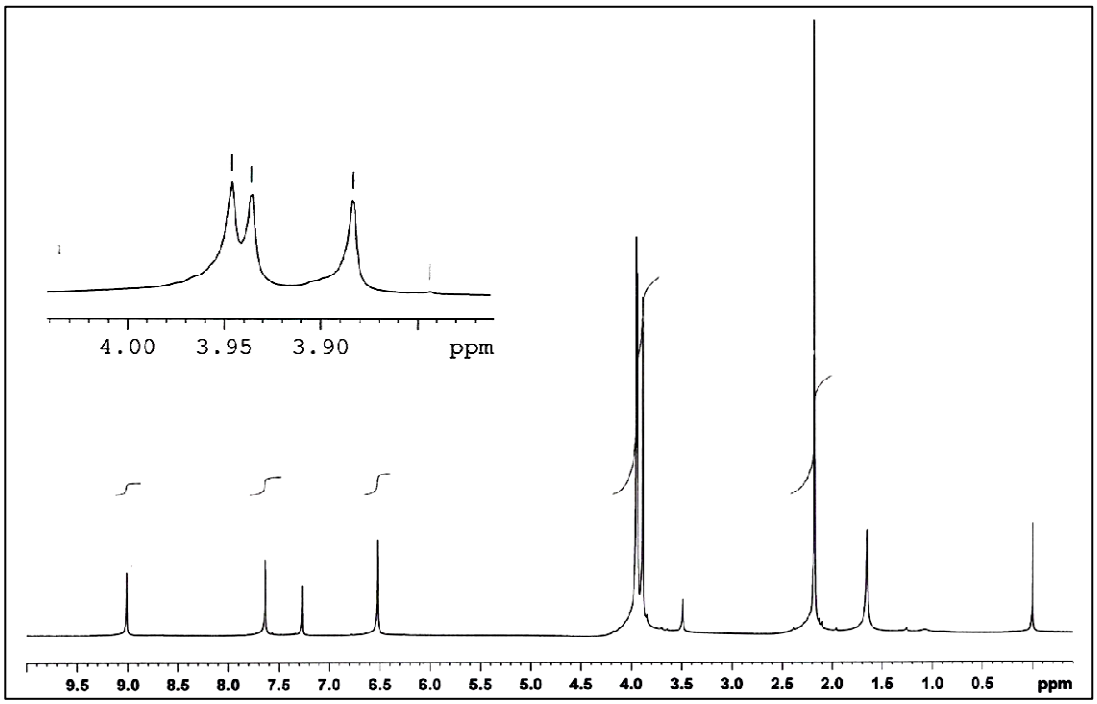

Figure 50 ^{1}H NMR (300 MHz, $CDCl_3$) spectrum of compound **PJ1**

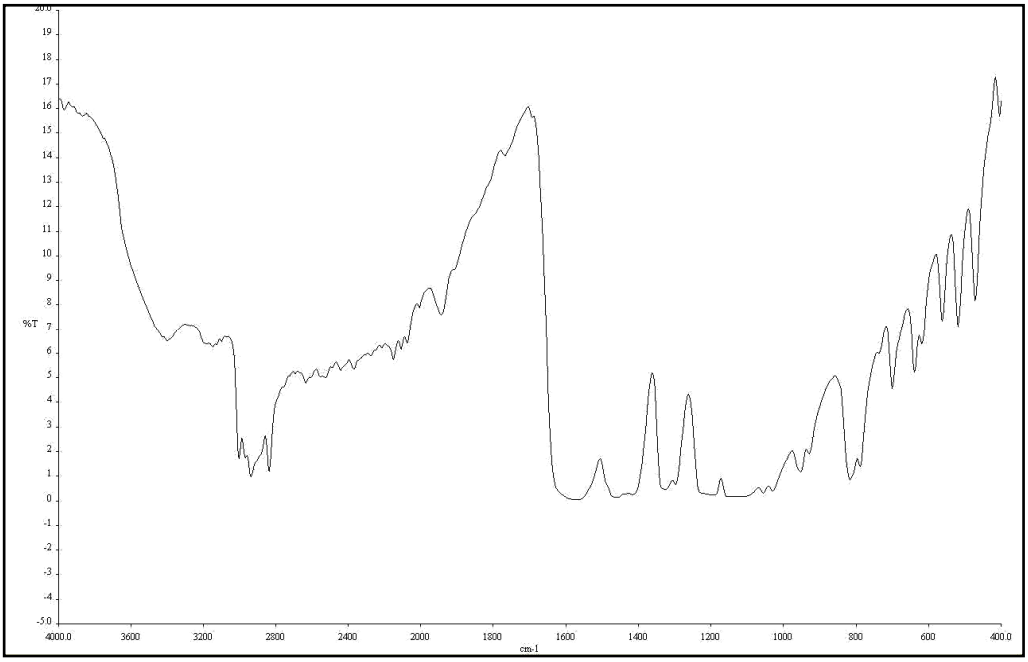

Figure 51 FT-IR (KBr) spectrum of compound **PJ2**

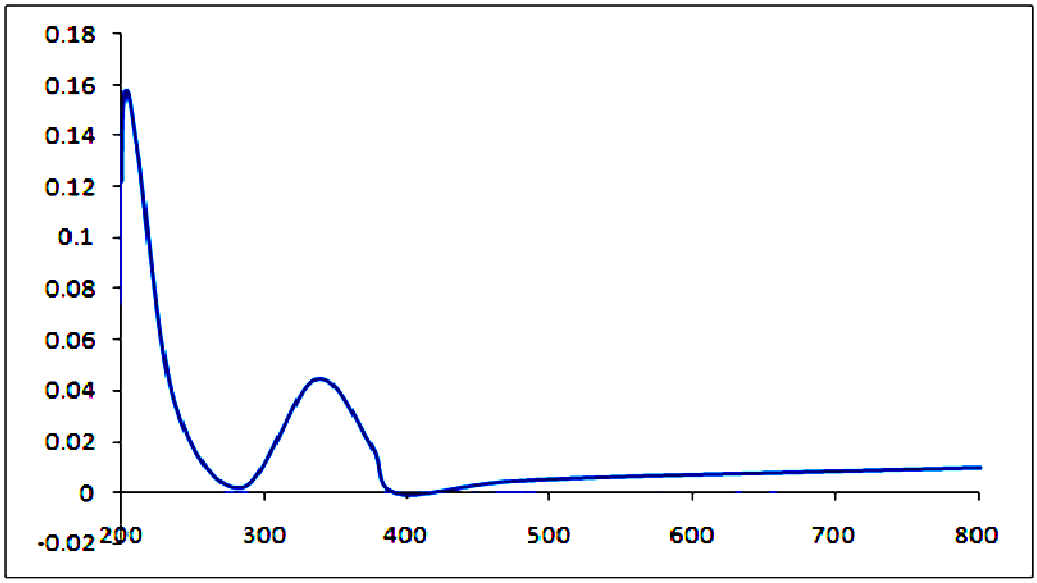

Figure 52 UV-Vis ($CHCl_3$) spectrum of compound **PJ2**

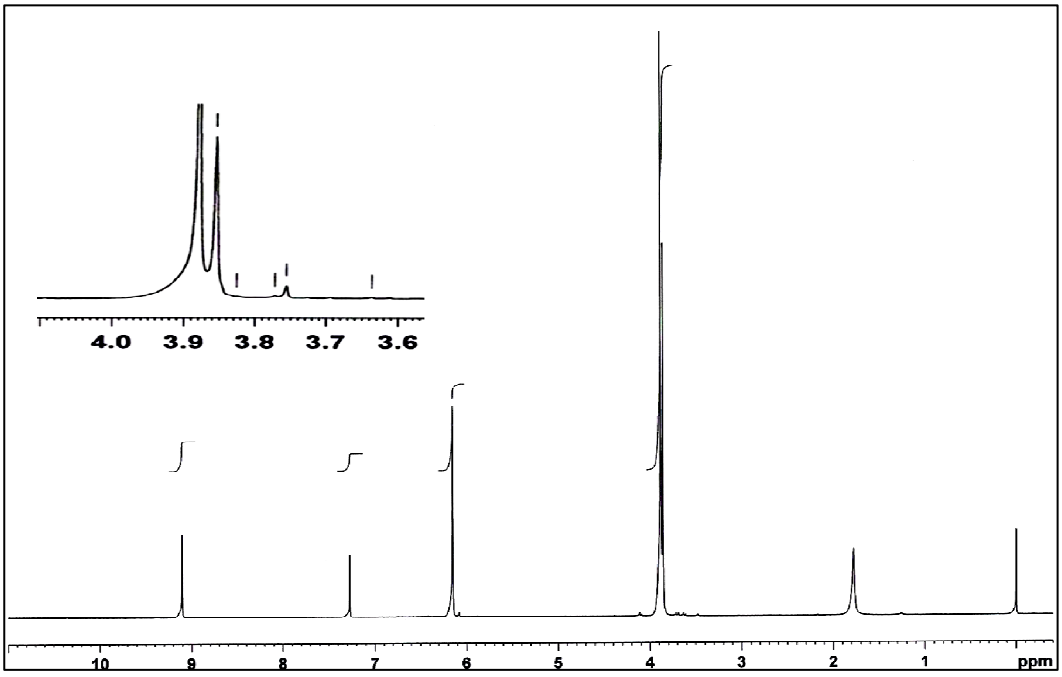

Figure 53 ^{1}H NMR (300 MHz, $CDCl_3$) spectrum of compound **PJ2**

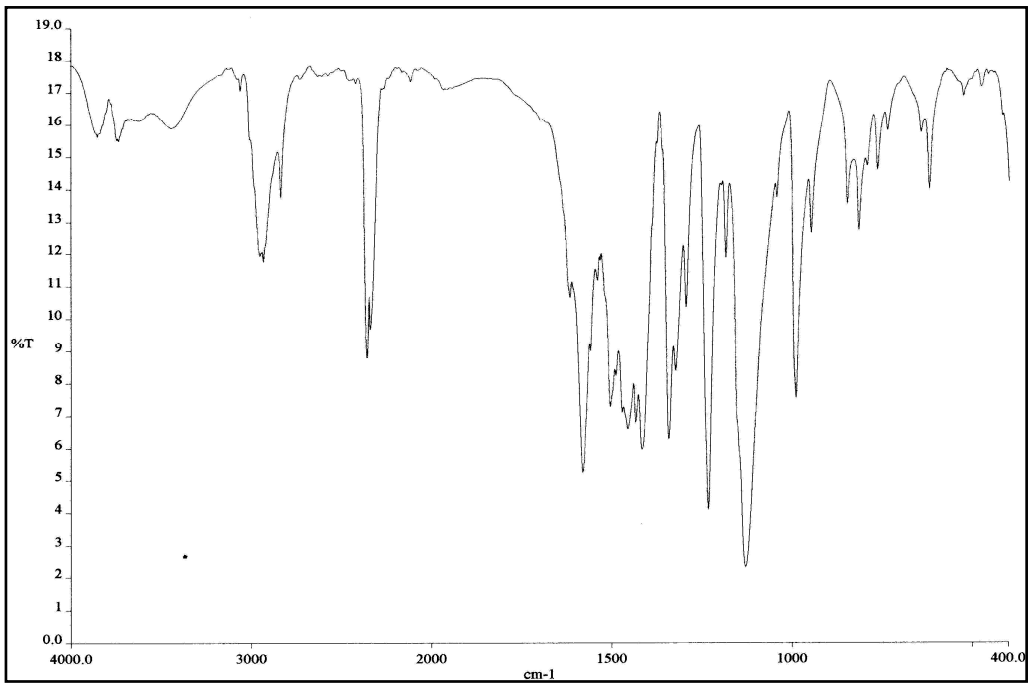

Figure 54 FT-IR (KBr) spectrum of compound **PJ3**

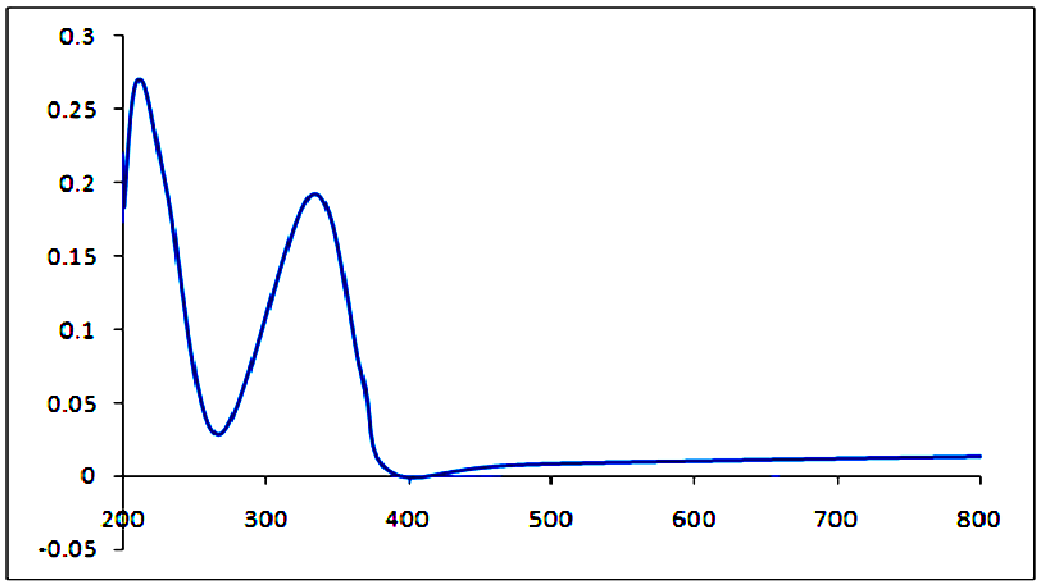

Figure 55 UV-Vis ($CHCl_3$) spectrum of compound **PJ3**

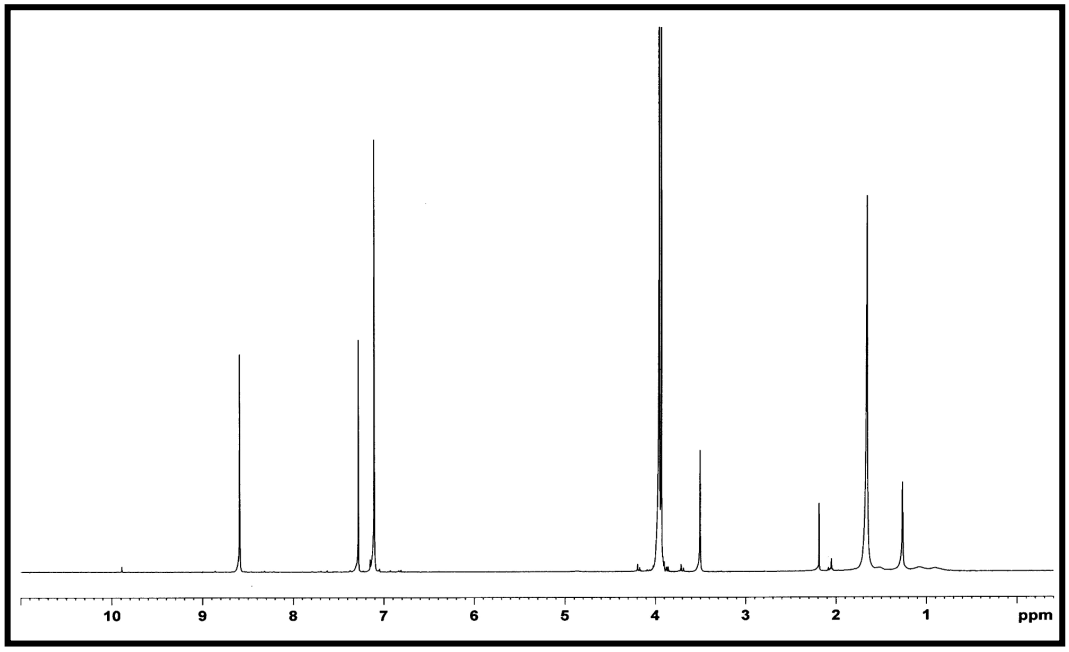

Figure 56 ^{1}H NMR (300 MHz, $CDCl_3$) spectrum of compound **PJ3**

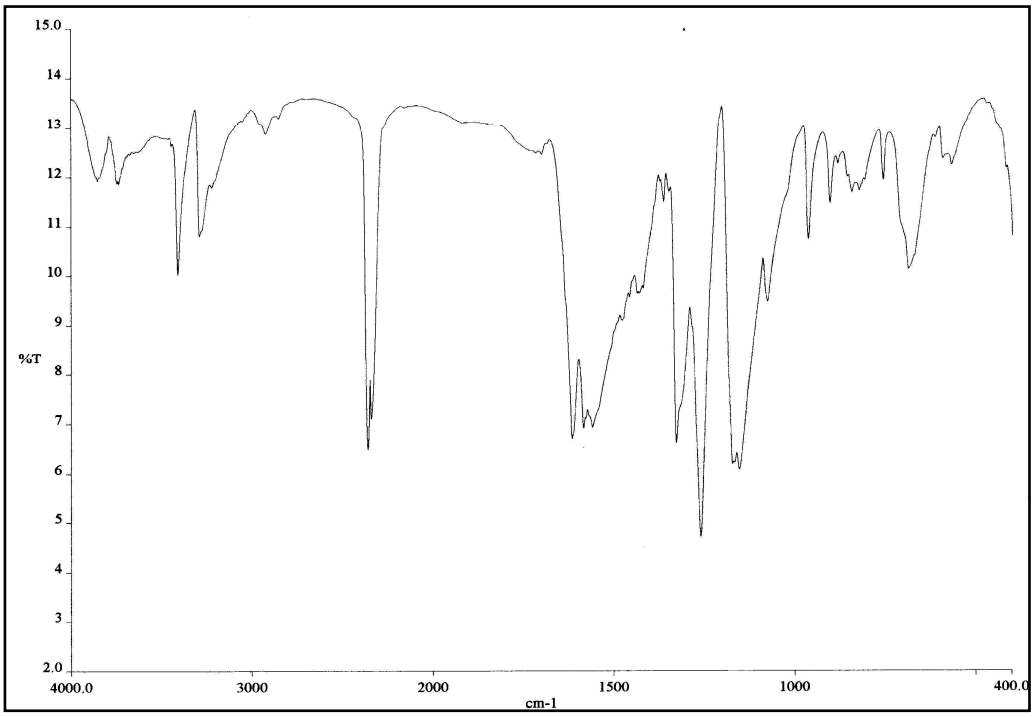

Figure 57 FT-IR (KBr) spectrum of compound **PJ4**

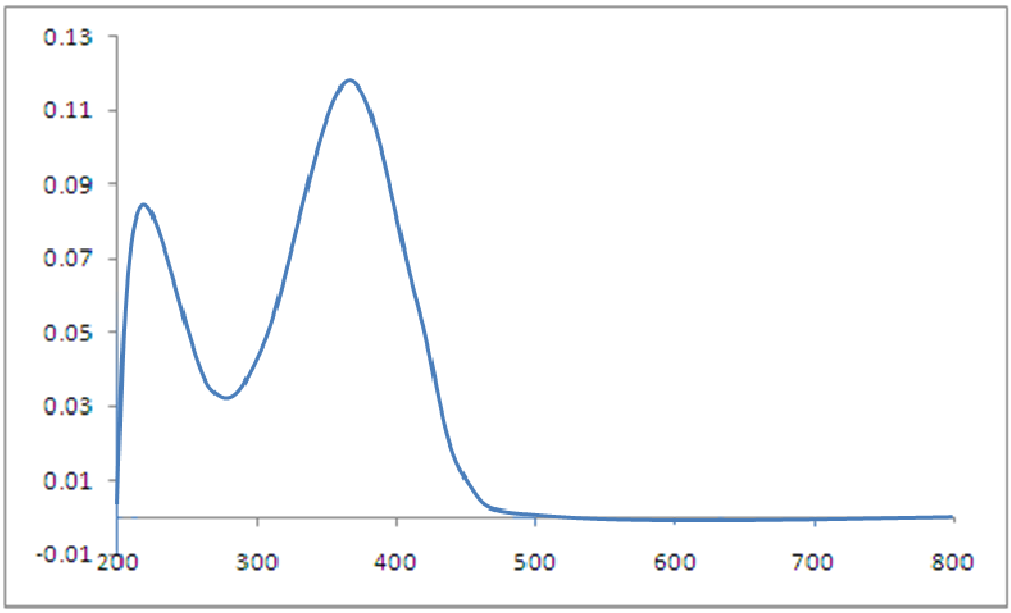

Figure 58 UV-Vis ($CHCl_3$) spectrum of compound **PJ4**

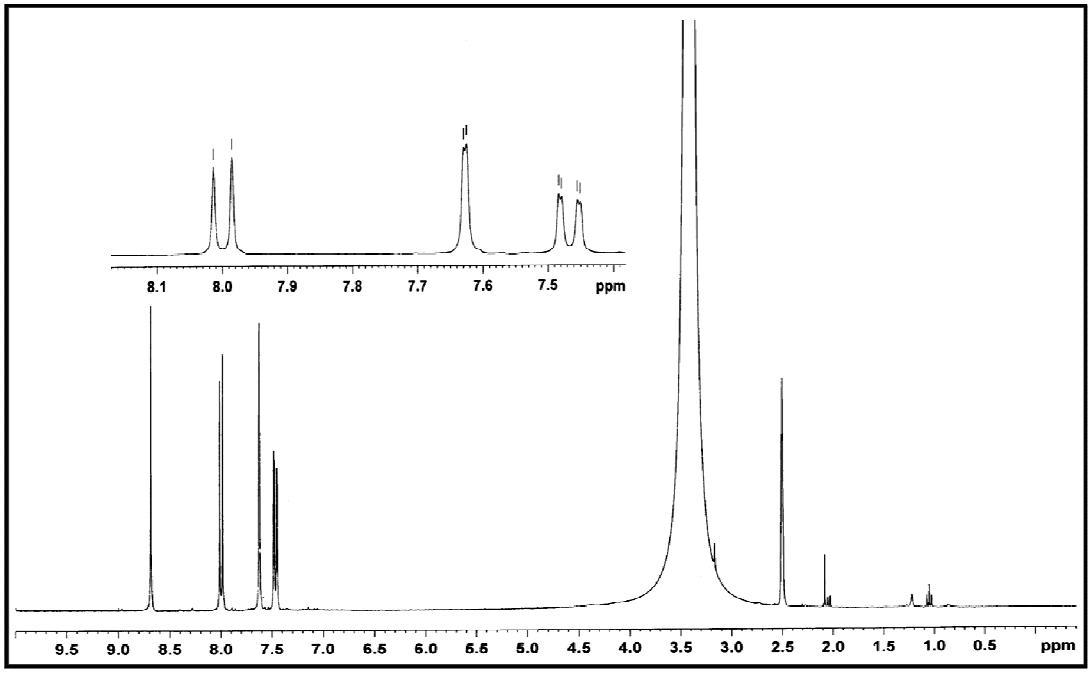

Figure 59 ^{1}H NMR (300 MHz, DMSO) spectrum of compound **PJ4**

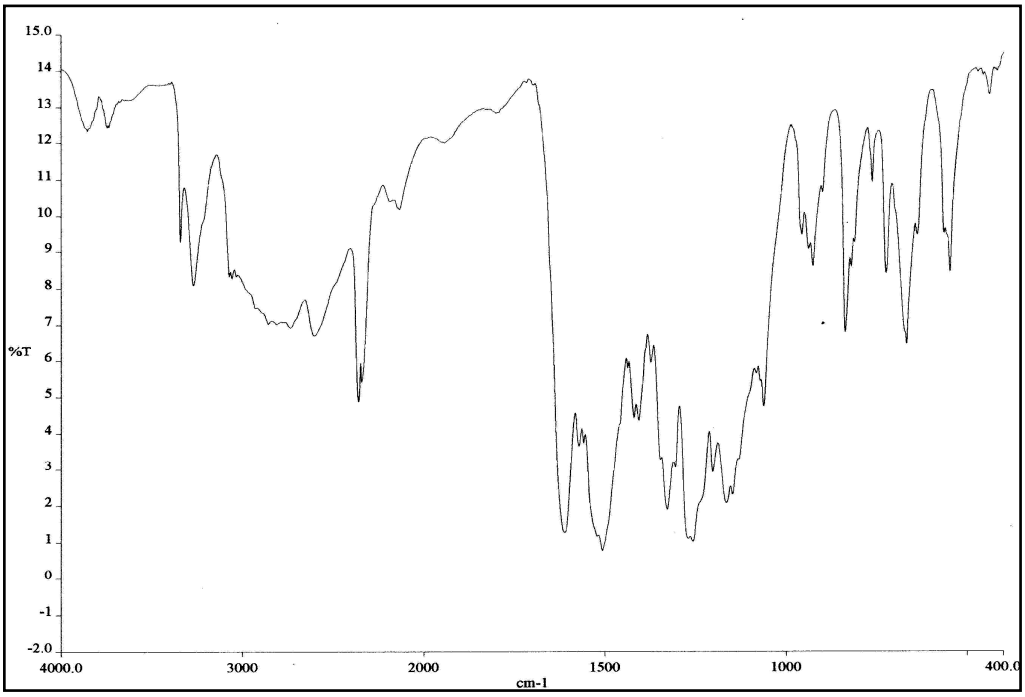

Figure 60 FT-IR (KBr) spectrum of compound **PJ5**

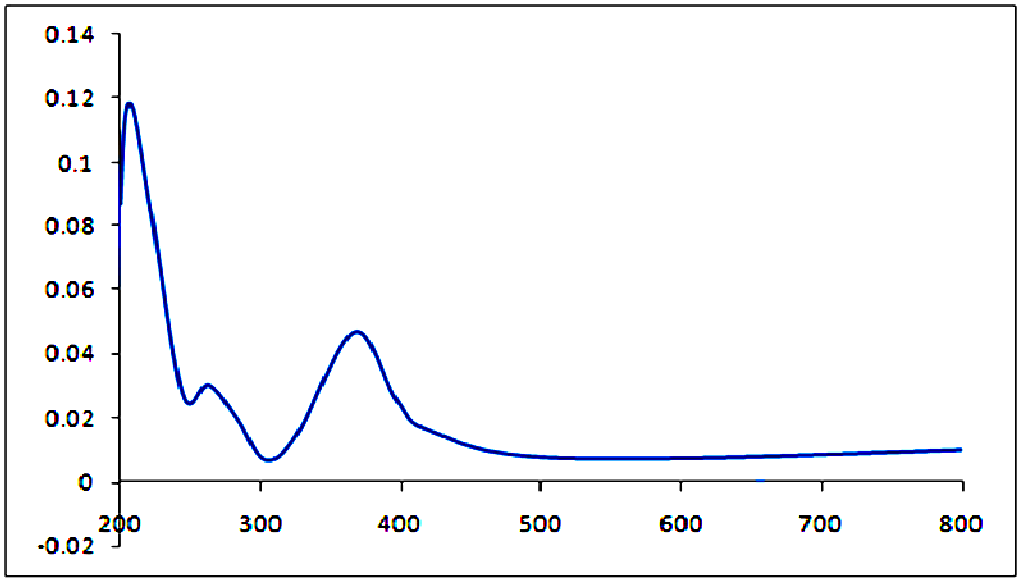

Figure 61 UV-Vis ($CHCl_3$) spectrum of compound **PJ5**

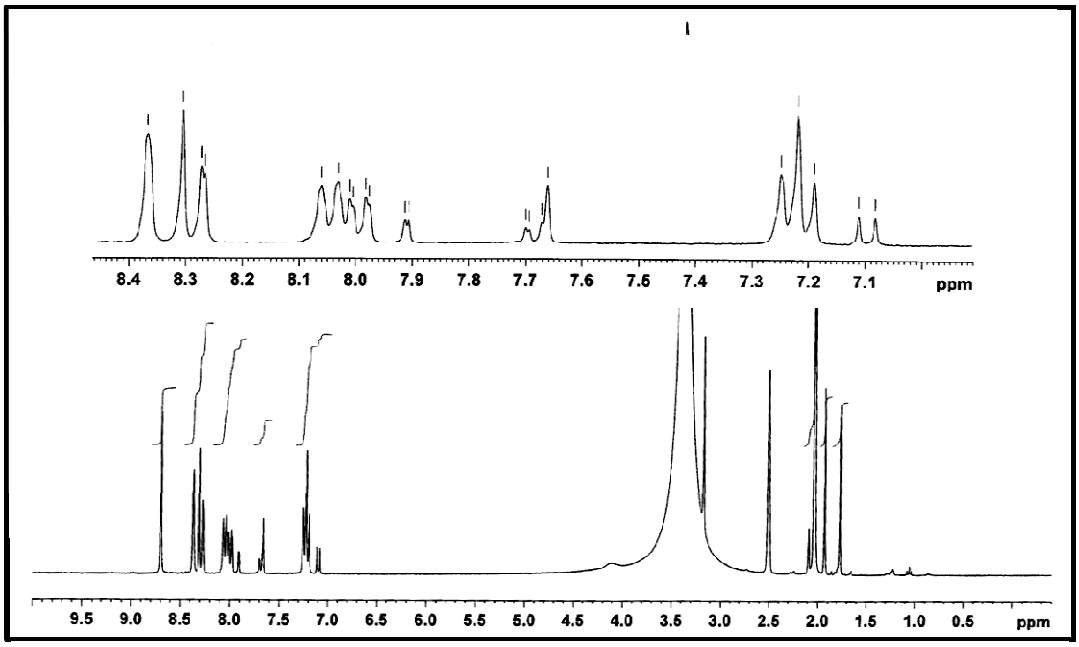

Figure 62 ^{1}H NMR (300 MHz, DMSO) spectrum of compound **PJ5**

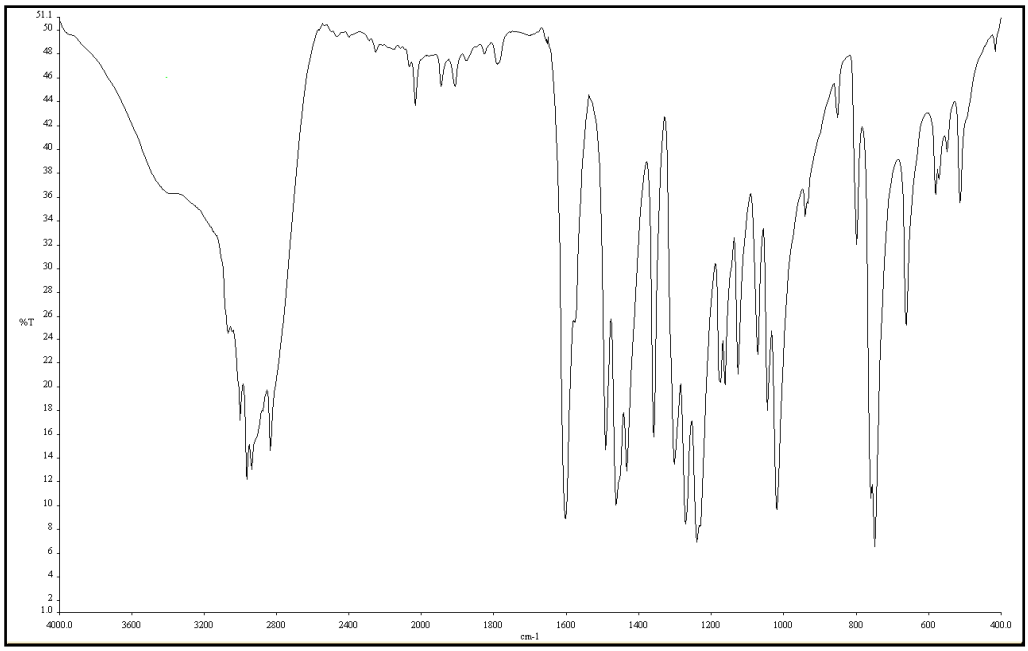

Figure 63 FT-IR (KBr) spectrum of compound **PJ6**

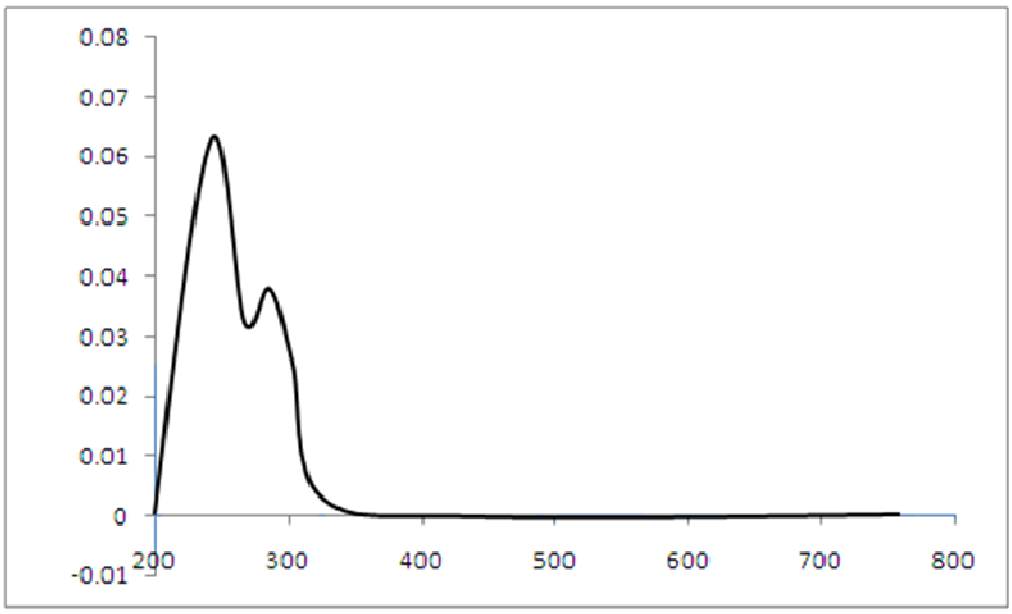

Figure 64 UV-Vis ($CHCl_3$) spectrum of compound **PJ6**

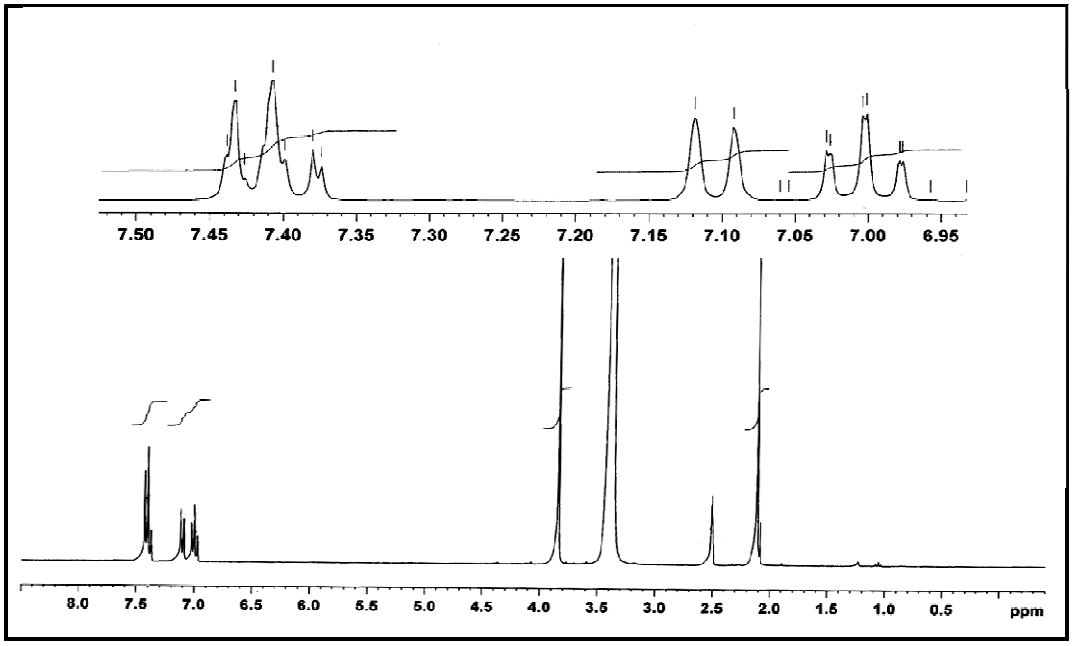

Figure 65 ^{1}H NMR (300 MHz, DMSO) spectrum of compound **PJ6**

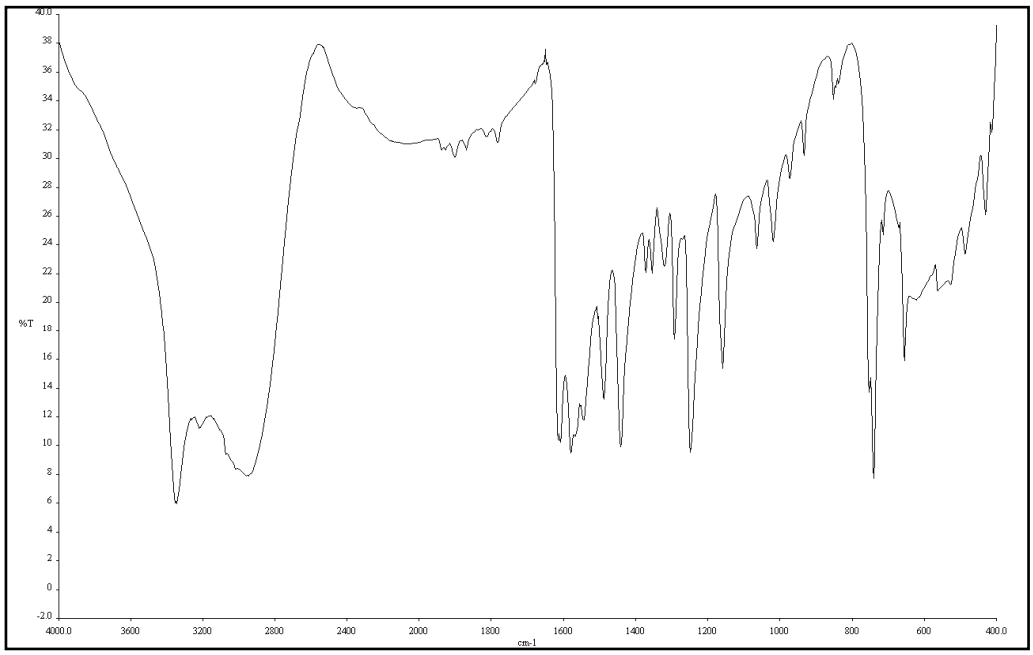

Figure 66 FT-IR (KBr) spectrum of compound **PJ7**

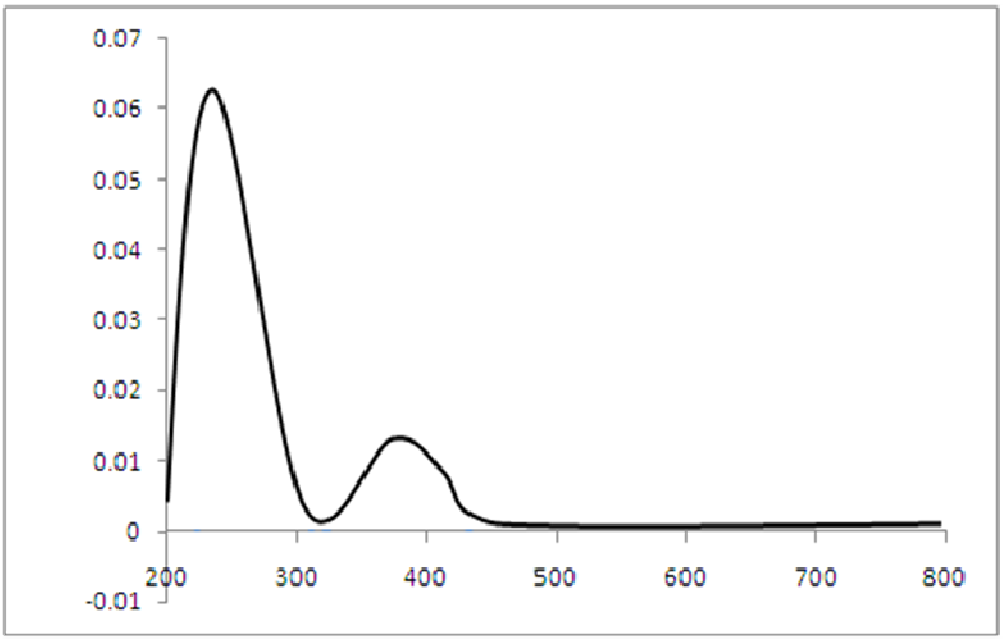

Figure 67 UV-Vis ($CHCl_3$) spectrum of compound **PJ7**

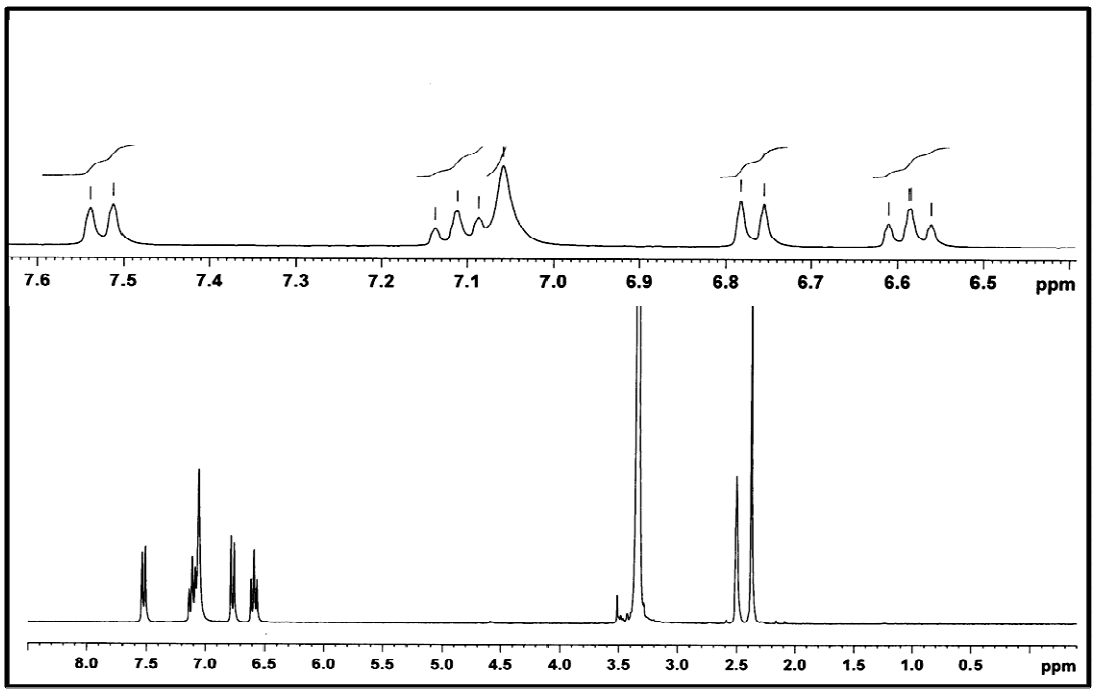

Figure 68 ^{1}H NMR (300 MHz, DMSO) spectrum of compound **PJ7**

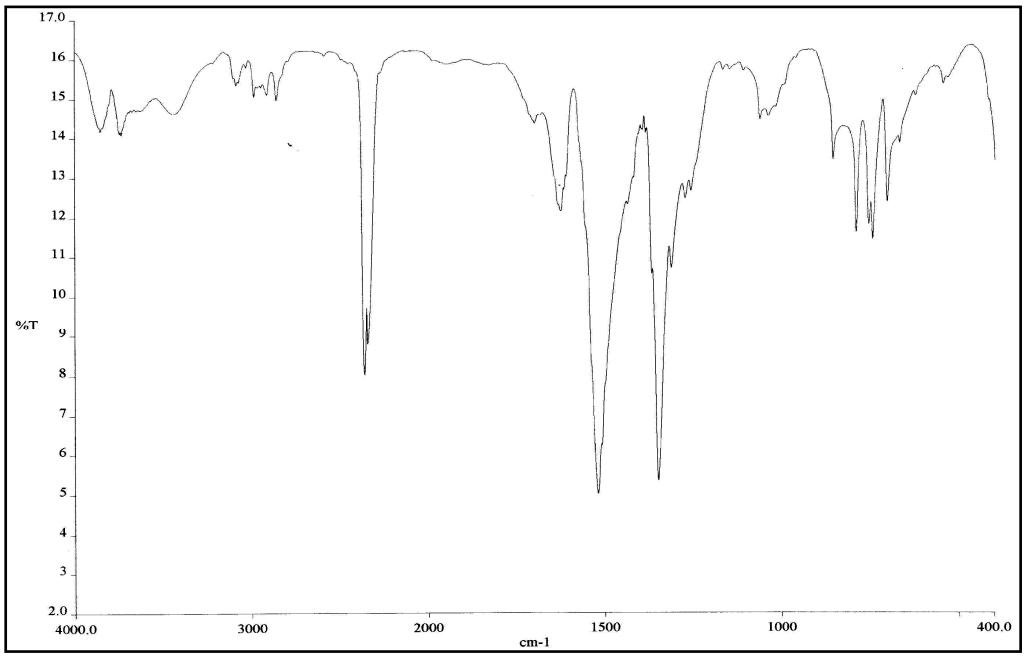

Figure 69 FT-IR (KBr) spectrum of compound **PJ8**

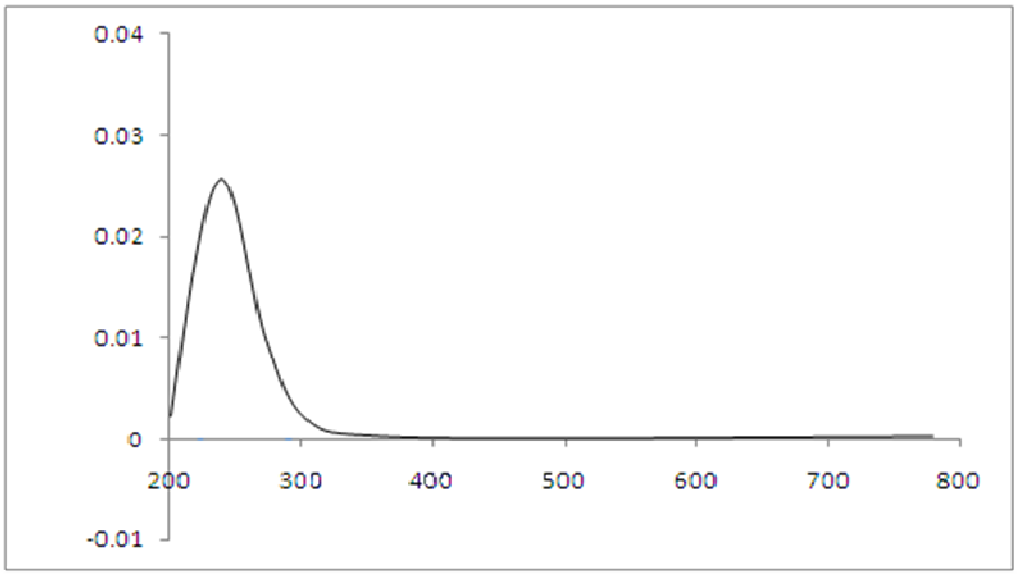

Figure 70 UV-Vis ($CHCl_3$) spectrum of compound **PJ8**

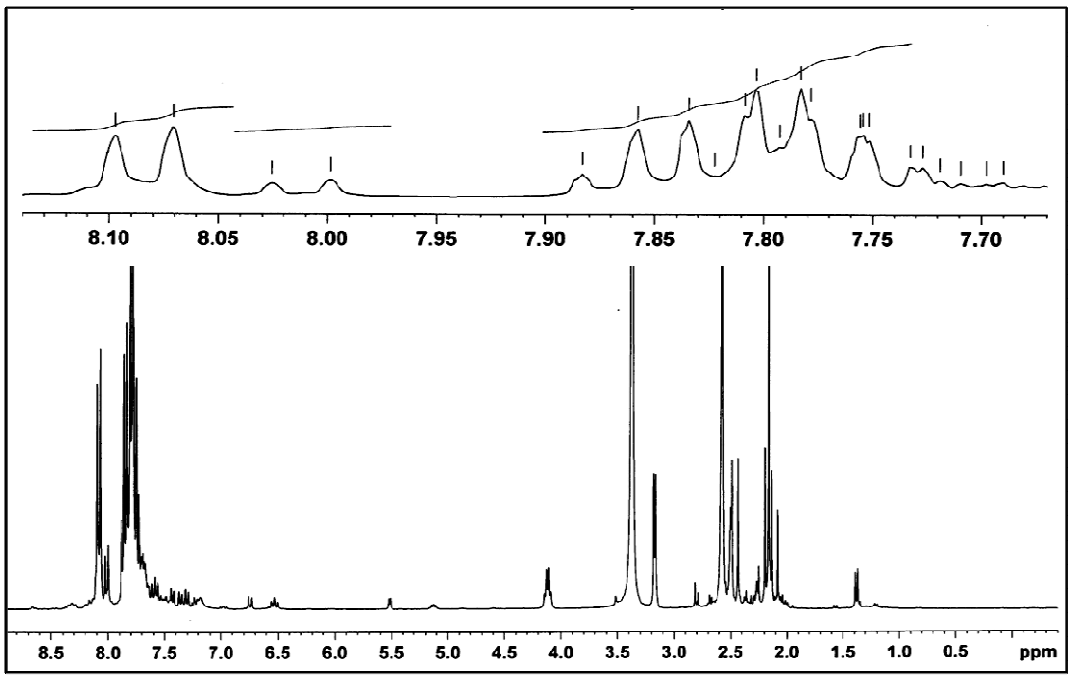

Figure 71 ^{1}H NMR (300 MHz, DMSO) spectrum of compound **PJ8**

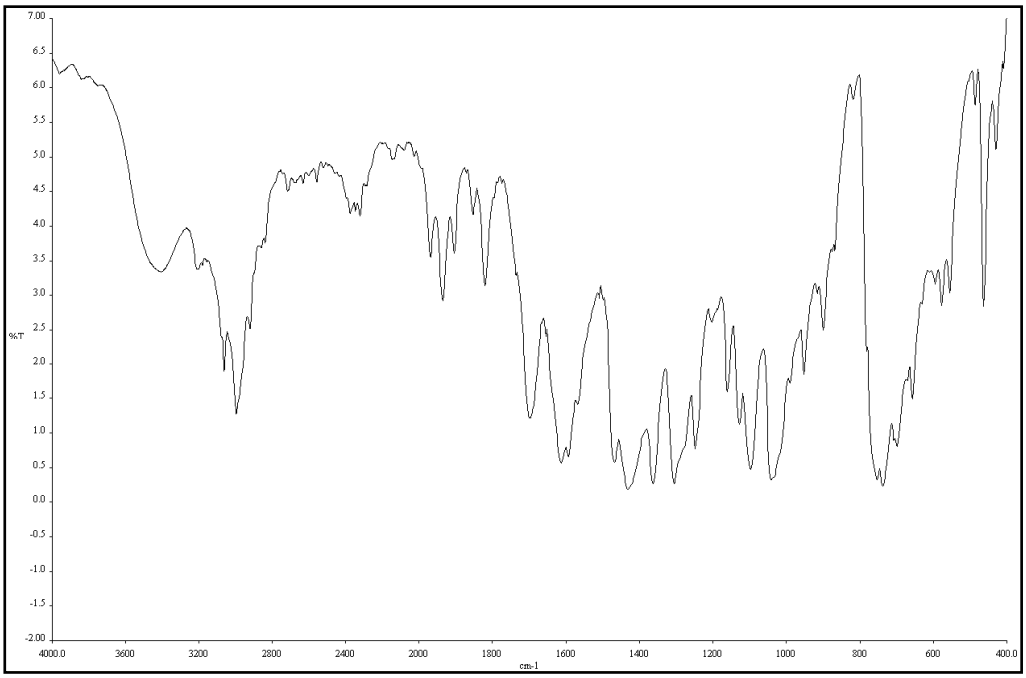

Figure 72 FT-IR (KBr) spectrum of compound **PJ9**

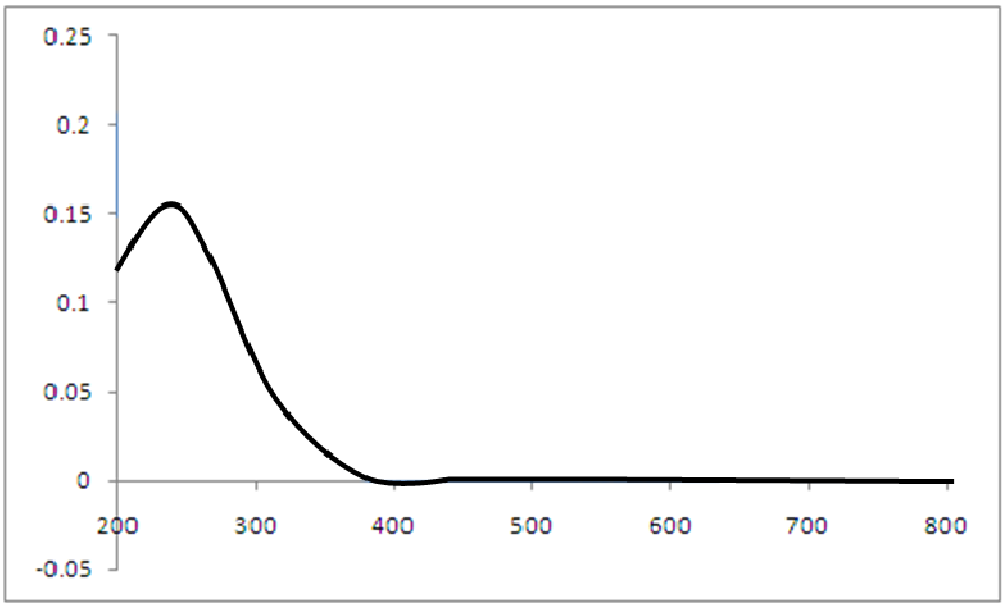

Figure 73 UV-Vis ($CHCl_3$) spectrum of compound **PJ9**

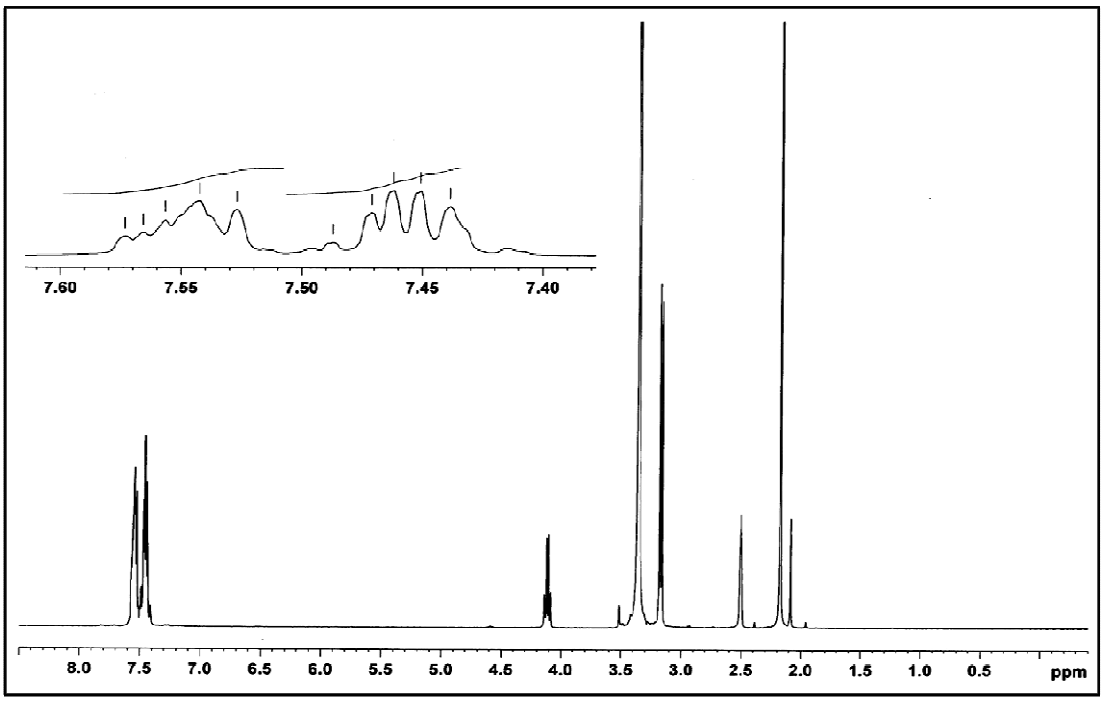

Figure 74 ^{1}H NMR (300 MHz, DMSO) spectrum of compound **PJ9**

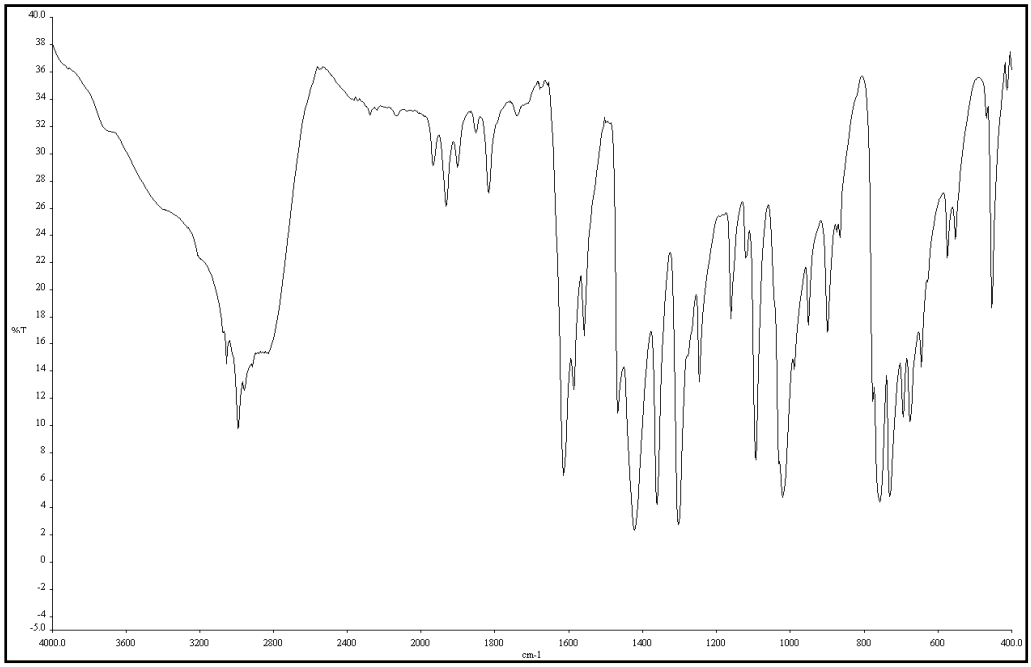

Figure 75 FT-IR (KBr) spectrum of compound **PJ10**

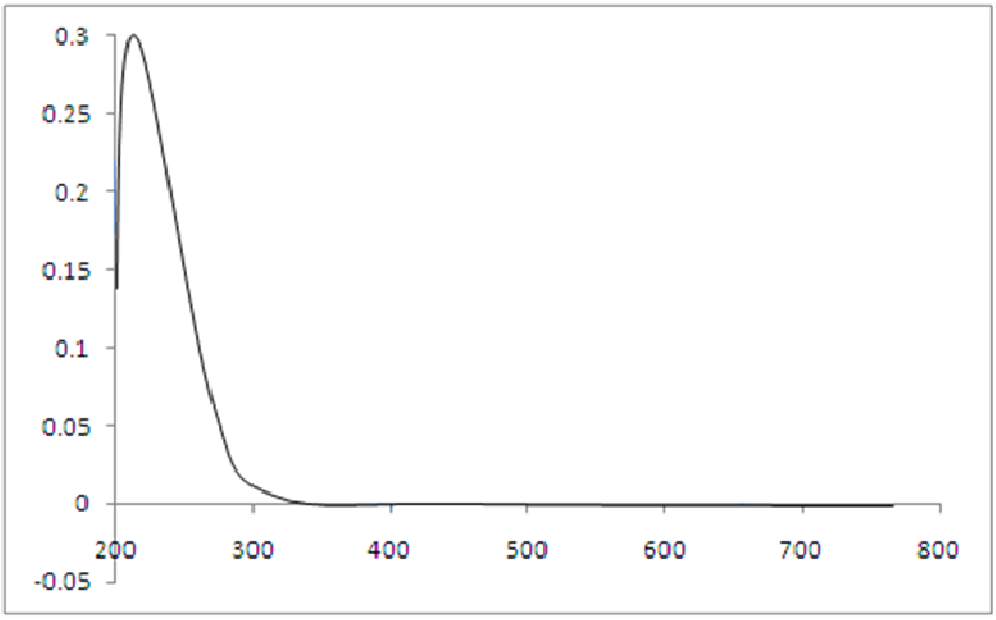

Figure 76 UV-Vis ($CHCl_3$) spectrum of compound **PJ10**

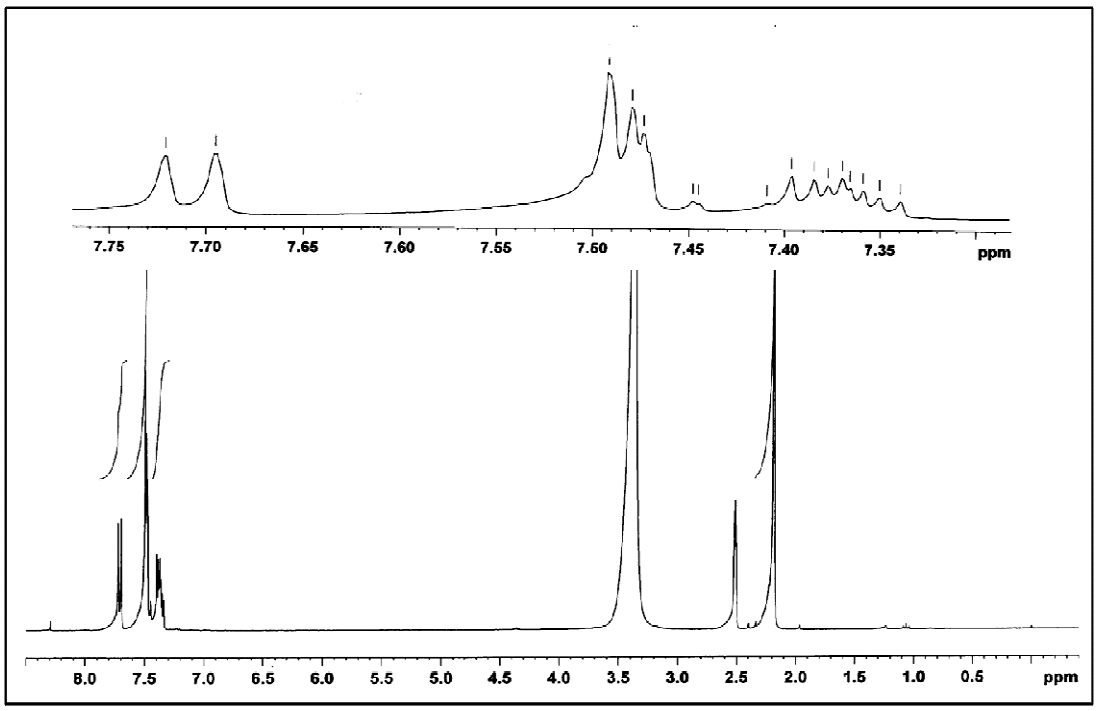

Figure 77 ^{1}H NMR (300 MHz, DMSO) spectrum of compound **PJ10**

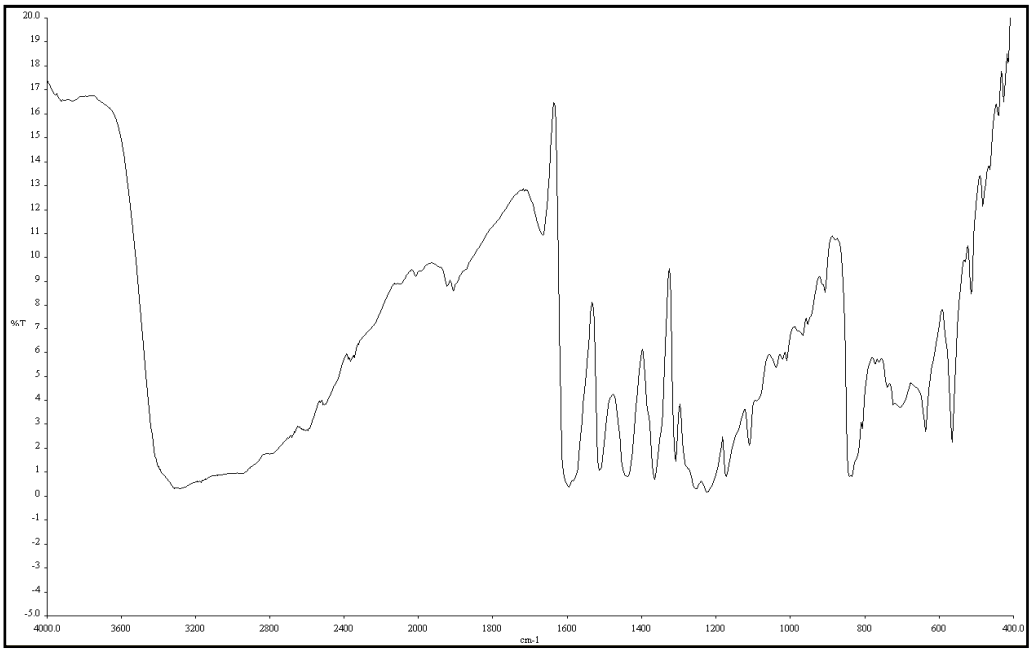

Figure 78 FT-IR (KBr) spectrum of compound **PJ11**

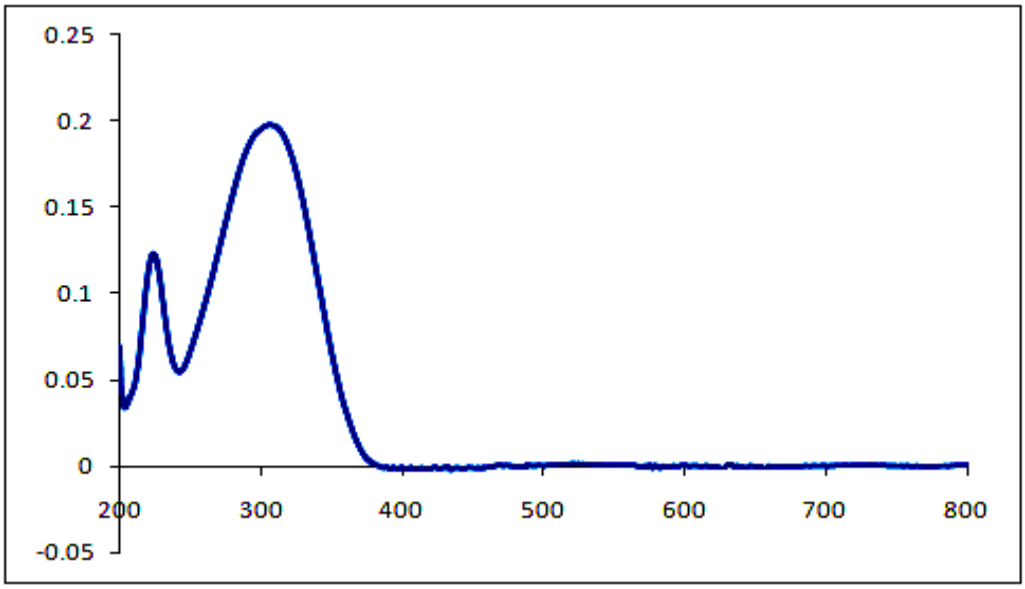

Figure 79 UV-Vis ($CHCl_3$) spectrum of compound **PJ11**

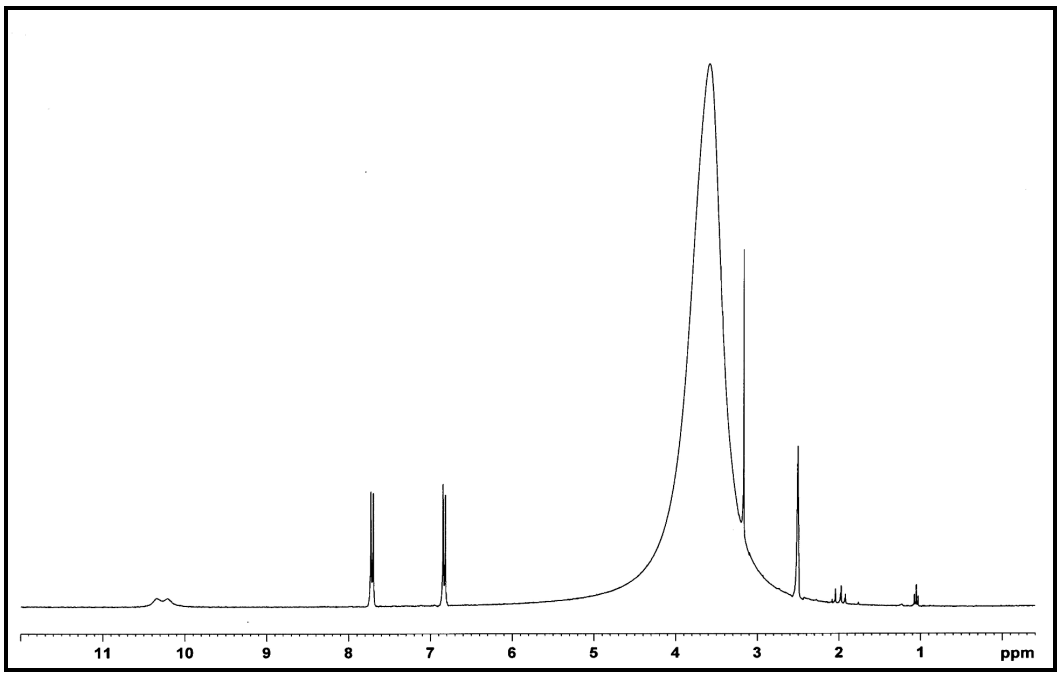

Figure 80 ^{1}H NMR (300 MHz, DMSO) spectrum of compound **PJ11**

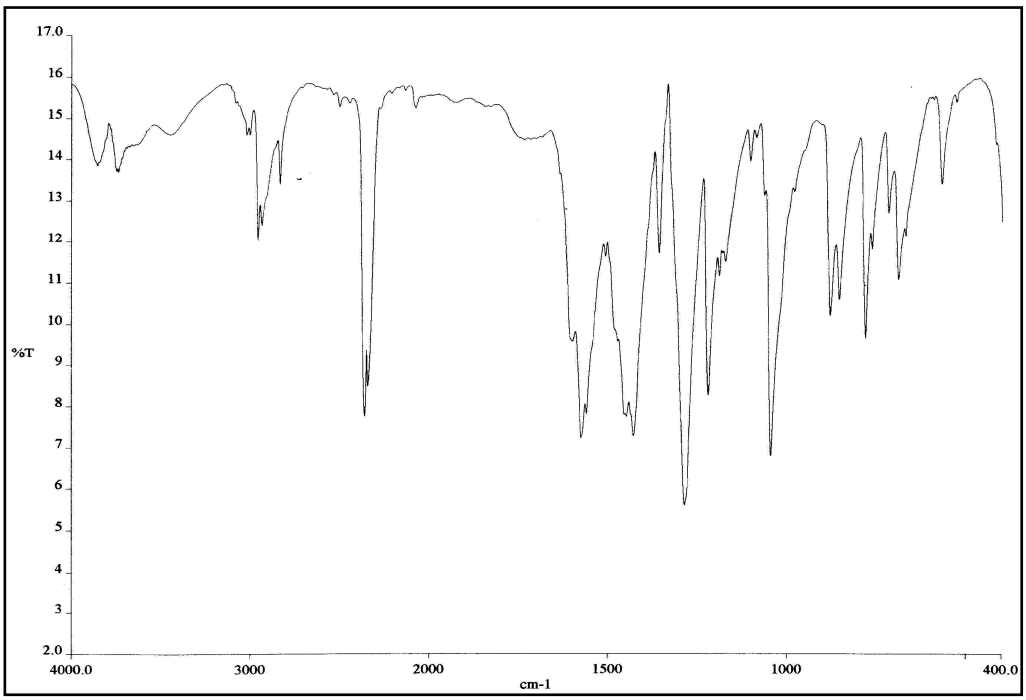

Figure 81 FT-IR (KBr) spectrum of compound **PJ12**

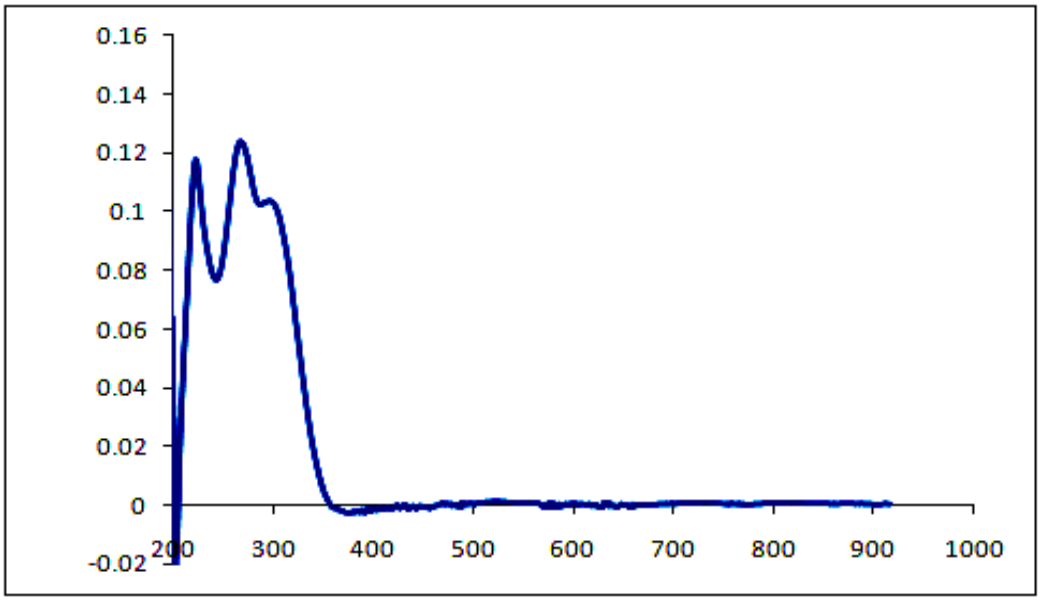

Figure 82 UV-Vis ($CHCl_3$) spectrum of compound **PJ12**

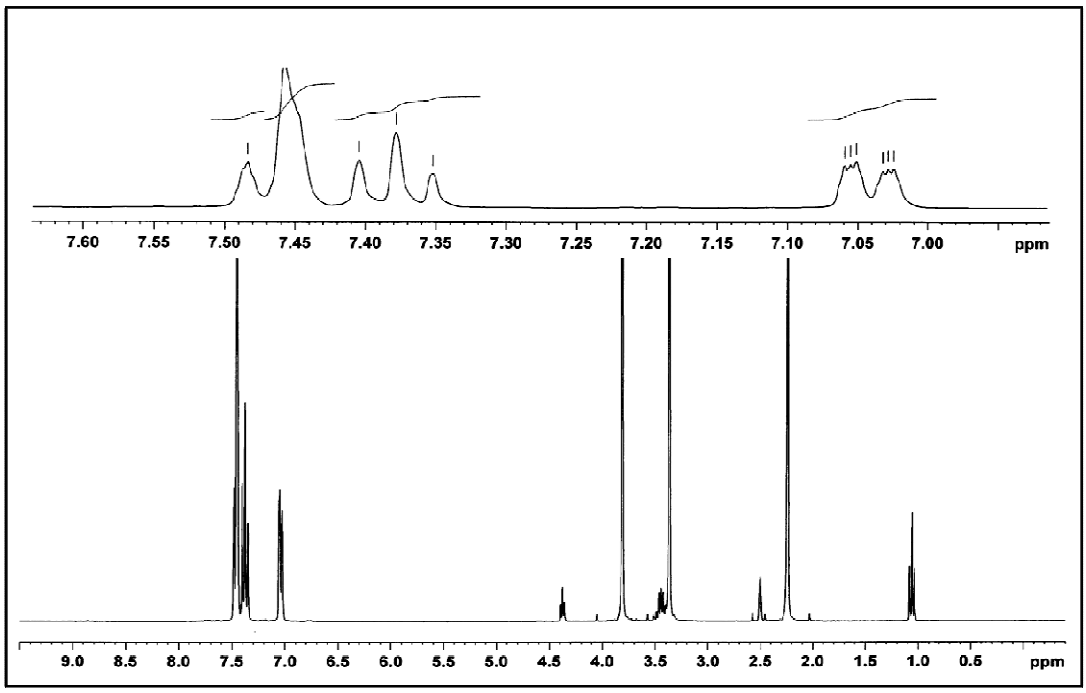

Figure 83 ^{1}H NMR (300 MHz, DMSO) spectrum of compound **PJ12**

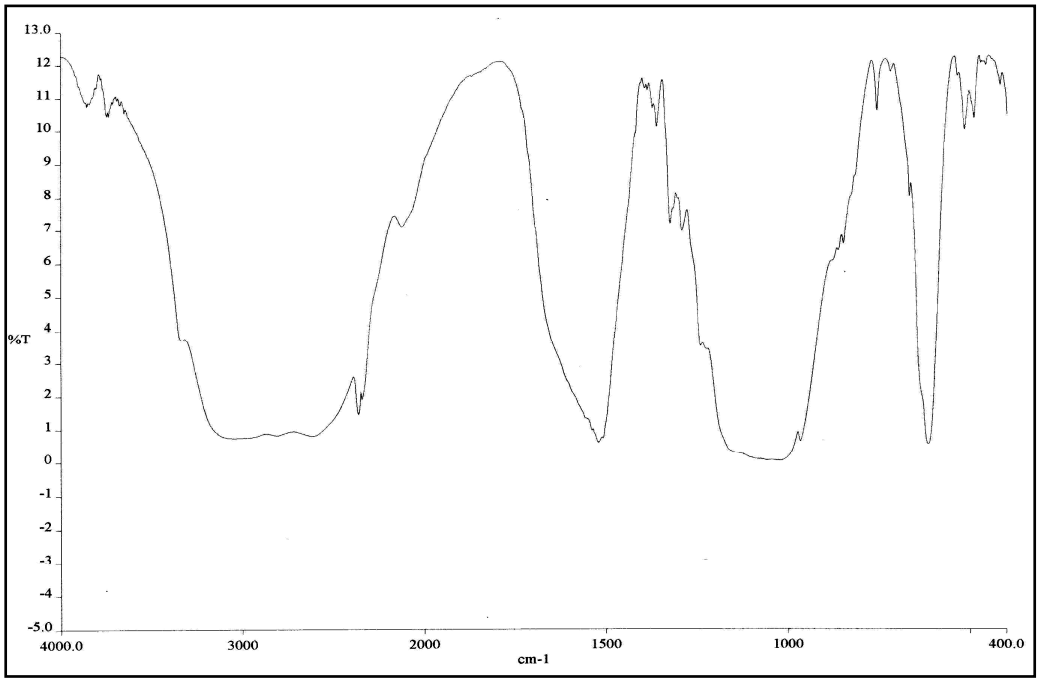

Figure 84 FT-IR (KBr) spectrum of compound **PJ13**

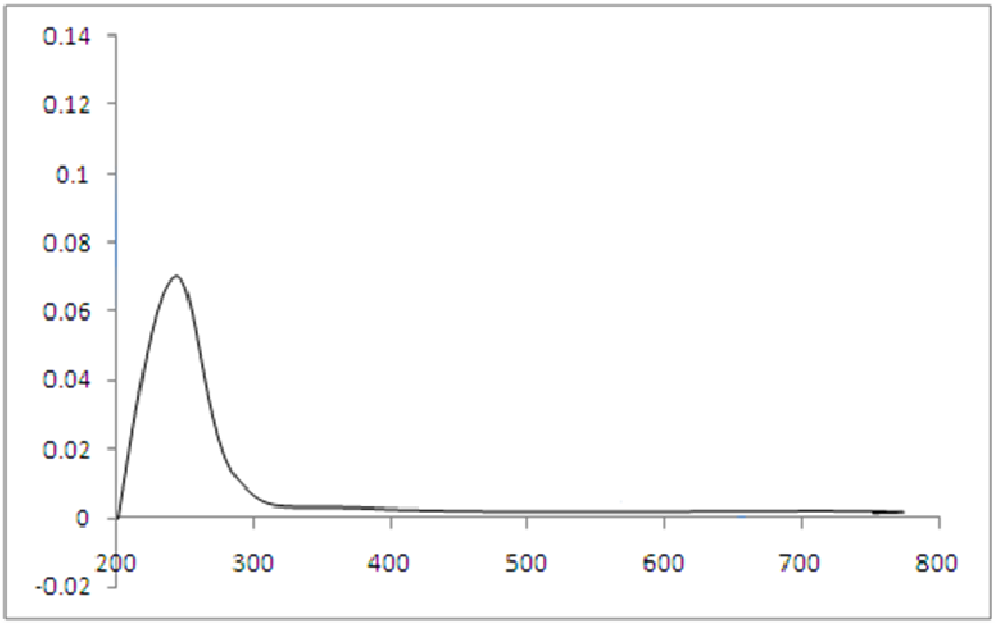

Figure 85 UV-Vis ($CHCl_3$) spectrum of compound **PJ13**

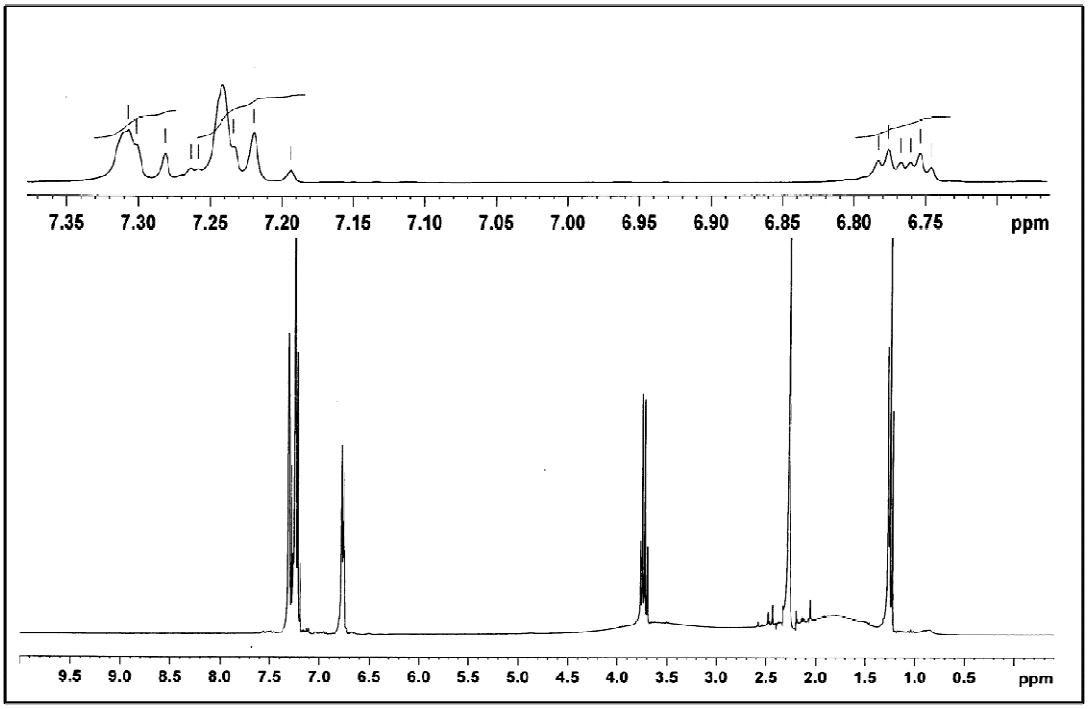

Figure 86 ^{1}H NMR (300 MHz, $CDCl_3$) spectrum of compound **PJ13**

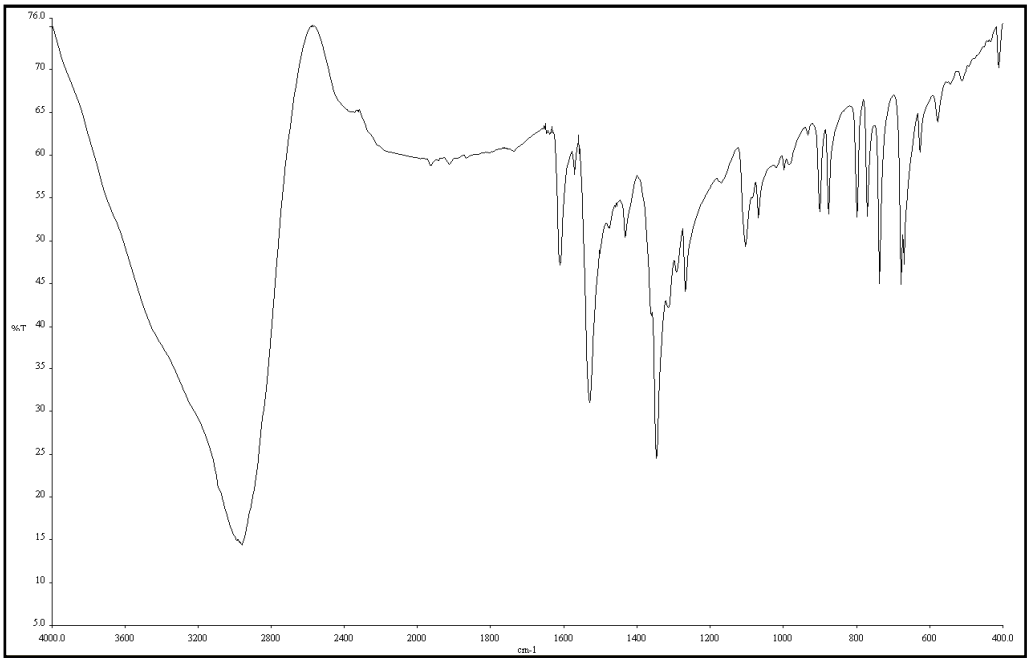

Figure 87 FT-IR (KBr) spectrum of compound **PJ14**

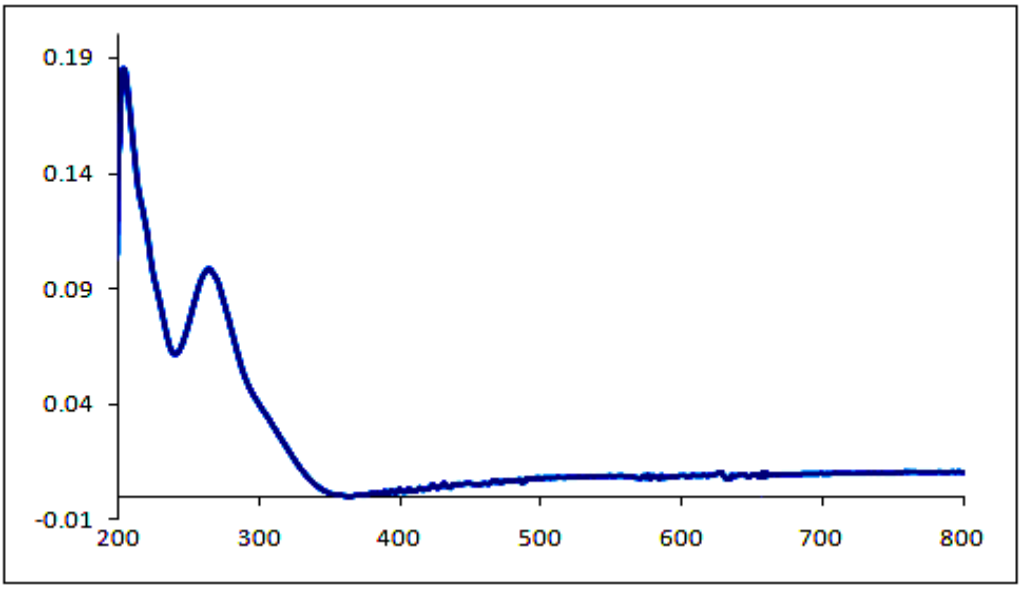

Figure 88 UV-Vis ($CHCl_3$) spectrum of compound **PJ14**

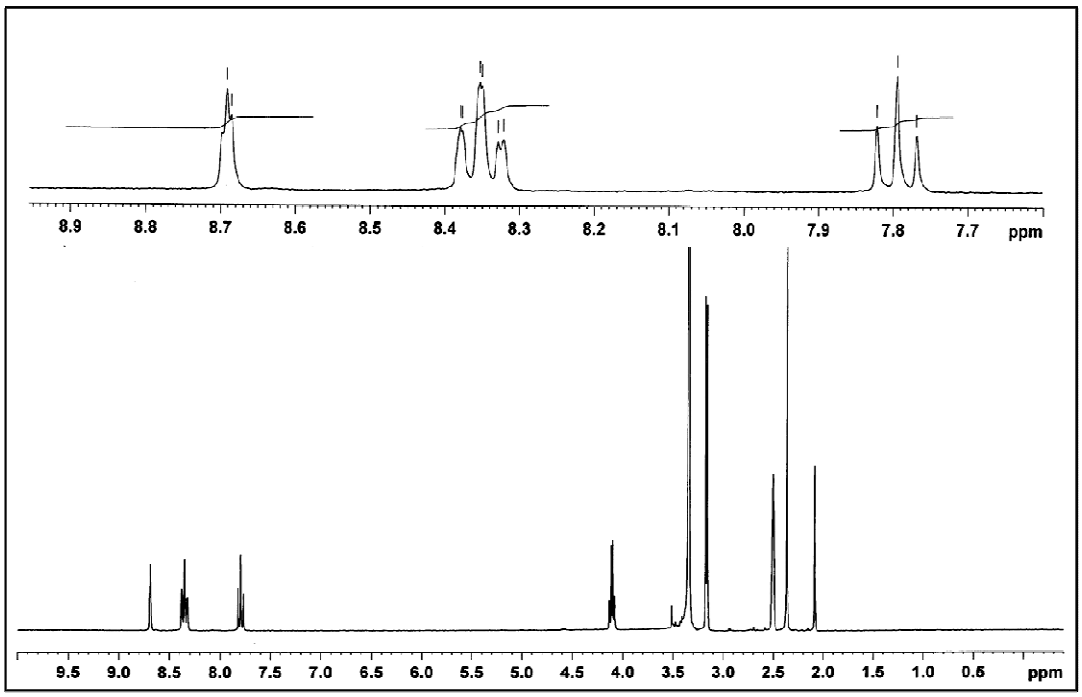

Figure 89 ^{1}H NMR (300 MHz, DMSO) spectrum of compound **PJ14**

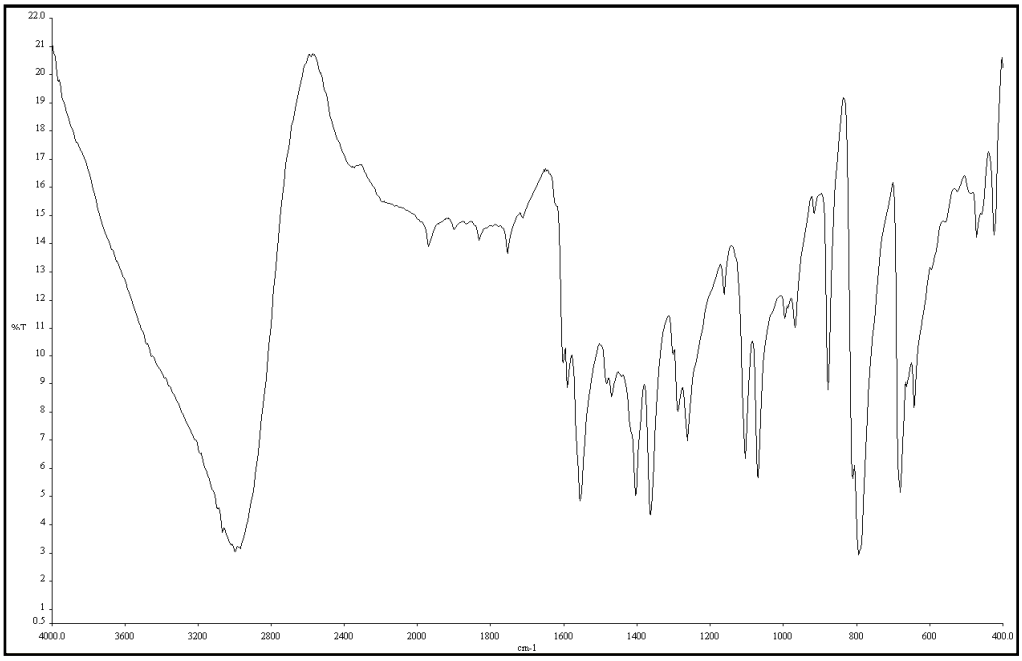

Figure 90 FT-IR (KBr) spectrum of compound **PJ15**

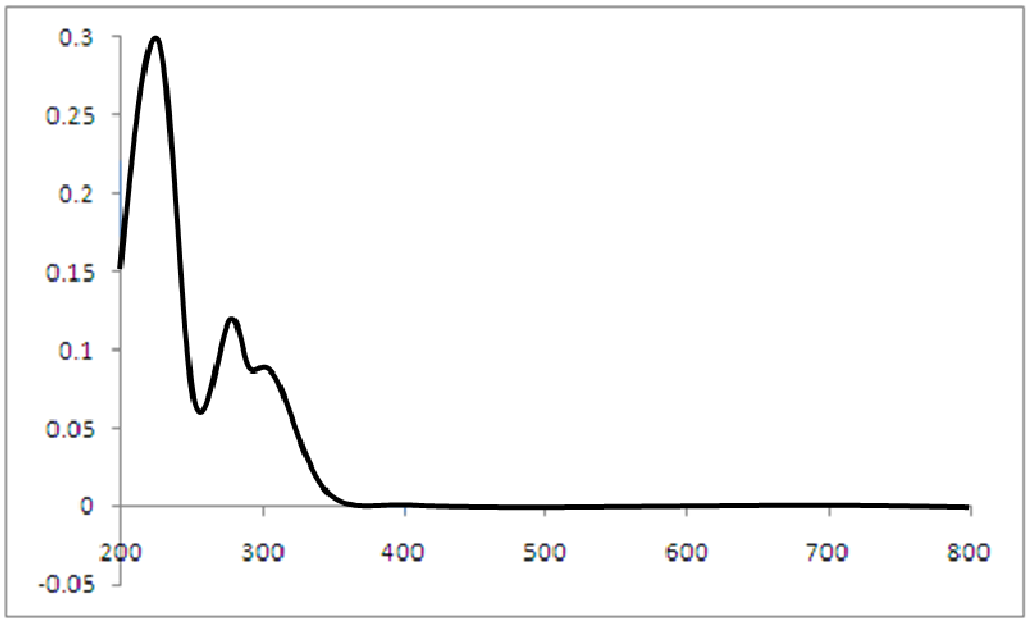

Figure 91 UV-Vis ($CHCl_3$) spectrum of compound **PJ15**

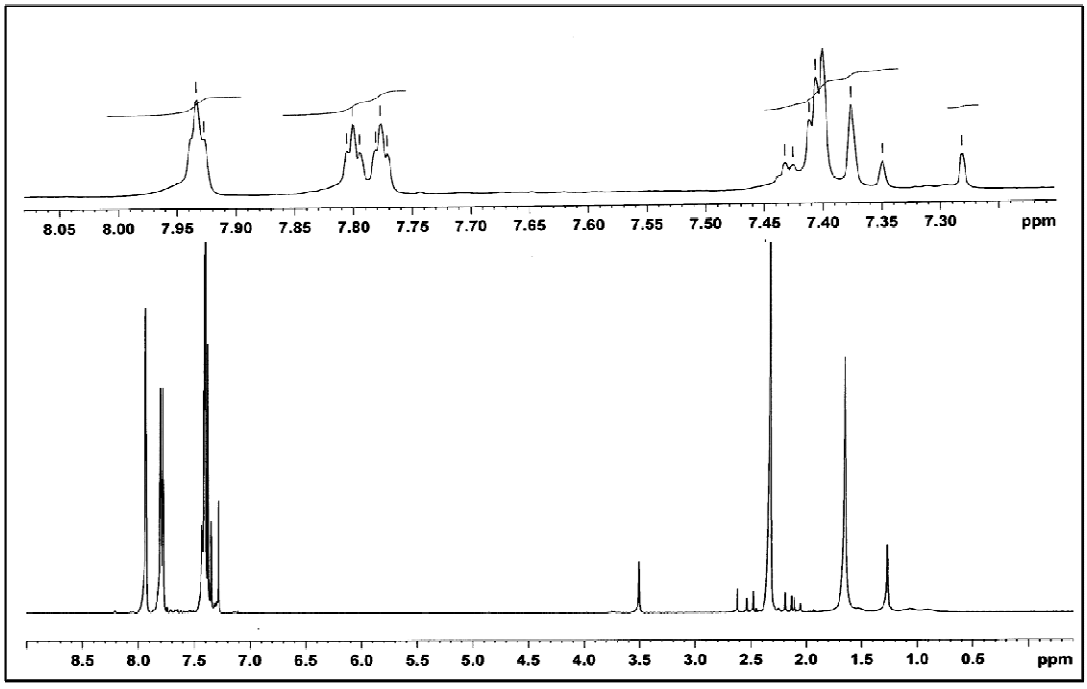

Figure 92 ^{1}H NMR (300 MHz, $CDCl_3$) spectrum of compound **PJ15**

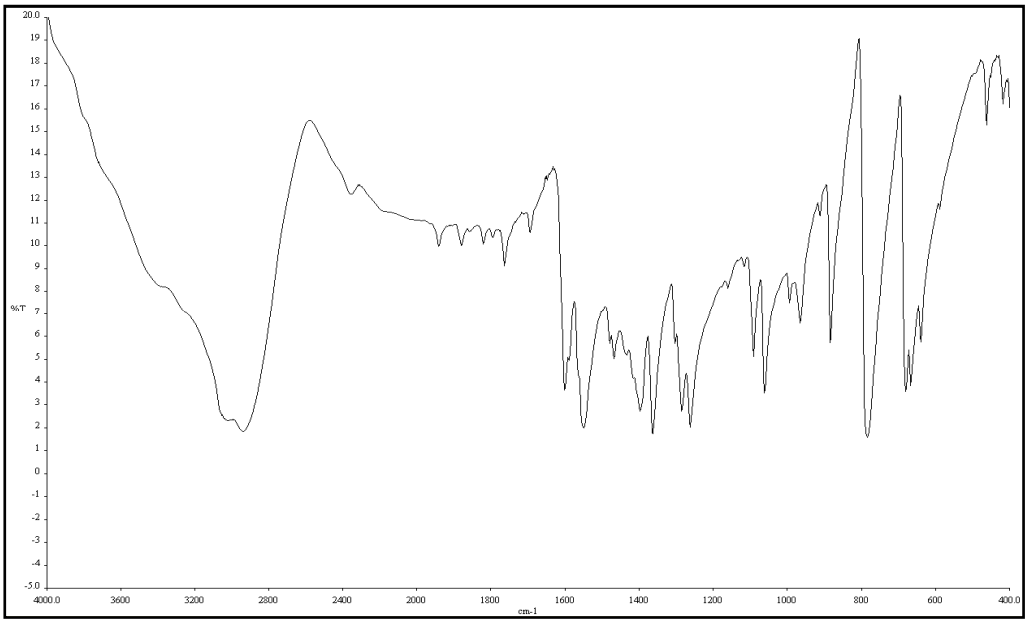

Figure 93 FT-IR (KBr) spectrum of compound **PJ16**

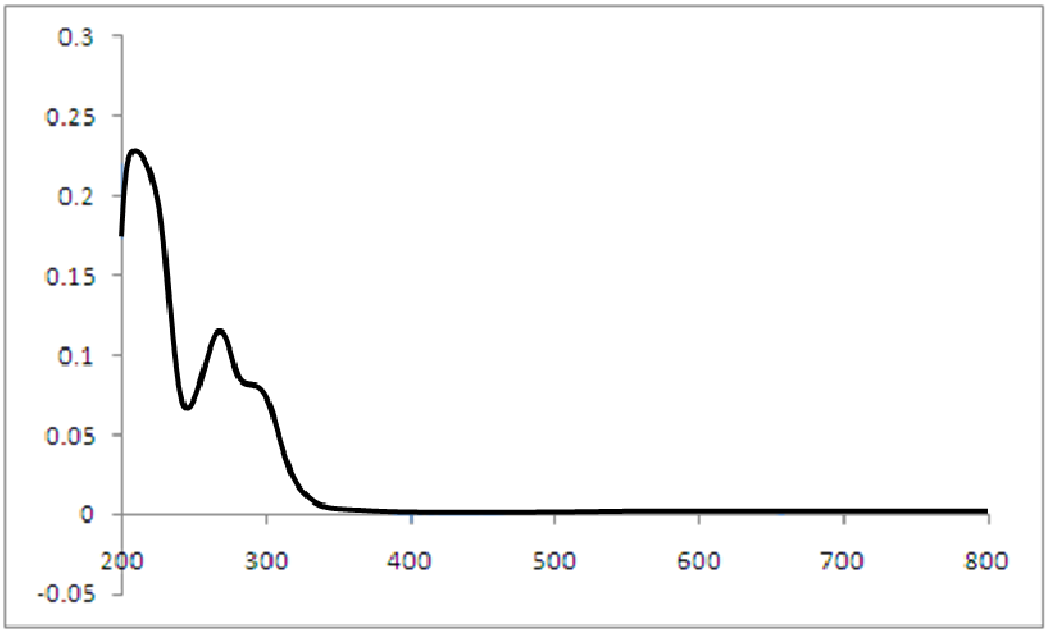

Figure 94 UV-Vis ($CHCl_3$) spectrum of compound **PJ16**

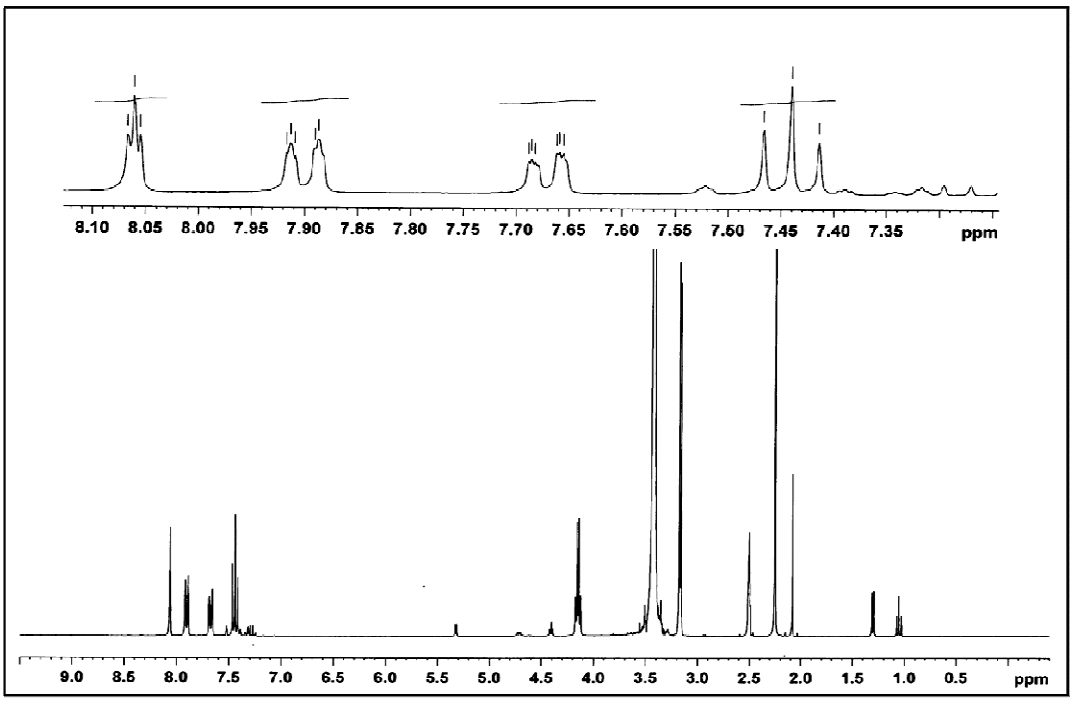

Figure 95 ^{1}H NMR (300 MHz, DMSO) spectrum of compound **PJ16**

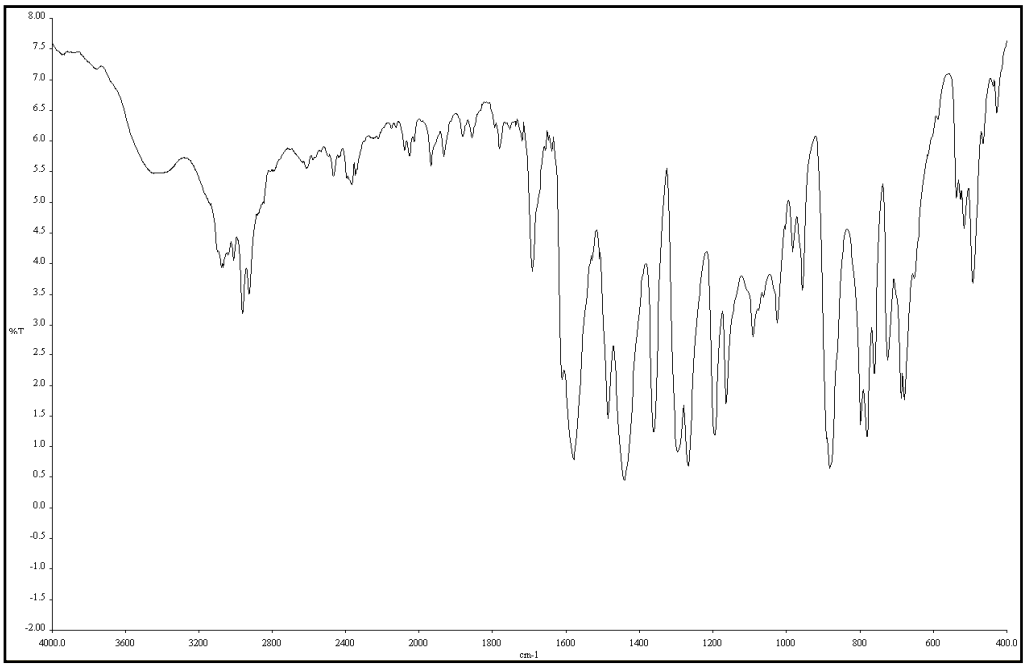

Figure 96 FT-IR (KBr) spectrum of compound **PJ17**

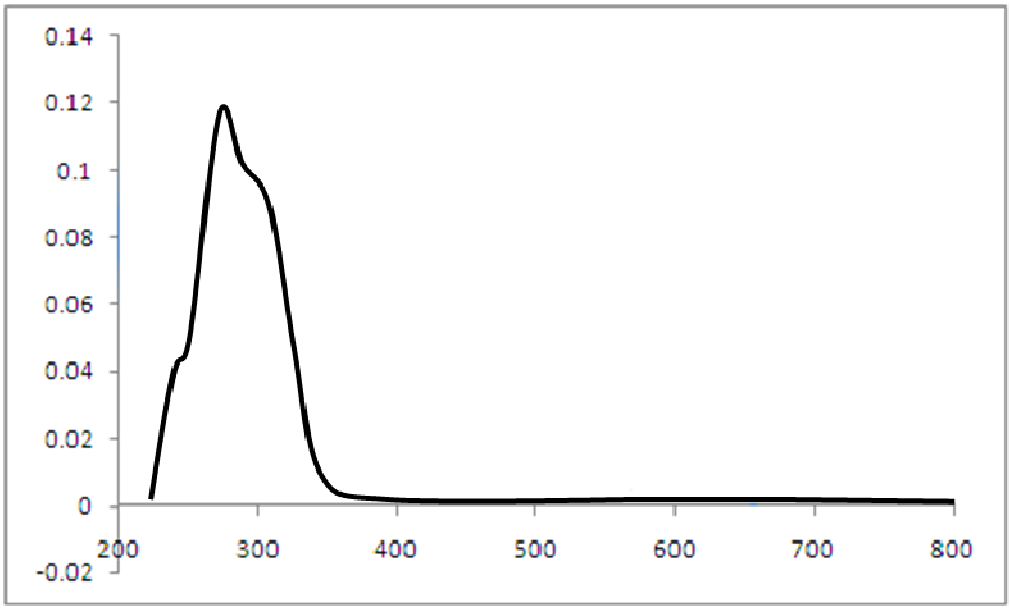

Figure 97 UV-Vis ($CHCl_3$) spectrum of compound **PJ17**

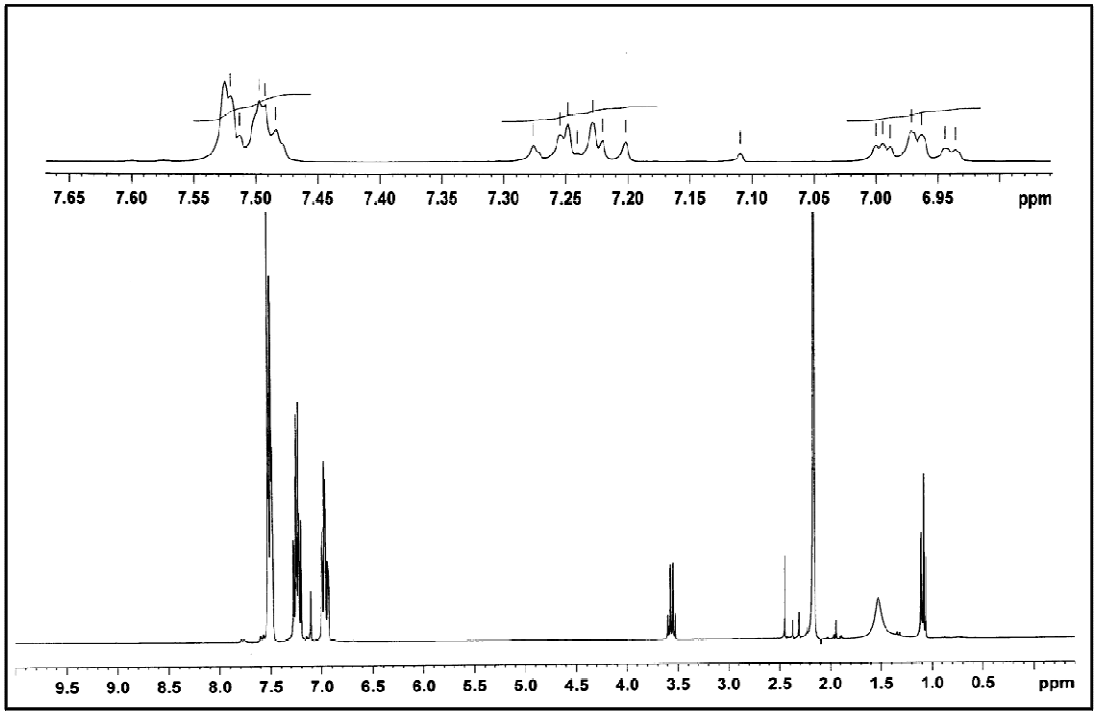

Figure 98 ^{1}H NMR (300 MHz, DMSO) spectrum of compound **PJ17**

VITAE

Name Miss Patcharaporn Jansrisewangwong

Student ID 5210220047

Educational Attainment

Degree	Name of Institution	Year of Graduation
B.Sc. (Chemistry)	Prince of Songkla University	2008

Scholarship Awards during Enrolment

Scholarship was awarded by the Center of Excellence for Innovation in Chemistry (PERCH-CIC), Commission on Higher Education, Ministry of Education.

List of Publication and proceedings

Publications

1. Fun, H.-K.; Jansrisewangwong, P.; Chantrapromma, S. (2010) "(*E,E*)-1,2-Bis(2,4,6-trimethoxybenzylidene)hydrazine", *Acta Cryst.*, **E66**, o2401-o2402.

2. Chantrapromma, S.; Jansrisewangwong, P.; Fun, H.-K. (2010) "(1*E*,2*E*)-1,2-Bis[1-(2-methoxyphenyl)ethylidene]hydrazine", *Acta Cryst.*, **E66**, o2994-o2995.

3. Jansrisewangwong, P.; Chantrapromma, S.; Fun, H.-K. (2010) "(*E,E*)-1,2-Bis[1-(2-bromophenyl)ethylidene]hydrazine", *Acta Cryst.*, **E66**, o2170.

4. Fun, H.-K.; Jansrisewangwong, P.; Karalai, C.; Chantrapromma, S.; (2011) "(*E,E*)-1,2-Bis(2,4,5-trimethoxybenzylidene)hydrazine", *Acta Cryst.*, **E67**, o1526-o1527.